Stony Brook University

Formation and Inhibition of Islet Amyloid in Type 2 Diabetes

A Dissertation Presented

by

Ling-Hsien Tu

to

The Graduate School

in Partial Fulfillment of the

Requirements

for the Degree of

Doctor of Philosophy

in

Chemistry

Stony Brook University

August 2014

Stony Brook University

The Graduate School

Ling-Hsien Tu

We, the dissertation committee for the above candidate for the

Doctor of Philosophy degree, hereby recommend

acceptance of this dissertation.

Daniel P. Raleigh, Ph. D., Dissertation Advisor
Professor and Vice-Chair, Department of Chemistry

Carlos Simmerling, Ph. D., Chairperson of Defense
Professor, Department of Chemistry

Elizabeth Boon, Ph. D., Third Member
Associate Professor, Department of Chemistry

Carlos de los Santos, Ph. D., Outside Member
Professor, Department of Pharmacological Sciences

This dissertation is accepted by the Graduate School

Charles Taber
Dean of the Graduate School

Abstract of the Dissertation

Formation and Inhibition of Islet Amyloid in Type 2 Diabetes

by

Ling-Hsien Tu

Doctor of Philosophy

in

Chemistry

Stony Brook University

2014

Amyloid fibrils are insoluble protein aggregates found in organs and tissues, and are structurally dominated by β-strands. Amyloid formation has been implicated in a wide range of human diseases. Each disease is characterized by a specific protein or peptide that aggregates in certain conditions. For example, the amyloid β protein (Aβ) forms amyloid plaques in the brain of patients with Alzheimer's disease and this leads to neuronal degeneration. Parkinson's disease, another common neurodegenerative disorder, is associated with the intracellular aggregation of α-synuclein to form Lewy bodies in the brains of patients. This dissertation focuses on a polypeptide hormone, human islet amyloid polypeptide (IAPP, also known as amylin), which is co-secreted with insulin from pancreatic β-cells and forms islet amyloid deposits in type 2 diabetes.

Although several models of IAPP aggregation have been proposed and inhibitors of amyloid formation have been developed, the mechanism of amyloid formation by IAPP is still not known. In this dissertation, the role of aromatic interaction was examined by mutational analysis of a series

of Phe to Leu mutants. We also investigated the role of the C-terminus of IAPP and its interaction with His-18 during amyloid formation by IAPP. Several potential inhibitors of IAPP amyloid formation including the non-steroid anti-inflammatory drugs, Aspirin and Ketoprofen, and the red wine ingredient, Resveratrol were tested. In addition, we characterized Matrix Metallopeptidase 9 (MMP 9) IAPP cleavage products to better understand how this protease regulates IAPP amyloid formation. These studies aim to provide new insights into the mechanism of IAPP aggregation and the screening of inhibitors.

Table of Contents

List of Figures

List of Tables

List of Abbreviations

2DIR	Two-dimensional infrared spectroscopy
8-37 IAPP	A peptide fragment corresponding to residues 8-37 of human islet amyloid polypeptide
Aβ	The proteolytical fragment of amyloid precursor protein which is responsible for amyloid formation in Alzheimers disease
Ac 8-37-IAPP	N-terminus acetylated 8-37 IAPP
AFM	Atomic force microscopy
ANS	Autonomic nervous system
CD	Circular dichroism
CGRP	Calcitonin gene-related peptide
CJD	Creutzfeld-Jakob disease
CNS	Central nervous system
CPE	Carboxypeptidase E
DMSO	Dimethyl sulfoxide
EGCG	(–)-Epigallocatechin 3-gallate
EPR	Electron paramagnetic resonance
ER	Endoplasmic reticulum
$F_{C\equiv N}$	*p*-Cyanophenylalanine
F15I-IAPP	a Phe-15 to Ile variant of human islet amyloid polypeptide
F15L-IAPP	a Phe-15 to Leu variant of human islet amyloid polypeptide
F15L/F23L IAPP	a Phe-15 to Leu, Phe-23 to Leu variant of human islet amyloid polypeptide
F15L/Y37L IAPP	a Phe-15 to Leu, Tyr-37 to Leu variant of human islet amyloid polypeptide
F15Nle	a Phe-15 to norleucine variant of human islet amyloid polypeptide
F15Tle	a Phe-15 to tert-leucine variant of human islet amyloid polypeptide
F23L	a Phe-23 to Leu variant of human islet amyloid polypeptide

F23L/Y37L	a Phe-23 to Leu, Tyr-37 to Leu variant of human islet amyloid polypeptide
FAP	Familial amyloid polyneuropathy
Fmoc	9-fluorenylmethoxycarbonyl
Fmoc-PAL-PEG	5-(4’-Fmoc-aminomethyl-3’,5-dimethoxyphenyl) valeric acid
free CT-IAPP	A human islet amyloid polypeptide variant with a free C-terminus
FRET	Fluorescence resonance energy transfer
FTIR	Fourier transform infrared spectroscopy
G24P-IAPP	a Gly-24 to Pro variant of human islet amyloid polypeptide
GFP	Green fluorescent protein
GSS	Gerstmann-Straussler-Schrinker syndrome
H18L	A His-18 to Leu variant of human islet amyloid polypeptide
H18Q	A His-18 to Gln variant of human islet amyloid polypeptide
H18Q free CT-IAPP	A His-18 to Gln variant of human islet amyloid polypeptide with a free acid C-terminus
HFIP	Hexafluoroisopropanol
HPLC	High performance liquid chromatography
I26P-IAPP	A Ile 26 to Gln variant of human islet amyloid polypeptide
IAPP	Islet amyloid polypeptide
IDE	Insulin-degrading enzyme
MALDI-TOP-MS	Matrix assisted laser desorption ionization-time of flight mass spectrometry
MBP	Maltose-binding protein
MD	Molecular dynamics
MMP9	Matrix metallopeptidase 9
N-MeG24, N-MeI26-Iapp	Residue Gly-24 and Ile-26 N-methylated islet amyloid polypeptide
NMR	Nuclear magnetic resonance
PAM	Peptidylglycine alpha-amidating monooxygenase
PAP 248-286	A peptide fragment corresponding to residues 248-286 of prostatic acid phosphatase

PC1/3	Subtilisin-like prohormone convertase enzyme 1/3
PC2	Subtilisin-like prohormone convertase enzyme 2
PNS	Peripheral nervous system
RALS	Right angle light scattering
S20G-IAPP	A Ser 20 to Gly variant of human islet amyloid polypeptide
STEM	Scanning transmission electron microscopy
t_{50}	Time required to reach 50% of the final fluorescence change in the thioflavin-T assays
TEM	Transmission electron microscopy
TFA	Trifluoroacetic acid
TFE	Trifluoroethanol
TTR	Transthyretin
v/v	Volume to volume
Y37L	A Tyr 37 to Leu variant of human islet amyloid polypeptide

Acknowledgments

I would like to express the deepest appreciation to my research advisor, Professor Daniel P. Raleigh for his continuous support of my Ph.D study, for his patience and encouragement during the past few years. His guidance helped me in all the time of research and writing of this thesis. His great enthusiasm for science also has inspired me and kept me motivated. I could not have imagined having a better advisor and mentor for my Ph.D study.

Besides my advisor, I would like to thank my thesis committee: Prof. Carlos Simmerling and Prof. Elizabeth Boon for their encouragement, insightful comments, and helpful discussion on my work. I also thank Prof. Carlos de los Santo who kindly served as my outside committee. It is been a pleasure interacting with such great scientists.

Thanks to all past and present group members, Dr. Andisheh Abedini, Dr. Bing Shan, Dr. Hümeyra Taşkent, Dr. Fanling Meng, Dr. Peter Marek, Dr. Shifeng Xiao, Dr. Wenli Meng, Dr. Vadim Patsalo, Dr. Ping Cao, Harris Noor, Hui Wang, Bowu Luan, Ivan Peran, Matt Watson, Rehana Akter, Amy Wong, Natalie Stenzoski, Xiaoxue Zhang, and Yuan Chen for their thoughtful discussion. I greatly enjoyed working with them. In particular, I would like to give my special thanks to Dr. Ping Cao for enlightening me the first glance of research and for collaborating on several projects.

Thank you to all scientists whom I have collaborated with over the years: Prof. Martin T. Zanni and Dr. Arnaldo L. Serrano from University of Wisconsin-Madison for 2D-IR studies; Prof. Steven Kahn, Dr. Sakeneh Zraika and Dr. Daneil Meier from University of Washington for MMP9 studies; Prof. Peter Tessier and Dr. Fanling Meng from Rensselaer Polytechnic Institute for protein domain antibody studies; Prof. Sheena Radford and Lydia Walker for IMS-MS studies.

My sincere thanks also goes to faculty and staff from Department of Chemistry and Department of Biochemistry and Cell Biology, especially to Ms. Kathrine Hughes, Dr. Bela Ruzsicska, and Dr. Susan van Horn who have helped me a lot in the past years. I also thank American Chemical Society Biological Division for travel support.

I am greatly grateful to all my friends in both US and Taiwan for their encouragement and support. Lastly and most importantly, I thank my family and my husband, Benson Su, for their endless love and support. I could not have accomplished this much without your help.

List of Publications

1. Cao, P.; **Tu, L. H.**; Abedini, A.; Levsh, O.; Akter, R.; Patsalo, V.; Schmidt, A. M.; Raleigh, D. P., Sensitivity of amyloid formation by human islet amyloid polypeptide to mutations at residue 20. *J. Mol. Biol.* **2012**, *421* (2-3), 282-295.

2. Cao, P.; Marek, P.; Noor, H.; Patsalo, V.; **Tu, L. H.**; Wang, H.; Abedini, A.; Raleigh, D. P., Islet amyloid: From fundamental biophysics to mechanisms of cytotoxicity. *Febs Lett.* **2013**, *587* (8), 1106-1118.

3. **Tu, L. H.**; Raleigh, D. P., Role of aromatic interactions in amyloid formation by islet amyloid polypeptide. *Biochemistry* **2013**, 52 (2), 333-342.

4. Cao,P.; Abedini A.; Wang H.; **Tu L. H.**; Zhang X.; Schmidt A. and Raleigh, D. P., Islet amyloid polypeptide toxicity and membrane interactions. *Proc. Natl. Acad. Sci. U.S.A.* **2013**, *110* (48), 19279-19284.

5. **Tu, L. H.**; Serrano, A. L.; Zanni, M. T.; Raleigh, D. P., Mutational analysis of pre-amyloid intermediates: The role of His-Tyr interactions in islet amyloid formation. *Biophys. J.* **2014**, *106* (7), 1520-1527.

6. Abedini, A.; Plesner, A.; Cao, P.; Zhang, J.; **Tu, L. H.**; Meng, F.; Middleton, C. T.; Wang, H.; Song, F.; Zanni, M. T.; Verchere C. B.; Raleigh, D. P.; Schmidt, A. M., Islet amyloid induced β-cell death is mediated by RAGE/Amylin intermediates. *Submitted.*

7. **Tu, L. H.**; Noor, H.; Cao, P.; Raleigh, D. P., Aspirin, diabetes and islet amyloid: Reexamination of the inhibition of amyloid formation by Aspirin and Ketoprofen. *ACS Chem. Biol.*, **2014**, *9* (7), 1632–1637.

8. **Tu, L. H.**; Young, L.; Wong, A.; Ashcroft A. E.; Radford, S. E.; Raleigh, D. P., Mutational analysis of the ability of resveratrol to inhibit amyloid formation by islet amyloid polypeptide: Critical evaluation of the importance of aromatic inhibitor and histidine inhibitor interactions. *In preparation*.

Chapter 1. Introduction

A wide range of human diseases arise due to the failure of peptides or proteins to adopt their native conformation, a process generally referred to as protein misfolding. An important subset of these diseases involve amyloid formation. Amyloids are insoluble fibrous protein aggregates formed by a wide range of proteins. Although there is no sequence similarity among amyloid forming proteins, the amyloid deposits all share specific structural features. In certain cases, amyloid fibrils can be functional and beneficial for the biological activity of living organisms. This introduction summarizes the current understanding of the general biophysical principles of amyloid formation and current strategies to prevent amyloid formation. The main focus of this thesis is on the amyloid formation by human islet amyloid polypeptide (IAPP, also known as Amylin), which is an endocrine hormone co-secreted with insulin from pancreatic β-cells and is responsible for islet amyloid deposits in type 2 diabetes.

1.1 General features of amyloid

1.1.1 Amyloid formation and human disease

More than thirty different human diseases have been associated with amyloid deposits including Alzheimer's disease, Parkinson's disease and type 2 diabetes [1-5]. These diseases can be broadly grouped into two forms: systemic and localized amyloidosis. In systemic amyloidosis, aggregation can take place in multiple organs including the liver, kidney, spleen, heart, joints, and muscles. The fibril forming protein is first synthesized by one or more tissues then transported via the blood

to other parts of the body. Localized amyloidosis is usually related to proteins synthesized in a specific organ and deposited within that same organ. General pathological features of amyloidosis include displacement of normal tissues, disruption of their function, and cell death. Diagnosis of amyloidosis is usually via tissue biopsy and treatment depends on the type of amyloidosis, but is often of limited effectiveness. Table 1.1 lists most of the known amyloid forming proteins and their target organs. Most conditions are sporadic (85%), some may be hereditary (10%), or transmissible (5%) [3].

Although the role of amyloids in diseases is not fully clear, cell toxicity via protein aggregation was initially linked to amyloid deposits [6-8]. More recently, studies have suggested that low molecular weight, metastable, soluble oligomers are the primary cause of toxicity [6, 9-16]. For example, the severity of Alzheimer's disease correlates with the level of low ordered oligomers of Amyloid β-peptide (Aβ) rather than with mature Aβ amyloid fibrils [17, 18]. In addition, transgenic mice show defects in cell function and cognitive impairment before accumulation of obvious amyloid plaques [19]. Parkinson's disease, the second most common neurodegenerative disorder, associated with the aggregation of α-synuclein in Lewy bodies, also appears to be involved in toxicity via early aggregates [10, 20]. The pathogenic species are considered to be the transient population present during the process of fibrillization. There is increasing evidence that prefibrillar aggregates from peptides and proteins other than Aβ and α-synuclein can be toxic to the cells or disrupt their function [9, 15, 16, 21, 22]. These intermediates might have interactions with cell membranes and perturb the integrity of lipid bilayers, ultimately leading to cell death [23-26]. However the mechanisms of toxicity are not known and other mechanisms of cellular toxicity, including caspase-mediated apoptosis, oxidative stress and generation of reactive oxygen species are also considered to be associated with oligomers [9, 27, 28].

1.1.2 The structure of amyloid fibrils

Amyloid fibrils are constructed from a number of protofilaments and have a characteristic highly ordered cross-β-sheet structure, in which a core of β-strands is aligned perpendicularly to the fibril axis and form extended regular β-sheets. These protofilaments pack together in a helical manner to form rope-like fibrils that are typically 10-20 nm wide [5, 29-31] (Figure 1-1). These fibrils have the ability to bind dyes such as thioflavin-T (ThT) and Congo red (CR) and can be imaged *in vitro* using transmission electron microscopy (TEM) or atomic force microscopy (AFM) [32-34].

The molecular details of amyloid fibril structures are not fully understood due to their poor solubility, large size and the noncrystalline nature of fibrils. Recently, however, the use of solid-state NMR [35-37] and X-ray crystallography [38, 39] have allowed considerable progress in the understanding of amyloid fibril structures. For example, a structure model of $A\beta_{1-40}$ has been proposed based on constraints from solid-state NMR studies and measurement of the mass-per-length from electron microscopy [35]. In this model, residues 12-24 and 30-40 form the core region of the fibrils with a β-strand conformation. These strands are connected by the loop consisting of residues 25-29, suggesting that a single cross-β unit comprises a two layered β-sheet structure. A simple $A\beta_{1-40}$ protofilament consists of two $A\beta_{1-40}$ cross-β units, and the width of the resulting four β-sheets is ~10 Å, as determined by scanning transmission electron microscopy (STEM). The other significant approach to define the structure of amyloid fibrils is to determine the structure microcrystals of amyloid-forming fragments. Until now, more than thirty such segments from 14 different proteins have been identified by Eisenberg and co-workers [40-42]. These segments form three-dimensional crystals that are believed to contain some of the features that are key characteristics of amyloid fibrils. In the case of the yeast prion protein Sup35, the segment

GNNQQNY forms both amyloid-like fibrils and closely related microcrystals, the latter which can be utilized to reveal the atomic structure by X-ray crystallography [40]. The structure of GNNQQNY consists of a pair of β-sheets that interact with each other through the side chains of Asn-2, Gln-4, and Asn-6 forming a tight and dry interface. More importantly, the inter-sheet spacing of microcrystals formed by amyloid-forming fragments, in general, matches the fibril patterns determined by X-ray fiber diffraction (~ 4.8 Å). Fragments of IAPP corresponding to the sequences NNGFAIL and SSTNVG have been crystallized and their structure are solved by Eisenberg's group. This has led to a model for the IAPP fibrils which differs somewhat from NMR study derived model. In Eisenberg's model, the β-sheets are made up of residues 8-18 and 23-37. These studies suggest that many amyloid fibrils could have core structures with similar features [30].

1.1.3 Mechanism of amyloid formation

The kinetics of amyloid formation are complex and difficult to describe due to the lack of structural information for all of the transition states and due to the lack of information about possible multiple pathways and heterogeneous oligomers. However, it is thought, based on experimental evidences that amyloid fibril formation occurs via a nucleation-dependent polymerization mechanism [43-45]. The formation of amyloid fibrils involves three distinct detectable phases (Figure 1-2). (i) The initial lag phase, which is theorized to be the time required for monomers to form an active nucleus, followed by (ii) an exponential fibril growth phase. Fibril growth is thought to occur rapidly by the addition of either monomers or oligomers to the nucleus. Finally, (iii) a saturation phase is reached in which the amyloid fibrils are in equilibrium with soluble peptides. In such a nucleation-dependent mechanism, preformed amyloid fibrils can promote further aggregation without nucleation. Therefore, the lag phase can be shortened or

entirely abolished when the "seeds" are added at the beginning of fibrillization. The seeding reaction is generally specific and its efficiency decreases dramatically as the sequence or fibril structure diverges between seeds and peptide monomers [46]. Secondary nucleation is also important for amyloid formation. Secondary nucleation pathways are usually defined as fragmentation, with a rate depending only upon the concentration of existing fibrils, or heterogeneous secondary nucleation which depends on both the concentration of monomers and existing fibrils [43, 47, 48]. In the latter case, the surface of already formed fibrils acts to catalyze formation of additional fibrils.

1.1.4 Inhibition of amyloid formation

As noted earlier, amyloid formation has been studied for years and more than thirty human proteins can form amyloid deposits that are associated with diseases. Many amyloid diseases are neurodegenerative and affect the elderly population. Others contribute to common disorders such as type 2 diabetes. Therefore, there is increasing interest in amyloid research. Methods used to inhibit amyloid induced cytotoxicity and protein aggregation have drawn considerable attention. Several of the recently developed strategies will be discussed below.

In some cases, small molecules have been designed to stabilize the native folded state of a protein and inhibit unfolding and aggregation. This approach is promising for proteins that have to undergo an unfolding transition to initiate amyloid formation. For example, transthyretin (TTR) is a tetrameric serum carrier of the thyroid hormone. The dissociation of the TTR tetramer is believed to be rate-limiting for amyloid fibril formation under moderately acidic conditions [49, 50]. A TTR mutation, which is associated with familial amyloid polyneuropathy (FAP), exhibits an enhanced rate of amyloid formation due to tetramer destabilization [50, 51]. The compound

tafamidis meglumine was rationally designed to stabilize the TTR tetramer and has been brought into clinical trials and approved for use in Europe [52, 53].

A large number of synthetic compounds, natural products and peptide-based inhibitors have been shown to inhibit the formation of amyloid fibrils by some proteins. Polyphenol compounds including curcumin, resveratrol, morin hydrate, epigallocatechin gallate (EGCG) and tannic acids are inhibitors of amyloid formation [54-56]. EGCG, a compound present in green tea, is notable for being an effective inhibitor of amyloid formation by Aβ, islet amyloid polypeptide (IAPP), α-synuclein, a fragment of prostatic acid phosphatase (PAP 248-286) and κ-casein [54, 55, 57-61]. In addition, EGCG is able to disaggregate preformed fibrils, which may be beneficial in the biological clearance of aggregates. EGCG is thought to act by diverting proteins into non-toxic off pathway aggregates [57, 60, 61]. The phenolic compound resveratrol, found in red wine, has also been shown to be effective against Aβ and IAPP amyloid fibril formation [62-65]. It is suggested to be able to remodel Aβ soluble oligomers and amyloid fibrils into high molecular weight aggregates that are unstructured and non-toxic [62]. Resveratrol can also inhibit lipid membrane-induced IAPP fibrillogenesis and keep intact cell morphology [65].

The development of peptide-based inhibitors of amyloid formation is another active field of research. The approaches for rational design of inhibitors include amino acid substitutions and side chain modifications of amyloidogenic regions, proline insertion, modification of the peptide termini or peptide backbone, use of D-amino acids, and synthetic α-helix mimetics to target amyloid intermediates [66]. Many side chain substitutions and modifications have focused on the central hydrophobic region of Aβ, the LVFFA motif [67, 68]. Replacement of the central Phe residues of $A\beta_{1-40}$ by Thr abolishes fibril formation [67]. Moreover, an octapeptide derived from

this region, QKLVTTAE, can be used as an inhibitor for native $A\beta_{1-40}$ [69]. Proline residues are unfavorable in β-sheets because of their rigid structure and a lack of the amide hydrogen needed for the hydrogen bonding found in β-sheets. Many studies have shown that substitution of Pro reduces fibril-forming capacity [70-73]. The point mutants I26P and G24P of human IAPP are both non-amyloidogenic and the combination of two mutant peptides can yield a highly effective inhibitor of IAPP and Aβ amyloid formation [74]. Rat IAPP, which differs from the human IAPP at six of the 37 positions, does not form amyloid fibrils and inhibits, albeit moderately, amyloid formation by human IAPP. There are three proline residues in the rat IAPP sequence while human IAPP has none. Substitution of Pro at key residues is likely the major reason for the non-amyloidogenicity of rat IAPP in comparison to human IAPP [73]. *N*-methyl amino acids can also prevent protein aggregation by destabilizing hydrogen-bonding interactions between individual β-strands [75-77]. A double *N*-methylated full length IAPP analog [(N-Me)G24, (N-Me)I26]-IAPP was designed for IAPP inhibition studies. This IAPP variant is highly soluble, nonamyloidogenic in homogeneous solution, noncytotoxic and blocks human IAPP amyloid formation and human IAPP induced cytotoxicity in cell culture [76]. Recent findings have suggested that the helical oligomeric intermediates may be the relevant cytotoxic species in IAPP and Aβ amyloid formation and helix-helix association may promote the formation of early β-sheet structures [9, 78, 79]. Thus, a series of pentameric pyridylamides and benzamides were synthesized as helical mimetics in order to target the transient helical intermediates in IAPP amyloid formation [80].

The design of inhibitors based on the amyloid fibril structure has also been developed recently. To date, the most detailed structural information of amyloid fibrils was determined by Eisenberg's laboratory. They designed inhibitors based on the crystal structures of protein segments to cap fibril ends and impede fibril growth. So far, two non-natural amino acid peptide inhibitors have

been described: the D-TLKIVW peptide inhibitor significantly delayed amyloid formation by the tau protein fragment and Trp-His-Lys-chAla-Trp-hydroxyTic hexapeptide containing Ala and Tyr/Pro derivative greatly reduced PAP 248-286 fibril mediated HIV infection [81]. Nowick's group designed macrocyclic β-sheet peptides which comprise two anti-parallel β-strands to prevent IAPP amyloid formation. One strand of the macrocycles contains a heptapeptide sequence derived from IAPP and the other stand contains an unnatural amino acid to avoid forming external hydrogen bonds. The heptapeptide in the macrocycles is designed to bind fibril β-sheets and the other strand can prevent fibril growth. Similar macrocycles also have been used to study the aggregation of other amyloidogenic proteins [82].

1.2 Islet amyloid polypeptide (IAPP)

1.2.1 Biosynthesis of IAPP

IAPP is a member of the calcitonin related peptide family and is similar in sequence and somewhat similar in biological activity to calcitonin gene-related peptide (CGRP). IAPP is initially expressed as an 89 residue pre-proprotein containing a 22 residue signal peptide which is cleaved in the endoplasmic reticulum (ER) [83, 84]. ProIAPP and proinsulin are both further processed by prohormone convertases PC2 and PC1/3, and by carboxypeptidase E (CPE) in the Golgi and in the secretory granules. PC2 cleaves proIAPP between Lys10 and Arg11, and PC1/3 cleaves between Lys50 and Arg51 [85, 86]. This numbering refers to the proIAPP sequence. CPE removes two basic amino acids that remain at the C terminus [87]. PC2 can process proIAPP at the C-terminal cleavage site in the absence of PC1/3, but less effectively [88]. The resulting peptide, which contains a C-terminal glycine residue, is converted by peptidylglycine alpha-amidating

monooxygenase (PAM) to produce an amidated C-terminus [89]. Mature IAPP also contains a disulfide bond between the two cysteine residues (Figure 1-3). Some studies have suggested that both the intramolecular disulfide bond and C-terminal amidation are necessary for full biological activity [90].

IAPP is stored and co-secreted with insulin in the secretory granules of the islet β-cells. The concentration of IAPP in the granule is in the millimolar range and is about 1-2% that of insulin [91]. The low pH environment and partially crystalline state of insulin are thought to prevent IAPP amyloid formation, even at such high concentrations, since the rate of IAPP fibril formation is highly pH dependent and insulin can act an inhibitor of IAPP aggregation [92-95]. The physiological role of IAPP is not completely clear, but it is believed to be involved in the regulation of glucose metabolism [96-98]. IAPP was found to be a potent inhibitor of glycogen synthesis in rat skeletal muscle [99] and was also shown to inhibit insulin-stimulated glucose transport *in vitro* [100]. In addition, IAPP also has been shown to dose-dependently reduce food intake and body weigh in animal models [101]. The peptide is also found in the brain and is believed to play a role in appetite control [102].

1.2.2 IAPP amyloid formation and type 2 diabetes

Pancreatic islet amyloid is a characteristic pathological feature of type 2 diabetes and IAPP is the major component of the amyloid deposits [103-105]. More than 80% of patients suffering from diabetes are found to have amyloid in the islets of Langerhans. However, the deposits have also been detected in healthy individuals [106-108]. Initially, it was thought that amyloid deposits discovered in the pancreas were composed of carbohydrates as they were stained by a dye used to stain starch [109]. Later it became apparent that amyloid deposits contain protein fibrils in which

the constituent proteins stack and adopt a β-sheet structure. In 1987, two groups independently identified the sequence of the component of islet amyloid, a 37 residue pancreatic hormone, encoded by a single copy of gene located on human chromosome 12 [104].

Islet amyloid is not the cause of type 2 diabetes, but IAPP contributes to β-cell dysfunction, cell death and the loss of β-cell mass [110-112]. It was first shown that IAPP is cytotoxic when added to islet cells in 1994 [110]. In order to investigate the role of IAPP and islet amyloidosis in type 2 diabetes, several groups have generated transgenic mice that carry the human IAPP gene in their chromosomal DNA. These groups have demonstrated that human IAPP transgenic mice can develop islet amyloid and hyperglycemia [113, 114]. Rapid amyloid formation also likely plays a role in the failure of pancreatic islet transplants. Amyloid deposits can be detected rapidly in diabetic mice transplanted with human islets [115]. Clinical trials with islet transplantation were not successful because, overall, only 10% of islet recipients can maintain normoglycemia without insulin therapy [116]. There was a progressive loss of the grafted β-cells in most of the subjects and widespread amyloid deposits were found in their implanted islets (Figure 1-4) [117, 118]. Xenotransplantation of islets using pigs or other animals which do not develop amyloid would be an attractive alternative for human diabetes, since porcine islets have been shown to have better glycemic maintenance in mice recipients and to prolong islet graft survival [119]. More recent findings have suggested that the process of IAPP amyloid formation or IAPP oligomeric intermediates, rather than mature amyloid fibrils, is toxic to cells [24, 120, 121]. A range of mechanisms have been proposed for IAPP induced β-cell toxicity. These include cell membrane permeabilization or disruption, formation of nonspecific ion channels, defects in autophagy, ER stress, localized islet inflammation, as well as activation of signaling pathways that regulate β-cell

apoptosis [122-128]. Research is underway for a better understanding of the mechanisms of IAPP toxicity and the literature is continually updated. For recent review see [129, 130].

1.2.3 Structural models of IAPP amyloid fibrils

IAPP amyloid fibrils consist of cross β-strands and have been characterized by circular dichroism (CD), two dimensional infrared spectroscopy (2D-IR), electron paramagnetic resonance spectroscopy, NMR and X-ray diffraction [131, 132]. However, an exact structural model of the IAPP monomer in its fibrillar state is still unclear. Two atomic level models have been proposed for IAPP amyloid fibrils [37, 133] and they have some common features (Figure 1-5). Both suggest that protofibrils are made up of two columns of IAPP monomers which adopt a U-shaped structure. Each polypeptide contains two regions of β-sheets that are linked by a loop. The first seven residues, containing the disulfide bond, are disordered. One of the models built by Dr. Tycko's group is based on solid-state NMR studies [37]. They used STEM to determine the mass-per-length value of the protofilament, and performed solid state NMR measurements on a series of isotopically labeled samples to obtain structural constraints on the fibril conformation. In this model, residues 8-17 and residues 28-37 form β-sheets (Figure 1-5). Another model developed by Prof. Eisenberg's group is based on X-ray crystallographic studies of small peptide fragments (Figure 1-6) [133]. They crystallized two fragments derived from IAPP and determined their atomic structure. The peptides studied were NNFGAIL corresponding to residues 21-27 and SSTNVG corresponding to residues 28-33. The SSTNVG fragment was chosen as the center core of their model because the intersheet distance most closely matches experimental fiber diffraction patterns [129]. In Eisenberg's model, two β-strands are composed of residues 8-17 and residues 23-37. The main difference between these two models lies in the details of side chain packing.

As discussed earlier, rat IAPP which does not form amyloid fibrils differs from human IAPP at only six of the 37 positions. Studies of human and rat IAPP have implied the 20-29 region as a critical amyloidogenic domain that modulates the properties of the entire sequence [73, 134, 135]. Interestingly, the 20-29 region is not part of the β-sheets in either model. This may suggest that the loop region is important for the kinetics of amyloid formation, even if it is not part of the β-sheet structure. Indeed, the only naturally occurring human IAPP mutation, S20G, is found in this region and may be associated with early onset type 2 diabetes in a small fraction of East-Asian population [136-138]. The Ser to Gly substitution of residue 20 dramatically accelerates IAPP amyloid formation, while a Ser to Lys substitution significantly slows amyloid formation [137].

1.2.4 Residue specific effects on IAPP amyloid formation

IAPP is conserved through evolution and has been characterized in mammals, birds, and fishes [139-141]. Not all species form islet amyloid: mouse, rat and canine do not form islet amyloid fibrils, whereas human, monkey and felines do. The ability to form amyloid is likely correlated with the primary sequence of IAPP. Mouse and rat IAPP contain three Pro residues at positions 25, 28 and 29, while the human and monkey sequences do not include any Pro. The Pro substitutions present in the mouse/rat IAPP sequence make it difficult to form amyloid fibrils since Pro is a well-known β-sheet breaker. Porcine and ferret IAPP also form amyloid fibrils, but are much less amyloidogenic than human IAPP (Figure 1-7) [128, 142].

A number of mutational studies have provided insight into the interactions involved in amyloid formation. However, it is difficult to compare experimental data as amyloid formation is sensitive to changes in buffer composition, pH, salt concentration, temperature and the presence of organic co-solvents. The rate of IAPP amyloid formation, for example, is strongly pH-dependent.

Aggregation of IAPP is considerably faster at high pH when His-18 and the N-terminus are deprotonated [93, 143]. Some studies have used 1-2% (v/v) hexafluoroisopropanol (HFIP) as a co-solvent. HFIP has been reported to significantly accelerate the rate of amyloid formation even at a low concentration [144]. Ionic strength and the choice of anion are also important factors that affect IAPP amyloid formation [145]. Another complexity is that truncated 8-37 IAPP is used in some of these studies.

Even though these mutational studies of amyloid formation contain many potential complications, they still provide a valuable data set. Here we summarize the available data from the studies using full length IAPP or 8-37 IAPP with an amidated C-terminus (Table 1-2) [71, 74, 133, 137, 143, 146-152]. Many studies have focused on the region between residues 20 and 29. Non-amyloidogenic rat IAPP contains three Pro residues in this region, so this region was thought to dictate amyloidogenic properties of IAPP. However, multiple Pro substitutions outside of this region have been shown to abolish human IAPP amyloid formation [150]. In contrast, single amino acid substitution of rat IAPP at residue 18 by the residue present in human IAPP can induce rat IAPP to form amyloid fibrils [153]. Therefore, the role of the 20-29 region in controlling IAPP's amyloidogenicity is still ambiguous.

Aromatic-hydrophobic and aromatic-aromatic interactions have been proposed to play a critical role in amyloid formation [135], but work from our own laboratory shows they are not required. Replacement of all three aromatic residues with Leu alters the rate of amyloid formation, but does not abolish the ability of IAPP to form amyloid fibrils [146]. A more detailed discussion of the role of aromatic residues is presented in Chapter 2.

Some of the studies focus on the examination of the putative helical regions of IAPP. A model for early stage of IAPP aggregation has been proposed. IAPP was found to adopt α-helical structure from residues 8-18 and residues 22-27 when IAPP was fused to maltose binding protein (MBP) and residue 15 was suggested to make important contacts when IAPP dimerized [151]. Therefore, a number of substitutions near residue 15 have also been examined. Ser, Ala and Asp substituents which are predicted to enhance helix association increased the rate of amyloid formation. Conversely, the substitution of Phe with Lys, decreased the rate of amyloid formation, which can be rationalized by this model, since the positive charge can disrupt the helical interface.

The role of amide side chain interactions in amyloid formation by IAPP was tested using the same strategy. Five of the asparagine side chains in truncated 8-37 IAPP were individually mutated and the effects on the rate of amyloid formation were determined. The authors found that different sites have drastically different impact on amyloid kinetics. Position 14 and 21 are considered more critical to amyloid formation [152].

1.2.5 Oligomeric intermediates in IAPP amyloid formation

The importance of on-pathway low order oligomers in IAPP amyloid formation is unclear, although they have been suggested to be the primary toxic species during aggregation [113, 154]. Identifying the size or structure of oligomeric intermediates in IAPP amyloid formation is difficult due to their fast conversion. Conventional biophysical techniques including CD, FTIR spectroscopy, and fluorescence-based assays are able to provide information on the protein's global conformation, but provide limited detail on specific region of proteins. As a result, these methods are not helpful for the study of oligomers in amyloid formation. Some studies have used the conformation-specific antibody A11 to detect oligomers [155, 156]. Immunoreactive A11 was

first widely used in Aβ and polyQ oligomerization, but its specificity for IAPP oligomers has not been fully determined. Artifact associated with use of this antibody are discussed in [15, 157]. Analytical ultracentrifugation and ^{19}F NMR studies have also failed to detect low order oligomers for human IAPP [158, 159]. In contrast, studies using photo-induced cross-linking and ion mobility spectrometry-mass spectrometry (IMS-MS) have identified oligomeric states, ranges from monomer to hexamer [160-161]. To date, several models for early oligomers have been proposed (Figure 1-8) and are summarized below [82, 151, 160, 163].

Helical intermediates may be important for IAPP amyloid formation. A number of experiments suggest that IAPP amyloid formation may involve a helical intermediate *in vitro* [78, 80, 151, 164]. Formation of helical intermediates could be advantageous for the formation of intermolecular β-sheets, because the helix association of N-terminal regions of IAPP would lead to a high local concentration of the amyloidogenic C-terminal regions [78, 165]. Eisenberg and coworkers proposed a model in support of this hypothesis based on their crystallographic studies. They solved the crystal structure of human IAPP fused to MBP and found a helix-helix homo-dimerization interface between two MBP-IAPP fusion proteins [151].

The use of IMS-MS and molecular dynamics (MD) modeling has led to a different model for early IAPP intermediates. This model suggests that IAPP dimers are assembled from β-hairpin-like monomers and that the β-strand is generally more stable and favorable than the helix in the formation of a dimer interface. Therefore, the model proposes that β-sheet rich oligomers are formed by direct side-by-side assembly of β-hairpin monomers [160]. However, the β-hairpins have all the hydrogen bonds within one monomer, but the fibrils have all the hydrogen bonds between monomers. Thus there will be a huge energetic penalty to rearrange the hairpins.

Another model for early intermediates proposes an antiparallel stable dimer generated by stacking of the His-18 and Tyr-37 side chains and is based on NMR studies conducted under acidic conditions using a recombinant form of IAPP [163]. However, this variant has a free C-terminus rather than physiologically relevant C-terminus. This leads to an obvious question: Is the His-Tyr interaction still present in the biologically relevant version of human IAPP with an amidated C-terminus? The role of His-Tyr interactions and the C-terminus in IAPP amyloid formation are described in more detail in Chapter 4.

A recent study based on 2D IR proposes a new model [82]. This model suggests that an oligomeric intermediate with parallel β-sheet forms during the lag phase of IAPP amyloid formation. Interestingly the β-sheet is found in a region that does not form β-sheet in the models of the fibrils. The authors observed the structural evolution from initial β-sheet to partially disordered loop for the region of IAPP residues 23-27 (FGAIL). This model might help to rationalize some mutational studies in this region. Breakage of the intermolecular FGAIL β-sheet intermediates could lead to a large energy barrier before fibril growth. Moreover, IAPP samples for these spectral measurements were prepared at much higher concentration compared to that used in other studies. It is not known whether IAPP at high concentration still follows the same pathway of fibrillization.

1.3 Figures

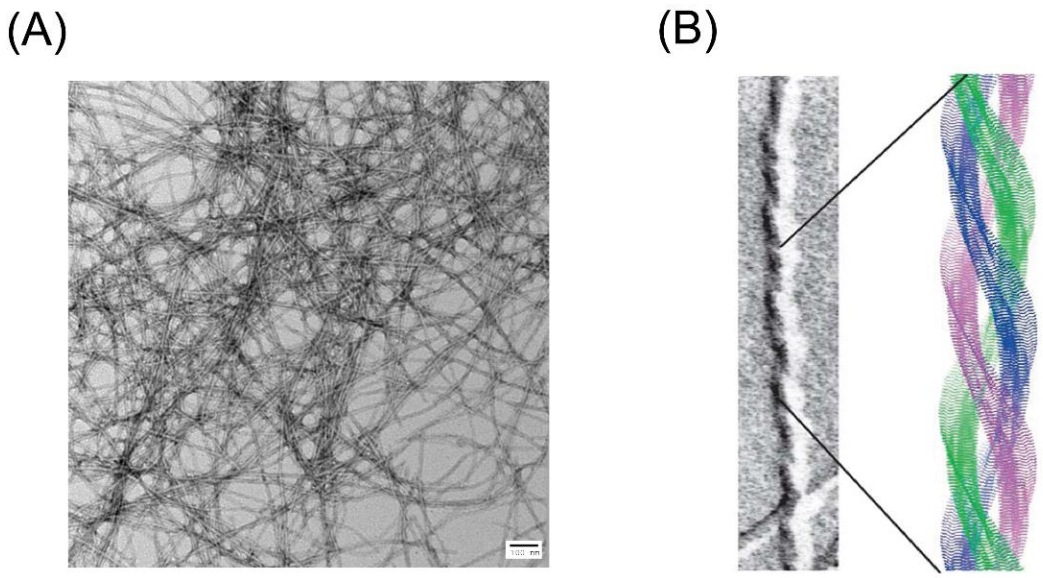

Figure 1-1: Structure and model of amyloid fibrils. (A) TEM image of amyloid fibrils formed by synthetic human IAPP *in vitro*. Scale bar represents 100 nm. This image was collected by the author. (B) The image on the right is a model of amyloid fibrils in which three protofilaments pack together in a helical manner. Figure is taken from reference 29.

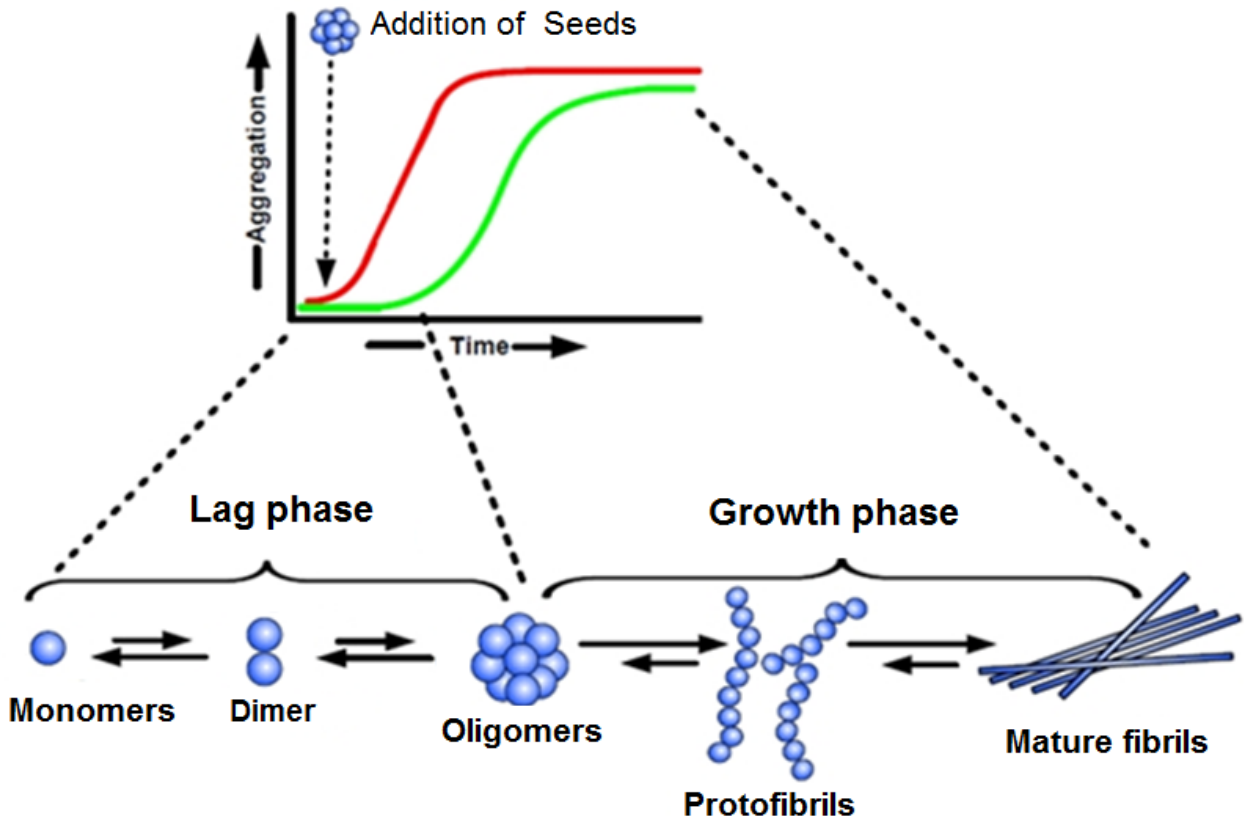

Figure 1-2: A nucleation-dependent polymerization model of amyloid aggregation. The kinetics of amyloid formation is represented by a sigmoidal curve. A lag phase which involves the formation of active seeds is followed by a rapid growth phase during which fibrils are formed (green curve). The rate limiting step in this process is the formation of seeds to promote aggregation. The lag phase can be bypassed by the addition of preformed seeds (red curve). Figure is taken from reference 166.

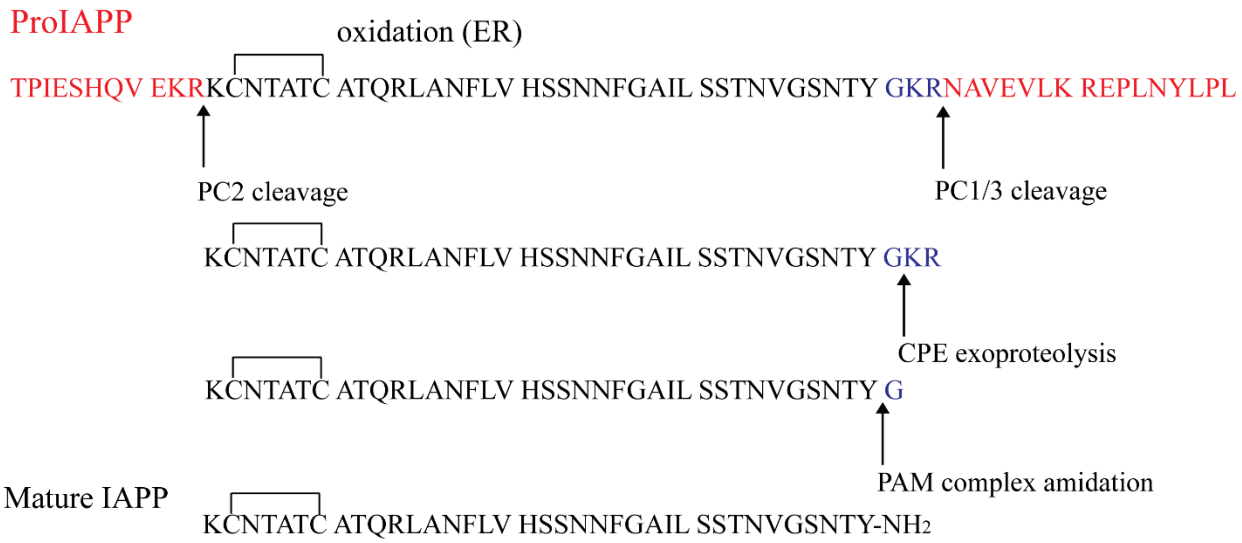

Figure 1-3: The processing of ProIAPP to mature IAPP in the Golgi and in the secretory granules of the islet β-cells. The major cleavage sites in each step are indicated by black arrows. Mature IAPP contains a disulfide bond and amidated C-terminus and both are important for IAPP's biological function.

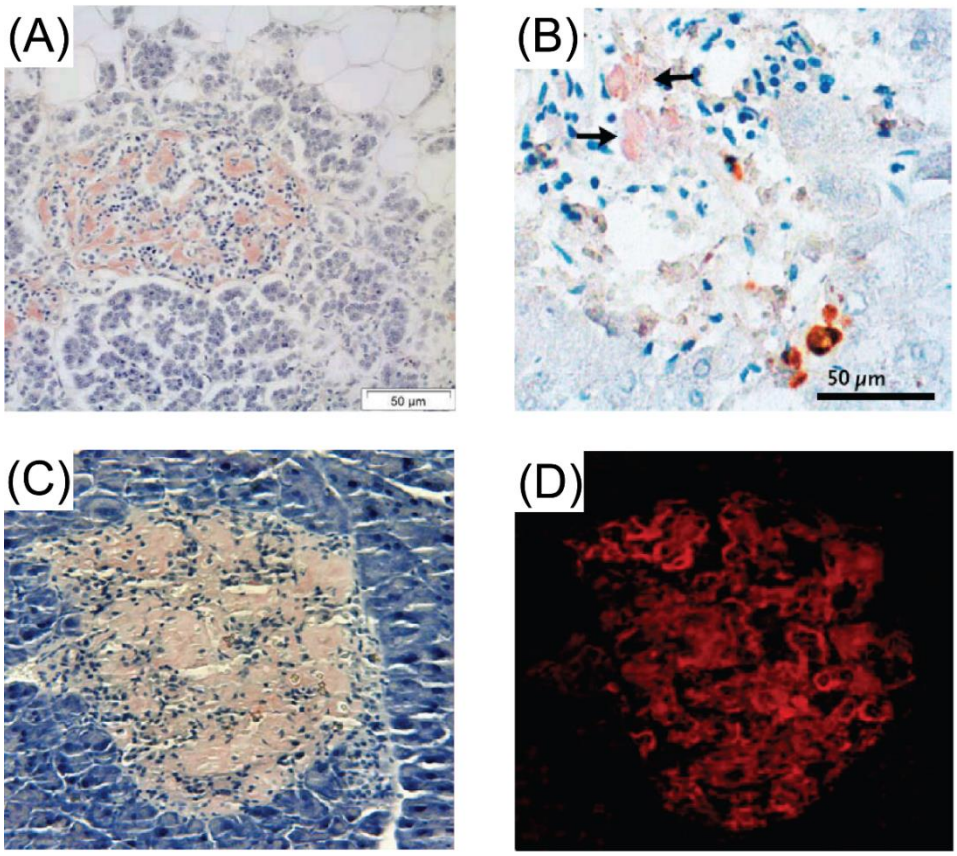

Figure 1-4: Pancreatic islet cells with extracellular amyloid deposits. (A) Typical amyloid deposits seen in a human type 2 diabetic islet stained pink. The section was stained for amyloid with Congo red. (B) Amyloid deposits are found in transplanted islets in a patient with type 1 diabetes (arrows). (C) The presence of amyloid is detected with Congo red in the islet of a human IAPP transgenic mouse. The Congo red stained amyloid is visible as pink deposits. (D) Image was obtained from the same pancreatic islet section as figure (C), but fluorescence microscopy was applied for better visualization (bright red). Figure is adapted from references 96, 126, and 127.

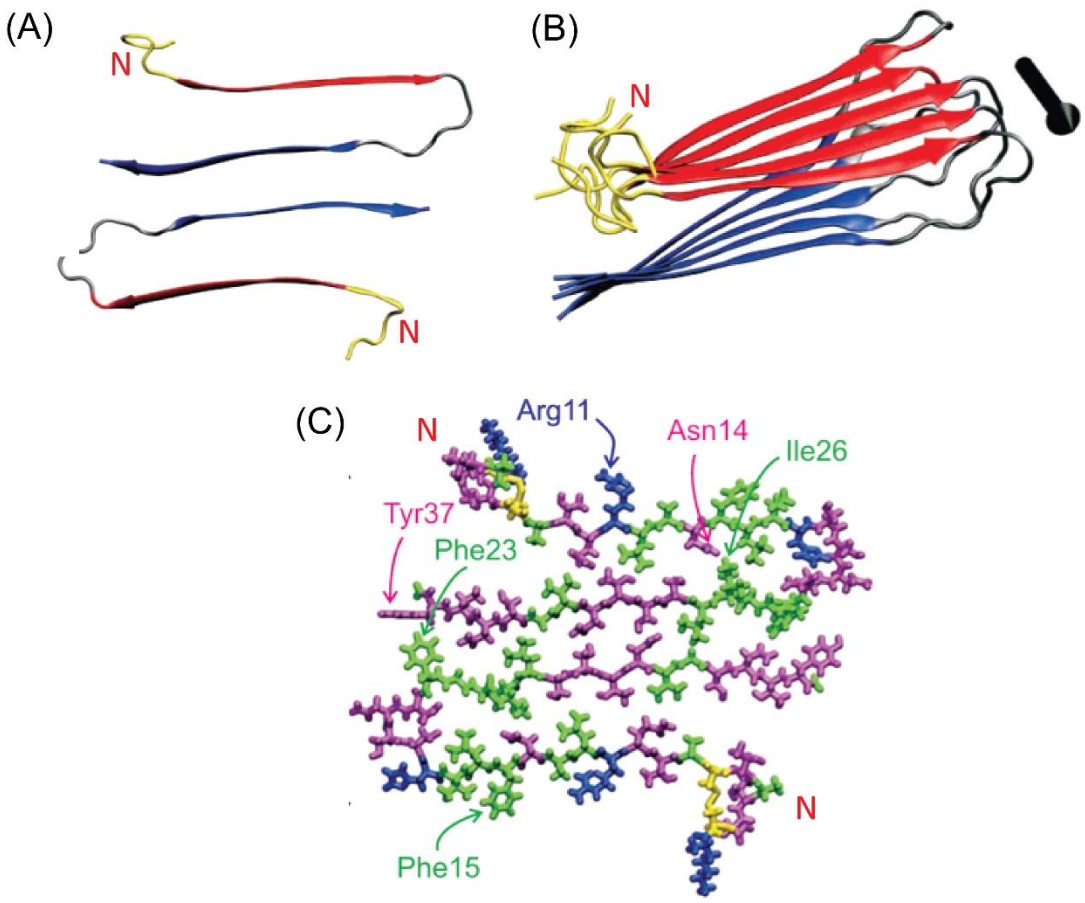

Figure 1-5: An atomic level model proposed for IAPP amyloid fibrils based on solid state NMR. (A) IAPP protofibrils consist of two columns of IAPP monomers and each polypeptide contains two β-sheet regions. (B) In register, parallel β-strands run perpendicular to the fibril axis as indicated by an arrow. N- and C-terminal β-strands segments are colored in red and blue respectively. Note the mainchain hydrogen bonds are between different IAPP molecules, not within one molecule. (C) All atom representations of this model are shown, with hydrophobic residues colored in green, polar residues colored in magenta, positively charged residues colored in blue, and disulfide-linked cysteine residues colored in yellow. The N-terminus is labeled in each figure. Figure is adapted from reference 37.

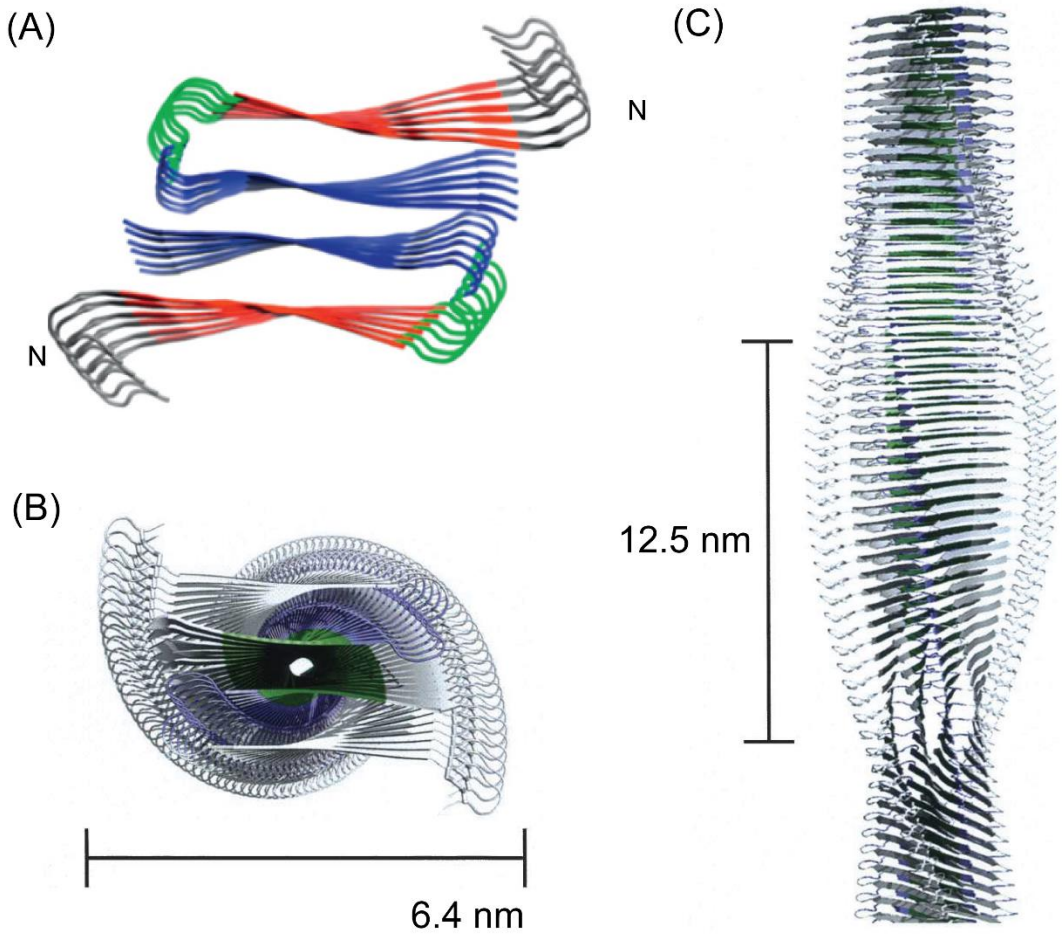

Figure 1-6: Atomic level model proposed for IAPP amyloid fibrils based on the crystal structure of two IAPP fragments, NNFGAIL and SSTNVG. (A) Residues 8-17, colored in red, and residues 23-37, colored in blue, form intermolecular β-sheets. (B) View down the axis of the fibril model with a diameter 64 Å. The residues are shown in green for SSTNVG. (C) View perpendicular to the axis of the fibril model with a length of 125 Å (4.8 Å per layer). Figure is adapted from reference 133.

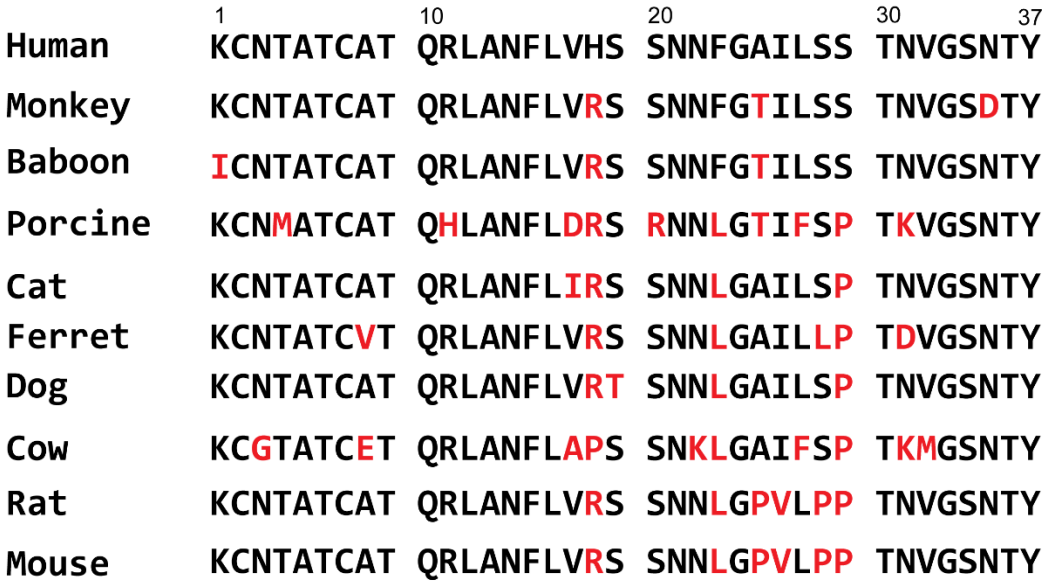

Figure 1-7: Primary sequence of IAPP from different species. Residues that differ from human IAPP are colored in red. The first six species (human to ferret) can develop islet amyloid and type 2 diabetes. Rats and mice do not develop islet amyloid. Cats, but not Dogs have been reported to form amyloid in vivo. All of the variants contain a disulfide bridge between residues 2 and 7 and have an amidated C-terminus.

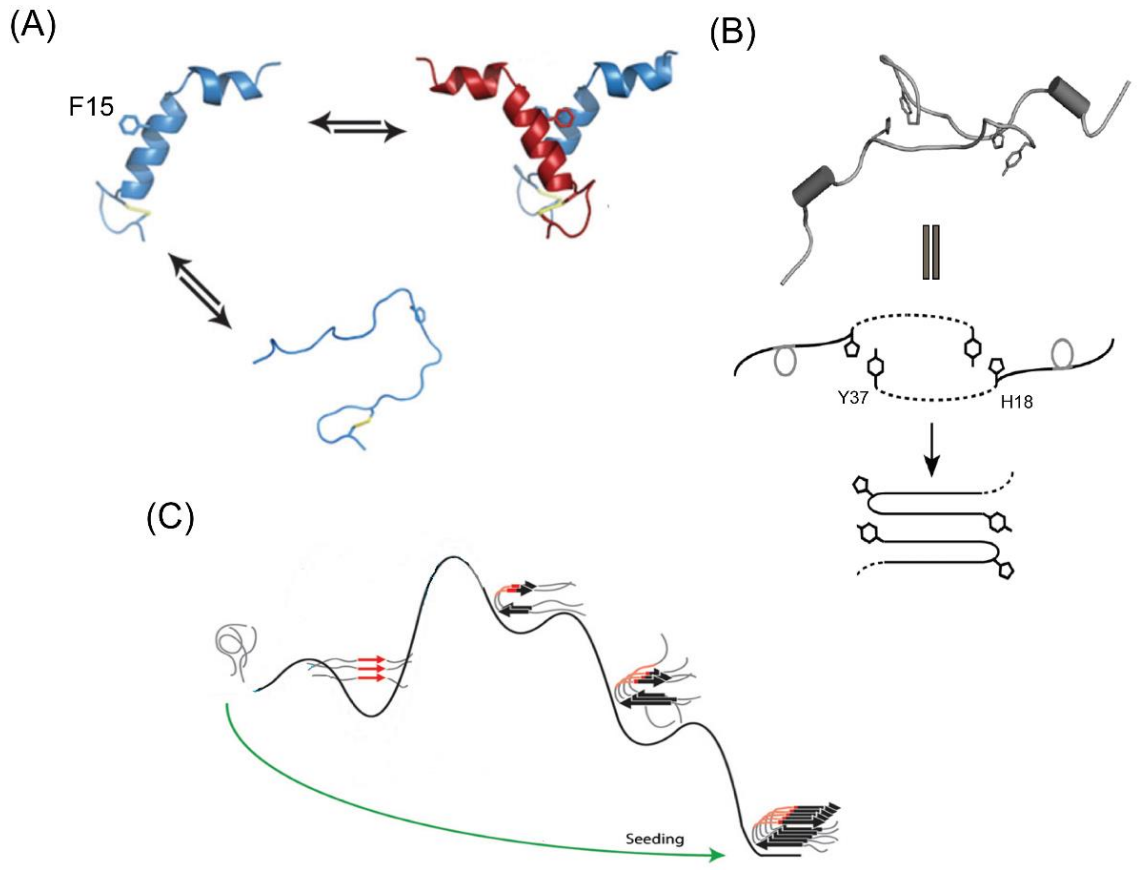

Figure 1-8: Models of IAPP oligomerization. (A) One model was proposed based on the crystal structure of a maltose binding protein-IAPP fusion protein. An ordered helical conformation of the IAPP monomer and dimerization were observed in the crystal. Phe 15 was suggested to be the key residue responsible for association [151]. (B) NMR studies suggest that stable dimers with antiparallel orientation of monomers were stabilized by stacking of His-18 and Tyr-37 [163]. This studies were carried out with a non-physiological variant with a free C-terminus. (C) A free energy landscape for IAPP aggregation is illustrated based on 2DIR studies. Reside 23-27, highlighted in red, were observed to form parallel β-sheets in the lag phase. The main free energy barrier during IAPP aggregation occurs during the transition of this β-sheet into the turn region in the IAPP fibrils [82]. Figure is adapted from references 82, 151, and 163.

1.4 Tables

Fibril protein	Precursor protein	Systemic and/or localized	Target organs
AL	Immunoglobulin light chain	S,L	All organs except CNS
AH	Immunoglobulin heavy chain	S, L	All organs except CNS
Aβ2M	β2-microglobulin, wild type	L	Musculoskeletal system
	β2-microglobulin, variant	S	ANS
ATTR	Transthyretin, wild type	S, L	Heart mainly in males, Tenosynovium
	Transthyretin, variants	S	PNS, ANS, heart, eye, leptomen.
AA	(Apo) serum amyloid A	S	All organs except CNS
AApoAI	Apolipoprotein A I, variants	S	Heart, liver, kidney, PNS, testis, larynx (C terminal variants), skin (C terminal variants)
AApoAII	Apolipoprotein A II, variants	S	Kidney
AApoAIV	Apolipoprotein A IV, wild type	S	Kidney medulla and systemic
ALys	Lysozyme, variants	S	Kidney
AFib	Fibrinogen α, variants	S	Kidney, primarily
ACys	Cystatin C, variants	S	PNS, skin
Aβ	Aβ protein precursor	L	CNS
APrP	Prion protein, wild type	L	CJD, fatal insomnia
	Prion protein, variants	L	CJD, GSS syndrome, fatal insomnia
ACal	(Pro)calcitonin	L	C-cell thyroid tumors
AIAPP	Islet amyloid polypeptide	L	Islets of langerhans, insulinomas
AANF	Atrial natriuretic factor	L	Cardiac atria
APro	Prolactin	L	Pituitary prolactinomas, aging pituitary
AIns	Insulin	L	Iatrogenic, local injection

Table 1.1: List of part of known extracellular fibril proteins in human. Table is taken from reference 5.

(A) Human IAPP	KCNTATCATQRLANFLVHSSNNFGAILSSTNVGSNTY	
I26P [71, 74]	----------P----------	X
G24P [71, 74]	----------P----------	X
3XL [146]	----------L-------L----------L	▼
S20G [137]	----------G----------	▲
S20K [137]	----------K----------	▼
Pramlintide, V25P S28P S29P [147]	----------P--PP--------	X
S28G[148]	----------G---------	X
I26D[148]	----------D----------	X
A13E[148]	----------E----------	X
L16Q[148]	----------Q----------	X
F15L[149]	----------L----------	▲
F23L[149]	----------L----------	▼
Y37L[149]	----------L	▼
F15LF23L[149]	----------L-------L----------	▼
F15LY37L[149]	----------L----------L	▼
F23LY37L[149]	----------L----------L	▼
F15NLe[149]	----------X----------	▼
F15I [149]	----------I----------	▼
F15TLe[149]	----------X----------	▼
H18Q[143]	----------Q----------	▲
H18L[143]	----------L----------	▲
(B) 8-37 IAPP	ATQRLANFLVHSSNNFGAILSSTNVGSNTY	
3XP [150]	---------P-P---------P--------	X
H18R [133]	----------R----------	—
F23L [133]	----------L----------	▼
H18RF23L [133]	----------R----L----------	▼
H18RS28PS29P [133]	----------R---------PP--------	X
H18RF23LA25PI26V [133]	----------R----L-PV----------	X
F15S [151]	-------S----------	▲
F15A [151]	-------A----------	▲
F15D [151]	-------D----------	▲
F15K [151]	-------K----------	▼
V17A [151]	---------A----------	▲
V17K [151]	---------K----------	—
N14A [152]	------A----------	X
N14L [152]	------L----------	X
N14S [152]	------S----------	X

N21L [152]	----------L----------	X
N21S [152]	----------S----------	X
N22L [152]	----------L----------	—
N31L [152]	----------L------	▼
N35L [152]	----------L--	▼
L12NN14L [152]	----N-L----------	X
N14LL16N [152]	------L-N----------	X
A13C [152]	-----C----------	▼
V17C [152]	---------C----------	▲
A25C [152]	----------C----------	▼
T30C [152]	----------C-------	▼
T36C [152]	----------C-	—

Table 1-2: Mutational studies of amyloid formation by full length IAPP (A) and the 8-37 fragment of IAPP (B). Residues which differ from human IAPP are indicated in red. Red X denotes an unnatural amino acid. NLe= norleucine. TLe= *tert*-leuceine. "—" no reported effect; "▲" The mutation is reported to lead to faster amyloid formation; "▼" The mutation is reported to lead to slower amyloid formation; "**X**" The mutant is reported to abolish amyloid formation. Data is collected from the indicated reference.

1.5 References

1. Sipe, J. D., Amyloidosis. *Crit. Rev. Clin. Lab. Sci.* **1994**, *31* (4), 325-354.

2. Koo, E. H.; Lansbury, P. T.; Kelly, J. W., Amyloid diseases: Abnormal protein aggregation in neurodegeneration. *Pro. Natl. Acad. Sci. U. S. A.* **1999**, *96* (18), 9989-9990.

3. Chiti, F.; Dobson, C. M., Protein misfolding, functional amyloid, and human disease. *Annu. Rev. Biochem.* **2006**, *75*, 333-366.

4. Bellotti, V.; Chiti, F., Amyloidogenesis in its biological environment: challenging a fundamental issue in protein misfolding diseases. *Curr. Opin. Struct. Biol.* **2008**, *18* (6), 771-779.

5. Sipe, J. D.; Benson, M. D.; Buxbaum, J. N.; Ikeda, S.; Merlini, G.; Saraiva, M. J. M.; Westermark, P., Amyloid fibril protein nomenclature: 2012 recommendations from the nomenclature committee of the international society of amyloidosis. *Amyloid* **2012**, *19* (4), 167-170.

6. Glabe, C.; Kayed, R.; Sokolov, Y.; Hall, J., Common structure and mechanism of soluble amyloid oligomer pathogenesis in degenerative diseases. *Neurobiol. Aging* **2004**, *25*, S75-S76.

7. Stefani, M., Generic cell dysfunction in neurodegenerative disorders: Role of surfaces in early protein misfolding, aggregation, and aggregate cytotoxicity. *Neuroscientist* **2007**, *13* (5), 519-531.

8. Lorenzo, A.; Razzaboni, B.; Weir, G. C.; Yankner, B. A., Pancreatic islet cell toxicity of amylin associated with type-2 diabetes mellitus. *Nature* **1994**, *368* (6473), 756-60.

9. Fandrich, M., Oligomeric intermediates in amyloid formation: Structure determination and mechanisms of toxicity. *J. Mol. Biol.* **2012**, *421* (4-5), 427-440.

10. Winner, B.; Jappelli, R.; Maji, S. K.; Desplats, P. A.; Boyer, L.; Aigner, S.; Hetzer, C.; Loher, T.; Vilar, M.; Campionic, S.; Tzitzilonis, C.; Soragni, A.; Jessberger, S.; Mira, H.; Consiglio, A.; Pham, E.; Masliah, E.; Gage, F. H.; Riek, R., In vivo demonstration that alpha-synuclein oligomers are toxic. *Proc. Natl. Acad. Sci. U. S. A.* **2011**, *108* (10), 4194-4199.

11. Heinitz, K.; Beck, M.; Schliebs, R.; Perez-Polo, J. R., Toxicity mediated by soluble oligomers of beta-amyloid (1-42) on cholinergic SN56.B5.G4 cells. *J. Neurochem.* **2006**, *98* (6), 1930-1945.

12. Stefani, M., Structural features and cytotoxicity of amyloid oligomers: Implications in Alzheimer's disease and other diseases with amyloid deposits. *Prog. Neurobiol.* **2012**, *99* (3), 226-245.

13. Haass, C.; Selkoe, D. J., Soluble protein oligomers in neurodegeneration: lessons from the Alzheimer's amyloid beta-peptide. *Nat. Rev. Mol. Cell Biol.* **2007**, *8* (2), 101-112.

14. Valincius, G.; Heinrich, F.; Budvytyte, R.; Vanderah, D. J.; McGillivray, D. J.; Sokolov, Y.; Hall, J. E.; Losche, M., Soluble amyloid beta-oligomers affect dielectric membrane properties by bilayer insertion and domain formation: Implications for cell toxicity. *Biophys. J.* **2008**, *95* (10), 4845-4861.

15. Zraika, S.; Hull, R. L.; Verchere, C. B.; Clark, A.; Potter, K. J.; Fraser, P. E.; Raleigh, D. P.; Kahn, S. E., Toxic oligomers and islet beta cell death: guilty by association or convicted by circumstantial evidence? *Diabetologia* **2010**, *53* (6), 1046-1056.

16. Ritzel, R. A.; Meier, J. J.; Lin, C. Y.; Veldhuis, J. D.; Butler, P. C., Human islet amyloid polypeptide oligomers disrupt cell coupling, induce apoptosis, and impair insulin secretion in isolated human islets. *Diabetes* **2007**, *56* (1), 65-71.

17. Wang, J.; Dickson, D. W.; Trojanowski, J. Q.; Lee, V. M. Y., The levels of soluble versus insoluble brain A beta distinguish Alzheimer's disease from normal and pathologic aging. *Expe. Neurol.* **1999**, *158* (2), 328-337.

18. McLean, C. A.; Cherny, R. A.; Fraser, F. W.; Fuller, S. J.; Smith, M. J.; Beyreuther, K.; Bush, A. I.; Masters, C. L., Soluble pool of A beta amyloid as a determinant of severity of neurodegeneration in Alzheimer's disease. *Annals Neurol.* **1999**, *46* (6), 860-866.

19. Moechars, D.; Dewachter, I.; Lorent, K.; Reverse, D.; Baekelandt, V.; Naidu, A.; Tesseur, I.; Spittaels, K.; Van Den Haute, C.; Checler, F.; Godaux, E.; Cordell, B.; Van Leuven, F., Early phenotypic changes in transgenic mice that overexpress different mutants of amyloid precursor protein in brain. *J. Biol. Chem.* **1999**, *274* (10), 6483-6492.

20. Sharon, R.; Bar-Joseph, I.; Frosch, M. P.; Walsh, D. M.; Hamilton, J. A.; Selkoe, D. J., The formation of highly soluble oligomers of alpha-synuclein is regulated by fatty acids and enhanced in Parkinson's disease. *Neuron* **2003**, *37* (4), 583-595.

21. Baglioni, S.; Casamenti, F.; Bucciantini, M.; Luheshi, L. M.; Taddei, N.; Chiti, F.; Dobson, C. M.; Stefani, M., Prefibrillar amyloid aggregates could be generic toxins in higher organisms. *J. Neurosci.* **2006**, *26* (31), 8160-8167.

22. Gazit, E., The role of prefibrillar assemblies in the pathogenesis of amyloid diseases. *Drug Future* **2004**, *29* (6), 613-619.

23. Demuro, A.; Mina, E.; Kayed, R.; Milton, S. C.; Parker, I.; Glabe, C. G., Calcium dysregulation and membrane disruption as a ubiquitous neurotoxic mechanism of soluble amyloid oligomers. *J. Biol. Chem.* **2005**, *280* (17), 17294-17300.

24. Janson, J.; Ashley, R. H.; Harrison, D.; McIntyre, S.; Butler, P. C., The mechanism of islet amyloid polypeptide toxicity is membrane disruption by intermediate-sized toxic amyloid particles. *Diabetes* **1999**, *48* (3), 491-498.

25. Terzi, E.; Holzemann, G.; Seelig, J., Interaction of Alzheimer beta-amyloid peptide (1-40) with lipid membranes. *Biochemistry* **1997**, *36* (48), 14845-14852.

26. Quist, A.; Doudevski, L.; Lin, H.; Azimova, R.; Ng, D.; Frangione, B.; Kagan, B.; Ghiso, J.; Lal, R., Amyloid ion channels: A common structural link for protein-misfolding disease. *Proc. Natl. Acad. Sci. U. S. A.* **2005**, *102* (30), 10427-10432.

27. Nakagawa, T.; Zhu, H.; Morishima, N.; Li, E.; Xu, J.; Yankner, B. A.; Yuan, J. Y., Caspase-12 mediates endoplasmic-reticulum-specific apoptosis and cytotoxicity by amyloid-beta. *Nature* **2000**, *403* (6765), 98-103.

28. Jakob-Roetne, R.; Jacobsen, H., Alzheimer's Disease: From pathology to therapeutic approaches. *Angew. Chem. Int. Ed.* **2009**, *48* (17), 3030-3059.

29. Kajava, A. V.; Aebi, U.; Steven, A. C., The parallel superpleated beta-structure as a model for amyloid fibrils of human amylin. *J. Mol. Biol.* **2005**, *348* (2), 247-252.

30. Sunde, M.; Serpell, L. C.; Bartlam, M.; Fraser, P. E.; Pepys, M. B.; Blake, C. C. F., Common core structure of amyloid fibrils by synchrotron X-ray diffraction. *J. Mol. Biol.* **1997**, *273* (3), 729-739.

31. Serpell, L. C.; Sunde, M.; Benson, M. D.; Tennent, G. A.; Pepys, M. B.; Fraser, P. E., The protofilament substructure of amyloid fibrils. *J. Mol. Biol.* **2000**, *300* (5), 1033-1039.

32. Levine, H., Thioflavine-T interaction with amyloid beta-sheet structures. *Amyloid* **1995**, *2* (1), 1-6.

33. Ban, T.; Hamada, D.; Hasegawa, K.; Naiki, H.; Goto, Y., Direct observation of amyloid fibril growth monitored by thioflavin T fluorescence. *J. Biol. Chem.* **2003**, *278* (19), 16462-16465.

34. Puchtler, H.; Sweat, F., Congo red as a stain for fluorescence microscopy of amyloid. *J. Histochem. Cytochem.* **1965**, *13* (8), 693-694

35. Petkova, A. T.; Ishii, Y.; Balbach, J. J.; Antzutkin, O. N.; Leapman, R. D.; Delaglio, F.; Tycko, R., A structural model for Alzheimer's beta-amyloid fibrils based on experimental constraints from solid state NMR. *Proc. Natl. Acad. Sci. U. S. A.* **2002**, *99* (26), 16742-16747.

36. Van der Wel, P. C. A.; Lewandowski, J. R.; Griffin, R. G., Solid-state NMR study of amyloid nanocrystals and fibrils formed by the peptide GNNQQNY from yeast prion protein Sup35p. *J.Am. Chem. Soc.* **2007**, *129* (16), 5117-5130.

37. Luca, S.; Yau, W. M.; Leapman, R.; Tycko, R., Peptide conformation and supramolecular organization in amylin fibrils: Constraints from solid-state NMR. *Biochemistry* **2007**, *46* (47), 13505-13522.

38. Nelson, R.; Sawaya, M. R.; Balbirnie, M.; Madsen, A. O.; Riekel, C.; Grothe, R.; Eisenberg, D., Structure of the cross-beta spine of amyloid-like fibrils. *Nature* **2005**, *435* (7043), 773-778.

39. Nelson, R.; Eisenberg, D., Recent atomic models of amyloid fibril structure. *Curr. Opin. Struc. Biol.* **2006**, *16* (2), 260-265.

40. Sawaya, M. R.; Sambashivan, S.; Nelson, R.; Ivanova, M. I.; Sievers, S. A.; Apostol, M. I.; Thompson, M. J.; Balbirnie, M.; Wiltzius, J. J. W.; McFarlane, H. T.; Madsen, A. O.; Riekel, C.;

Eisenberg, D., Atomic structures of amyloid cross-beta spines reveal varied steric zippers. *Nature* **2007**, *447* (7143), 453-457.

41. Goldschmidt, L.; Teng, P. K.; Riek, R.; Eisenberg, D., Identifying the amylome, proteins capable of forming amyloid-like fibrils. *Proc. Natl. Acad. Sci. U. S. A.* **2010**, *107* (8), 3487-3492.

42. Wiltzius, J. J. W.; Sievers, S. A.; Sawaya, M. R.; Cascio, D.; Popov, D.; Riekel, C.; Eisenberg, D., Atomic structure of the cross-beta spine of islet amyloid polypeptide (amylin). *Protein Sci.* **2008**, *17* (9), 1467-1474.

43. Xue, W. F.; Homans, S. W.; Radford, S. E., Systematic analysis of nucleation-dependent polymerization reveals new insights into the mechanism of amyloid self-assembly. *Proc. Natl. Acad. Sci. U. S. A.* **2008,** *105* (26), 8926-8931.

44. Lomakin, A.; Chung, D. S.; Benedek, G. B.; Kirschner, D. A.; Teplow, D. B., On the nucleation and growth of amyloid beta-protein fibrils: Detection of nuclei and quantitation of rate constants. *Proc. Natl. Acad. Sci. U. S. A.* **1996**, *93* (3), 1125-1129.

45. Ferrone, F., Analysis of protein aggregation kinetics. *Method. Enzymol.* **1999**, *309*, 256-274.

46. O'Nuallain, B.; Williams, A. D.; Westermark, P.; Wetzel, R., Seeding specificity in amyloid growth induced by heterologous fibrils. *J. Biol. Chem.* **2004**, *279* (17), 17490-17499.

47. Padrick, S. B.; Miranker, A. D., Islet amyloid: Phase partitioning and secondary nucleation are central to the mechanism of fibrillogenesis. *Biochemistry* **2002**, *41* (14), 4694-4703.

48. Bishop, M. F.; Ferrone, F. A., Kinetics of nucleation-controlled polymerization-a perturbation treatment for use with a secondary pathway. *Biophys. J.* **1984**, *46* (5), 631-644.

49. Lai, Z. H.; Colon, W.; Kelly, J. W., The acid-mediated denaturation pathway of transthyretin yields a conformational intermediate that can self-assemble into amyloid. *Biochemistry* **1996**, *35* (20), 6470-6482.

50. Hou, X.; Aguilar, M. I.; Small, D. H., Transthyretin and familial amyloidotic polyneuropathy - Recent progress in understanding the molecular mechanism of neurodegeneration. *Febs J.* **2007**, *274* (7), 1637-1650.

51. McCutchen, S. L.; Colon, W.; Kelly, J. W., Transthyretin mutation Leu-55-Pro significantly alters tetramer stability and increases amyloidogenicity. *Biochemistry* **1993**, *32* (45), 12119-12127.

52. Bulawa, C. E.; Connelly, S.; Devit, M.; Wang, L.; Weigel, C.; Fleming, J. A.; Packman, J.; Powers, E. T.; Wiseman, R. L.; Foss, T. R.; Wilson, I. A.; Kelly, J. W.; Labaudiniere, R., Tafamidis, a potent and selective transthyretin kinetic stabilizer that inhibits the amyloid cascade. *Proc. Natl. Acad. Sci. U. S. A.* **2012**, *109* (24), 9629-9634.

53. Coelho, T.; Maia, L. F.; da Silva, A. M.; Cruz, M. W.; Plante-Bordeneuve, V.; Lozeron, P.; Suhr, O. B.; Campistol, J. M.; Conceicao, I. M.; Schmidt, H. H. J.; Trigo, P.; Kelly, J. W.; Labaudinie, R.; Chan, J.; Packman, J.; Wilson, A.; Grogan, D. R., Tafamidis for transthyretin familial amyloid polyneuropathy a randomized, controlled trial. *Neurology* **2012**, *79* (8), 785-792.

54. Porat, Y.; Abramowitz, A.; Gazit, E., Inhibition of amyloid fibril formation by polyphenols: Structural similarity and aromatic interactions as a common inhibition mechanism. *Chem. Bio. Drug Des.* **2006**, *67* (1), 27-37.

55. Bastianetto, S.; Krantic, S.; Quirion, R., Polyphenols as potential inhibitors of amyloid aggregation and toxicity: Possible significance to Alzheimer's disease. *Med. Chem.* **2008**, *8* (5), 429-435.

56. Ferreira, N.; Saraiva, M. J.; Almeida, M. R., Natural polyphenols inhibit different steps of the process of transthyretin (TTR) amyloid fibril formation. *Febs Lett.* **2011**, *585* (15), 2424-2430.

57. Bieschke, J.; Russ, J.; Friedrich, R. P.; Ehrnhoefer, D. E.; Wobst, H.; Neugebauer, K.; Wanker, E. E., EGCG remodels mature alpha-synuclein and amyloid-beta fibrils and reduces cellular toxicity. *Proc. Natl. Acad. Sci. U. S. A.* **2010**, *107* (17), 7710-7715.

58. Bastianetto, S.; Yao, Z. X.; Papadopoulos, V.; Quirion, R., Neuroprotective effects of green and black teas and their catechin gallate esters against beta-amyloid-induced toxicity. *Euro. J. Neurosci.* **2006**, *23* (1), 55-64.

59. Hauber, I.; Hohenberg, H.; Holstermann, B.; Hunstein, W.; Hauber, J., The main green tea polyphenol epigallocatechin-3-gallate counteracts semen-mediated enhancement of HIV infection. *Proc. Natl. Acad. Sci. U. S. A.* **2009**, *106* (22), 9033-9038.

60. Cao, P.; Raleigh, D. P., Analysis of the inhibition and remodeling of islet amyloid polypeptide amyloid fibers by flavanols. *Biochemistry* **2012**, *51* (13), 2670-2683.

61. Raleigh, D. P.; Meng, F. L.; Abedini, A.; Plesner, A.; Verchere, C. B., The flavanol (-)-epigallocatechin 3-gallate inhibits amyloid formation by islet amyloid polypeptide, disaggregates amyloid fibrils, and protects cultured cells against IAPP-induced toxicity. *Biochemistry* **2010**, *49* (37), 8127-8133.

62. Ladiwala, A. R. A.; Lin, J. C.; Bale, S. S.; Marcelino-Cruz, A. M.; Bhattacharya, M.; Dordick, J. S.; Tessier, P. M., Resveratrol selectively remodels soluble oligomers and fibrils of amyloid A beta into off-pathway conformers. *J. Biol. Chem.* **2010**, *285* (31), 24228-24237.

63. Mishra, R.; Sellin, D.; Radovan, D.; Gohlke, A.; Winter, R., Inhibiting islet amyloid polypeptide fibril formation by the red wine compound resveratrol. *Chembiochem* **2009**, *10* (3), 445-449

64. Feng, Y.; Wang, X. P.; Yang, S. G.; Wang, Y. J.; Zhang, X.; Du, X. T.; Sun, X. X.; Zhao, M.; Huang, L.; Liu, R. T., Resveratrol inhibits beta-amyloid oligomeric cytotoxicity but does not prevent oligomer formation. *Neurotoxicology* **2009**, *30* (6), 986-995.

65. Evers, F.; Jeworrek, C.; Tiemeyer, S.; Weise, K.; Sellin, D.; Paulus, M.; Struth, B.; Tolan, M.; Winter, R., Elucidating the mechanism of lipid membrane-induced IAPP fibrillogenesis and its inhibition by the red wine compound resveratrol: A synchrotron X-ray reflectivity study. *J. Am. Chem. Soc.* **2009**, *131* (27), 9516-9521.

66. Sciarretta, K. L.; Gordon, D. J.; Meredith, S. C., Peptide-based inhibitors of amyloid assembly. *Method Enzymol*. **2006**, 413, 273-312.

67. Esler, W. P.; Stimson, E. R.; Ghilardi, J. R.; Lu, Y. A.; Felix, A. M.; Vinters, H. V.; Mantyh, P. W.; Lee, J. P.; Maggio, J. E., Point substitution in the central hydrophobic cluster of a human beta-amyloid congener disrupts peptide folding and abolishes plaque competence. *Biochemistry* **1996**, *35* (44), 13914-13921.

68. Tjernberg, L. O.; Naslund, J.; Lindqvist, F.; Johansson, J.; Karlstrom, A. R.; Thyberg, J.; Terenius, L.; Nordstedt, C., Arrest of beta-amyloid fibril formation by a pentapeptide ligand. *J. Biol. Chem.* **1996**, *271* (15), 8545-8548.

69. Hughes, S. R.; Goyal, S.; Sun, J. E.; GonzalezDeWhitt, P.; Fortes, M. A.; Riedel, N. G.; Sahasrabudhe, S. R., Two-hybrid system as a model to study the interaction of beta-amyloid peptide monomers. *Proc. Natl. Acad. Sci. U. S. A.* **1996**, *93* (5), 2065-2070.

70. Moriarty, D. F.; Raleigh, D. P., Effects of sequential proline substitutions on amyloid formation by human amylin (20-29). *Biochemistry* **1999,** *38* (6), 1811-1818.

71. Abedini, A.; Meng, F. L.; Raleigh, D. P., A single-point mutation converts the highly amyloidogenic human islet amyloid polypeptide into a potent fibrillization inhibitor. *J. Am. Chem. Soc.* **2007**, *129* (37), 11300-11301 .

72. Wood, S. J.; Wetzel, R.; Martin, J. D.; Hurle, M. R., Prolines and amyloidogenicity in fragments of the Alzheimer's peptide beta/A4. *Biochemistry* **1995**, *34* (3), 724-730.

73. Westermark, P.; Engstrom, U.; Johnson, K. H.; Westermark, G. T.; Betsholtz, C., Islet amyloid polypeptide: pinpointing amino acid residues linked to amyloid fibril formation. *Proc. Natl. Acad. Sci. U. S. A.* **1990**, *87* (13), 5036-40.

74. Meng, F. L.; Raleigh, D. P.; Abedini, A., Combination of kinetically selected inhibitors in trans leads to highly effective inhibition of amyloid formation. *J. Am. Chem. Soc.* **2010**, *132* (41), 14340-14342.

75. Gordon, D. J.; Tappe, R.; Meredith, S. C., Design and characterization of a membrane permeable N-methyl amino acid-containing peptide that inhibits A beta (1-40) fibrillogenesis. *J. Pept. Res.* **2002**, *60* (1), 37-55.

76. Kapurniotu, A.; Schmauder, A.; Tenidis, K., Structure-based design and study of non-amyloidogenic, double N-methylated IAPP amyloid core sequences as inhibitors of IAPP amyloid formation and cytotoxicity. *J. Mol. Biol.* **2002**, *315* (3), 339-350.

77. Kokkoni, N.; Stott, K.; Amijee, H.; Mason, J. M.; Doig, A. J., N-methylated peptide inhibitors of beta-amyloid aggregation and toxicity. Optimization of the inhibitor structure. *Biochemistry* **2006**, *45* (32), 9906-9918.

78. Abedini, A.; Raleigh, D. P., A critical assessment of the role of helical intermediates in amyloid formation by natively unfolded proteins and polypeptides. *Protein Eng. Des. Sel.* **2009**, *22* (8), 453-459.

79. Williamson, J. A.; Miranker, A. D., Direct detection of transient alpha-helical states in islet amyloid polypeptide. *Protein Sci.* **2007**, *16* (1), 110-117.

80. Saraogi, I.; Hebda, J. A.; Becerril, J.; Estroff, L. A.; Miranker, A. D.; Hamilton, A. D., Synthetic alpha-helix mimetics as agonists and antagonists of islet amyloid polypeptide aggregation. *Angew. Chem. Int. Ed.* **2010**, *49* (4), 736-739.

81. Sievers, S. A.; Karanicolas, J.; Chang, H. W.; Zhao, A.; Jiang, L.; Zirafi, O.; Stevens, J. T.; Munch, J.; Baker, D.; Eisenberg, D., Structure-based design of non-natural amino-acid inhibitors of amyloid fibril formation. *Nature* **2011**, *475* (7354), 96-117.

82. Buchanan, L. E.; Dunkelberger, E. B.; Tran, H. Q.; Cheng, P. N.; Chiu, C. C.; Cao, P.; Raleigh, D. P.; de Pablo, J. J.; Nowick, J. S.; Zanni, M. T., Mechanism of IAPP amyloid fibril formation involves an intermediate with a transient beta-sheet. *Proc. Natl. Acad. Sci. U.S.A.* **2013**, *110* (48), 19285-19290.

83. Betsholtz, C.; Svensson, V.; Rorsman, F.; Engstrom, U.; Westermark, G. T.; Wilander, E.; Johnson, K.; Westermark, P., Islet amyloid polypeptide (IAPP) - cDNA cloning and identification of an amyloidogenic region associated with the species-specific occurrence of age-related diabetes-mellitus. *Expe. Cell Res.* **1989**, *183* (2), 484-493.

84. Sanke, T.; Bell, G. I.; Sample, C.; Rubenstein, A. H.; Steiner, D. F., An islet amyloid peptide is derived from an 89-amino acid precursor by proteolytic processing. *J. Biol. Chem.* **1988**, *263* (33), 17243-17246.

85. Badman, M. K.; Shennan, K. I.; Jermany, J. L.; Docherty, K.; Clark, A., Processing of pro-islet amyloid polypeptide (proIAPP) by the prohormone convertase PC2. *Febs Lett.* **1996**, *378* (3), 227-231.

86. Marzban, L.; Trigo-Gonzales, G.; Zhu, X. R.; Rhodes, C. J.; Halban, P. A.; Steiner, D. F.; Verchere, C. B., Role of beta-cell prohormone convertase (PC) 1/3 in processing of pro-islet antyloid polypeptide. *Diabetes* **2004**, *53* (1), 141-148.

87. Marzban, L.; Soukhatcheva, G.; Verchere, C. B., Role of carboxypeptidase E in processing of pro-islet amyloid polypeptide in beta-cells. *Endocrinology* **2005**, *146* (4), 1808-1817.

88. Wang, J.; Xu, J.; Finnerty, J.; Furuta, M.; Steiner, D. F.; Verchere, C. B., The prohormone convertase enzyme 2 (PC2) is essential for processing pro-islet amyloid polypeptide at the NH2-terminal cleavage site. *Diabetes* **2001**, *50* (3), 534-539.

89. Martinez, A.; Montuenga, L. M.; Springall, D. R.; Treston, A.; Cuttitta, F.; Polak, J. M., Immunocytochemical localization of peptidylglycine alpha-amidating monooxygenase enzymes (PAM) in human endocrine pancreas. *J. Histochem. Cytochem.* **1993**, *41* (3), 375-380.

90. Roberts, A. N.; Leighton, B.; Todd, J. A.; Cockburn, D.; Schofield, P. N.; Sutton, R.; Holt, S.; Boyd, Y.; Day, A. J.; Foot, E. A.; Willis, A. C.; Reid, K. B. M.; Cooper, G. J. S., Molecular and functional-characterization of amylin, a peptide associated with type-2 diabetes-mellitus. *Proc. Natl. Acad. Sci. U. S. A.* **1989**, *86* (24), 9662-9666.

91. Kahn, S. E.; Dalessio, D. A.; Schwartz, M. W.; Fujimoto, W. Y.; Ensinck, J. W.; Taborsky, G. J.; Porte, D., Evidence of cosecretion of islet amyloid polypeptide and insulin by beta-cells. *Diabetes* **1990**, *39* (5), 634-638.

92. Charge, S. B.; de Koning, E. J.; Clark, A., Effect of pH and insulin on fibrillogenesis of islet amyloid polypeptide *in vitro*. *Biochemistry* **1995**, *34* (44), 14588-93.

93. Abedini, A.; Raleigh, D. P., The role of His-18 in amyloid formation by human islet amyloid polypeptide. *Biochemistry* **2005**, *44* (49), 16284-16291.

94. Hutton, J. C., The internal pH and membrane-potential of the insulin-secretory granule. *Biochem. J.* **1982**, *204* (1), 171-178.

95. Larson, J. L.; Miranker, A. D., The mechanism of insulin action on islet amyloid polypeptide fiber formation. *J. Mol. Biol.* **2004**, *335* (1), 221-231.

96. Westermark, P.; Andersson, A.; Westermark, G. T., Islet amyloid polypeptide, islet amyloid, and diabetes mellitus. *Physiol. Rev.* **2011**, *91* (3), 795-826.

97. Scherbaum, W. A., The role of amylin in the physiology of glycemic control. *Expe. Clini. Endocrinol. Diabetes* **1998**, *106* (2), 97-102.

98. Young, D. A.; Deems, R. O.; Deacon, R. W.; McIntosh, R. H.; Foley, J. E., Effects of amylin on glucose-metabolism and glycogenolysis *in vivo and in vitro*. *Am. J. Physiol.* **1990**, *259* (3), E457-E461.

99. Cooper, G. J. S.; Leighton, B.; Dimitriadis, G. D.; Parrybillings, M.; Kowalchuk, J. M.; Howland, K.; Rothbard, J. B.; Willis, A. C.; Reid, K. B. M., Amylin found in amyloid deposits in human type-2 diabetes-mellitus may be a hormone that regulates glycogen-metabolism in skeletal-muscle. *Proc. Natl. Acad. Sci. U.S.A.* **1988**, *85* (20), 7763-7766.

100. Zierath, J. R.; Galuska, D.; Engstrom, A.; Johnson, K. H.; Betsholtz, C.; Westermark, P.; Wallberghenriksson, H., Human islet amyloid polypeptide at pharmacological levels inhibits insulin and phorbol ester-stimulated glucose-transport in vitro incubated human muscle strips. *Diabetologia* **1992**, *35* (1), 26-31.

101. Rushing P. A.; Hagan, M. M.; Seeley R. J.; Lutz, T. A.; D' Alessio, D. A.; Air, E. L.; Woods S. C., Inhibition of central amylin signaling increases food intake and body adiposity in rats. Endocrinology **2001**, *142* (11), 5035-5038.

102. Lutz, T.A., Control of energy homeostasis by amylin. *Cell. Mol. Life Sci.* **2012**, *69* (12), 1947–1965.

103. Cooper, G. J. S.; Willis, A. C.; Clark, A.; Turner, R. C.; Sim, R. B.; Reid, K. B. M., Purification and characterization of a peptide from amyloid-rich pancreases of type-2 diabetic-patients. *Proc. Natl. Acad. Sci. U.S.A.***1987**, *84* (23), 8628-8632.

104. Mosselman, S.; Hoppener, J. W. M.; Zandberg, J.; Vanmansfeld, A. D. M.; Vankessel, A. H. M. G.; Lips, C. J. M.; Jansz, H. S., Islet amyloid polypeptide - Identification and chromosomal localization of the human-gene. *Febs Lett.* **1988**, *239* (2), 227-232.

105. Hull, R. L.; Westermark, G. T.; Westermark, P.; Kahn, S. E., Islet amyloid: A critical entity in the pathogenesis of type 2 diabetes. *J. Clini. Endocrinol. Metab.* **2004**, *89* (8), 3629-3643.

106. Westerma.P, Quantitative studies of amyloid in islets of Langerhans. *Ups. J. Med. Sci.* **1972**, *77* (2), 91-94.

107. Maloy, A. L.; Longnecker, D. S.; Greenberg, E. R., The relation of islet amyloid to the clinical type diabetes. *Human Pathol.* **1981**, *12* (10), 917-922.

108. Narita, R.; Toshimori, H.; Nakazato, M.; Kuribayashi, T.; Toshimori, T.; Kawabata, K.; Takahashi, K.; Masukura, S., Islet amyloid polypeptide (IAPP) and pancreatic-islet amyloid deposition in diabetes and nondiabetic patients. *Diabetes Res. Clin. Pract.* **1992**, *15* (1), 3-14.

109. Ahronheim, J. H., The nature of the hyaline material in the pancreatic islands in diabetes mellitus. *Am. J. Pathol.* **1943**, *19* (5), 873-882.

110. Lorenzo, A.; Razzaboni, B.; Weir, G. C.; Yankner, B. A., Pancreatic-islet cell toxicity of amylin associated with type-2 diabetes-mellitus. *Nature* **1994**, *368* (6473), 756-760.

111. Hull, R. L.; Andrikopoulos, S.; Verchere, C. B.; Vidal, J.; Wang, F.; Cnop, M.; Prigeon, R. L.; Kahn, S. E., Increased dietary fat promotes islet amyloid formation and beta-cell secretory dysfunction in a transgenic mouse model of islet amyloid. *Diabetes* **2003**, *52* (2), 372-379.

112. Jurgens, C. A.; Toukatly, M. N.; Fligner, C. L.; Udayasankar, J.; Subramanian, S. L.; Zraika, S.; Aston-Mourney, K.; Carr, D. B.; Westermark, P.; Westermark, G. T.; Kahn, S. E.; Hull, R. L., beta-cell loss and beta-cell apoptosis in human type 2 diabetes are related to islet amyloid deposition. *Am. J. Pathol.* **2011**, *178* (6), 2632-2640.

113. Verchere, C. B.; DAlessio, D. A.; Palmiter, R. D.; Weir, G. C.; BonnerWeir, S.; Baskin, D. G.; Kahn, S. E., Islet amyloid formation associated with hyperglycemia in transgenic mice with pancreatic beta cell expression of human islet amyloid polypeptide. *Proc. Natl. Acad. Sci. U.S.A.* **1996**, *93* (8), 3492-3496.

114. Janson, J.; Soeller, W. C.; Roche, P. C.; Nelson, R. T.; Torchia, A. J.; Kreutter, D. K.; Butler, P. C., Spontaneous diabetes mellitus in transgenic mice expressing human islet amyloid polypeptide. *Proc. Natl. Acad. Sci. U.S.A.* **1996**, *93* (14), 7283-7288.

115. Westermark, G. T.; Westermark, P.; Nordin, A.; Tornelius, E.; Andersson, A., Formation of amyloid in human pancreatic islets transplanted to the liver and spleen of nude mice. *Ups. J. Med. Sci.* **2003**, *108* (3), 193-203.

116. Swift, S. M.; Clayton, H. A.; London, N. J. M.; James, R. F. L., The potential contribution of rejection to survival of transplanted human islets. *Cell Transplant.* **1998**, *7* (6), 599-606.

117. Westermark, G. T.; Westermark, P.; Berne, C.; Korsgren, O.; Nordic Network Clin Islet, T., Widespread amyloid deposition in transplanted human pancreatic islets. *N. Eng. J. Med.* **2008**, *359* (9), 977-979.

118. Hoppener, J. W. M.; Lips, C. J. M., Role of islet amyloid in type 2 diabetes mellitus. *Int. J. Biochem. Cell Biol.* **2006**, *38* (5-6), 726-736.

119. Potter, K. J.; Abedini, A.; Marek, P.; Klimek, A. M.; Butterworth, S.; Driscoll, M.; Baker, R.; Nilsson, M. R.; Warnock, G. L.; Oberholzer, J.; Bertera, S.; Trucco, M.; Korbutt, G. S.; Fraser, P. E.; Raleigh, D. P.; Verchere, C. B., Islet amyloid deposition limits the viability of human islet grafts but not porcine islet grafts. *Proc. Natl. Acad. Sci. U. S. A.* **2010**, *107* (9), 4305-4310.

120. Zraika, S.; Hull, R. L.; Verchere, C. B.; Clark, A.; Potter, K. J.; Fraser, P. E.; Raleigh, D. P.; Kahn, S. E., Toxic oligomers and islet beta cell death: guilty by association or convicted by circumstantial evidence? *Diabetologia* **2010**, *53* (6), 1046-56.

121. Weise, K.; Radovan, D.; Gohlke, A.; Opitz, N.; Winter, R., Interaction of hIAPP with model raft membranes and pancreatic beta-cells: Cytotoxicity of hIAPP oligomers. *Chembiochem* **2010**, *11* (9), 1280-1290.

122. Zraika, S.; Hull, R. L.; Udayasankar, J.; Aston-Mourney, K.; Subramanian, S. L.; Kisilevsky, R.; Szarek, W. A.; Kahn, S. E., Oxidative stress is induced by islet amyloid formation and time-dependently mediates amyloid-induced beta cell apoptosis. *Diabetologia* **2009**, *52* (4), 626-635.

123. Khemtemourian, L.; Killian, J. A.; Hoppener, J. W. M.; Engel, M. F. M., Recent insights in islet amyloid polypeptide-induced membrane disruption and its role in beta-cell death in type 2 diabetes mellitus. *Expe. Diabetes Res.* **2008**, 421287.

124. Subramanian, S. L.; Hull, R. L.; Zraika, S.; Aston-Mourney, K.; Udayasankar, J.; Kahn, S. E., cJUN N-terminal kinase (JNK) activation mediates islet amyloid-induced beta cell apoptosis in cultured human islet amyloid polypeptide transgenic mouse islets. *Diabetologia* **2012**, *55* (1), 166-174.

125. Zhang, S. P.; Liu, J. X.; Dragunow, M.; Cooper, G. J. S., Fibrillogenic amylin evokes islet beta-cell apoptosis through linked activation of a caspase cascade and JNK1. *J. Biol. Chem.* **2003**, *278* (52), 52810-52819.

126. Masters, S. L.; Dunne, A.; Subramanian, S. L.; Hull, R. L.; Tannahill, G. M.; Sharp, F. A.; Becker, C.; Franchi, L.; Yoshihara, E.; Chen, Z.; Mullooly, N.; Mielke, L. A.; Harris, J.; Coll, R. C.; Mills, K. H. G.; Mok, K. H.; Newsholme, P.; Nunez, G.; Yodoi, J.; Kahn, S. E.; Lavelle, E. C.; O'Neill, L. A. J., Activation of the NLRP3 inflammasome by islet amyloid polypeptide provides a mechanism for enhanced IL-1 beta in type 2 diabetes. *Nat. Immunol.* **2010**, *11* (10), 897-904.

127. Rivera, J. F.; Gurlo, T.; Daval, M.; Huang, C. J.; Matveyenko, A. V.; Butler, P. C.; Costes, S., Human-IAPP disrupts the autophagy/lysosomal pathway in pancreatic beta-cells: protective role of p62-positive cytoplasmic inclusions. *Cell Death Differ.* **2011**, *18* (3), 415-426.

128. Morita, S.; Sakagashira, S.; Shimajiri, Y.; Eberhardt, N. L.; Kondo, T.; Kondo, T.; Sanke, T., Autophagy protects against human islet amyloid polypeptide-associated apoptosis. *J. Diabetes Invest.* **2011**, *2* (1), 48-55.

129. Abedini, A.; Schmidt, A. M., Mechanisms of islet amyloidosis toxicity in type 2 diabetes. *Febs Lett.* **2013**, *587* (8), 1119-1127.

130. Cao, P.; Marek, P.; Noor, H.; Patsalo, V.; Tu, L. H.; Wang, H.; Abedini, A.; Raleigh, D. P., Islet amyloid: From fundamental biophysics to mechanisms of cytotoxicity. *Febs Lett.* **2013**, *587* (8), 1106-1118.

131. Makin, O. S.; Serpell, L. C., Structural characterisation of islet amyloid polypeptide fibrils. *J. Mol. Biol.* **2004**, *335* (5), 1279-1288.

132. Jayasinghe, S. A.; Langen, R., Identifying structural features of fibrillar islet amyloid polypeptide using site-directed spin labeling. *J. Biol. Chem.* **2004**, *279* (46), 48420-48425.

133. Wiltzius, J. J.; Sievers, S. A.; Sawaya, M. R.; Cascio, D.; Popov, D.; Riekel, C.; Eisenberg, D., Atomic structure of the cross-beta spine of islet amyloid polypeptide (amylin). *Protein Sci.* **2008**, *17* (9), 1467-74.

134. Johnson, K.H.; O'Brien, T.D.; Betsholtz, C.; Westermark, P., Islet amyloid polypeptide: mechanisms of amyloidogenesis in the pancreatic islets and potential roles in diabetes mellitus. *Lab. Invest.* **1992**, *66*, 522–535.

135. Azriel, R.; Gazit, E., Analysis of the structural and functional elements of the minimal active fragment of islet amyloid polypeptide (IAPP) - An experimental support for the key role of the phenylalanine residue in amyloid formation. *J. Biol. Chem.* **2001**, *276* (36), 34156-34161.

136. Park, K.; Jaikaran, E. T. A. S.; Clark, A.; Verchere, C. B., Increased amyloid fibril formation and beta cell toxicity of S20G mutant human islet amyloid polypeptide (IAPP). *Diabetes* **2002**, *51*, A386-A386.

137. Cao, P.; Tu, L. H.; Abedini, A.; Levsh, O.; Akter, R.; Patsalo, V.; Schmidt, A. M.; Raleigh, D. P., Sensitivity of amyloid formation by human islet amyloid polypeptide to mutations at residue 20. *J. Mol. Biol.* **2012**, *421* (2-3), 282-295.

138. Sakagashira, S.; Hiddinga, H. J.; Tateishi, K.; Sanke, T.; Hanabusa, T.; Nanjo, K.; Eberhardt, N. L., S20G mutant amylin exhibits increased in vitro amyloidogenicity and increased intracellular cytotoxicity compared to wild-type amylin. *Am. J. Pathol.* **2000**, *157* (6), 2101-2109.

139. Nishi, M.; Chan, S. J.; Nagamatsu, S.; Bell, G. I.; Steiner, D. F., Conservation of the sequence of islet amyloid polypeptide in five mammals is consistent with its putative role as an islet hormone. *Proc. Natl. Acad. Sci. U.S.A.* **1989**, *86* (15), 5738-5742.

140. Westermark, G. T.; Falkmer, S.; Steiner, D. F.; Chan, S. J.; Engstrom, U.; Westermark, P., Islet amyloid polypeptide is expressed in the pancreatic islet parenchyma of the teleostean fish,

Myoxocephalus (cottus) scorpius. *Compar. Biochem. Physiol. B-Biochem. Mol. Biol.* **2002**, *133* (1), 119-125.

141. Miyazato, M.; Nakazato, M.; Shiomi, K.; Aburaya, J.; Kangawa, K.; Matsuo, H.; Matsukura, S., Molecular-forms of islet amyloid polypeptide (IAPP amylin) in four mammals. *Diabetes Res. Clin. Pract.* **1992**, *15* (1), 31-36.

142. Zhang, X.; Cheng, B. A.; Gong, H.; Li, C. Z.; Chen, H.; Zheng, L.; Huang, K., Porcine islet amyloid polypeptide fragments are refractory to amyloid formation. *Febs Lett.* **2011**, *585* (1), 71-77.

143. Tu, L.H.; Serrano, A. L.; Zanni, M. T.; Raleigh, D. P., Mutational analysis of preamyloid intermediates: The role of His-Tyr interactions in islet amyloid formation. *Biophys. J.* **2014**, 106 (7), 1520-1527.

144. Yanagi, K.; Ashizaki, M.; Yagi, H.; Sakurai, K.; Lee, Y. H.; Goto, Y., Hexafluoroisopropanol induces amyloid fibrils of islet amyloid polypeptide by enhancing both hydrophobic and electrostatic interactions. *J. Biol. Chem.* **2011**, *286* (27), 23959-23966.

145. Marek, P. J.; Patsalo, V.; Green, D. F.; Raleigh, D. P., Ionic strength effects on amyloid formation by amylin are a complicated interplay among Debye screening, ion selectivity, and Hofmeister effects. *Biochemistry* **2012**, *51* (43), 8478-8490.

146. Marek, P.; Abedini, A.; Song, B. B.; Kanungo, M.; Johnson, M. E.; Gupta, R.; Zaman, W.; Wong, S. S.; Raleigh, D. P., Aromatic interactions are not required for amyloid fibril formation by islet amyloid polypeptide but do influence the rate of fibril formation and fibril morphology. *Biochemistry* **2007**, *46* (11), 3255-3261.

147. Weyer, C.; Maggs, D. G.; Young, A. A.; Kolterman, O. G., Amylin replacement with pramlintide as an adjunct to insulin therapy in type 1 and type 2 diabetes mellitus: A physiological approach toward improved metabolic control. *Curr. Pharma. Des.* **2001**, *7* (14), 1353-1373.

148. Fox, A.; Snollaerts, T.; Casanova, C. E.; Calciano, A.; Nogaj, L. A.; Moffet, D. A., Selection for nonamyloidogenic mutants of islet amyloid polypeptide (IAPP) identifies an extended region for amyloidogenicity. *Biochemistry* **2010**, *49* (36), 7783-7789.

149. Tu, L. H.; Raleigh, D. P., Role of Aromatic interactions in amyloid formation by islet amyloid polypeptide. *Biochemistry* **2013**, *52* (2), 333-342.

150. Abedini, A.; Raleigh, D. P., Destabilization of human IAPP amyloid fibrils by proline mutations outside of the putative amyloidogenic domain: Is there a critical amyloidogenic domain in human IAPP? *J. Mol. Biol.* **2006**, *355* (2), 274-281.

151. Wiltzius, J. J. W.; Sievers, S. A.; Sawaya, M. R.; Eisenberg, D., Atomic structures of IAPP (amylin) fusions suggest a mechanism for fibrillation and the role of insulin in the process. *Protein Sci.* **2009**, *18* (7), 1521-1530.

152. Koo, B. W.; Hebda, J. A.; Miranker, A. D., Amide inequivalence in the fibrillar assembly of islet amyloid polypeptide. *Protein Eng. Des. Sel.* **2008**, *21* (3), 147-154.

153. Green, J.; Goldsbury, C.; Min, T.; Sunderji, S.; Frey, P.; Kistler, J.; Cooper, G.; Aebi, U., Full-length rat amylin forms fibrils following substitution of single residues from human amylin. *J. Mol. Biol.* **2003**, *326* (4), 1147-1156.

154. Haataja, L.; Gurlo, T.; Huang, C. J.; Butler, P. C., Islet amyloid in type 2 diabetes, and the toxic oligomer hypothesis. *Endocr. Rev.* **2008**, *29* (3), 303-316.

155. Kayed, R.; Head, E.; Sarsoza, F.; Saing, T.; Cotman, C. W.; Necula, M.; Margol, L.; Wu, J.; Breydo, L.; Thompson, J. L.; Rasool, S.; Gurlo, T.; Butler, P.; Glabe, C. G., Fibril specific, conformation dependent antibodies recognize a generic epitope common to amyloid fibrils and fibrillar oligomers that is absent in prefibrillar oligomers. *Mol. Neurodegener.* **2007**, *2*. 18

156. Kayed, R.; Head, E.; Thompson, J. L.; McIntire, T. M.; Milton, S. C.; Cotman, C. W.; Glabe, C. G., Common structure of soluble amyloid oligomers implies common mechanism of pathogenesis. *Science* **2003**, *300* (5618), 486-489.

157. Zhao, H. L.; Sui, Y.; Guan, J. Amyloid oligomers in diabetic and nondiabetic human pancreas. *Transl. Res*. 2009, *153*, 24–32

158. Vaiana, S. M.; Ghirlando, R.; Yau, W. M.; Eaton, W. A.; Hofrichter, J., Sedimentation studies on human amylin fail to detect low-molecular-weight oligomers. *Biophys. J.* **2008**, *94* (7), L45-L47.

159. Suzuki, Y.; Brender, J. R.; Hartman, K.; Ramamoorthy, A.; Marsh, E. N. G., Alternative pathways of human islet amyloid polypeptide aggregation distinguished by F-19 nuclear magnetic resonance-detected kinetics of monomer consumption. *Biochemistry* **2012**, *51* (41), 8154-8162.

160. Dupuis, N. F.; Wu, C.; Shea, J. E.; Bowers, M. T., The amyloid formation mechanism in human IAPP: Dimers have beta-strand monomer-monomer interfaces. *J. Am. Chem. Soc.* **2011**, *133* (19), 7240-7243.

161. Cheng, B. A.; Liu, X. R.; Gong, H.; Huang, L. Q.; Chen, H.; Zhang, X.; Li, C. Z.; Yang, M. Y.; Ma, B. J.; Jiao, L. H.; Zheng, L.; Huan, K., Coffee components inhibit amyloid formation of human islet amyloid polypeptide in vitro: Possible link between coffee consumption and diabetes mellitus. *J. Agricul. Food Chem.* **2011**, *59* (24), 13147-13155.

162. Young, L. M.; Cao, P.; Raleigh, D. P.; Ashcroft, A. E.; Radford, S. E., Ion mobility spectrometry-mass spectrometry defines the oligomeric intermediates in amylin amyloid formation and the mode of action of inhibitors. *J. Am. Chem. Soc.* **2014**, *136* (2), 660-670.

163. Wei, L.; Jiang, P.; Xu, W. X.; Li, H.; Zhang, H.; Yan, L. Y.; Chan-Park, M. B.; Liu, X. W.; Tang, K.; Mu, Y. G.; Pervushin, K., The molecular basis of distinct aggregation pathways of islet amyloid polypeptide. *J. Biol. Chem.* **2011**, *286* (8), 6291-6300.

164. Williamson, J. A.; Loria, J. P.; Miranker, A. D., Helix stabilization precedes aqueous and bilayer-catalyzed fiber formation in islet amyloid polypeptide. *J. Mol. Bio.* **2009**, *393* (2), 383-396.

165. Abedini, A.; Raleigh, D. P., A role for helical intermediates in amyloid formation by natively unfolded polypeptides? *Phys. Biol.* **2009**, *6* (1), 15005

166. Kumar, S.; Walter, J., Phosphorylation of amyloid beta (A beta) peptides - A trigger for formation of toxic aggregates in Alzheimer's disease. *Aging* **2011**, *3* (8), 803-812.

Chapter 2. Role of aromatic interactions in amyloid formation by islet amyloid polypeptide

Abstract

Aromatic-aromatic and aromatic-hydrophobic interactions have been proposed to play a role in amyloid formation by a range of polypeptides including islet amyloid polypeptide. IAPP contains three aromatic residues Phe-15, Phe-23, and Tyr-37. The ability of all single aromatic to leucine mutants, all double aromatic to leucine mutants and the triple leucine mutant to form amyloid were examined. Amyloid formation was almost twice as rapid for the F15L mutant relative to wild-type, but was almost three fold slower for the Y37L mutant and almost two fold slower for F23L mutant. Amyloid fibrils formed from each of the single mutants were effective at seeding amyloid formation by wild-type IAPP, implying that the fibril structures are similar. The F15L/F23L double mutant has a larger effect than the F15L/Y37L double mutant on the rate of amyloid formation, even though a Y37L substitution has more drastic consequences in the wild-type background than does the F23L mutation, suggesting non-additive effects between the different sites. The triple leucine mutant and the F23L/Y37L double mutant are the slowest to form amyloid. Phe-15 has been proposed to make important contacts early in the aggregation pathway, but the F15L mutant data indicates that they are not optimal. A set of variants containing natural and unnatural amino acids at position 15, which were designed to conserve hydrophobicity, but which alter α-helix and β- sheet propensity, were analyzed to determine the properties of this position that control the rate of amyloid formation. There is no correlation between β-sheet propensity at this position and the rate of amyloid formation, but there is a correlation with α-helical propensity.

NOTE: The material presented in this chapter has been published (Ling-Hsien Tu and Daniel P. Raleigh "Role of aromatic interactions in amyloid formation by islet amyloid polypeptide" *Biochemistry* **2013**, 52 (2), 333-342). This chapter contains direct excerpts from the manuscript, which was written by me with suggestions and revisions from Professor Daniel P. Raleigh.

2.1 Introduction

The details of amyloid formation are still not well understood, especially for those proteins that are intrinsically disordered in their monomeric states. Aromatic−aromatic interactions have been proposed to play an important role in amyloid formation, particularly for IAPP [1−3]. IAPP contains three aromatic residues, Phe-15, Phe-23, and Tyr-37 (Figure 2.1), and a triple aromatic to leucine mutant forms amyloid at a significantly reduced rate compared to that of the wild type [2]; however, the effects of single site substitutions or double mutations have not been examined. Phe to Tyr FRET studies suggest that aromatic residues may make contacts during the early stages of amyloid formation [4]. However, experiments with variants that contain the fluorescent Tyr analogue 4-cyanophenylalanine argue that the aromatic side chains remain solvated during the lag phase and suggest that aromatic−aromatic interactions involving Tyr-37 do not develop during the lag phase [5]. Thus, the role of the aromatic residues in amyloid formation by IAPP is not clear. In fact, the details of the early stages of IAPP amyloid formation are not well understood. This is a topic of current interest because intermediates along the pathway of amyloid formation may be the most toxic entities and could be targets for inhibitor design [6, 7]. The role of Phe-15 is particularly interesting because this position is believed to make contacts important for the initial oligomerization [8]. Here we examine a comprehensive set of aromatic to leucine mutants as well

as a set of F15 variants containing natural and unnatural amino acids that preserve hydrophobicity but alter secondary structure propensity to deduce the role aromatic residues play in amyloid formation by IAPP.

2.2 Materials and methods

2.2.1 Peptide synthesis and purification.

Peptides were synthesized on a 0.25 mmol scale using a CEM microwave peptide synthesizer and 9-fluorylmethoxycarbonyl (Fmoc) chemistry. Fmoc-protected pseudoproline dipeptide derivatives were incorporated at positions 9 and 10, 19 and 20, and 27 and 28 to facilitate the synthesis [9]. Solvents were ACS-grade. All other reagents were purchased from Advanced Chemtech, PE-Biosystems, Sigma, and Fisher Scientific. 5-(4′-Fmoc-aminomethyl-3′,5-dimethoxyphenol) valeric acid (PAL-PEG) resin was used to form an amidated C-terminus. Standard Fmoc reaction cycles were used. The first residue attached to the resin, β-branched residues, Arg, and all pseudoproline dipeptide derivatives were doubly coupled. The peptide was cleaved from the resin through the use of standard trifluoroacetic acid (TFA) methods. Crude peptides were partially dissolved in 20% acetic acid (v/v), frozen in liquid nitrogen, and lyophilized to increase their solubility. The dry peptide was dissolved in dimethyl sulfoxide (DMSO) at room temperature to promote the formation of the disulfide bond [10, 11]. The peptides were purified by reverse-phase high-performance liquid chromatography (HPLC) using a Vydac C18 preparative column (10 mm × 250 mm). A two-buffer gradient was used: buffer A consisting of 100% H_2O and 0.045% HCl (v/v) and buffer B consisting of 80% acetonitrile, 20% H_2O, and 0.045% HCl. HCl was used as the counterion instead of TFA to reduce the residual amount of TFA

because TFA can influence amyloid formation. Analytical HPLC was used to check the purity of peptides before use. Peptides were analyzed by mass spectrometry using a Bruker MALDI-TOF MS instrument to confirm the molecular weight: wild-type IAPP, expected 3903.3, observed 3902.1; F15-IAPP, expected 3871.3, observed 3872.0; F23-IAPP, expected 3871.3, observed 3871.3; Y37-IAPP, expected 3855.4, observed 3853.8; F15L/F23L-IAPP, expected 3835.3, observed 3834.0; F15L/Y37L-IAPP, expected 3821.3, observed 3819.8; F23L/Y37L-IAPP, expected 3821.3, observed 3820.0; 3XL-IAPP, expected 3787.2, observed 3785.1; F15I-IAPP, expected 3871.3, observed 3871.5; F15NLe-IAPP, expected 3871.3, observed 3872.1; F15TLe-IAPP, expected 3871.3, observed 3872.0.

2.2.2 Sample preparation.

A 1.6 mM peptide solution was prepared in 100% hexafluoro-2-propanol (HFIP) and stored at −20 °C. Stock solution was filtered using a 0.45 μm GHP Acrodisc 13 syringe to remove preformed aggregates. For the seeding assays, preformed wild-type IAPP and single mutant fibrils were produced from kinetic experiments. The solution was incubated, and thioflavin-T fluorescence was monitored to ensure fibril formation had occurred. Seeds were used within 12 h to ensure reproducibility.

2.2.3 Thioflavin-T fluorescence assays.

Fluorescence experiments were performed on an Applied Phototechnology fluorescence spectrophotometer using an excitation wavelength of 450 nm and an emission wavelength of 485 nm. The excitation and emission slits were set at 6 nm, and a 1.0 cm cuvette was used. Solutions were prepared by diluting the filtered stock into Tris buffer and thioflavin-T solution immediately before the measurement. The final concentrations were 16 μM peptide and 32 μM thioflavin-T in

2% HFIP and 20 mM Tris buffer (pH 7.4) for all experiments. All solutions were stirred during the fluorescence experiments to maintain homogeneity. Stirring is known to accelerate IAPP amyloid formation. For the seeding assays, 1.6 mM peptide stock solutions in HFIP were diluted into the seeded buffer solution to give final concentrations of 16 μM peptide, 32 μM thioflavin-T, 1.6 μM seed (in monomer units), and 2% HFIP in pH 7.4, 20 mM Tris buffer For kinetic experiments without HFIP, solutions were prepared by adding pH 7.4, 20 mM Tris buffer containing thioflavin-T to lyophilized dry peptides for a final peptide concentration of 16 μM. These studies were conducted using a Beckman Coulter DTX880 plate reader without stirring.

2.2.4 Circular dichroism (CD) experiments.

CD experiments were performed using an Applied Photophysics Chirascan CD spectrometer. The solutions for the CD experiments were prepared by diluting the filtered stock peptide solutions into 20 mM Tris buffer (pH 7.4). The final peptide concentration was 16 μM in 2% HFIP. Spectra were recorded from 190 to 260 nm at 1 nm intervals in a quartz cuvette with a 0.1 cm path length at 25 °C. CD experiments used the same stock solutions as the thioflavin-T fluorescence measurements. A background spectrum was subtracted from the collected data.

2.2.5 *Transmission electron microscopy (TEM).*

TEM was performed at the Life Science Microscopy Center at Stony Brook University. Samples were aliquots from the same solutions that were used for the fluorescence measurements. 5 uL of the peptide solution was placed on a carboncoated Formvar 300 mesh copper grid for 1 min and then negatively stained with saturated uranyl acetate for 1 min.

2.3 Results and discussion

2.3.1 Analysis of amyloid formation by aromatic to Leu variants.

The sequence of IAPP and the solid-state NMR-derived model of IAPP amyloid protofibrils [12] are shown in Figure 2-1. The molecule contains three aromatic residues. Phe-15 and Tyr-37 are conserved among all known IAPP sequences; Phe-23 is not, but it is substituted with only leucine (Figure 1-6). A set of seven aromatic to leucine variants were prepared: all three single mutants, the complete set of double mutants, and the triple mutant. Leu was used because it is the closest natural nonaromatic substitution for Tyr and Phe in terms of size and hydrophobicity. An additional set of variants was prepared to examine the role of Phe-15 in detail. The rate of amyloid formation was measured using fluorescence-detected thioflavin-T binding assays. Thioflavin-T is a small dye whose quantum yield is enhanced when it binds to amyloid fibrils [13]. The molecule is believed to bind to grooves on the surface of the amyloid fibrils. Thioflavin-T assays reliably report on IAPP amyloid formation kinetics, and the compound does not alter the aggregation kinetics under the conditions used here [5]. Amyloid formation by IAPP follows a sigmoidal time course in which no detectable amyloid fibrils are formed during the lag phase. The lag phase is followed by a growth phase during which fibrils develop and elongate, eventually leading to a steady state where fibrils are in equilibrium with soluble protein. Thioflavin-T curves for the wild type and single mutants are displayed in Figure 2-2A, and the data for the double and triple mutants are shown in Figure 2-2B. Amyloid formation by wild-type IAPP is rapid under the conditions of these experiments (2% HFIP, 20 mM Tris buffer, pH 7.4, and constant stirring). IAPP amyloid formation has been widely studied by dilution from HFIP, and we chose this protocol to facilitate comparison to earlier studies. Additional studies, described below, were performed without HFIP. The kinetic analysis reveals a number of interesting features. All of the mutants, with the exception

of F15L-IAPP, show a decreased rate of amyloid formation and an increased lag time. In contrast, replacement of Phe-15 accelerates amyloid formation, decreasing the lag time by a factor of almost 2. Phe-15 has been proposed to be involved in the early steps of amyloid formation, but the data show that the Phe-15 is not the optimal residue at this site in terms of amyloid formation. The role of Phe-15 is considered in more detail below. The other single mutants form amyloid more slowly with the most pronounced effect observed for the Tyr-37 to Leu mutant, which has a lag time that is a factor of 3 longer than that of wild-type IAPP. The lag time for F23L-IAPP is almost 2-fold longer than that of the wild-type. The F15L/Y37L double mutant forms amyloid more rapidly than the Y37L single mutant, but more slowly than the wild type, indicating that the acceleration caused by the Phe-15 substitution partially compensates for the slowing caused by the Tyr-37 to Leu replacement. The other mutants are much slower in forming amyloid than wild-type IAPP. F15L/F23L-IAPP is 4-fold slower, while F23L/Y37L-IAPP and 3XL-IAPP are ~7.5-fold slower. The lag times and t_{50} values for all of the mutants are listed in Table 2.1. T_{50} is the time required to reach half the final intensity in a thioflavin-T assay and is commonly used as a quantitative measure of amyloid formation. The differences observed for t_{50} values and the lag times between different peptides are much larger than the experimental uncertainty. For example, analysis of a set of 25 independent measurements conducted on wild-type IAPP over the course of two years with more than five separate batches of peptide yielded a standard deviation in t_{50} of <20% (Figure 2-3). The calculated standard deviations for independent measurements conducted on an individual batch of peptide are even smaller, <10% in all cases and often significantly smaller. TEM images of aliquots removed at the end of each kinetic run confirm the presence of extensive amyloid fibrils (Figure 2-4). CD confirms the presence of β-sheet structure in all samples (Figure 2-5). The differences in the rates of amyloid formation are unlikely to be due to small variations in

concentration from sample to sample, because the lag time for amyloid formation by IAPP has been shown to be largely independent of peptide concentration for the conditions (2% HFIP with constant stirring) and concentrations used here [14]. Small changes in pH can affect the rate of amyloid formation by IAPP because the lag time depends on the protonation state of His-18 and the N terminus [15]; however, all samples were at the same pH to within 0.1 pH unit. Control experiments with wild-type IAPP show that the lag time varies by only 10% between pH 7.2 and 7.6 in the buffer used here. This variation in pH is much wider than that observed in our experiments, and the effect on the lag time in the control studies is much weaker than the differences in the lag times observed for the different mutants. Variations in the final HFIP concentration can also alter the rate of amyloid formation, but the HFIP concentration was fixed at 2% (v/v). We also plotted the kinetic data as normalized fluorescence intensity versus normalized time, t/t_{50} of wild-type, to facilitate a comparison of the shape of the kinetic progress curves of the mutants with that of the wild type (Figure 2-6). The normalized curves for wild-type IAPP, F15L-IAPP, F23LIAPP, and F15L/F23L-IAPP are very similar in shape. This is consistent with the mutants and wild-type IAPP having a similar mode of assembly but does not prove that they do. The normalized curve for F15L/Y37L-IAPP shows some differences relative to that of the wild type in the early stage of fibril formation, while the normalized plot for Y37L-IAPP has a slight difference in the growth phase. The F23L/Y37L-IAPP and 3XL-IAPP mutants have the slowest rates of amyloid formation and display the largest differences in normalized progress curves.

2.3.2 The single mutants form amyloid fibrils that are similar to wild-type fibrils.

TEM and CD studies outlined above suggest that the morphologies of the fibrils formed by wild-type IAPP and the mutants are similar. We investigated the structural similarity between wild-type

and mutant fibrils in more detail by conducting seeding experiments. Preformed amyloid fibrils can serve as a template for the addition of monomers, resulting in a bypassing of the lag phase. Seeding is usually much more effective when fibrils are used as seeds for their own monomers [16, 17]. We first examined seeding of wild-type IAPP by wild-type fibrils (Figure 2-7, gray curve). A bypass of the lag phase was observed as expected. We then tested the ability of preformed F15L-IAPP, F23L-IAPP, and Y37L-IAPP amyloid fibrils to seed wild-type IAPP (Figure 2-7, red, blue, and green curves). The curves perfectly overlap with the curve from the wild-type seeding study, showing that the mutant fibrils seed wild-type IAPP efficiently. This argues that the single-mutant fibrils share significant structural similarity with wild-type fibrils.

2.3.3 Nonadditive effects on amyloid formation are observed between different sites.

The effect of some of the double mutations is not equal to the additive effect of the two individual mutations (Figure 2-8). For a simple protein folding reaction, nonadditive effects can be detected by comparing the effect of mutations on folding rate constants. Independent effects will lead to additive effects on the log of the folding rate or multiplicative effects on the rate constants. Amyloid formation is more complex, involving multiple steps and possible parallel pathways with heterogeneous intermediates; thus, it is not possible to readily relate a simple thioflavin-T progress curve to microscopic rate constants. Nonetheless, a semiquantitative comparison can be obtained using values of t_{50} or the length of the lag phase. We first analyzed the effect caused by a single mutation relative to the wild type by calculating the ratio of the t_{50} of the single mutant to the t_{50} of the wild type. The expected additive effects (stars in Figure 2-8) are estimated by multiplying the parameters calculated for two single mutations. Assuming independent additive effects, the F15L/F23L double mutant is expected to form amyloid on the same time scale as or even slightly faster than the wild type. However, the value of t_{50} for the

F15L/F23L double mutant is 4-fold larger than the wild-type t_{50}. The F15L/Y37L double mutant forms amyloid close to the rate expected if the effect of the Phe-15 mutation and the effect of the Tyr-37 mutation are additive. The F23L/Y37L double mutant has the most significant effect on the rate of amyloid formation (7.2-fold larger than that of the wild type), but the effect is even greater than expected from simple additivity (4.8-fold). To summarize, both the F15L/F23L and F23L/Y37L double mutants form amyloid more slowly than predicted from simple additive effects, with the largest deviation observed for the F15L/F23L double mutant.

2.3.4 Sensitivity of position 15 to amyloid formation.

F15L-IAPP is a rare example of a mutation that accelerates amyloid formation. This region of IAPP has been proposed to be involved in the early stages of oligomerization [8], and it is of interest to determine the properties of this site that impact the rate of amyloid formation. Secondary structure propensity is likely a key feature. Work from several groups suggests that helical intermediates are important in the pathway of IAPP fibrillation [8, 18−23]. For example, crystallographic studies of IAPP fused to MBP showed that the segments corresponding to residues 8−18 and 22−27 are helical in the construct [8]. NMR studies have shown that human and rat IAPP have a tendency to preferentially sample helical ϕ and ψ angles between residues 8 and 22 in the monomeric state [18]. These observations have led to models that postulate that initial oligomerization is driven by the thermodynamic linkage between helix formation and self-association [18, 20−23]. Phe-15 is within the putative helical region and has been proposed to make important contacts during the early stages of amyloid formation [8, 24]. We prepared a series of variants with isomeric four-carbon side chains at position 15 to probe the factors that control amyloid formation. We compared the effects of Leu, norleucine (four-carbon unbranched side chain), Ile, and tert-leucine (tertbutyl side chain) on amyloid formation (Figure 2-9A). These

amino acids have side chains with similar hydrophobicities [25], but different α-helix and β-sheet propensities (Table 2-2). The substitutions have significantly different effects upon the kinetics of amyloid formation (Figure 2-9B and 2-9C). The Phe-15 to *tert*-leucine variant, F15TLe-IAPP, which has three methyl groups on the β-carbon, takes much longer to form amyloid than the wild type (Figure 2-9B, purple), even though TLe has the highest β-sheet propensity [26−28]. The F15I-IAPP mutant (Figure 2-9C, green curve), with its β-branched side chain, also forms amyloid more slowly than wild-type IAPP, F15L-IAPP, or the F15 to norleucine mutant (F15NLe-IAPP), even though Ile has a higher β-sheet propensity. TEM images confirm that all of the Phe-15 variants form amyloid fibrils and have a morphology similar to that of wild-type fibrils (Figure 2-10). Seeding experiments were used to further probe the structure of the amyloid fibrils formed by the variants. Each variant was as efficient at seeding amyloid formation by wild-type IAPP as were wild-type seeds (Figure 2-11), arguing that the structures of the mutant fibrils are similar to wild-type fibrils. The data show that the rate of amyloid formation does not correlate with β-sheet propensity at this position even though residue 15 is located in a β-strand in all known models of IAPP amyloid fibrils [12, 28]. There is a stronger correlation with α-helical propensity. TLe has by far the lowest α-helical propensity [26, 30], and this variant is by far the slowest to form amyloid. Ile has the second lowest helical propensity, and the Ile variant is the second slowest to form amyloid. Phe, the wild-type residue, Leu, and NLe have relatively high α-helical propensities, and these variants form amyloid more rapidly. Earlier work, using truncated variants of IAPP, has shown that replacement of Phe-15 with Ser or Ala increases the rate of amyloid formation [8]. Both of these residues have higher helical propensity than Phe.

2.3.5 The effect of Phe-15 substitutions upon amyloid formation is independent of the presence of HFIP.

HFIP and other fluoridated alcohols accelerate amyloid formation by IAPP, and even low levels of fluoridated alcohol co-solvent can promote helix formation [14, 15]. We examined the set of Phe-15 variants in the absence of HFIP to ensure that the results were not biased by the presence of the co-solvent. The lag times for wild-type IAPP and the Phe-15 variants range from hours to days without HFIP and without stirring. The order of fibril formation by wild-type IAPP and the Phe-15 variants is the same in the presence or absence of HFIP (Figure 2-12 and Table 2-3). TLe, with the lowest α-helical propensity and highest β-sheet propensity, takes the longest time to form amyloid fibrils, while the Ile variant has a longer lag phase and longer growth phase than the wild type. Variants with unbranched side chains at position 15 form amyloid faster. We also compared the three single aromatic to leucine mutants in the absence of HFIP and found the same rank order as observed in 2% HFIP; F15L-IAPP formed amyloid more rapidly than the wild type, while both F23L-IAPP and Y37L-IAPP did so more slowly than the wild type, with Y37L-IAPP being the slowest (Table 2-3). These experiments confirm that the results are not an artifact of solvent composition.

2.4 Conclusions

The data presented here reveal that the three aromatic residues make different contributions to IAPP amyloid assembly kinetics, with the Tyr-37 substitution having the largest effect. Apparent nonadditive effects were observed between Phe-15 and Phe-23 and between Phe-23 and Tyr-37. The effects should be interpreted with caution because, as noted, amyloid formation is a complex process involving multiple steps and the analysis of nonadditive interactions is less straightforward than analysis of the simple folding of globular proteins. Nontheless, the results are significant, with

the strongest effect observed between Phe-15 and Phe-23. Phe-23 is located in a region proposed to be important for the early stages of the development of β-sheet structure [31], while Phe-15 has been suggested to be involved in early stages of oligomerization. The observation of nonadditivity might reflect synergy between these processes. *p*-Cyanophenylalanine Tyr FRET measurements argue that Phe-23 and Tyr-37 do not make persistent contacts in the lag phase beyond any formed in the dead time of kinetic measurements [5]. Thus, any nonadditive interactions between Phe-23 and Tyr-37 are unlikely to result from long-lived direct contacts formed in the lag phase. It is worth noting that the relative deviation from simple additive behavior is smaller for this pair than for the duo of Phe-15 and Phe-23. The two residues are distant from each other in an individual chain; however, the supermolecular structure of the protofibrils brings Phe-23 in one chain close to Tyr-37 in the adjacent stack of monomers (Figure 2-1), and this might account for nonadditivity. The Phe-23C_β to Tyr-37C_β distances are 12.2 ± 3.5 Å in the NMR-based model of IAPP amyloid. Phe-15 is within the region proposed to be important for early contact formation during IAPP oligomerization, and several groups have proposed that the initial events involve helix formation with the region of residues 8−20 or 8−22 [8, 20, 21, 23]. In this model, initial association is driven by the thermodynamic linkage between helix formation and oligomerization. Our analysis of the effect of substitutions at position 15 is broadly consistent with this model because the substitutions with high β-sheet propensity, but low α-helical propensity, have longer lag phases than the wild type. Substitutions with high α-helical propensity and lower β-sheet propensity form amyloid more rapidly with shorter lag phases. It is interesting to compare these results with a recent study of aromatic residues in the Alzheimer's Aβ peptide [32]. Aβ contains a pair of adjacent Phe residues at positions 19 and 20. The peptide still forms amyloid if both are replaced with Leu or Ile, indicating that aromatic side chains are not required at these sites. These substitutions have the

opposite effect in Aβ compared to IAPP; faster amyloid formation was observed for the substitution that increased β-sheet propensity (Ile) compared to the one that lowered β-sheet propensity (Leu). In a separate study, the consequences of a series of substitutions at position-19 were examined in a Aβ-GFP construct [33]. Amyloid formation was found to be dependent on the β-sheet propensity, with a higher β-sheet propensity correlating with enhanced aggregation, although no kinetic data were obtained. Aβ, like IAPP, has been proposed to populate a helical intermediate during amyloid formation *in vitro* [34]. Within this context, one can still rationalize the effects of Phe-19 mutations and Phe-19 and Phe-20 double mutations; perhaps the helical structure does not include this segment of Aβ, or perhaps helical structure in this portion of the chain introduces new interactions that slow aggregation.

2.5 Figures

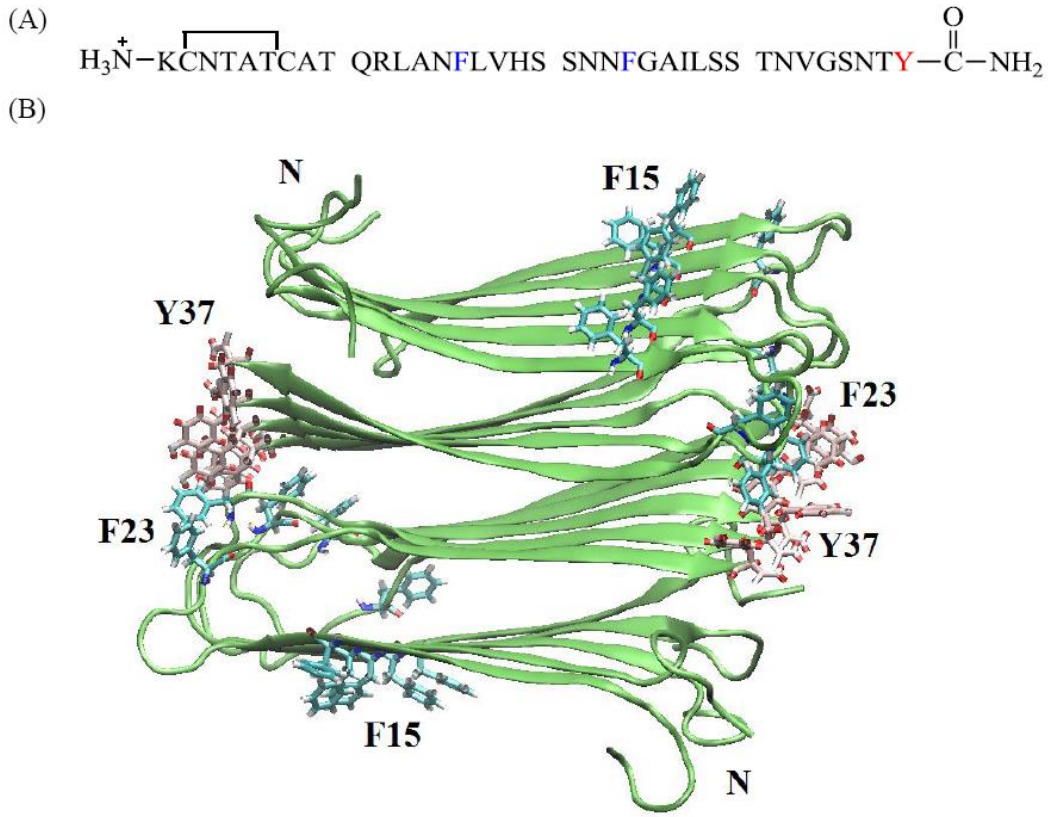

Figure 2-1: IAPP sequence and locations of aromatic residues in model of IAPP protofibrils. (A) Primary sequence of human IAPP. IAPP contains a disulfide bridge between residues 2 and 7. The C-terminus is amidated, and the N-terminus is free. The aromatic residues are colored in blue (Phe-15 and Phe-23) and red (Tyr-37). (B) Diagram of the solid-state NMR-derived model of IAPP protofibrils [26]. The aromatic residues and the N-terminus are labeled. Phe-23 (blue) and Tyr-37 (red) are colored differently as an aid to the eye.

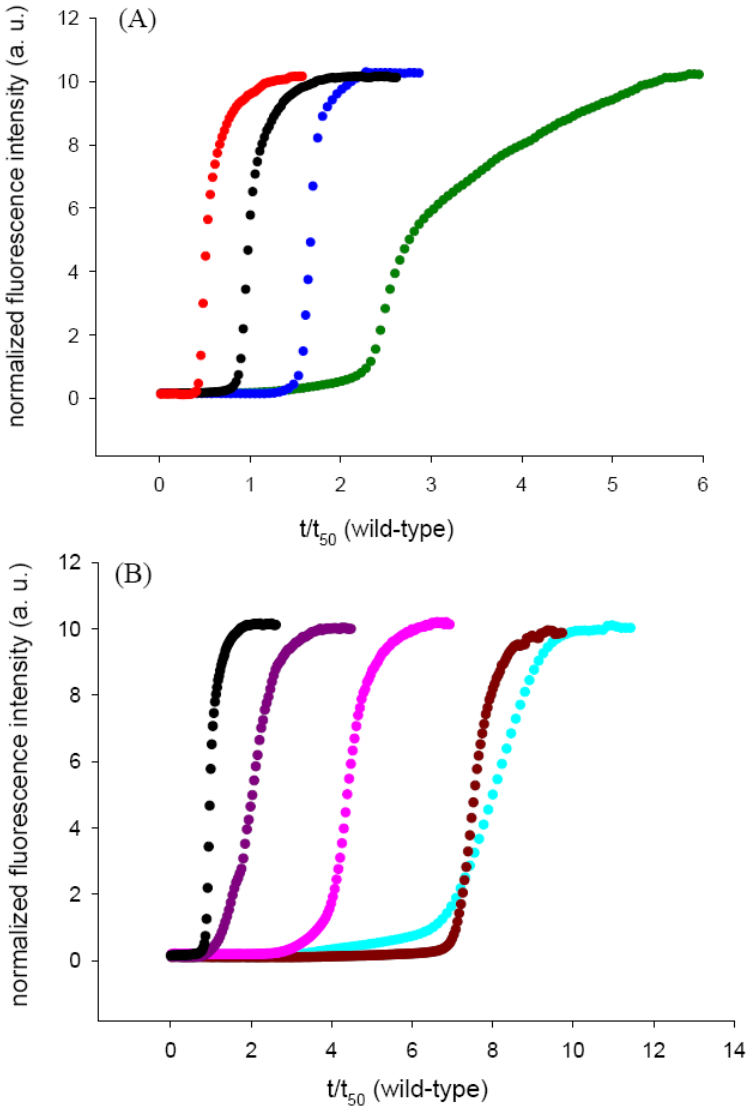

Figure 2-2: Substitution of the aromatic residues in IAPP alters the kinetics of amyloid formation. Thioflavin-T fluorescence-monitored kinetic experiments. (A) Single mutants compared to the wild type: black for wild-type IAPP, red for F15L-IAPP, blue for F23L-IAPP, and green for Y37L-IAPP. (B) Multiple mutants compared to the wild type: black, wild-type IAPP; purple, F15L/Y37L-IAPP; pink, F15L/F23L-IAPP; brown, F23L/Y37L-IAPP; and light blue, 3XL-IAPP. All experiments were conducted in pH 7.4, 20 mM Tris buffer and 2% HFIP with constant stirring at 25 °C.

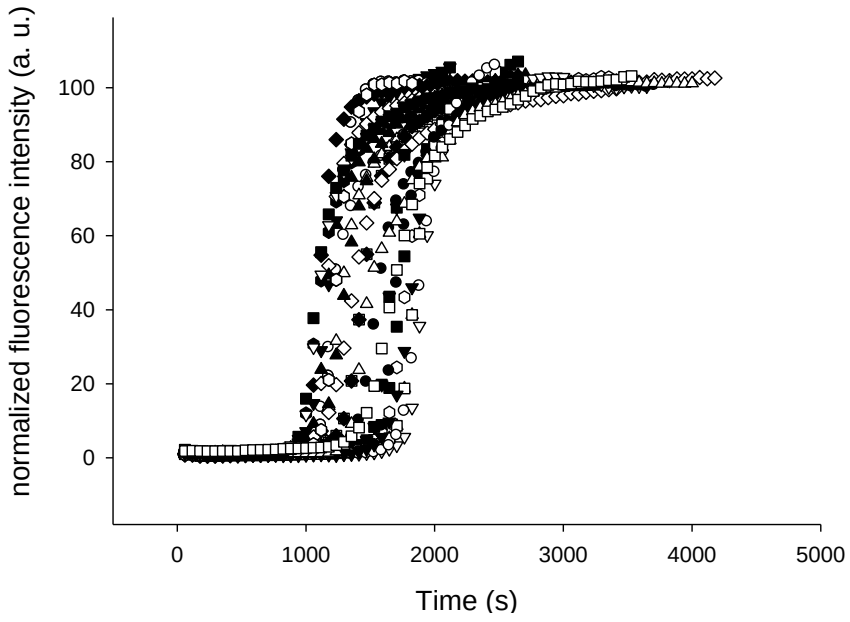

Figure 2-3: Comparison of 25 separate thioflavin-T fluorescence monitored kinetic experiments conducted on wild-type human IAPP. At least five different batches of peptide were examined over a two year time period. All the experiments were conducted under the same conditions, 25 ^{o}C, pH 7.4 20 mM Tris buffer, and 2% (v/v) HFIP with constant stirring.

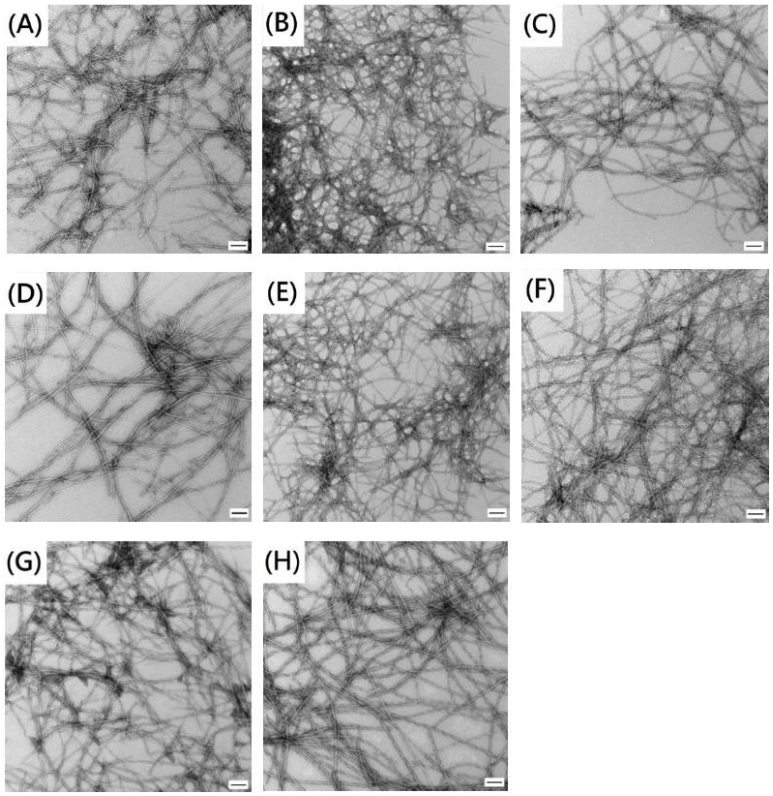

Figure 2-4: All aromatic mutants form amyloid. TEM images recorded at the end of the kinetic runs depicted in Figure 2-2: (A) wild-type IAPP, (B) F15L-IAPP, (C) F23L-IAPP, (D) Y37L-IAPP, (E) F15L/F23L-IAPP, (F) F15L/Y37L-IAPP, (G) F23L/Y37L-IAPP, and (H) 3XL-IAPP. Scale bars represent 100 nm.

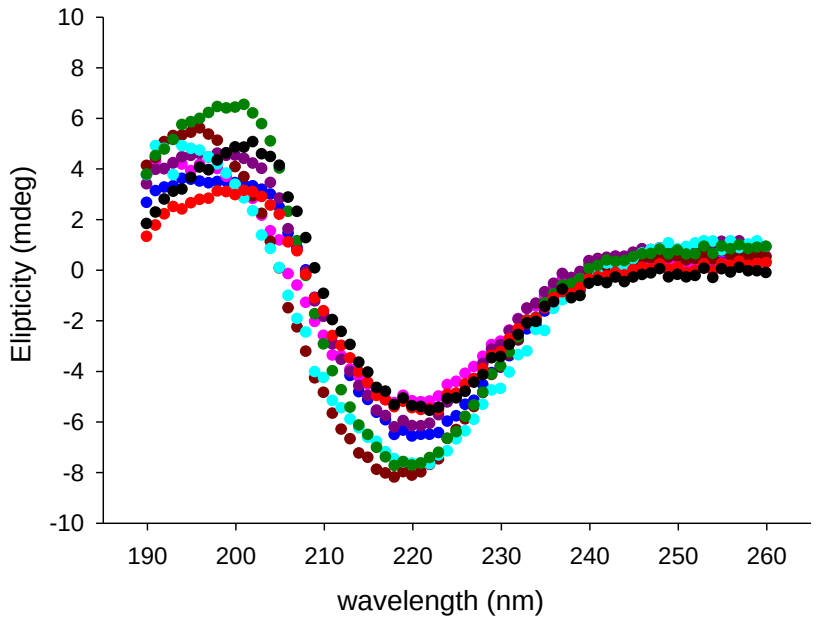

Figure 2-5: CD spectra collected at the end of the kinetic experiments shown in Figure 2-2. Black, wild-type IAPP; red, F15L-IAPP; blue, F23L-IAPP; green, Y37L-IAPP; pink, F15L/F23L-IAPP; purple, F15L/Y37L-IAPP; brown, F23L/Y37L-IAPP; light blue, 3XL-IAPP.

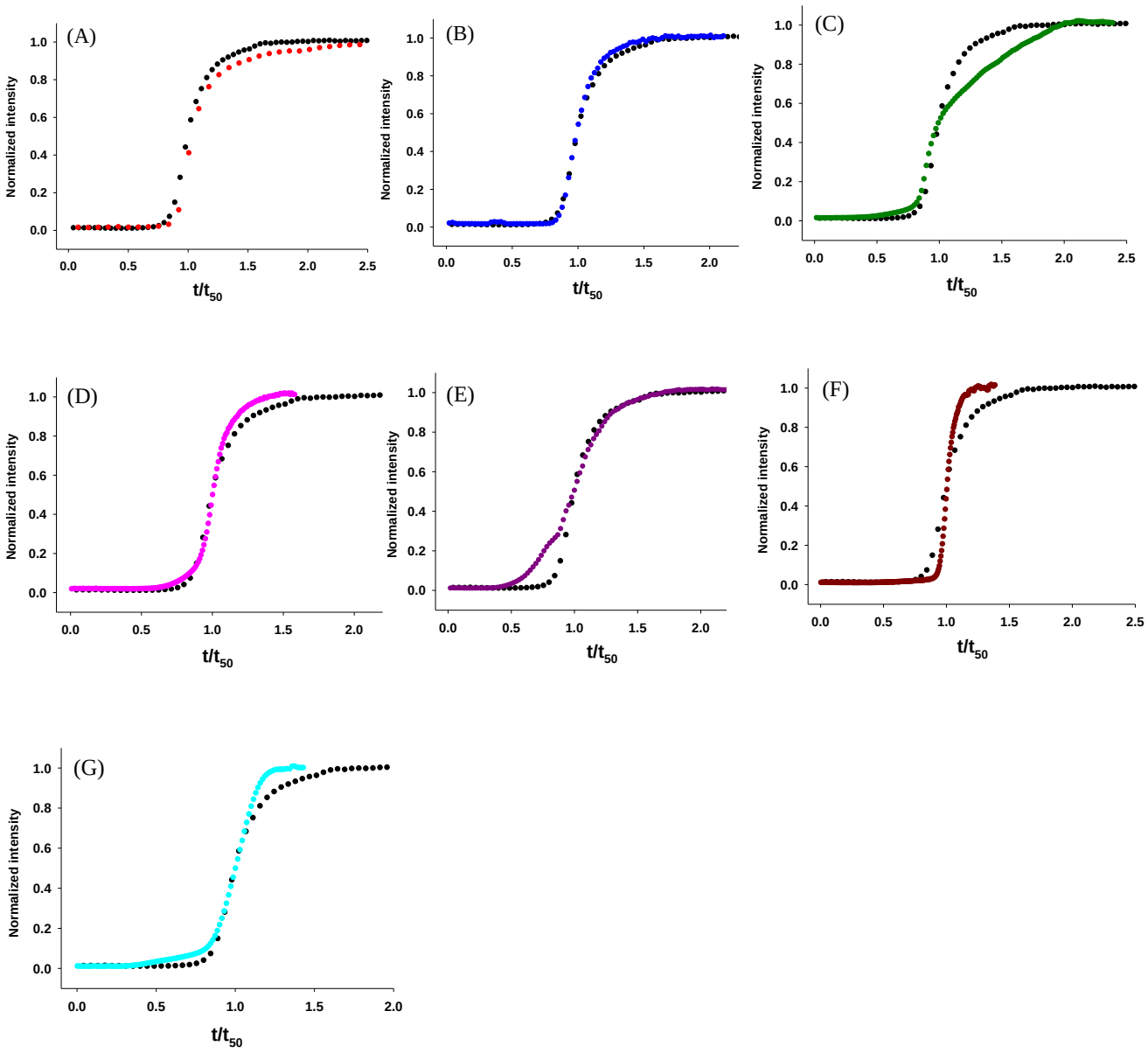

Figure 2-6: Comparison of normalized kinetic curves for reactions in 2% HFIP, pH 7.4 20 mM Tris buffer with constant stirring. The vertical scale is normalized such that the full scale is from 0 to 1.0 for each sample and the horizontal scale is t/t_{50}. (A) wild-type IAPP (black) and F15L-IAPP (red), (B) wild-type IAPP (black) and F23L-IAPP (blue), (C) wild-type IAPP (black) and Y37L-IAPP (green), (D) wild-type IAPP (black) and F15L/F23L-IAPP (pink), (E) wild-type IAPP (black) and F15L/Y37L-IAPP (purple), (F) wild-type IAPP (black) and F23L/Y37L-IAPP (brown), (G) wild-type IAPP (black) and 3XL-IAPP (light blue).

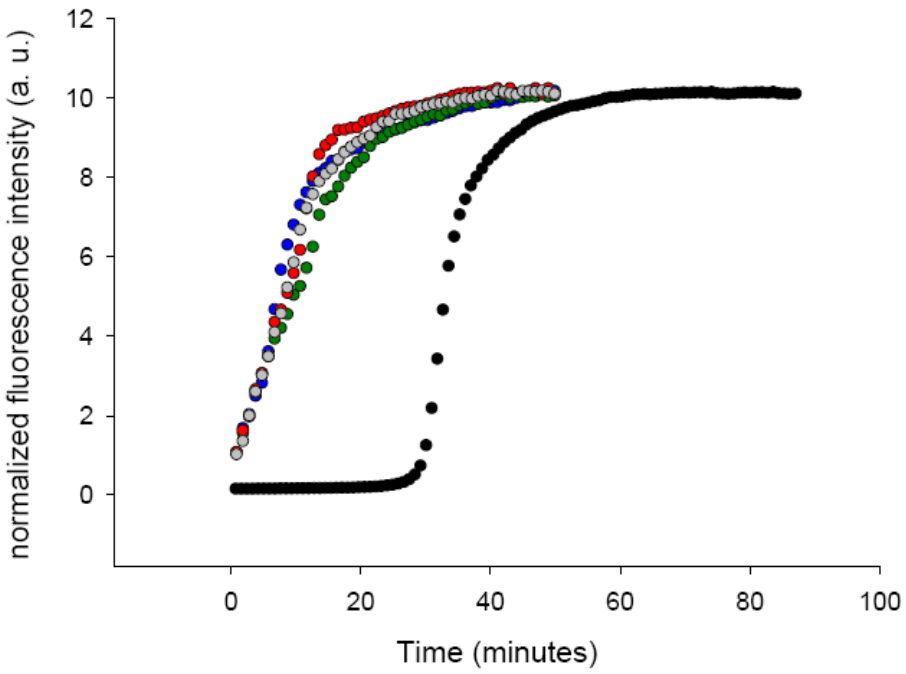

Figure 2-7: Aromatic mutants effectively seed amyloid formation by wild-type IAPP. Thioflavin-T fluorescence-monitored seeding experiments are shown: black for unseeded wild-type IAPP amyloid formation, gray for wild-type IAPP seeded by wild-type IAPP amyloid fibrils, red for wild-type IAPP seeded by F15L-IAPP amyloid fibrils, blue for wild-type IAPP seeded by F23L-IAPP amyloid fibrils, and green for wild-type IAPP seeded by Y37L-IAPP amyloid fibrils.

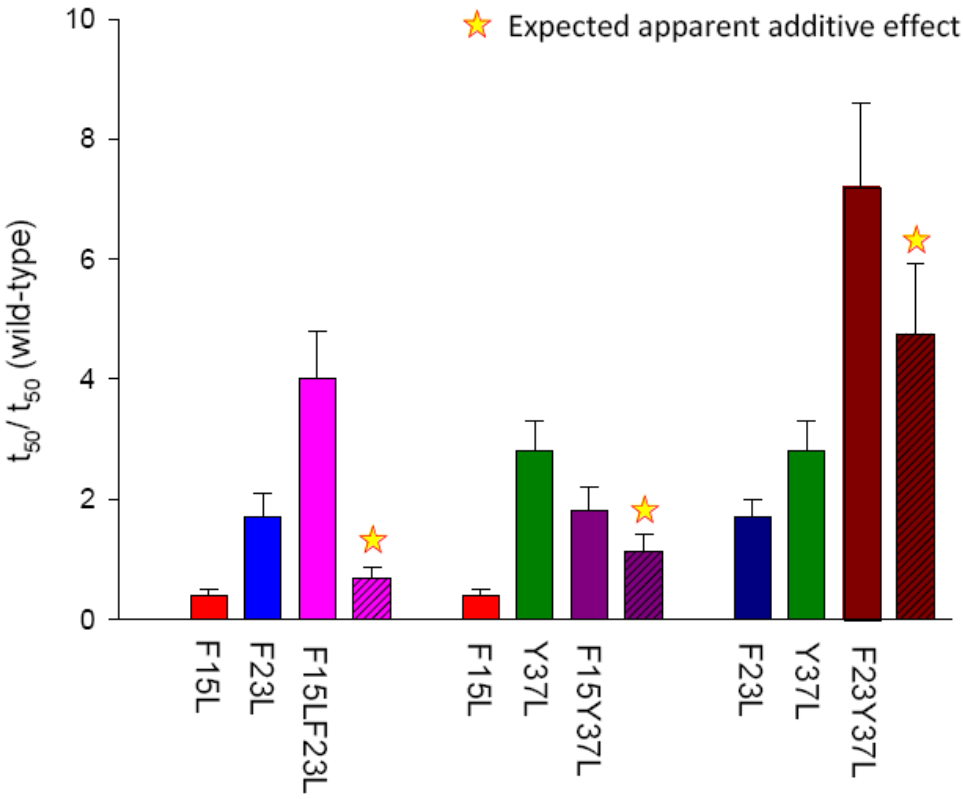

Figure 2-8: Nonadditive effects of double mutants. The bar graphs show the different effects caused by single mutants and the corresponding double mutants on amyloid formation. Stars denote the expected additive result. The uncertainties represent the standard deviations for experimental data and the propagated uncertainty for calculated values.

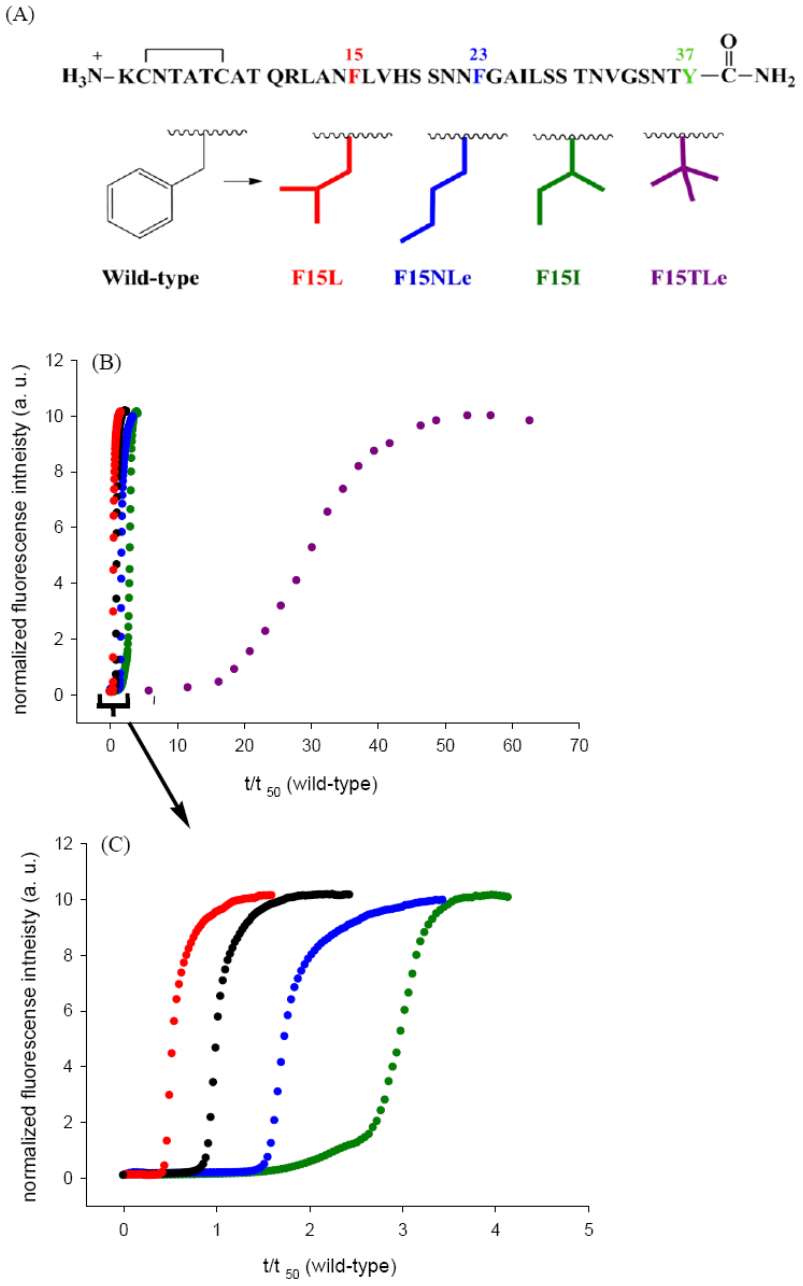

Figure 2-9: The rate of amyloid formation is affected by substitution at position 15, but there is no correlation with β-sheet propensity. (A) A series of variants with isomeric four-carbon side chains were analyzed. These "mutations" change α-helix propensity and β-sheet propensity but maintain hydrophobicity. (B) Thioflavin-T fluorescence-monitored kinetic experiments: black for wild-type IAPP, red for F15L-IAPP, blue for F15NLe-IAPP, green for F15I-IAPP, and purple for F15TLe-IAPP. (C) Enlarged plot covering the range of t/t_{50} (wild-type) from 0 to 5.

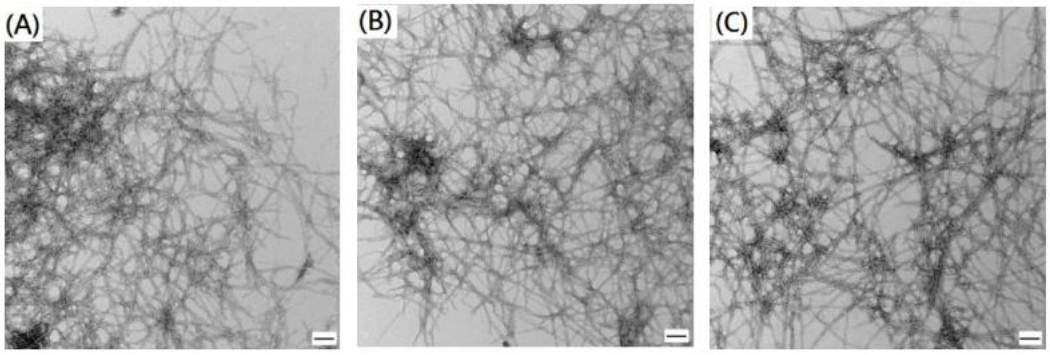

Figure 2-10. All position 15 variants form amyloid. TEM images recorded at the end of the kinetic runs depicted in Figure 2-9: (A) F15NLe-IAPP, (B) F15I-IAPP, and (C) F15TLe-IAPP. Scale bar represents 100 nm.

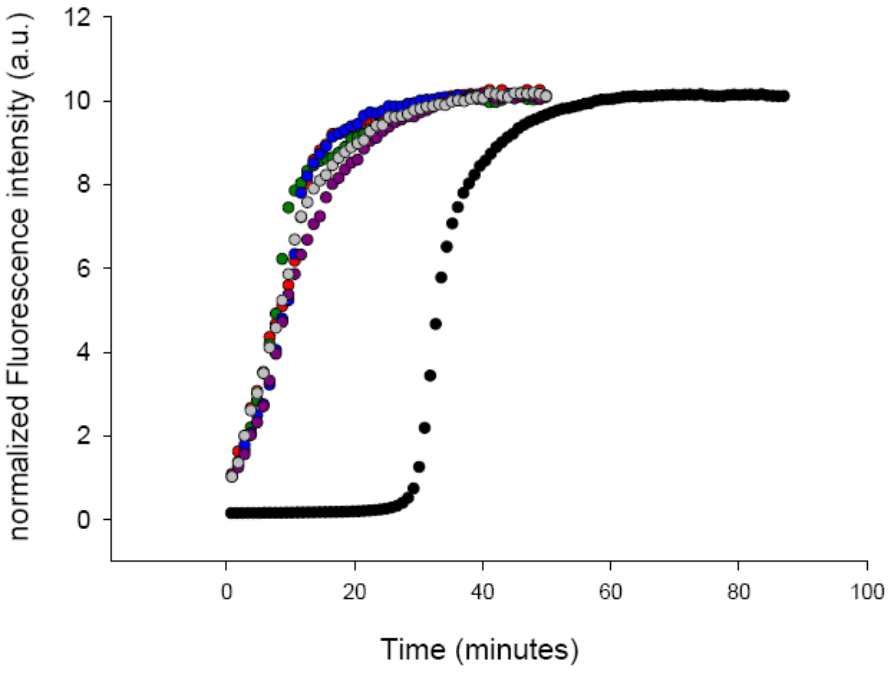

Figure 2-11: Position 15 variants effectively seed amyloid formation by wild-type IAPP. The results of thioflavin-T fluorescence-monitored seeding experiments are shown: black for unseeded wild-type IAPP amyloid formation, gray for wild-type IAPP seeded by wild-type IAPP amyloid fibrils, red for wild-type IAPP seeded by F15L-IAPP amyloid fibrils, blue for wild-type IAPP seeded by F15NLe-IAPP amyloid fibrils, green for wild-type IAPP seeded by F15I-IAPP amyloid fibrils, and purple for wild-type IAPP seeded by F15TLe-IAPP amyloid fibrils.

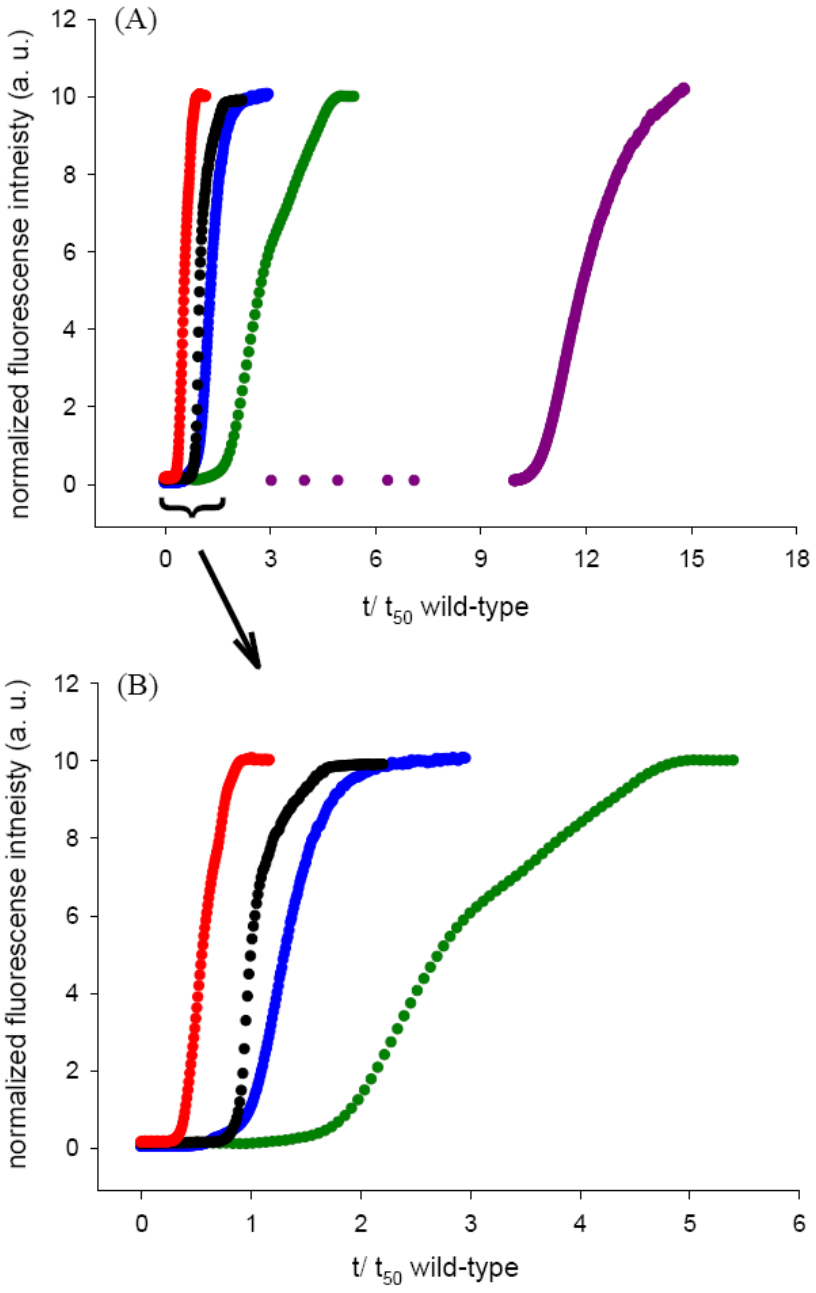

Figure 2-12: Rank order of amyloid formation by the F15 variants is independent of HFIP. (A) Thioflavin-T fluorescence-monitored kinetic experiments in the absence of HFIP without stirring. The final peptide concentration is 16 μM in 20 mM Tris buffer (pH 7.4): black for wild-type IAPP, red for F15L-IAPP, blue for F15NLe-IAPP, green for F15I-IAPP, and purple for F15TLe-IAPP. (B) Enlarged plot covering the range of t/t_{50} (wild-type) from 0 to 6.

2.6 Tables

peptide	Lag time[a] (s)	t_{50}[b] (s)	lag time/ wild-type lag time	t_{50}/ t_{50} of wild-type
Wild-type	1310±280[c]	1470±280		
F15L-IAPP	490±50	640±40	0.4±0.1[d]	0.4±0.1
F23L-IAPP	2230±220	2470±220	1.7±0.4	1.7±0.3
Y37L-IAPP	2790±90	4160±100	2.1±0.5	2.8±0.5
F15L/F23L-IAPP	5100±60	5850±30	3.9±0.8	4.0±0.8
F15L/Y37L-IAPP	1790±140	2650±100	1.4±0.3	1.8±0.4
F23L/Y37L-IAPP	9670±150	10600±500	7.4±1.6	7.2±1.4
3XL	9210±260	10950±250	7.0±1.5	7.4±1.4

[a]. The lag time is defined here as the time required to reach 10% of the final fluorescence change in the thioflavin-T assays. [b]. t_{50} is the time required to reach 50% of the final fluorescence change in the thioflavin-T assays. [c]. The quoted uncertainty is the standard deviation. [d]. The uncertainty was determined by standard propagation of error.

Table 2-1: Comparison of kinetic parameters for wild-type IAPP and aromatic to leucine mutants. Experiments performed at 25 °C and pH 7.4 in 20 mM Tris buffer and 2% (v/v) HFIP with constant stirring.

	Π[a]	Volume (Å^3)[b]	P_α[c]	P_β[d]
Phe	1.79	105.9	< Leu, NLe	1.43
Leu	1.70	92.7	0.75	1.1
Ile	1.80	92.4	0.56	1.71
NLe	1.70	93.0	0.85	< Phe
TLe	1.51	94.0	0.15	>Phe

[a]. Hydrophobicity of amino acids [25]. [b]. Molecular volumes of amino acids side chain based on Chem 3D ultra 9.0 calculations. [c]. α-helix propensity of amino acids [26, 30] [d]. β-sheet propensity of amino acids [26-28].

Table 2-2: Values for amino acid hydrophobicity, side chain volume, α-helix propensity, and β-sheet propensity.

(A) peptide	wild-type	F15L	F23L	Y37L	F15NLe	F15I	F15TLe
lag time (h)	16±1.3[a]	9.8±0.1	38±0.6	42±2.3	20±1.7	41±2.3	267±4
t_{50} (h)	23±0.9	11±0.1	42±1.7	63±2.8	31±1.3	61±5.8	276±6

(B) mutant	HFIP	F15L	F23L	Y37L	F15NLe	F15I	F15TLe
lag time/ wild-type lag time	present	0.4 ±0.08[b]	1.7±0.4	2.1±0.5	1.9±0.4	2.3±0.5	22±5
t_{50}/ t_{50} of wild-type	present	0.4±0.08	1.7±0.3	2.8±0.5	1.8±0.4	2.9±0.6	28±6
lag time/ wild-type lag time	absent	0.6±0.08	2.4±0.2	2.6±0.3	1.3±0.1	2.6±0.3	17±1.4
t_{50}/ t_{50} of wild-type	absent	0.5±0.02	1.8±0.1	2.7±0.2	1.3±0.1	2.7±0.3	12±0.5

[a]. The quoted uncertainty is the standard deviation. [b]. The uncertainty was calculated by standard propagation of error.

Table 2-3: (A) Kinetic parameters for wild-type IAPP, single aromatic to Leu mutants, and Phe-15 variants for amyloid Formation in the absence of HFIP and (B) comparison of kinetic parameters normalized with respect to the wild-type for single aromatic to Leu mutants and Phe-15 variants in the presence and absence of HFIP. Experiments were conducted at 25 °C and pH 7.4 in 20 mM Tris buffer in the presence and absence of HFIP.

2.7 References

1. Gazit, E., A possible role for pi-stacking in the self-assembly of amyloid fibrils. *Febs. J.* **2002**, *16* (1), 77-83.

2. Marek, P.; Abedini, A.; Song, B. B.; Kanungo, M.; Johnson, M. E.; Gupta, R.; Zaman, W.; Wong, S. S.; Raleigh, D. P., Aromatic interactions are not required for amyloid fibril formation by islet amyloid polypeptide but do influence the rate of fibril formation and fibril morphology. *Biochemistry* **2007**, *46* (11), 3255-3261.

3. Tracz, S. M.; Abedini, A.; Driscoll, M.; Raleigh, D. P., Role of aromatic interactions in amyloid formation by peptides derived from human amylin. *Biochemistry* **2004**, *43* (50), 15901-15908.

4. Padrick, S. B.; Miranker, A. D., Islet amyloid polypeptide: Identification of long-range contacts and local order on the fibrillogenesis pathway. *J. Mol. Biol.* **2001**, *308* (4), 783-794.

5. Marek, P.; Mukherjee, S.; Zanni, M. T.; Raleigh, D. P., Residue-specific, real-time characterization of lag-phase species and fibril growth during amyloid formation: A combined fluorescence and IR study of *p*-cyanophenylalanine analogs of islet amyloid polypeptide. *J. Mol. Biol.* **2010**, *400* (4), 878-888.

6. Lorenzo, A.; Razzaboni, B.; Weir, G. C.; Yankner, B. A., Pancreatic-islet cell toxicity of amylin associated with type-2 diabetes-mellitus. *Nature* **1994**, *368* (6473), 756-760.

7. Butler, A. E.; Janson, J.; Bonner-Weir, S.; Ritzel, R.; Rizza, R. A.; Butler, P. C., beta-Cell deficit and increased beta-cell apoptosis in humans with type 2 diabetes. *Diabetes* **2003**, *52* (1), 102-110.

8. Wiltzius, J. J. W.; Sievers, S. A.; Sawaya, M. R.; Eisenberg, D., Atomic structures of IAPP (amylin) fusions suggest a mechanism for fibrillation and the role of insulin in the process. *Protein Sci.* **2009**, *18* (7), 1521-1530.

9. Abedini, A.; Raleigh, D. P., Incorporation of pseudoproline derivatives allows the facile synthesis of human IAPP, a highly amyloidogenic and aggregation-prone polypeptide. *Org. Lett.* **2005**, *7* (4), 693-696.

10. Tam, J. P.; Wu, C. R.; Liu, W.; Zhang, J. W., Disulfide bond formation in peptides by dimethyl-sulfoxide- Scope and applications. *J. Am. Chem. Soc.* **1991**, *113* (17), 6657-6662.

11. Abedini, A.; Singh, G.; Raleigh, D. P., Recovery and purification of highly aggregation-prone disulfide-containing peptides: Application to islet amyloid polypeptide. *Anal. Biochem.* **2006**, *351* (2), 181-186.

12. Luca, S.; Yau, W. M.; Leapman, R.; Tycko, R., Peptide conformation and supramolecular organization in amylin fibrils: Constraints from solid-state NMR, *Biochemistry* **2007**, 46 (47), 13505-13522.

13. Levine, H., Thioflavin-T interaction with synthetic Alzheimers-disease beta-amyloid peptides - Detection of amyloid aggregation in solution. *Protein Sci.* **1993**, *2* (3), 404-410.

14. Padrick, S. B.; Miranker, A. D., Islet amyloid: Phase partitioning and secondary nucleation are central to the mechanism of fibrillogenesis. *Biochemistry* **2002**, *41* (14), 4694-4703.

15. Abedini, A.; Raleigh, D. P., The role of His-18 in amyloid formation by human islet amyloid polypeptide. *Biochemistry* **2005**, *44* (49), 16284-16291.

16. O'Nuallain, B.; Williams, A. D.; Westermark, P.; Wetzel, R., Seeding specificity in amyloid growth induced by heterologous fibrils. *J. Biol. Chem.* **2004**, *279* (17), 17490-17499.

17. Krebs, M. R. H.; Morozova-Roche, L. A.; Daniel, K.; Robinson, C. V.; Dobson, C. M., Observation of sequence specificity in the seeding of protein amyloid fibrils. *Protein Sci.* **2004**, *13* (7), 1933-1938.

18. Williamson, J. A.; Miranker, A. D., Direct detection of transient alpha-helical states in islet amyloid polypeptide. *Protein Sci.* **2007**, *16* (1), 110-117.

19. Nanga, R. P. R.; Brender, J. R.; Xu, J. D.; Hartman, K.; Subramanian, V.; Ramamoorthy, A., Three-dimensional structure and orientation of rat islet amyloid polypeptide protein in a membrane environment by solution NMR spectroscopy. *J. Am. Chem. Soc.* **2009**, *131* (23), 8252-8261.

20. Abedini, A.; Raleigh, D. P., A critical assessment of the role of helical intermediates in amyloid formation by natively unfolded proteins and polypeptides. *Protein Eng. Des. Sel.* **2009**, *22* (8), 453-459.

21. Abedini, A.; Raleigh, D. P., A role for helical intermediates in amyloid formation by natively unfolded polypeptides? *Phys. Biol.* **2009**, *6* (1), 15005.

22. Cao, P.; Meng, F.; Abedini, A.; Raleigh, D. P., The ability of rodent islet amyloid polypeptide to inhibit amyloid formation by human islet amyloid polypeptide has important implications for the mechanism of amyloid formation and the design of inhibitors. *Biochemistry* **2010**, *49* (5), 872-881.

23. Williamson, J. A.; Loria, J. P.; Miranker, A. D., Helix stabilization precedes aqueous and bilayer-catalyzed fiber formation in islet amyloid polypeptide. *J. Mol. Biol.* **2009**, *393* (2), 383-396.

24. Gilead, S.; Wolfenson, H.; Gazit, E., Molecular mapping of the recognition interface between the islet amyloid polypeptide and insulin. *Angew. Chem. Int. Ed.* **2006**, *45* (39), 6476-6480.

25. Fauchere, J. L.; Charton, M.; Kier, L. B.; Verloop, A.; Pliska, V., Amino acid side chain parameters for correlation studies in biology and pharmacology. *Int. J. Pept. Protein Res.* **1988**, *32* (4), 269-278.

26. Paterson, Y.; Leach, S. J., Effect of side-chain branching on theoretically predicted conformational space available to amino-acid-residues. *Macromolecules* **1978**, *11* (2), 409-415.

27. Minor, D. L.; Kim, P. S., Measurement of the beta-sheet-forming propensities of amino-acids, *Nature* **1994**, *367* (6464), 660-663.

28. Street, A. G.; Mayo, S. L., Intrinsic beta-sheet propensities result from van der Waals interactions between side chains and the local backbone. *Proc. Natl. Acad. Sci. U.S.A.* **1999**, *96* (1), 9074-9076.

29. Wiltzius, J. J.; Sievers, S. A.; Sawaya, M. R.; Cascio, D.; Popov, D.; Riekel, C.; Eisenberg, D., Atomic structure of the cross-beta spine of islet amyloid polypeptide (amylin). *Protein Sci.* **2008**, *17* (9), 1467-1474.

30. Lyu, P. C.; Sherman, J. C.; Chen, A.; Kallenbach, N. R., Alpha-helix stabilization by natural and unnatural amino-acids with alkyl side-chains. *Proc. Natl. Acad. Sci. U.S.A.* **1991**, *88* (17), 5317-5320.

31. Shim, S. H.; Gupta, R.; Ling, Y. L.; Strasfeld, D. B.; Raleigh, D. P.; Zanni, M. T., Two-dimensional IR spectroscopy and isotope labeling defines the pathway of amyloid formation with residue-specific resolution. *Proc. Natl. Acad. Sci. U.S.A.* **2009**, *106* (16), 6614-6619.

32. Armstrong, A. H.; Chen, J.; McKoy, A. F.; Hecht, M. H., Mutations that replace aromatic side chains promote aggregation of the Alzheimer's A beta peptide. *Biochemistry* **2011**, *50* (19), 4058-4067.

33. de Groot, N. S.; Aviles, F. X.; Vendrell, J.; Ventura, S., Mutagenesis of the central hydrophobic cluster in Aβ 42 Alzheimer's peptide: Side-chain properties correlate with aggregation propensities, *Febs J.* **2006**, *273* (3), 658-668.

34. Kirkitadze, M. D.; Condron, M. M.; Teplow, D. B., Identification and characterization of key kinetic intermediates in amyloid beta-protein fibrillogenesis. *J. Mol. Biol.* **2001**, *312* (5), 1103

Chapter 3. Biophysical characterization of matrix metallopeptidase 9 (MMP9) IAPP cleavage products

Abstract

Prevention of IAPP accumulation via peptidases degradation is of interest and several enzymes in islets have been found to play a role in this process. Matrix Metallopeptidase 9 (MMP9) is one of the enzymes reported to be capable of degrading IAPP and subsequently limit amyloid formation. Here we used matrix-assisted laser desorption/ionization time-of-flight (MALDI-TOF) mass spectroscopy to identify MMP9 cleavage products and two cleavage sites were determined. The four resulting fragments of IAPP (1-15, 16-37, 1-25 and 26-37) were synthesized and their ability to form amyloid fibrils was evaluated via thioflavin-T binding assays, CD and TEM. Fragments 1-15, 1-25, and 26-37 are not amyloidogenic and do not alter amyloid formation by intact human IAPP. In contrast, fragment 16-37 can form amyloid by itself and accelerates IAPP amyloid formation. However, we demonstrate that MMP9 can inhibit fibril formation of fragment 16-37 by cleaving it into even smaller fragments.

3.1 Introduction

Several enzymes including neprilysin, matrix metalloproteinase (MMP) 2, MMP9, and insulin-degrading enzyme (IDE) have been studied for their role in IAPP aggregation [1-6]. However, the mechanism of cleavage of IAPP and prevention of IAPP amyloid formation by these enzymes is not fully determined. This chapter describes the studies of MMP9. Neprilysin is a 90-110 kDa zinc

metalloproteinase. The physiological role of neprilysin varies depending on tissue localization. In studies of Alzheimer's disease, neprilysin was shown to degrade Aβ, the main peptide component of the amyloid deposits found in this disease [7-9]. Neprilysin is also expressed and active in islets, but the potential role of neprilysin in inhibiting amyloid formation in islets is ambiguous. Therefore, IAPP degradation by neprilysin is of great interest. IDE, known alternatively as insulysin, was first identified as a degrading enzyme because of its ability to cleave the B chain of the hormone insulin. Both Aβ and IAPP have been shown to be substrates of IDE [5, 10]. Inhibition of this enzyme results in reduced IAPP degradation and increased amyloid deposits in insulinoma cells [6]. More recently, two other enzymes, MMP2 and MMP9 were also shown to be capable of degrading Aβ and IAPP [4, 11, 12], but MMP 2 activity was not detected in either human IAPP transgenic or nontransgenic mouse islets. Conversely, MMP9 is expressed and active in the islets of mouse models. Inhibition of MMP9 activity was shown to result in increased amyloid deposits and β-cell apoptosis [4]. Therefore, MMP9 may play an important role in regulation of IAPP amyloid formation *in vivo*.

MMP9 degradation of IAPP is selective. Rat IAPP was not cleaved with incubation of MMP9. Ala^{25}-Ile^{26} is the putative site of MMP9 cleavage on human IAPP [4]. This cleavage site is within the region that might be critical for amyloid formation. To date, the cleavage products have not been tested for their amyloidogenicity nor their effect on full length human IAPP amyloid formation. In this study, we determine the mechanism of MMP9 in preventing islet amyloid formation.

3.2 Materials and methods

3.2.1 MALDI-TOF mass spectroscopy analysis of cleavage products.

Wild-type IAPP 10 μM was incubated at 37 ºC with MMP9 which was purchased from EMD Millipore. The enzyme is supplied in 50 mM HEPES, 10 mM $CaCl_2$, 20% glycerol, and 0.005% BRIJ-35 detergent. After 22 h incubation, the solution was desalted using Millipore C18 zip tips, and mixed with the matrix α-cyano-4-hydroxycinnamic acid before measurement.

3.2.2 Peptide synthesis and purification.

Wild-type IAPP and IAPP fragments were synthesized on a 0.25 mmol scale using Fmoc chemistry on a CEM microwave peptide synthesizer. Fmoc-Phe-PEG-PS resin and Fmoc-Ala-PEG-PS resin were used in the synthesis of fragment 1-15 and fragment 1-25, respectively. Fmoc-PAL-PEG-PS resin was used in order to incorporate the amidated C-terminus in wild-type IAPP, fragment 16-37 and 26-37. Standard Fmoc reaction cycles were used. The first residue attached to the resin, β-branched residues, Arg, and all pseudoproline dipeptide derivatives were double coupled. Fmoc protected pseudoproline dipeptide derivatives were incorporated at positions 9-10, 19-20, and 27-28 to facilitate the synthesis [13]. The peptide was cleaved from the resin through the use of standard TFA methods. Crude peptides were partially dissolved in 20 % acetic acid (v/v), and lyophilized to increase their solubility. The dry peptides were then redissolved in dimethyl sulfoxide (DMSO) at room temperature to promote the formation of disulfide bonds [14, 15]. Analytical HPLC was used to monitor the process of oxidation. The peptides were purified by reverse-phase HPLC using a Vydac C18 preparative column (10 mm x 250 mm). A two buffer gradient system was used: buffer A consisted of 100% H_2O and 0.045% HCl (v/v) and buffer B consisted of 80% acetonitrile, 20% H_2O and 0.045% HCl (v/v). HCl was used as the counterion

since residual TFA can influence amyloid formation. Analytical HPLC was used to check the purity of peptides before use. Peptides were analyzed by mass spectrometry using a Bruker MALDI-TOF MS to confirm the molecular weight. Wild-type IAPP, expected *m/z:* 3903.3, observed 3902.1; fragment 1-15 IAPP, expected 1639.9, observed 1639.9; fragment 1-25 IAPP expected 2667.0, observed 2667.1; fragment 16-37, expected 2282.5, observed 2283.3; fragment 26-37 IAPP, expected 1254.4, observed 1254.2.

3.2.3 Sample preparation.

A 1.6 mM peptide solution was prepared in 100% HFIP and stored at -20 ^{o}C. Before aliquoting the desired amount, solutions were filtered using a 0.22 μm syringe filter. For kinetic experiments, aliquots of the filtered stock solution were lyophilized for 20 to 24 h, and then diluted into pH 7.4, 20 mM Tris buffer and thioflavin-T solution. The final concentration of wild-type IAPP and fragments was 16 uM.

3.2.4 Thioflavin-T and p-cyanophenylalanine (p-cyanoPhe) fluorescence assays.

Thioflavin-T fluorescence studies were conducted using a Beckman Coulter DTX880 plate reader. An excitation wavelength of 430 nm and emission wavelength of 485 nm was used. *p*-CyanoPhe fluorescence studies were performed on an Applied Photo technology fluorescence spectrophotometer. *p*-cyanoPhe fluorescence was excited at 240 nm and emission was monitored at 296 nm.

3.2.5 Circular dichroism (CD) experiments.

CD experiments were performed at 25 ^{o}C using an Applied Photophysics Chirascan circular dichroism spectrometer. The peptide solutions for the CD experiments were prepared by diluting

the lyophilized dry peptide into 20 mM Tris-HCl buffer at pH 7.4. The final concentration of peptide was 16 μM. Spectra were recorded from 190 to 260 nm at 1 nm intervals in a quartz cuvette with a 0.1 cm path length at 25 ºC. CD experiments used the same reaction solutions as the thioflavin-T fluorescence measurements. A background spectrum was subtracted from the collected data.

3.2.6 Transmission electron microscope (TEM).

TEM was performed at the Life Science Microscopy Center at the State University of New York at Stony Brook. Samples were aliquots from the same reaction solutions that were used for the fluorescence measurements. 5 μL of peptide solution was placed on carbon-coated 300- mesh copper grid for 1 min and then negatively stained with saturated uranyl acetate for 1 min.

3.3 Results and discussion

3.3.1 Identification of cleavage products produced by MMP9

We first used MALDI-TOF mass spectroscopy to identify the principle cleavage products of MMP9 digestion. Human IAPP (10 μM) was incubated with 0.2 uM of MMP 9 at pH 7.5 and 37 ºC for 22 h and the reaction products were analyzed. The major peaks in the mass spectrum corresponded to *m/z* = 1641.4 and 2669.1 (Figure 3-1). These are consistent with fragments corresponding to residues 1-15 and 1-25. We did not detect peaks corresponding to residues 16-37 and 26-37. It is possible that these fragments were too hydrophobic to be ionized or further digested. The complete set of cleavage product could not be determined. However, the spectrum would suggest that MMP9 cleavage sites are Phe^{15}-Leu^{16} and Ala^{25}-Ile^{26}. Ala-Ile is also found as cleavage site when MMP9 cleaved another amyloidogenic protein, $A\beta_{1-40}$ [11].

3.3.2 MMP9 cleavage products are not amyloidogenic except for the 16-37 fragment.

To explore the potential mechanism of IAPP degradation by MMP9, we synthesized each of the potential major fragments and tested their ability to form amyloid using fluorescence detected thioflavin-T binding assays, CD and TEM. As noted earlier, thioflavin-T is a small dye whose quantum yield increases when it binds to amyloid fibrils. The exact mode of dye binding is not known, but it is thought to bind in grooves on the surface of the amyloid fibrils which are produced by the in-register alignment of sidechains [16]. Thioflavin-T has been shown to accurately report the time course of IAPP amyloid formation, without influencing e the kinetics of assembly under the conditions used here [17]. However, the dye is not completely amyloid specific and it is important to confirm the results of thioflavin-T experiments with an independent approach. Thus we also recorded TEM images of all reaction products as well as CD spectra. Thioflavin-T fluorescence curves for each of the fragments and for full length human IAPP (positive control) are displayed in Figure 3-2.

The time course observed for human IAPP is typical, and a lag phase on the order of 15 h is observed followed by a growth phase. TEM images of aliquots are recorded at the end of the reactions and reveal dense mats of amyloid fibrils, and CD spectra reveal the presence of β-sheet structure (Figure 3-3). Very different results are found with the fragments. The fluorescence profile is flat for fragments 1-15, 1-25, and 26-37, with no enhancement of thioflavin-T fluorescence detected over the entire time course (Figure 3-2). TEM images recorded for aliquots collected at the end of the reactions confirm the absence of fibrils and CD spectra show no significant β-sheet structure. In contrast, the 16-37 fragment forms amyloid fibrils aggressively with no apparent lag phase. Again, TEM and CD were used to confirm its ability to form fibrils.

3.3.3 Nonamyloidogenic cleavage products do not affect amyloid formation by full length human IAPP.

It is possible that the fragments could act as inhibitors of amyloid formation by uncleaved human IAPP or might even accelerate IAPP amyloid formation. There are a number of IAPP mutants which act as effective inhibitors of wild-type amyloid formation which also share the common feature of having the mutations localized in the C-terminal half of the molecule [18, 19]. This suggests that the N-terminal portion of the molecule might act as a recognition motif which allows binding to wild-type IAPP, while the substitution in the C-terminal region prevents the development of the cross-β amyloid structure. There have also been reports of peptides which accelerate amyloid formation [20]. Thus it is important to test the effects of the MMP9 cleavage products on IAPP amyloid formation. Addition of the nonamyloidogenic fragments 1-15, 1-25 and 26-37 at several ratios had no effect on the kinetics of amyloid assembly. Thioflavin-T fluorescence curves and TEM images of the various mixtures are displayed in Figure 3-4, together with a positive control (full length human IAPP). The t_{50} values, the time to 50% completion and final value of the thioflavin-T intensity are similar for all of these samples. TEM images are also very similar to the control study (Figure 3-5) arguing that fragments 1-15, 1-25 and 26-37 do not alter the kinetics of IAPP amyloid formation.

3.3.4 The 16-37 fragment accelerates amyloid formation by full length human IAPP.

We also tested the effect of the 16-37 fragment on IAPP amyloid formation. This fragment is the only cleavage product that is able to form amyloid fibrils by itself, although we did not detect its signal in mass spectrum. Several different ratios of the 16-37 fragment to human IAPP were examined by thioflavin T binding assay. A 1:1 mixture of human IAPP and the 16-37 fragment

exhibits a t_{50} that is much shorter than that observed for human IAPP alone (Figure 3-6). In experiments containing a 5-fold and 10-fold excess of the 16-37 fragment, the thioflavin-T fluorescence develops very quickly. Because the 16-37 fragment is also amyloidogenic and thioflavin-T can bind to most fibrils, it is difficult to discriminate the fibrils formed by the fragment or by human IAPP, or by mixtures using thioflavin T assays.

We further used *p*-cyanophenylalanine fluorescence (*p*-cyanoPhe or $F_{C\equiv N}$) to directly probe the amyloid formation by human IAPP in the presence of the amyloidogenic fragment. $F_{C\equiv N}$ is an unnatural amino acid that can be incorporated into peptides or proteins. The fluorescence quantum yield is high in water and low when the cyano group is buried in hydrophobic environments such as the interior of amyloid fibrils [21, 22]. Previous studies have demonstrated that the substitution of any of three aromatic residues in IAPP by $F_{C\equiv N}$ does not perturb the kinetics of amyloid formation, and the method using $F_{C\equiv N}$ variant to specifically monitor amyloid formation by human IAPP in the presence of other amyloidogenic proteins is successful [23]. Figure 3-6C displays the thioflavin-T and *p*-cyanoPhe fluorescence time course for the F15$F_{C\equiv N}$ IAPP variant in 2% HFIP with consistent stirring (black and red curves). The kinetic curve of amyloid formation in the presence of the 16-37 fragment at a 5-fold excess is very different from the control experiments. A much shorter lag phase is observed suggesting that the 16-37 fragment accelerates amyloid formation by human IAPP. Additional studies without the presence of organic co-solvent were also performed to ensure that the results were not biased (Figure 3-6D).

3.3.5 The 16-37 fragment can be further cleaved by MMP9.

We first identified MMP9 cleavage products, by incubating human IAPP with MMP9. Thioflavin-T was applied to probe possible fibril formation. If the 16-37 fragment is the final

cleavage product, then we should be able to observe the thioflavin T fluorescence signal due to its ability to form amyloid fibrils. However, there was no detectable fluorescence change for the entire incubation. Therefore, it is plausible that the peptide could be further cleaved by MMP9. To determine whether MMP9 degrades the 16-37 fragment, we incubated this fragment with MMP9 at 37 ^{o}C in a buffer solution containing thioflavin-T at pH 7.5. Thioflavin-T fluorescence was monitored and MALDI-TOF mass spectroscopy was used to determine cleavage products. TEM images were also recorded for samples collected from the fragment and MMP9 mixture. Figure 3-7 shows that MMP9 inhibits the 16-37 fragment fibril formation by cleaving this peptide at Ala^{25}-Ile^{26}. Only some non-fibrillar aggregates were detected in the mixtures of MMP9 and the 16-37 fragment. The mass spectrum clearly shows a peak corresponding to the cleavage product, the 16-25 fragment.

3.4 Conclusions

Our data shows that MMP9 can degrade human IAPP and is consistent with previous data [14]. However, in that study, there is faint but detectable signal for full length IAPP in mass spectra and only one cleavage product was identified. It is likely possible that we used higher enzyme concentration and had a longer time incubation to completely degrade IAPP in our study.

MMP9 cleaves IAPP at two positions, Phe^{15}-Leu^{16} and Ala^{25}-Ile^{26}, as identified by MALDI mass spectrometry. We recognized the peaks corresponding to the 1-15 and 1-25 fragments, but the peaks from the 16-37 and 26-37 fragments do not appear in the mass spectra. In general, peptides with many hydrophobic residues are not easy to be detected by MALDI. These two missing fragments could be too hydrophobic to be ionized or could be further digested by MMP9. A control

mass experiment (Figure 3-8) reveals that only faint signal is detected when the concentration of the 26-37 fragment is as low as that of human IAPP. The 16-37 fragment could be further digested, as shown by an observation of the 16-25 fragment when MMP9 was added to this peptide.

We also tested the ability of the resulting fragments to form amyloid fibrils and tested their inhibitory effect on full length IAPP amyloid formation. The 1-15, 1-25 and 26-37 fragments are not amyloidogenic. TEM images confirmed that these fragments do not form fibrils or small aggregates. These three fragments also do not affect the kinetics of IAPP amyloid formation or the morphologies of IAPP amyloid fibrils. TEM images of fibrils produced in each case are also similar to each other. In contrast, the 16-37 fragment is capable of forming fibrils in isolation. This peptide does not contain the flexible N-terminal part nor has any positive or negative charged residues. That may explain why this peptide forms amyloid much faster than IAPP. Use of *p*-cyanoPhe fluorescence provides direct evidence that the 16-37 fragment can promote IAPP amyloid formation.

Taken together, we have demonstrated that MMP9 inhibits amyloid formation by human IAPP and by the 16-37 fragment via degradation of the peptides. The resulting fragments become inactive. MMP9 can significantly reduce islet amyloid deposition. Thus, maintaining or increasing MMP9 in islets could potentially prevent IAPP amyloid formation and protect β-cells. The observation that the 16-37 fragment accelerates amyloid formation by wild-type IAPP is interesting and elucidation of its mode of action might provide clues as to free energy barriers involved in amyloid formation.

3.5 Figures

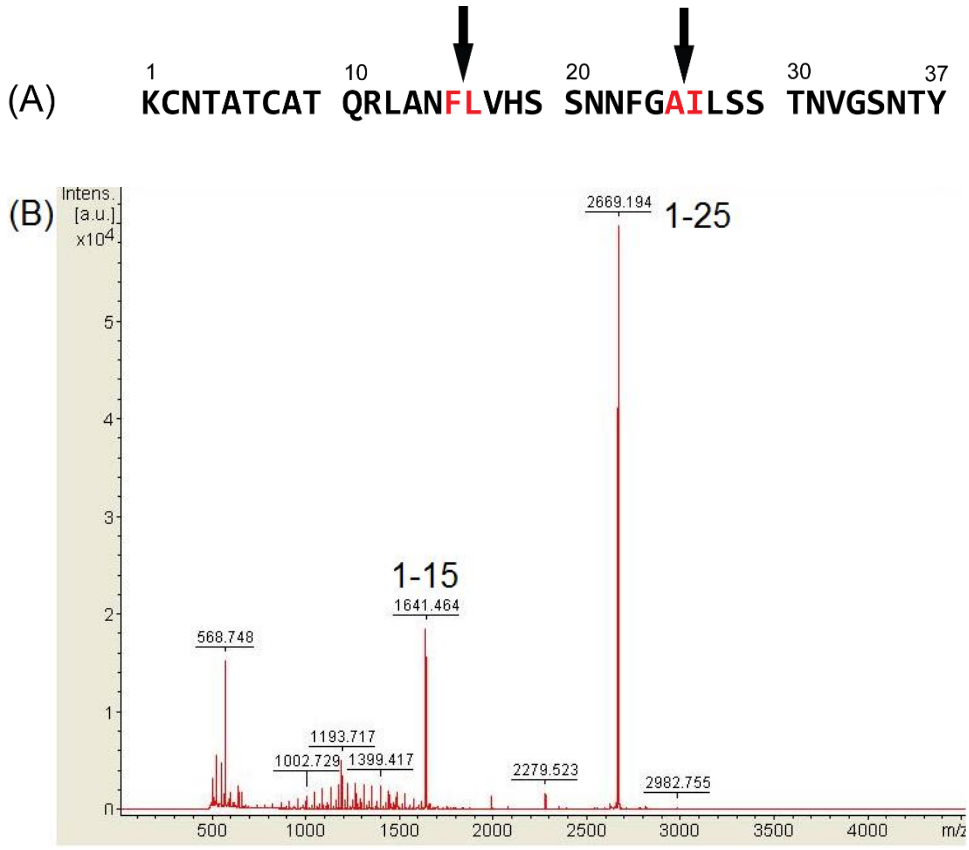

Figure 3-1: Identification of MMP9 cleavage products. (A) Primary sequence of human IAPP. The putative cleavage sites are indicated by arrows. (B) Peaks *m/z* = 1641.4 and 2669.1 are corresponding to residues 1-15 and 1-25, suggesting that Phe^{15}-Leu^{16} and Ala^{25}-Ile^{26} are the two major cleavage sites. Peak *m/z* = 568.7 was identified as contaminant of matrix.

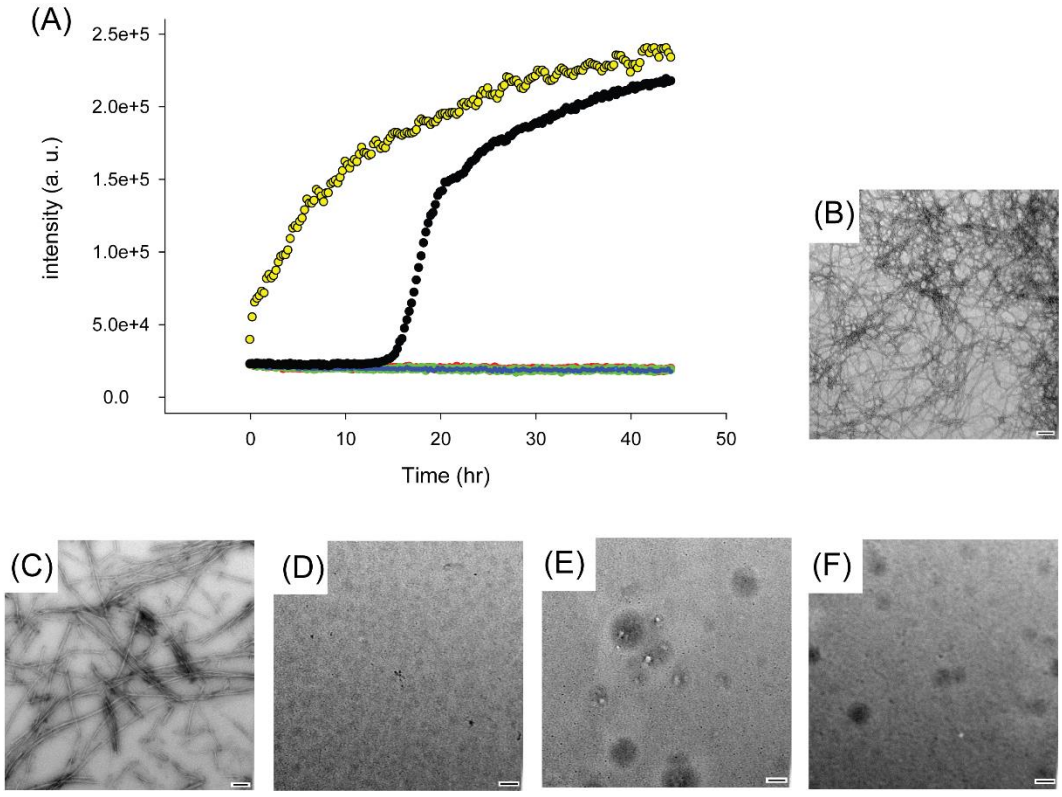

Figure 3-2: Thioflavin-T monitored kinetics of amyloid formation by human IAPP and four IAPP fragments. TEM images collected at the end of the reaction (45h) are also shown. (A) Black, human IAPP; yellow, the 16-37 fragment; red, the 1-15 fragment; green, the 1-25 fragment; blue, the 26-37 fragment. All experiments were conducted in 20 mM, pH 7.4 Tris buffer without stirring at 25 ^{o}C. (B) TEM image of amyloid fibrils formed by human IAPP. (C) TEM image of amyloid fibrils formed by the 16-37 fragment. (D) TEM image of a sample of the 1-15 fragment. (E) TEM image of a sample of the 1-25 fragment. (F) TEM image of a sample of the 26-37 fragment. Scale bars represent 100 nm.

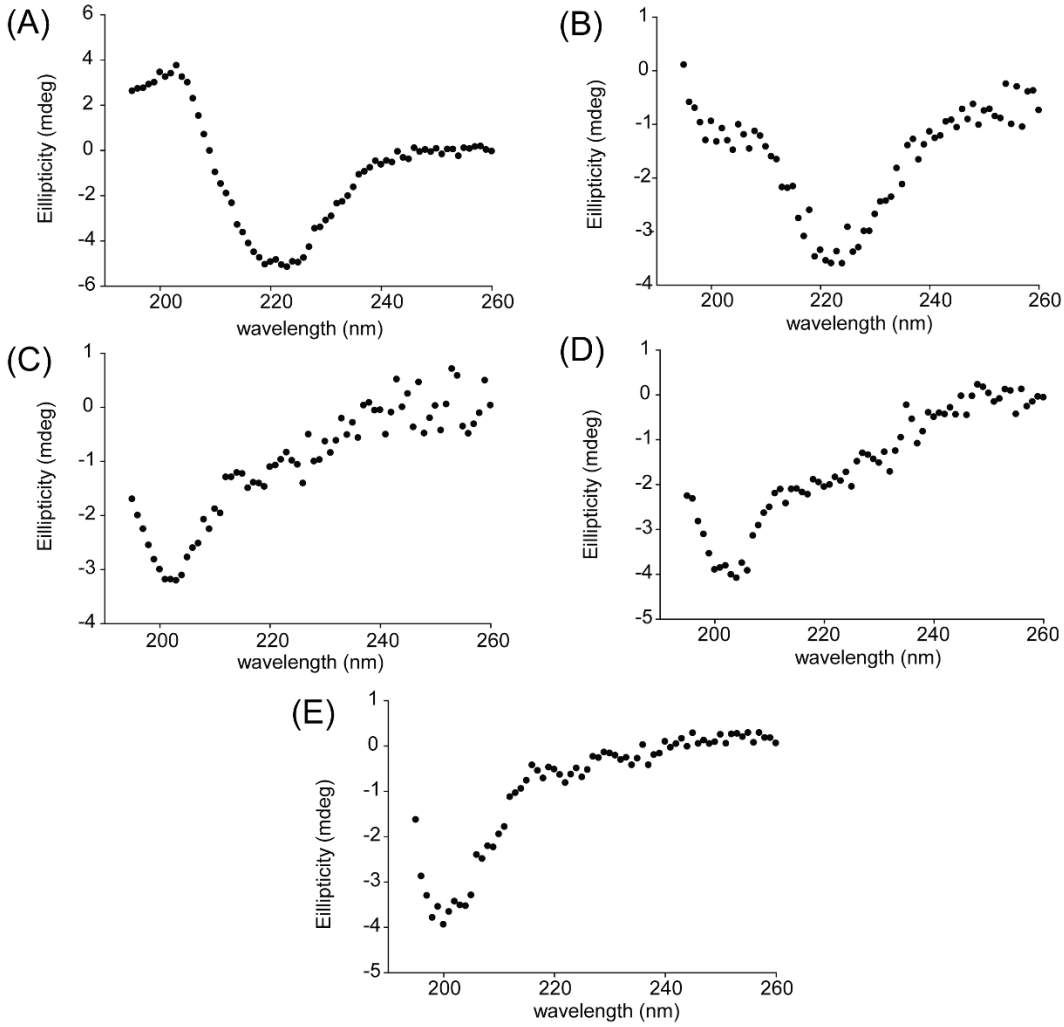

Figure 3-3: CD spectra of human IAPP and the four cleavage fragments collected at the end of thioflavin-T kinetic experiments are shown: (A) Human IAPP. (B) The 16-37 fragment. (C) The 1-15 fragment. (D) The 1-25 fragment. (E) The 26-37 fragment. (A) and (B) show the typical β-sheet signals suggesting the formation of amyloid fibrils.

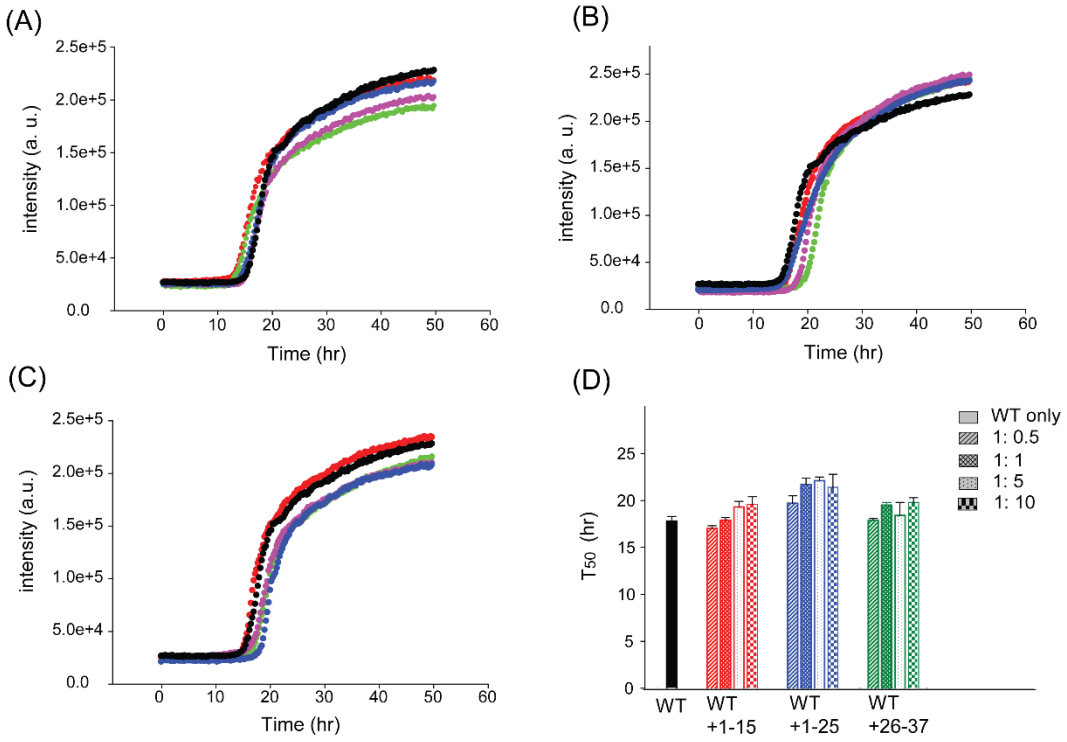

Figure 3-4: The 1-15, 1-25 and 26-37 fragments do not alter amyloid formation by full length human IAPP. Thioflavin-T fluorescence monitored kinetics are shown: (A) human IAPP (black) and human IAPP with the 1-15 fragment; (B) human IAPP (black) and human IAPP with the 1-25 fragment; (C) human IAPP (black) and human IAPP with the 26-37 fragment at 1: 0.5 (red), 1:1 (green), 1:5 (pink) and 1:10 (blue) ratios. All experiments were conducted in pH 7.4, 20 mM Tris buffer without stirring at 25 ºC. Human IAPP concentration is 16 μM. (D) The comparison of t_{50} of human IAPP kinetics in the presence or absence of fragments.

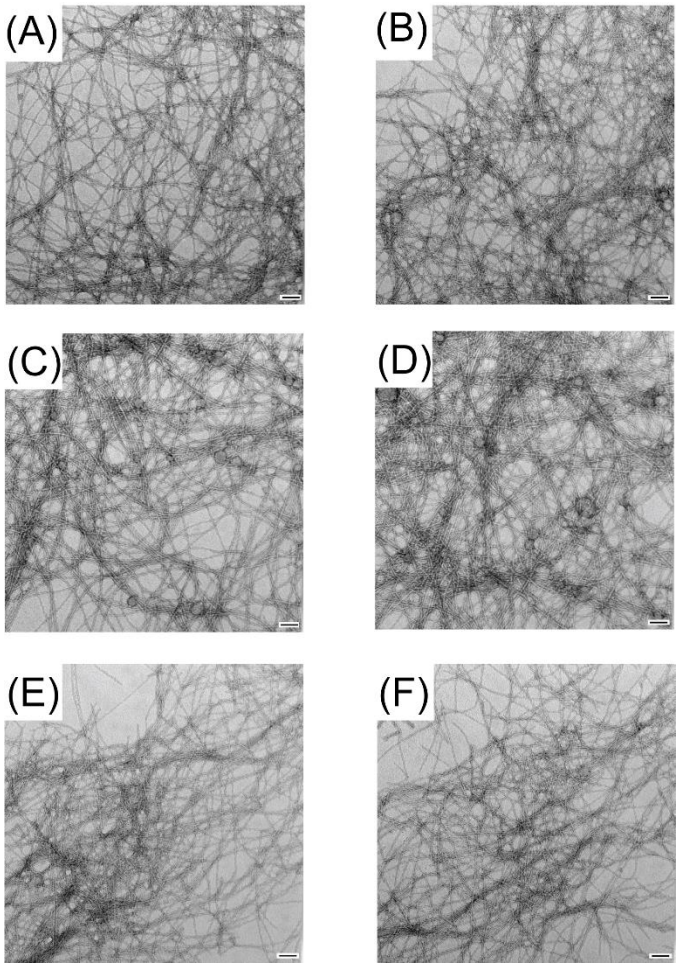

Figure 3-5: The 1-15, 1-25 and 26-37 fragments do not alter the morphologies of amyloid fibrils formed by human IAPP. Samples were removed from at the end of the kinetic reactions shown in Figure 3-4, and TEM images are recorded for (A) 1:1 mixture of human IAPP and the 1-15 fragment; (B) 1:5 mixture of human IAPP and the 1-15 fragment; (C) 1:1 mixture of human IAPP and the 1-25 fragment; (D) 1:5 mixture of human IAPP and the 1-25 fragment; (E) 1:1 mixture of human IAPP and the 26-37 fragment; (F) 1:5 mixture of human IAPP and the 26-37 fragment. Scale bars represent 100 nm.

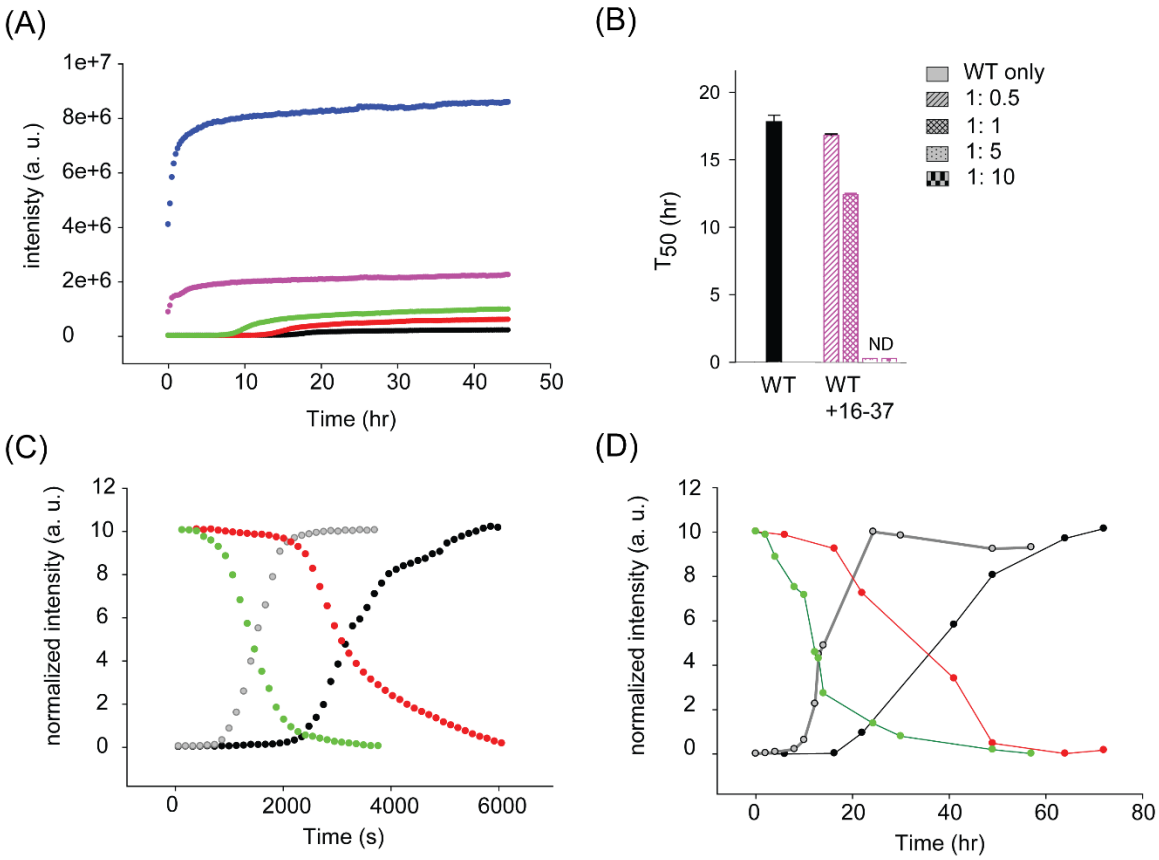

Figure 3-6: The 16-37 fragment accelerates amyloid formation by human IAPP. (A) Thioflavin-T fluorescence monitored kinetics of amyloid formation by human IAPP (black), human IAPP and the 16-37 fragment at 1: 0.5 ratio (red), human IAPP and the 16-37 fragment at 1:1 ratio (green), human IAPP and the 16-37 fragment at 1:5 ratio (pink) and human IAPP and the 16-37 fragment at 1:10 ratio (blue). (B) Comparison of t_{50} of amyloid formation by human IAPP in the presence or absence of fragment 16-37. ND: t_{50} is not able to be determined due to fast increases in fluorescence intensity. (C) Thioflavin-T (black) and *p*-cyanoPhe fluorescence (red) kinetics of $F15F_{C\equiv N}$ IAPP variant. The grey curve is the thioflavin-T monitored kinetic trace of $F15F_{C\equiv N}$ IAPP with a 5-fold excess of the 16-37 fragment and the green curve is the *p*-cyanoPhe kinetic trace of $F15F_{C\equiv N}$ IAPP with a 5-fold excess of the 16-37 fragment. Experiments are conducted at 25 ^{o}C, pH 7.4 20 mM Tris buffer with 2% HFIP and constant stirring. (D) Same as figure C, but experiments were performed without 2% HFIP and without stirring.

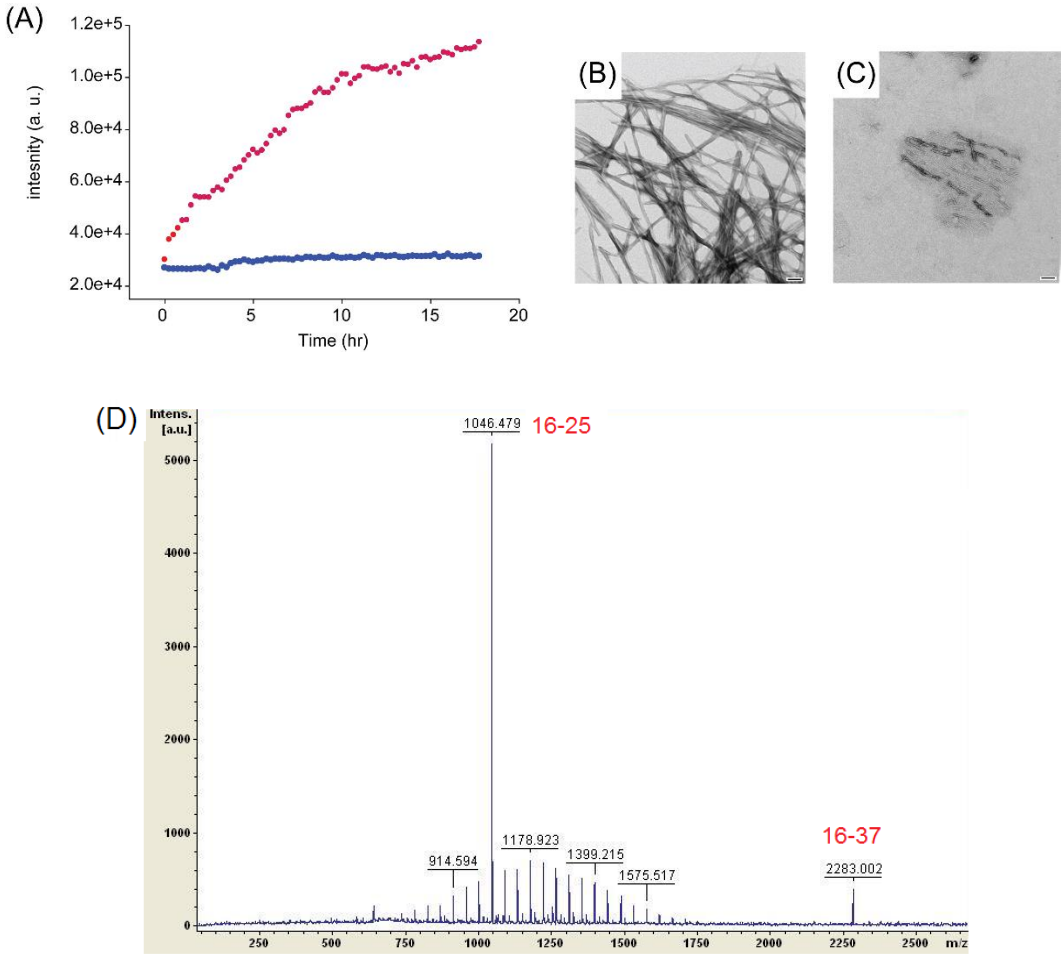

Figure 3-7: MMP9 degrades the 16-37 fragment and inhibits its ability to form fibrils. (A) Thioflavin-T fluorescence monitored kinetic of the 16-37 fragment with (blue curve) and without (red curve) MMP9. (B) TEM image of amyloid fibrils formed by the 16-37 fragment in the absence of MMP9. (C) TEM image recorded for a sample of the 16-37 fragment in the presence of MMP9. Scale bars represent 100 nm. (D) MALDI mass spectrum shows that Ala^{25}-Ile^{26} is the major MMP9 cleavage site for degradation of the 16-37 fragment.

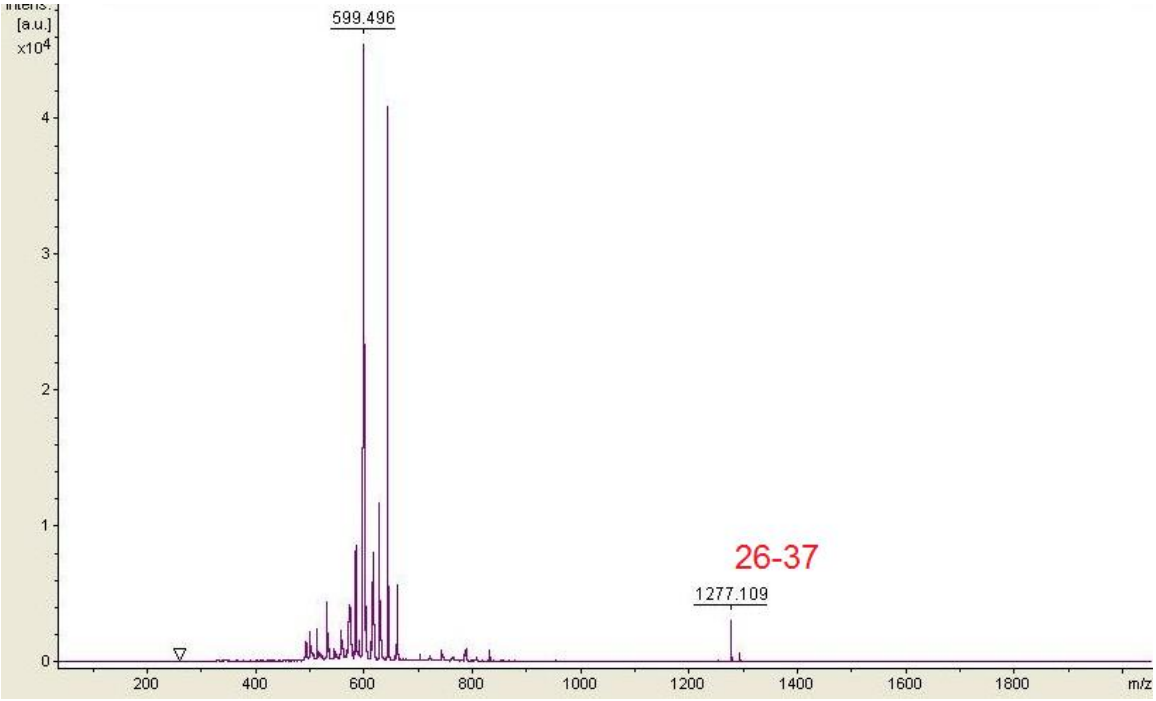

Figure 3-8: The 26-37 fragment is a highly hydrophobic peptide. Only faint signal of the 26-37 fragment was shown on MALDI mass spectrum when it was prepared at the same concentration as that of human IAPP.

3.6 References

1. Zraika, S.; Hull, R. L.; Udayasankar, J.; Clark, A.; Utzschneider, K. M.; Tong, J.; Gerchman, F.; Kahn, S. E., Identification of the amyloid-degrading enzyme neprilysin in mouse islets and potential role in islet amyloidogenesis. *Diabetes* **2007**, *56* (2), 304-310.

2. Zraika, S.; Aston-Mourney, K.; Marek, P.; Hull, R. L.; Green, P. S.; Udayasankar, J.; Subramanian, S. L.; Raleigh, D. P.; Kahn, S. E., Neprilysin impedes islet amyloid formation by inhibition of fibril formation rather than peptide degradation. *J. Biol. Chem.* **2010**, 285 (24), 18177-18183

3. Guan, H.; Chow, K. M.; Shah, R.; Rhodes, C. J.; Hersh, L. B., Degradation of islet amyloid polypeptide by neprilysin. *Diabetologia* **2012**, *55* (11), 2989-2998.

4. Aston-Mourney, K.; Zraika, S.; Udayasankar, J.; Subramanian, S. L.; Green, P. S.; Kahn, S. E.; Hull, R. L., Matrix metalloproteinase-9 reduces islet amyloid formation by degrading islet amyloid polypeptide. *J. Biol. Chem.* **2013**, *288* (5), 3553-3559.

5. Bennett, R. G.; Duckworth, W. C.; Hamel, F. G., Degradation of amylin by insulin-degrading enzyme. *J. Biol. Chem.* **2000**, *275* (47), 36621-36625.

6. Bennett, R. G.; Hamel, F. G.; Duckworth, W. C., An insulin-degrading enzyme inhibitor decreases amylin degradation, increases amylin-induced cytotoxicity, and increases amyloid formation in insulinoma cell cultures. *Diabetes* **2003**, *52* (9), 2315-2320.

7. Guan, H.; Liu, Y. X.; Daily, A.; Police, S.; Kim, M. H.; Oddo, S.; LaFerla, F. M.; Pauly, J. R.; Murphy, M. P.; Hersh, L. B., Peripherally expressed neprilysin reduces brain amyloid burden: A novel approach for treating Alzheimer's disease. *J. Neurosci. Res.* **2009**, 87 (6), 1462-1473.

8. Kanemitsu, H.; Tomiyama, T.; Mori, H., Human neprilysin is capable of degrading amyloid beta peptide not only in the monomeric form but also the pathological oligomeric form. *Neuroscience Letters* **2003**, *350* (2), 113-116.

9. Hersh, L. B.; Rodgers, D. W., Neprilysin and amyloid beta peptide degradation. *Curr. Alzheimer Res.* **2008**, *5* (2), 225-231.

10. Chesneau, V.; Vekrellis, K.; Rosner, M. R.; Selkoe, D. J., Purified recombinant insulin-degrading enzyme degrades amyloid beta-protein but does not promote its oligomerization. *Biochem. J.* **2000**, *351*, 509-516.

11. Backstrom, J. R.; Lim, G. P.; Cullen, M. J.; Tokes, Z. A., Matrix metalloproteinase-9 (MMP-9) is synthesized in neurons of the human hippocampus and is capable of degrading the amyloid-beta peptide (1-40). *J. Neurosci.* **1996**, *16* (24), 7910-7919.

12. Yan, P.; Hu, X. Y.; Song, H. W.; Yin, K. J.; Bateman, R. J.; Cirrito, J. R.; Xiao, Q. L.; Hsu, F. F.; Turk, J. W.; Xu, J.; Hsu, C. Y.; Holtzman, D. M.; Lee, J. M., Matrix metalloproteinase-9 degrades amyloid-beta fibrils in vitro and compact plaques in situ. *J. Biol. Chem.* **2006**, *281* (34), 24566-24574.

13. Abedini, A.; Raleigh, D. P., Incorporation of pseudoproline derivatives allows the facile synthesis of human IAPP, a highly amyloidogenic and aggregation-prone polypeptide. *Org. Lett.* **2005**, *7* (4), 693-696.

14. Tam, J. P.; Wu, C. R.; Liu, W.; Zhang, J. W., Disulfide bond formation in peptides by dimethyl-sulfoxide - Scope and applications. *J. Am. Chem. Soc.* **1991**, *113* (17), 6657-6662.

15. Abedini, A.; Singh, G.; Raleigh, D. P., Recovery and purification of highly aggregation-prone disulfide-containing peptides: Application to islet amyloid polypeptide. *Ana. Biochem.* **2006**, *351* (2), 181-186.

16. Levine, H., Thioflavin-T interaction with amyloid beta-sheet structures. *Amyloid* **1995**, *2* (1), 1-6.

17. Marek, P.; Gupta, R.; Raleigh, D. P., The fluorescent amino acid p-cyanophenylalanine provides an intrinsic probe of amyloid formation. *Chembiochem* **2008**, *9* (9), 1372-1374.

18. Abedini, A.; Meng, F. L.; Raleigh, D. P., A single-point mutation converts the highly amyloidogenic human islet amyloid polypeptide into a potent fibrillization inhibitor. *J. Am. Chem. Soc.* **2007**, *129* (37), 11300-11301

19. Meng, F. L.; Raleigh, D. P.; Abedini, A., Combination of kinetically selected inhibitors in trans leads to highly effective inhibition of amyloid formation. *J. Am. Chem. Soc.***2010**, *132* (41), 14340-14342.

20. Dunkelberger, E. B.; Buchanan, L. E.; Marek, P.; Cao, P.; Raleigh, D. P.; Zanni, M. T., Deamidation accelerates amyloid formation and alters amylin fiber structure. *J. Am. Chem. Soc.* **2012**, *134* (30), 12658-12667.

21. Tucker, M. J.; Oyola, R.; Gai, F., A novel fluorescent probe for protein binding and folding studies: p-cyano-phenylalanine. *Biopolymers* **2006**, *83* (6), 571-576.

22. Getahun, Z.; Huang, C. Y.; Wang, T.; De Leon, B.; DeGrado, W. F.; Gai, F., Using nitrile-derivatized amino acids as infrared probes of local environment. *J. Am. Chem. Soc.* **2003**, *125* (2), 405-411.

23. Marek, P.; Mukherjee, S.; Zanni, M. T.; Raleigh, D. P., Residue-specific, real-time characterization of lag-phase species and fibril growth during amyloid formation: A combined fluorescence and IR study of p-cyanophenylalanine analogs of islet amyloid polypeptide. *J. Mol. Biol.* **2010**, *400* (4), 878-888.

Chapter 4. Mutational analysis of preamyloid intermediates: The role of His-Tyr interactions in islet amyloid formation

Abstract

Formation of islet amyloid is complex and characterizing preamyloid oligomers is an important topic because oligomeric intermediates are postulated to be the most toxic species produced during fibril formation. A range of competing models for early oligomers have been proposed. The role of the amidated C-terminus in amyloid formation by IAPP and in stabilizing oligomers is not known. Studies with unamidated IAPP have provided evidence for formation of an antiparallel dimer at pH 5.5, stabilized by stacking of His-18 and Tyr-37, but it is not known if this interaction is formed in the physiological form of the peptide. Analysis of a set of variants with a free and with an amidated C-terminus shows that disrupting the putative His-Tyr interaction accelerates amyloid formation, indicating that it is not essential. Amidation to generate the physiologically relevant form of IAPP accelerates amyloid formation, demonstrating that the advantages conferred by C-terminal amidation outweigh increased amyloidogenicity. The analysis of this variant argues that IAPP is not under strong evolutionary pressure to reduce amyloidogenicity. Analysis of an H18Q mutant of IAPP shows that the charge state of the N-terminus is an important factor controlling the rate of amyloid formation, even though the N-terminal region of IAPP is believed to be flexible in the amyloid fibrils.

NOTE: The material presented in this chapter has been published (Tu, L.H.; Serrano, A. L.; Zanni, M. T.; Raleigh, D. P., Mutational analysis of preamyloid intermediates: The role of His-Tyr

interactions in islet amyloid formation. *Biophys. J.* **2014,** 106 (7), 1520-1527). This chapter contains direct excerpts from the manuscript, which was written by me with suggestions and revisions from Professor Daniel P. Raleigh and Martin T. Zanni. Arnaldo L. Serrano performed the two-dimensional infrared spectroscopy experiments.

4.1 Introduction

The role of the C-terminus in IAPP amyloid formation is relatively unexplored, but recent solution NMR studies using recombinant human IAPP strongly suggested that His-18 and Tyr-37 make early contacts during amyloid formation by an unamidated variant of IAPP at acidic pH [1]. His-aromatic amino acid interactions are known to be important in globular proteins [2], but have not been widely considered in the context of amyloid formation, and it is not known if these interactions are formed in the naturally occurring amidated form of IAPP or whether they are important if present. A model of an antiparallel stable dimer generated by stacking of the side chains of His-18 and Tyr-37 was proposed based on the NMR studies [1]. However, removal of the charged carboxylate and replacement with a neutral amide group to generate the physiological form of IAPP could alter interactions with the His side chain. In addition, the interactions involving His-18 and a charged C-terminus should be weaker at physiological pH because the pKa of His-18 is expected to be near, or below 7 in the monomeric state. Thus, the fraction of peptide with a protonated His-18 will decrease as the pH rises to physiological valves. Along these lines, previous studies of C-terminus amidated IAPP variants that contain the fluorescent Tyr/Phe analog 4-cyanophenylalanine argued that the aromatic side chains remain solvated during the lag phase and suggested that aromatic-aromatic interactions involving Tyr-37 or interactions of Tyr-37 with a

neutral His do not develop during the lag time [3]. Other models of low order oligomers have been proposed; including, for example, the formation of helical intermediates or the generation of dimers involving a side-by-side arrangement of β-hairpin monomers [4-8]. Thus, the role of potential His-18-Tyr-37 interactions is not clear, and the role of C-terminus in amyloid formation is not completely defined, nor is the nature of early structure acquisition clear. These issues are important because some inhibitors may target early oligomeric structures, and because oligomeric intermediates are thought to be the most toxic species [9-11]. Here, we investigate the role of the C-terminus of IAPP and its interaction with His-18 during amyloid formation by IAPP.

4.2 Materials and methods

4.2.1 Peptide synthesis and purification

Peptides were synthesized on a 0.1 mmol scale using a CEM Liberty microwave peptide synthesizer, and 9-fluornylmethoxycarbonyl (Fmoc) chemistry. Solvents used were ACS-grade. Fmoc-PAL-PEG-PS resin was used to form an amidated C-terminus. Fmoc-L-Tyr (*Ot*Bu)-PEG-PS resin was used for the preparation of peptides with a free C-terminus. Standard Fmoc reaction cycles were used. Fmoc protected pseudoproline dipeptide derivatives were incorporated at positions 9–10, 19–20, and 27–28 as previous described [12]. A maximum temperature of 50 ^{o}C was used for the coupling of His and Cys to reduce the possibility of racemization [13]. Peptides were cleaved from the resin by standard TFA methods. Crude peptides were partially dissolved in 20% acetic acid (v/v), frozen in liquid nitrogen, and lyophilized to increase their solubility. The dry peptide was redissolved in DMSO at room temperature to promote the formation of the disulfide bond [14, 15]. Analytic HPLC was used to ensure the completion of oxidation. Peptides

were purified by HPLC using a Vydac or Proto 300 C18 preparative column (10 mm x 250 mm). A two buffer gradient was used: buffer A consisted of 100% H_2O and 0.045% HCl (v/v) and buffer B included 80% acetonitrile, 20% H_2O, and 0.045% HCl. HCl was used as the counterion instead of TFA because residual TFA can influence amyloid formation. Analytical HPLC was used to check the purity of peptides before use. MALDI-TOF mass spectrometry confirmed the correct molecular mass. hIAPP, expected 3903.3, observed 3902.8; H18Q-hIAPP, expected 3894.3, observed 3894.4; H18L-hIAPP, expected 3879.3, observed 3879.3; free CT-hIAPP, expected 3904.2, observed 3903.8; free H18Q CT-IAPP, expected 3895.3, observed 3895.9.

4.2.2 Sample preparation

Peptides were dissolved in 100% HFIP at a concentration of 1.6 mM and stored at -20 ^{o}C. For kinetic studies, 8 uL aliquots were lyophilized and redissolved in 800 uL of 20 mM Tris buffer, pH 7.4. For the seeding assays, preformed fibrils were produced from kinetic studies. The solution was incubated and thioflavin-T fluorescence was monitored to ensure that fibril formation had occurred. Seeds were freshly prepared to ensure reproducibility.

4.2.3 Thioflavin-T fluorescence assays

For kinetic assays, solutions were prepared by adding 20 mM, pH 7.4 Tris buffer containing thioflavin-T to lyophilized dry peptides for a final peptide concentration of 16 uM. For the seeding assays, preformed fibrils mixed with Tris buffered thioflavin-T solution were added to the lyophilized dry hIAPP samples. The final condition was 16 uM peptide, 32 uM thioflavin-T, 1.6 uM seeds (in monomer units), and 20 mM Tris buffer at pH 7.4. Measurements were made at 25 ^{o}C using a Beckman Coulter DTX880 plate reader without stirring.

4.2.4 Transmission electron microscopy (TEM)

TEM was performed at the Life Science Microscopy Center at Stony Brook University. Aliquots were removed from the same solutions that were used for the fluorescence measurements. 5 uL of peptide solution was placed on a carbon-coated Formvar 300 mesh copper grid for 1 min and then negatively stained with saturated uranyl acetate for another 1 min.

4.2.5 Two-dimensional infrared spectroscopy (2DIR)

Samples for 2DIR were prepared at 0.5 mM in 20 mM pH 7.4 Tris buffer in D_2O, in a CaF_2 infrared cell with a 56 mm Teflon spacer, after overnight deuterium exchange in 100% HFIP-d (Aldrich). 2DIR spectra were collected as described previously [16]. Briefly, 60 fs mid-IR pulses centered at 6 mm, generated by optical parametric amplification of light from a regeneratively amplified Ti: sapphire laser system, were split into pump and probe beams, the former of which was sent through a Ge-based mid-IR acoustooptic pulse shaper to generate the pump pulse pair needed for 2D spectra and to provide shot-to-shot phase cycling. After passing through the excitation region of the pump beam, the probe beam was detected and digitized with a 64 element MCT detector array system (Infrared Systems). The pump and probe beams were polarized parallel in all experiments.

4.3 Results and discussion

4.3.1 Design of a model system to study the role of His-18 and Tyr-37 interactions in IAPP amyloid formation

The primary sequences of human IAPP (hIAPP) and designed mutants are shown in Figure 4.1A. The molecule contains a single histidine at position 18 and three aromatic residues, including a

single tyrosine at the C-terminus. Several structural models of hIAPP amyloid fibrils have been proposed; one based on the analysis of small peptide fragments of hIAPP and two based on solid-state NMR studies [17, 18]. His-18 is buried in the core of the fibril in the model based on crystallographic studies, and in one of the NMR-based models. However, calculations performed at the level of the linearized Poisson-Boltzmann equation argue that the network of interactions formed by His-18 is enough to overcome the desolvation barrier for a neutral His side chain [19]. The C-terminal Tyr is part of the ordered β-sheet core in all models and the parallel in register β-structures mean that the C-terminus of the one polypeptide chain is close to the C-terminus of its neighbors. Thus, there should be considerable charge repulsion in amyloid fibrils formed from variants with a free C-terminus, provided of course that they adopt the same structure.

To investigate the potential importance of His-18 and Tyr-37 interactions, we synthesized hIAPP variants in which His-18 was replaced by the neutral residues, Gln and Leu. These substitutions were chosen because they are roughly similar in volume to His. Obviously, they differ in shape and hydrophobicity and these factors could influence amyloid formation. However, the use of two different substitutions at position 18 helps to ensure that any conclusions are robust. Additional variants were prepared with a free C-terminus and substitutions at position-18. (Figure 4-2A). The rate of amyloid formation was measured using fluorescent detected thioflavin-T binding assays [20].

The data collected for hIAPP show a typical sigmoidal curve (Figure 4-1B, *dots*). The H18Q-hIAPP single mutant forms amyloid fibrils moderately faster than hIAPP (Figure 4-1B, *squares*) and the fibril morphology is similar to hIAPP fibrils as judged by TEM and 2DIR (Figure 4-1C and 1D, and Figure 4-3). This argues that any interactions between His-18 and the C-terminus Tyr are not critical for amyloid formation because their disruption at physiologically relevant pH does

not inhibit amyloid formation, but actually accelerates it. When His-18 is replaced by Leu, a less polar substitution than Gln, even more dramatic effects are observed and amyloid formation is much faster. No apparent lag phase is observed for H18L-hIAPP (Figure 4-1B, *triangles*). The protonated state of His-18 significantly affects the rate of amyloid formation [21], however the pH used in these studies is 7.4 ±0.2, and His-18 is expected to be largely deprotonated under these conditions. Hence, the effects are unlikely to be due simply to removal of a positive charge.

4.3.2 IAPP variants with a free C-terminus behave differently than C-terminal amidated IAPP

Previous work has shown that the natural amidated form of hIAPP and an IAPP variant with a free acid at its C-terminus form a different distribution of oligomers during the aggregation process [22], but putative His-18 and Tyr-37 interactions have not been probed.

To examine the possible role of interactions between His-18 and the C-terminus, we synthesized variants of hIAPP with a free acid C-terminus (denoted free CT-hIAPP, Figure 4-2A). This is the same form that was used in the solution NMR studies that defined the head-to-tail dimers [1]. Free CT-hIAPP formed amyloid much more slowly than hIAPP, by a factor of 4, as judged by the t_{50} value of the two kinetic profiles (Figure 4-2B, *dots and squares*). TEM images revealed differences in fibril morphology. hIAPP formed long and dense fibrils, whereas the free CT-hIAPP fibrils are shorter and curly (Figure 4-2C and 2D). We also prepared an hIAPP variant with a free acid C-terminus and a His-to-Gln substitution (denoted H18Q free CT-IAPP, Figure 4-2A) to analyze the impact of replacing His-18 in the free carboxylate background. H18Q free CT-IAPP formed amyloid faster than free CT-hIAPP (Figure 4-2B, *triangles and squares*). Again, the data show that replacement of His-18 accelerates amyloid formation and thus indicates that His-18-Tyr-37 interactions are not essential for amyloid formation in either background at pH 7.4. We used 2DIR

to probe the secondary structure of amyloid fibrils formed by the different variants. The IR transitions of the Amide-I' modes of proteins are sensitive to secondary structure and 2DIR has been used to monitor secondary structure as well as the packing of individual peptides in IAPP amyloid [23, 24]. 2DIR spectra were recorded for all of the samples and are displayed in Figure 4-3.The spectra are broadly similar to previously reported spectra of hIAPP [24]. The slice along the diagonal in the 2DIR contains similar information to a traditional linear IR spectrum, but with more prominent β-sheet signal because β-sheets and α-helices have stronger transitions than random coils in 2D IR spectra [25]. The diagonal slices are very similar and all display a prominent, sharp peak centered near 1617–1620 cm^{-1}, a frequency range that corresponds to β-sheet structure. The data shows that all of the variants form β-sheet-rich aggregates.

4.3.3 Nonadditive effects are observed with multiple mutations

hIAPP with a free C-terminus formed amyloid significantly more slowly than wild-type (WT) hIAPP with a 4-fold longer t_{50}, whereas the His to Gln mutation at position 18 slightly accelerated the process (~20%). If the effects of the changes are independent there should be no synergy between them and the effect of a double mutation should be the sum of the individual effects. This approach is widely used in studies of protein folding and protein stability where the processes under consideration can usually be described by simple models using a limited number of thermodynamic states [26]. Amyloid formation is significantly more complex and may involve multiple pathways and heterogeneous distributions of intermediates. In addition, it is presently impossible to measure rate constants for each of the microscopic steps in amyloid formation and, instead, t_{50} or the lag time is often used as a proxy for the time constant. However, t_{50} and the lag time likely cannot be related to the lifetime of a single kinetic step. These considerations indicate that there are considerable complications in using a double mutant cycle type approach to analyze

amyloid kinetics, nonetheless, a semiquantitative analysis can still provide insight. If $1/t_{50}$ is used as a proxy for the rate, i.e., t_{50} is used as a proxy for an individual time constant, then one expects additive effects on the value of $\ln(1/t_{50})$ if two substitutions are independent, or equivalently, multiplicative effects on $(1/t_{50})$. Here, we used the ratio $(t_{50}/t_{50\text{-WT}})$ where $t_{50\text{-WT}}$ is the t_{50} of normal amidated WT hIAPP. The expected additive effect was estimated by multiplying this parameter (t_{50} of single mutant/$t_{50\text{-WT}}$) calculated for the two single substitutions. The analysis revealed that the observed effects were not equal to the result expected for noninteracting sites (Figure 4-4). The t_{50} for H18Q free CT-IAPP is 0.8 that of hIAPP, whereas the expected result, assuming independent effects, is 3.2-fold. This analysis suggests that the C-terminal carboxylate interacts with His-18, but that the interaction does not favor amyloid formation.

4.3.4 Amyloid fibrils formed by IAPP variants with a free acid C-terminus do not seed amyloid formation by hIAPP

We further examined the structural similarity between hIAPP fibrils and the fibrils formed by different hIAPP variants using seeding experiments. Preformed hIAPP fibrils can be used as seeds to seed amyloid formation by monomeric hIAPP leading to a bypassing of the lag phase. Seeding is generally specific and structural differences between different proteins impact seeding efficiencies [27, 28]. We first seeded hIAPP with hIAPP fibrils as a control. As expected, a bypass of the lag phase was observed and a significant increase in thioflavin-T fluorescence in the first few hours was detected (Figure 4-5, *open circles*). We then tested the ability of fibrils formed by the different variants to seed hIAPP. When hIAPP was seeded by preformed H18Q-hIAPP fibrils, a curve similar to the control study was observed, suggesting that H18Q- hIAPP formed fibrils that are very similar to those generated by hIAPP fibrils (Figure 4-5, *diamonds*). In striking contrast, either of the variants with a free C-terminus is much less effective at seeding amyloid formation

by hIAPP and a significant lag phase is still observed. (Figure 4-5, *squares and triangles*). This result highlights the importance of the C-terminus and strongly suggests that there are differences in the details of the fibril structure formed by amidated and unamidated hIAPP. It is striking that simply replacing an amide group at the C-terminus by a carboxylate has more effect than replacing His-18 by residues that differ significantly in shape and polarity.

4.3.5 Analysis of H18Q-hIAPP reveals that the protonation state of the N-terminus affects the rate of amyloid formation

The rate of human IAPP amyloid formation is pH dependent and is faster above pH 7 than below. This is likely due in part to the deprotonation of His-18, but the free N-terminus could also contribute [21, 29]. Our H18Q-hIAPP mutant allows us to probe the role of the protonation state of the N-terminus in a background where no other groups titrate with a similar pKa. Amyloid formation by the mutant is approximately 4-fold faster at pH 7.5 relative to the rate at pH 5.0 (Figure 4-6 and Figure 4-7). The data highlights the contribution of the N-terminal charge state to amyloid formation and reveals that the pKa of the free N-terminus is below 7.5. All models of IAPP amyloid fibril postulate that the N-terminus is flexible, thus the strong dependence of the rate of amyloid formation on its charge state is striking.

4.4 Conclusions

The analysis presented here clearly shows that interactions involving His-18 and the C-terminus Tyr are not essential for amyloid formation and, furthermore, show that disrupting this potential interaction in both backgrounds enhances the rate of amyloid formation. Previous work, using recombinant IAPP with a free C-terminus, provided good evidence, via NMR, for interactions

between His-18 and the C-terminus at pH 5.5 [1]. This led to a model for formation of a head-to-tail dimer. Such interactions are expected to be stronger in the IAPP variant with a free C-terminus at low pH because the negatively charged carboxylate will make stronger interactions with His-18, which will be positively charged at pH 5.5. The data presented here show that if such interactions are formed in the physiologically relevant amidated form at physiological pH they do not promote amyloid formation, but rather hinder it.

Does this mean that the C-terminus of IAPP does not interact with the side chain of His-18? Not necessarily. The observation of nonadditive effects between the C-terminus and His-18 is consistent with formation of an interaction, although the effects are small. However, this does not imply that head-to-tail dimers are formed; they may be, but the fact that replacement of His-18 accelerates amyloid formation is broadly consistent with other models of early intermediates. The helical intermediate model predicts that the key contacts are made in the region of residues 8 to 18 and replacement of His might improve packing in this region [4-6]. The β-hairpin model involves two intramolecular β-hairpins packing together via strand-strand interactions in the region of residues 11 to 18 and residues 23 to 32 [7]. Again, replacement of His-18 could modify these interactions and might reduce unfavorable interactions between two polar side chains.

Replacement of the neutral amidated C-terminus with a negatively charged free carboxylate significantly decreased the rate of amyloid formation, consistent with previous studies [21], even though the change decreases the net charge on the polypeptide, showing that the rate of aggregation does not correlate with the net charge of the peptide although electrostatic interactions and peptide ion interactions are important in IAPP aggregation [19]. There is a parallel with the solubility of globular proteins; to a rough first approximation, proteins are the least soluble when the pH equals

the protein pI, but there are numerous examples where proteins are actually less soluble when pH does not equal the pI.

The fact that hIAPP variants with a free C-terminus are significantly less amyloidogenic argues that hIAPP is not under strong evolutionary pressure to minimize amyloidogenicity. The advantages of a modified C-terminus, enhanced resistance to proteases and possibly higher biological activity clearly outweigh the deleterious effects of increased *in vitro* amyloidogenicity. The likely explanations are that, until very recently, type 2 diabetes and islet amyloid did not significantly affect the young, thus prevention of islet amyloid was not under strong evolutionary pressure. A second, but not exclusive, possibly is that *in vitro* amyloidogenicity does not directly correlate with *in vivo* amyloidogenicity. The latter point may be relevant for hIAPP because hIAPP normally does not form amyloid *in vivo* even though it is stored in the secretary granule at concentrations that lead to rapid amyloid formation *in vitro*.

4.5 Figures

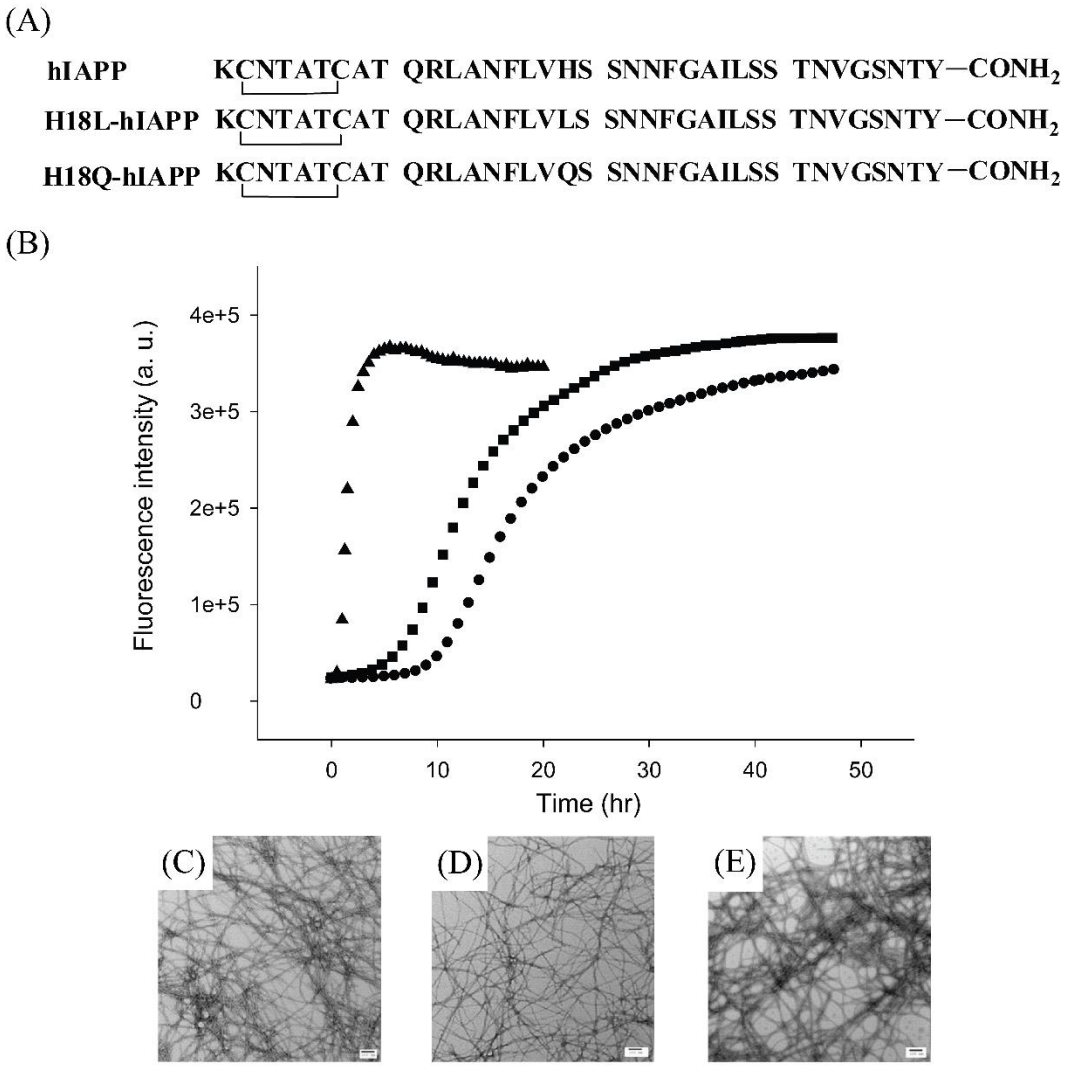

Figure 4-1: (A) Primary sequence of hIAPP and the two IAPP variants designed to study the potential His-18-Tyr-37 interaction in the naturally occurring amidated background. All peptides contain a disulfide bridge between residues 2 and 7, and an amidated C-terminus. (B) Thioflavin-T fluorescence monitored kinetic experiments are shown: *Dots*, hIAPP; *Squares*, H18Q-hIAPP; *Triangles*, H18LhIAPP. All experiments were conducted in 20 mM, pH 7.4 Tris buffer, without stirring at 25 ^{o}C. TEM image of the amyloid fibrils formed by hIAPP (C); H18Q-hIAPP (D); H18L-hIAPP (E). Scale bars represent 100 nm.

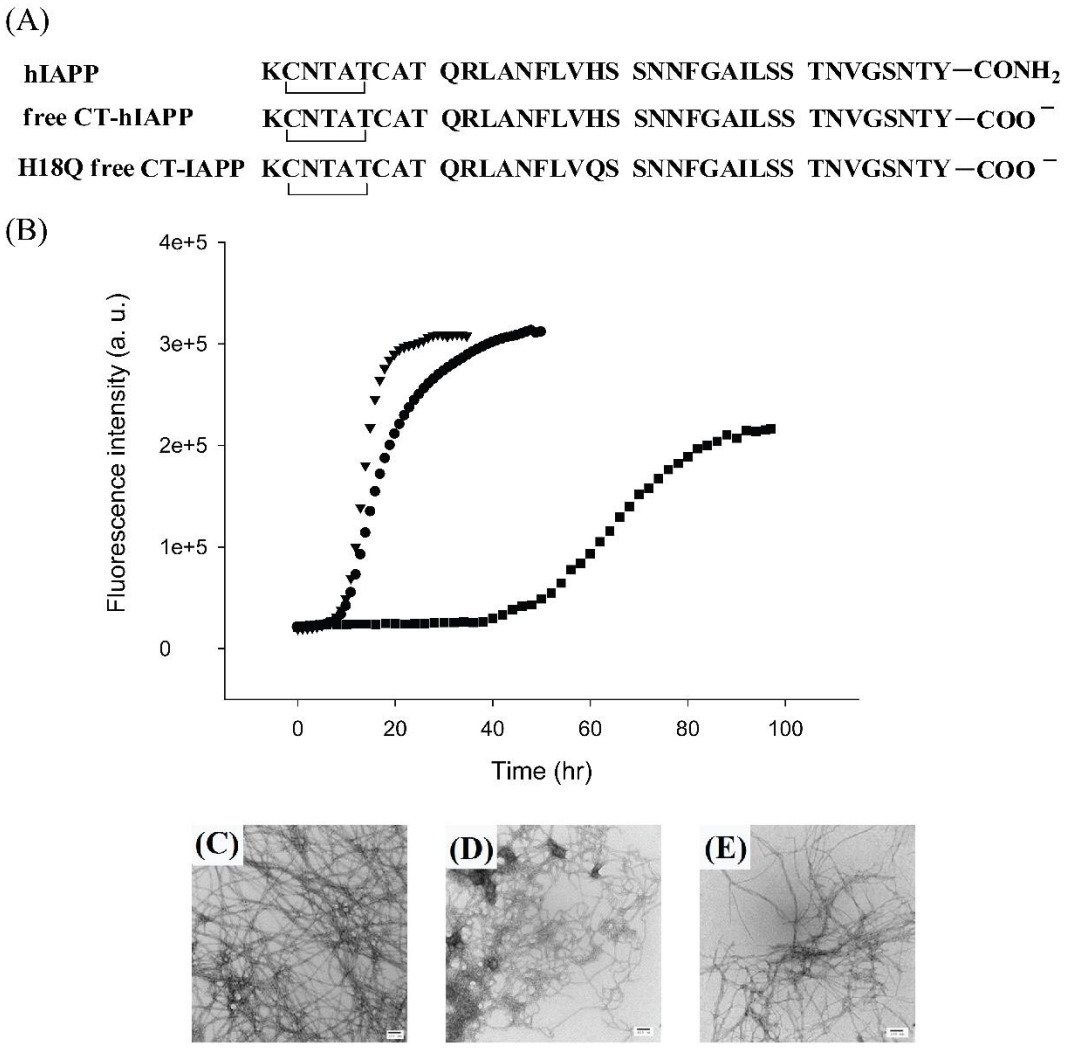

Figure 4-2: (A) Primary sequence of hIAPP and the two IAPP variants with a free C-terminus. All peptides contain a disulfide bridge between residues 2 and 7. (B) Thioflavin-T fluorescence monitored kinetic experiments are shown: *Dots*, hIAPP; *Triangles*, H18Q free CT-IAPP; *Squares*, free CT-hIAPP. All experiments were conducted in 20 mM, pH 7.4 Tris buffer without stirring at 25 ^{o}C. (C) TEM image of the amyloid fibrils formed by hIAPP. The micrograph is the same as the one shown in Figure 4-1. (D) TEM image of the amyloid fibrils formed by free CT-hIAPP. (E) TEM image of the amyloid fibrils formed by H18Q free CT-IAPP. Scale bars represent 100 nm.

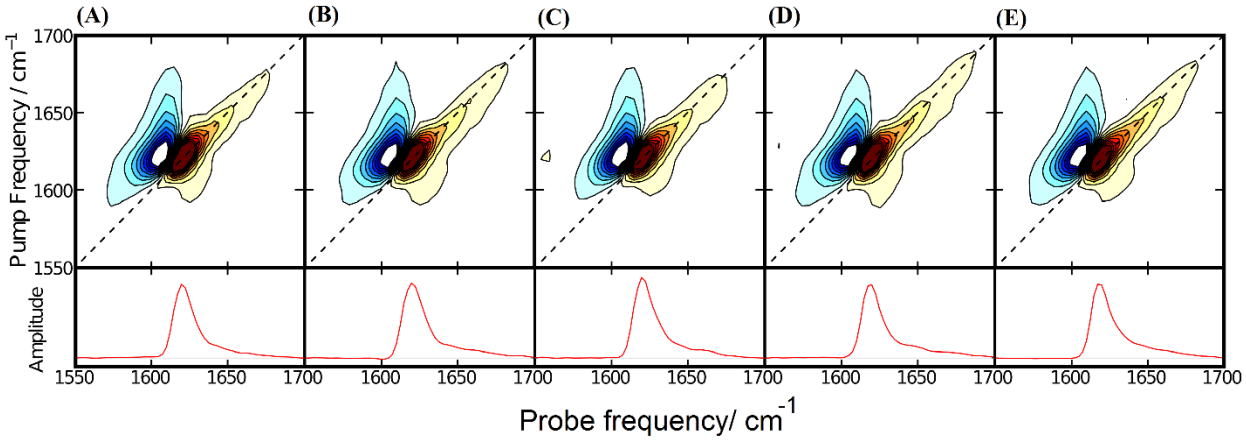

Figure 4-3: Two-dimensional infrared spectroscopy confirms that all peptides form amyloid fibrils. (A) hIAPP. (B) H18L-hIAPP. (C) H18Q-hIAPP. (D) Free CT-hIAPP. (E) H18Q free CT-IAPP. The diagonal slices of each spectrum are shown at the bottom of the figure.

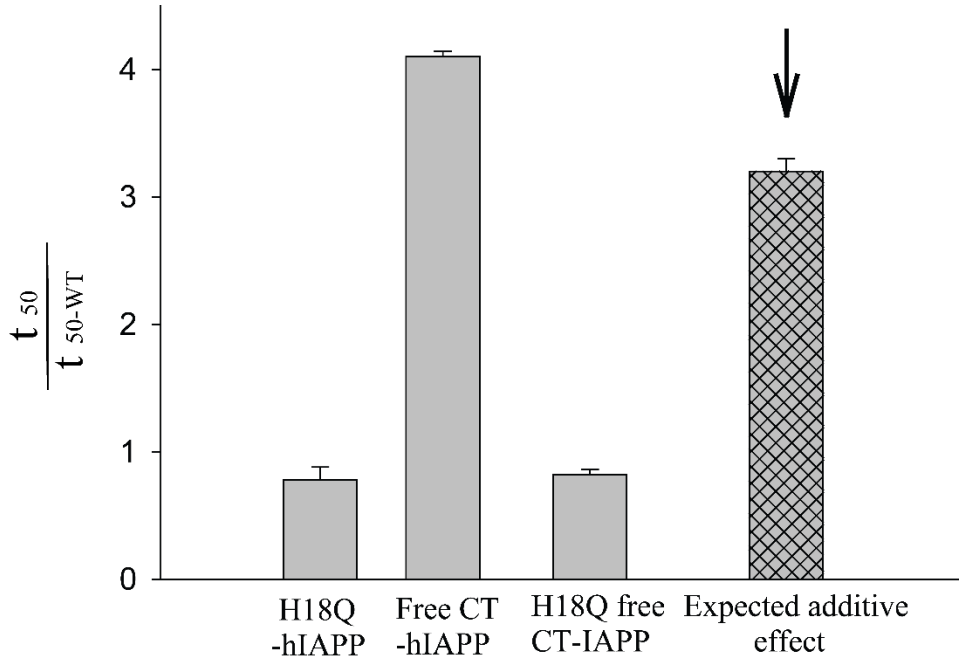

Figure 4-4: Nonadditive effects were observed between the C-terminus and His-18. The histogram shows the effect caused by mutation or by modification of the C-terminus. The expected additive result is indicated by the arrow.

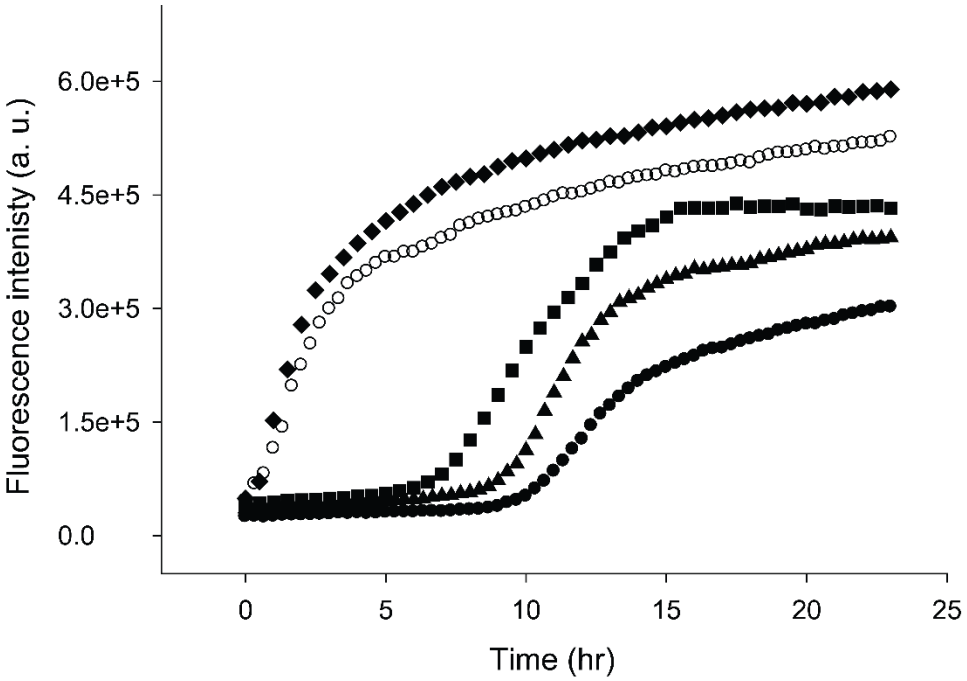

Figure 4-5: Amyloid fibrils formed by IAPP variants with a free acid C-terminus are much less effective at seeding amyloid formation by hIAPP than amyloid fibrils formed by variants with an amidated C-terminus. Thioflavin-T fluorescence monitored kinetic experiments are shown: *Dots*, unseeded hIAPP; *Open circles*, hIAPP seeded by hIAPP amyloid fibrils; *Diamonds*, hIAPP seeded by H18Q-hIAPP amyloid fibrils; *Triangles*, hIAPP seeded by free CT-hIAPP amyloid fibrils; *Squares*, hIAPP seeded by free H18Q CT-IAPP amyloid fibrils. Seeds were present at 10% concentration in monomer units.

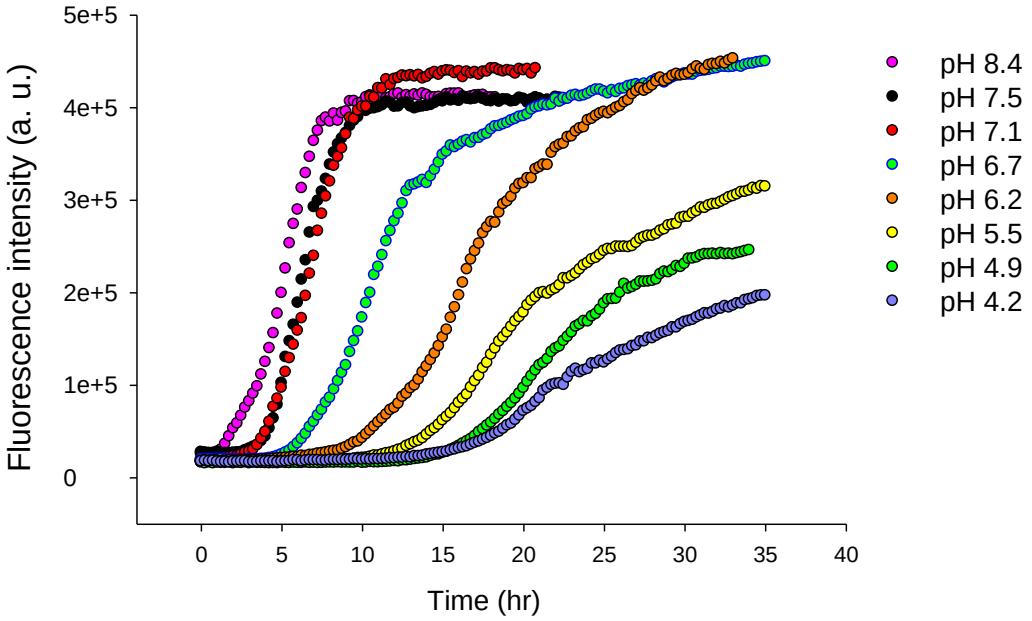

Figure 4-6: Kinetics of amyloid formation by H18Q-hIAPP in different pH conditions. The curves were used to measure the t_{50} values shown in Figure 4-7. Experiments were conducted at 25 ^{o}C. The peptide concentration was 20 uM.

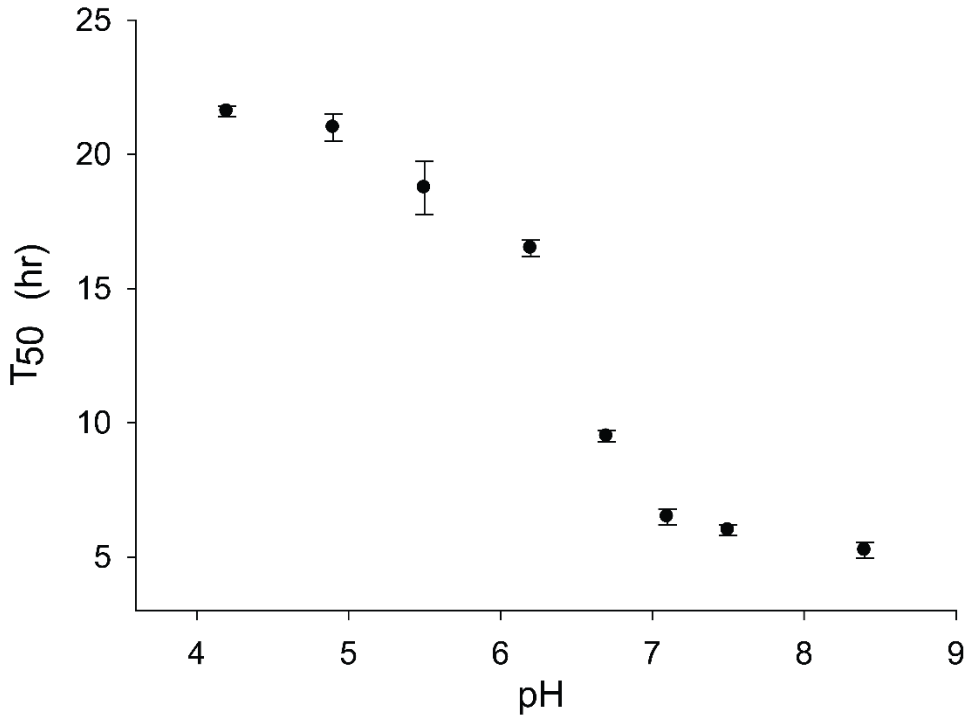

Figure 4-7: The pH dependence of amyloid formation by H18Q-hIAPP shows that the charge state of the N-terminus plays an important role in amyloid formation. Values of t_{50} are plotted versus pH. Experiments were conducted at 25 ^{o}C in 20 mM Tris buffer. The error bars were derived by conducting 3 to 4 independent measurements for each pH. The pH was adjusted by addition of small amounts of HCl. The maximum added Cl^{-}, beyond that present in the Tris buffer, due to the addition of HCl was 5 mM.

4.6 References

1. Wei, L.; Jiang, P.; Xu, W. X.; Li, H.; Zhang, H.; Yan, L. Y.; Chan-Park, M. B.; Liu, X. W.; Tang, K.; Mu, Y. G.; Pervushin, K., The molecular basis of distinct aggregation pathways of islet amyloid polypeptide. *J. Biol. Chem.* **2011**, *286* (8), 6291-6300.

2. Meurisse, R.; Brasseur, R.; Thomas, A., Aromatic side-chain interactions in proteins. Near- and far-sequence His-X pairs. *Biochim. Biophys. Acta.* **2003**, *1649* (1), 85-96.

3. Marek, P.; Gupta, R.; Raleigh, D. P., The fluorescent amino acid *p*-cyanophenylalanine provides an intrinsic probe of amyloid formation. *Chembiochem* **2008**, *9* (9), 1372-1374.

4. Abedini, A.; Raleigh, D. P., A critical assessment of the role of helical intermediates in amyloid formation by natively unfolded proteins and polypeptides. *Protein Eng. Des. Sel.* **2009**, *22* (8), 453-459.

5. Abedini, A.; Raleigh, D. P., A role for helical intermediates in amyloid formation by natively unfolded polypeptides? *Phys. Biol*. **2009**, *6* (1), 15005. 18

6. Wiltzius, J. J. W.; Sievers, S. A.; Sawaya, M. R.; Eisenberg, D., Atomic structures of IAPP (amylin) fusions suggest a mechanism for fibrillation and the role of insulin in the process. *Protein Sci.* **2009**, *18* (7), 1521-1530.

7. Dupuis, N. F.; Wu, C.; Shea, J. E.; Bowers, M. T., The amyloid formation mechanism in human IAPP: Dimers have beta-strand monomer-monomer interfaces. *J. Am. Chem. Soc.* **2011**, *133* (19), 7240-7243.

8. Williamson, J. A.; Miranker, A. D., Direct detection of transient alpha-helical states in islet amyloid polypeptide. *Protein Sci.* **2007**, *16* (1), 110-117.

9. Janson, J.; Ashley, R. H.; Harrison, D.; McIntyre, S.; Butler, P. C., The mechanism of islet amyloid polypeptide toxicity is membrane disruption by intermediate-sized toxic amyloid particles. *Diabetes* **1999**, *48* (3), 491-498.

10. Klein, W. L.; Stine, W. B.; Teplow, D. B., Small assemblies of unmodified amyloid beta-protein are the proximate neurotoxin in Alzheimer's disease. *Neurobiol. Aging* **2004**, *25* (5), 569-580.

11. Baglioni, S.; Casamenti, F.; Bucciantini, M.; Luheshi, L. M.; Taddei, N.; Chiti, F.; Dobson, C. M.; Stefani, M., Prefibrillar amyloid aggregates could be generic toxins in higher organisms. *J. Neurosci.* **2006**, *26* (31), 8160-8167.

12. Abedini, A.; Raleigh, D. P., Incorporation of pseudoproline derivatives allows the facile synthesis of human IAPP, a highly amyloidogenic and aggregation-prone polypeptide. *Org. Lett.* **2005**, *7* (4), 693-696.

13. Marek, P.; Mukherjee, S.; Zanni, M. T.; Raleigh, D. P., Residue-specific, real-time characterization of lag-phase species and fibril growth during amyloid formation: A combined fluorescence and IR study of p-cyanophenylalanine analogs of islet amyloid polypeptide. *J. Mol. Biol.* **2010**, *400* (4), 878-888.

14. Tam, J. P.; Wu, C. R.; Liu, W.; Zhang, J. W., Disulfide bond formation in peptides by dimethyl-sulfoxide-Scope and applications. *J. Am. Chem. Soc.* **1991**, *113* (17), 6657-6662.

15. Abedini, A.; Singh, G.; Raleigh, D. P., Recovery and purification of highly aggregation-prone disulfide-containing peptides: Application to islet amyloid polypeptide. *Anal. Biochem.* **2006**, *351* (2), 181-186.

16. Middleton, C. T.; Woys, A. M.; Mukherjee, S. S.; Zanni, M. T., Residue-specific structural kinetics of proteins through the union of isotope labeling, mid-IR pulse shaping, and coherent 2D IR spectroscopy. *Methods.* **2010**, *52* (1), 12-22.

17. Wiltzius, J. J.; Sievers, S. A.; Sawaya, M. R.; Cascio, D.; Popov, D.; Riekel, C.; Eisenberg, D., Atomic structure of the cross-beta spine of islet amyloid polypeptide (amylin). *Protein Sci.* **2008**, *17* (9), 1467-74.

18. Luca, S.; Yau, W. M.; Leapman, R.; Tycko, R., Peptide conformation and supramolecular organization in amylin fibrils: Constraints from solid-state NMR. *Biochemistry* **2007**, *46* (47), 13505-13522.

19. Marek, P. J.; Patsalo, V.; Green, D. F.; Raleigh, D. P., Ionic strength effects on amyloid formation by amylin are a complicated interplay among debye screening, ion selectivity, and hofmeister effects. *Biochemistry* **2012**, *51* (43), 8478-8490.

20. Levine, H., Thioflavin-T interaction with amyloid beta-sheet structures. *Amyloid* **1995**, *2* (1), 1-6.

21. Abedini, A.; Raleigh, D. P., The role of His-18 in amyloid formation by human islet amyloid polypeptide. *Biochemistry* **2005**, *44* (49), 16284-16291.

22. Chen, M. S.; Zhao, D. S.; Yu, Y. P.; Li, W. W.; Chen, Y. X.; Zhao, Y. F.; Li, Y. M., Characterizing the assembly behaviors of human amylin: a perspective derived from C-terminal variants. *Chem. Comm.* **2013**, *49* (18), 1799-1801.

23. Strasfeld, D. B.; Ling, Y. L.; Shim, S. H.; Zanni, M. T., Tracking fiber formation in human islet amyloid polypeptide with automated 2D-IR spectroscopy. *J. Am. Chem. Soc.* **2008**, *130* (21), 6698-6699

24. Shim, S. H.; Gupta, R.; Ling, Y. L.; Strasfeld, D. B.; Raleigh, D. P.; Zanni, M. T., Two-dimensional IR spectroscopy and isotope labeling defines the pathway of amyloid formation with residue-specific resolution. *Proc. Natl. Acad. Sci. U.S.A.* **2009**, *106* (16), 6614-6619.

25. Grechko, M.; Zanni, M. T., Quantification of transition dipole strengths using 1D and 2D spectroscopy for the identification of molecular structures via exciton delocalization: Application to alpha-helices. *J. Chem. Phys.* **2012**, *137* (18), 184202

26. Horovitz, A., Double-mutant cycles: A powerful tool for analyzing protein structure and function. *Fold. Des.* **1996**, *1* (6), R121-R126.

27. O'Nuallain, B.; Williams, A. D.; Westermark, P.; Wetzel, R., Seeding specificity in amyloid growth induced by heterologous fibrils. *J. Biol. Chem.* **2004**, *279* (17), 17490-17499.

28. Krebs, M. R. H.; Morozova-Roche, L. A.; Daniel, K.; Robinson, C. V.; Dobson, C. M., Observation of sequence specificity in the seeding of protein amyloid fibrils. *Protein Sci.* **2004**, *13* (7), 1933-1938.

29. Li, Y.; Xu, W. X.; Mu, Y. G.; Zhang, J. Z. H., Acidic pH retards the fibrillization of human islet amyloid polypeptide due to electrostatic repulsion of histidines. *J. Chem. Phys.* **2013**, *139* (5), 055102

Chapter 5. Aspirin, diabetes and amyloid: Reexamination of the inhibition of amyloid formation by aspirin and ketoprofen

Abstract

There are no therapeutic strategies for the treatment or prevention of islet amyloidosis. The non-steroid anti-inflammatory drug (NSAID) aspirin and ketoprofen, at clinically relevant doses, have been proposed to inhibit amyloid formation by IAPP and thus may hold promise for treatment of islet amyloidosis. These compounds are potentially attractive given the importance of inflammation in islet amyloidosis and given the fact that there are no anti islet amyloid agents in the clinic. We show that aspirin, even in 20 fold excess, has no effect on the kinetics of amyloid formation by IAPP as judged by thioflavin-T binding, right angle light scattering (RALS) and TEM, nor does it alter the morphology of resulting amyloid fibrils. Aspirin showed no ability to disaggregate preformed IAPP amyloid fibrils under the conditions of these studies, 25 ^{o}C and pH 7.4. Ketoprofen is similarly ineffective at inhibiting IAPP amyloid formation. The compounds do, however, interfere with CD- and Congo red-based assays of IAPP amyloid formation. This study highlights the importance of using multiple methods to follow amyloid formation when screening inhibitors.

NOTE: The material presented in this chapter has been published (Tu, L.H.; Noor, H.; Cao, P.; Raleigh, D. P., Aspirin, diabetes and amyloid: Reexamination of the inhibition of amyloid formation by Aspirin and Ketoprofen. *ACS Chem. Biol.* **2014**, *9* (7), 1632–1637). This chapter

contains direct excerpts from the manuscript, which was written by me with suggestions and revisions from Professor Daniel P. Raleigh.

5.1 Introduction

Analogs of human IAPP which are less aggregation prone than wild-type human IAPP have been approved as an adjunct to insulin therapy [1], but there is no treatment for islet amyloidosis, and there are no any approved therapeutic strategies to prevent islet amyloid deposition. The search for inhibitors of amyloid aggregation and amyloid formation is an active area of research [2-9], but comparatively few anti IAPP amyloid compounds have been developed and the vast majority of those are not drug like. Recently, the intriguing possibility that clinically relevant doses of the non-steroid anti-inflammatory drug (NSAID), aspirin and ketoprofen may inhibit IAPP amyloid formation and might disaggregate preformed IAPP amyloid fibrils has been raised [10]. This could open very attractive, inexpensive therapeutic approaches if the compounds were indeed effective anti-IAPP amyloid agents, particularly as inflammation is believed to play a role in islet amyloidosis toxicity and a central role in type-2 diabetes [11-17]. Here we critically examine the effects of aspirin and ketoprofen on IAPP amyloid formation and the effects of aspirin on preformed IAPP amyloid fibrils. Aspirin does not inhibit IAPP amyloid formation, even when added at 20-fold excess, and is unable to disassemble preformed IAPP amyloid. Ketoprofen is similarly ineffective at inhibiting amyloid formation. The reasons for the discrepancy with prior reports are examined and it is concluded that they are due to interference of the compounds with the analytical assays used and with the difficulty in analyzing small changes in CD spectra. The implications for the testing of amyloid inhibitors are discussed. The present study emphasizes the

necessity of employing multiple techniques to avoid false positive or false negatives in inhibition assays.

5.2 Materials and methods

5.2.1 Peptide synthesis and purification

Human IAPP was synthesized on a 0.1 mmol scale using a CEM Liberty microwave peptide synthesizer utilizing Fmoc chemistry. Solvents used were ACS-grade. The methods have been described previously [18, 19]. In order to afford a peptide with an amidated C-terminus, Fmoc-PAL-PEG-PS resin was used and purchased from Life Technologies. Standard Fmoc reaction cycles were used. Fmoc protected pseudoproline dipeptide derivatives were incorporated at positions 9-10, 19-20, and 27-28 to facilitate the synthesis. The β-branched residues, Arg, and all pseudoproline dipeptide derivatives were double coupled. A maximum temperature of 50 ^{o}C was used for the coupling of His and Cys in order to reduce the possibility of racemization. Peptides were cleaved from the resin by standard TFA methods; ethanedithiol, thioanosole and anisole were used as scavengers. Crude peptide was partially dissolved in 20% acetic acid (v/v), frozen in liquid nitrogen, and lyophilized to increase their solubility. The dry peptide was redissolved in 100% DMSO at room temperature to promote the formation of the disulfide bond [20, 21]. Peptide was purified by reverse-phase HPLC using a Proto 300 C18 preparative column (10 mm x 250 mm). A two buffer gradient was used: buffer A consisted of 100% H_2O and 0.045% HCl (v/v) and buffer B included 80% acetonitrile, 20% H_2O and 0.045% HCl. HCl was used as the counterion instead of TFA since residual TFA can influence amyloid formation. MALDI-TOF mass spectrometry confirmed the correct molecular weight (expected 3903.3 Da, observed 3902.8 Da).

5.2.2 Sample preparation

Human IAPP was first dissolved in 100% HFIP at a concentration of 1.6 mM and then filtered to remove any preformed amyloid aggregates. For thioflavin-T fluorescence assays, aliquots were lyophilized and redissolved in pH 7.4, 20 mM Tris buffer at the desired concentration. Aspirin and ketoprofen were prepared in 100% DMSO.

5.2.3 Thioflavin-T fluorescence assays

Solutions were prepared by adding pH 7.4, 20 mM Tris buffer and thioflavin-T to lyophilized dry peptides for a final peptide concentration of 16 μM. For the studies of aspirin and ketoprofen, 0.25% DMSO was present in the solution. Samples were incubated in the 96-well black plate. Measurements were made at 25 ^{o}C using a Beckman Coulter DTX880 plate reader without stirring. An excitation filter of 430 nm and an emission filter of 485 nm were used. To test the potential disaggregation activity of aspirin, peptide was first incubated in a low-binding 96-well plate and monitored using plate reader to ensure the formation of amyloid fibrils. Aspirin was added at 20-fold excess after amyloid formation.

5.2.4 Right Angle Light Scattering assays (RALS)

Solutions were prepared by adding pH 7.4, 20 mM Tris buffer without thioflavin-T to lyophilized dry peptides for a final peptide concentration of 16 μM. Samples are incubated in the low binding microcentrifuge tubes. Experiments were conducted using an Applied Phototechnology Fluorescence Spectrophotometer. RALS assays used an excitation and emission wavelength of 500 nm.

5.2.5 Transmission electron microscopy (TEM)

TEM was performed at the Life Science Microscopy Center at Stony Brook University. Aliquots were removed from the same solutions that were used for the fluorescence measurements. 5 μL of peptide solution was placed on carbon-coated Formvar 300 mesh copper grid for one minute and then negatively stained by incubation with saturated uranyl acetate for another one minute.

5.2.6 *Circular dichroism (CD) experiments*

CD experiments were performed using an Applied Photophysics Chirascan circular dichroism spectrometer. The solutions for the CD experiments were prepared by diluting the filtered stock peptide solutions into 20 mM Tris buffer at pH 7.4. The final concentration of peptide was 16 μM in 1 % HFIP. Spectra were recorded from 198 to 260 nm at 1 nm intervals in a quartz cuvette with 0.1 cm path length at 25 ^{o}C. Data were averaged from three scans. A background spectrum was subtracted from the collected data.

5.3 Results and discussion

5.3.1 Aspirin does not inhibit amyloid formation by IAPP

IAPP sequence and the structure of aspirin and ketoprofen are shown in Figure 5-1. We first examined the effects of aspirin on the kinetics of amyloid formation using fluorescence detected thioflavin-T binding assays. This is the standard assay in this field. Figure 5-2 displays the results of kinetic experiments conducted in the presence of aspirin. The expected sigmoidal time course is observed in the absence of aspirin with a t_{50}, defined as the time required to reach half of the total signal change in the thioflavin-T assay, of 20 h. Addition of aspirin, up to even a 20-fold excess, had no detectable effect on the rate of amyloid formation, as judged by the values of t_{50}. The compound also had no detectable effect on the final thioflavin-T intensity. Thioflavin-T binding assays are indirect since they rely on the binding of an extrinsic probe, and can sometimes

give misleading results [22], but they do have the advantage that they report on the kinetics of IAPP amyloid formation in the absence of conflicting factors. We also used TEM to monitor the effects of aspirin. Aliquots were removed from each sample at the end of kinetic experiments, blotted onto TEM grids and imaged. Extensive mats of fibrils were observed in the sample of IAPP alone and in all of the samples that contained aspirin.

Initial reports of the ability of aspirin to inhibit IAPP amyloid formation did not use thioflavin-T assays or TEM, but rather used CD and Congo red binding assays. It is possible, although unlikely, that thioflavin-T could displace aspirin from IAPP and interfere with its effects. This does not seem plausible since thioflavin-T has no such effect on a wide range of other inhibitors [23, 24] and does not bind to pre-amyloid intermediates. Nonetheless, we also tested the effects of aspirin in the absence of thioflavin-T using right angle light scattering (RALS) and TEM. Similar aggregation curves are observed in the presence and in the absence of a 20-fold excess of aspirin using RALS (Figure 5-3). TEM of the samples reveals the presence of dense mats of fibrils in each sample. Note that these samples did not contain thioflavin-T.

5.3.2 Aspirin is not capable of disaggregating preformed IAPP amyloid fibrils

We next examined the ability of aspirin to disaggregate preformed IAPP amyloid fibrils. Some, but not all inhibitors of amyloid formation have this property. We monitored amyloid formation using thioflavin-T assays (Figure 5-4) and then added a 20-fold excess of aspirin after amyloid formation was complete and the reaction had reached the saturation phase. Aliquots were removed for TEM analysis just before addition of aspirin, immediately afterwards and 48 h later. Addition of the compound did not perturb the thioflavin-T time course, in contrast, compounds which disaggregate amyloid fibrils lead to a decay in the thioflavin-T signal as a function of time

[2]. The TEM images recorded before and after addition of aspirin are very similar and reveal extensive deposits of amyloid fibrils, confirming that compound does not disaggregate IAPP amyloid (Figure 5-4B to 4D). In addition, CD spectra recorded before and after the addition of aspirin have an identical shape, consistent with a high degree of β-structure, although there is a modest decrease in intensity. Furthermore, no changes in the CD spectra are observed upon further incubation of up to 12 h (Figure 5-5). The CD studies are fully consistent with thioflavin-T, TEM, and RALS experiments.

5.3.3 Ketoprofen is not an inhibitor of IAPP amyloid formation

The NSAID ketoprofen has also been proposed to be an inhibitor of IAPP amyloid formation, again on the basis of Congo red assays and CD spectroscopy. We examined the ability of the compound to inhibit amyloid formation by human IAPP using TEM to directly test its effect on amyloid formation (Figure 5-6). TEM analysis revealed the presence of extensive mats of amyloid fibrils in all samples, showing that the compound is not an IAPP amyloid inhibitor.

5.4 Conclusions

The data presented here show that aspirin and ketoprofen do not inhibit IAPP amyloid formation under the conditions used, pH 7.4 and 25 ^{o}C. Why do the conclusions of this study differ from previous work? The earlier studies used trifluroethanol (TFE) to promote amyloid formation. TFE and HFIP stabilize secondary structure of peptides and even modest amount of HFIP or TFE can accelerate amyloid formation [25]. The use of a non-aqueous solvent to induce amyloid formation may contribute to the different conclusions, but the methods used also play a role. The previous study made use of CD and absorbance detected Congo red binding assays. The reported CD spectra

are different in the presence of high concentrations of aspirin, however, the reported spectrum, even at the highest concentration of aspirin, is not that of a random coil, and has a shape consistent with significant β-sheet intensity. In addition, the absorbance of aspirin and ketoprofen in the range of 200-250 nm can interfere with CD measurements. We employed different conditions to induce amyloid formation here and observed no change in the shape of the CD spectrum upon the addition of aspirin to preformed amyloid fibrils. Congo red binding was also used to test for the presence of amyloid in the original studies. Congo red staining is a classic method to probe amyloid formation, particularly for *ex-vivo* amyloid deposits and usually involves monitoring birefringence, but the absorbance-based assays are also employed. In either case, the dye is an extrinsic probe and it has been shown that it is not amyloid specific [26]. In the case of absorbance assays, addition of compounds can interfere by contributing background absorbance or by interfering with the binding of the dye. These considerations and the data presented here highlight the importance of using multiple probes to study amyloid inhibition, particularly methods such as TEM, which directly detect amyloid fibrils.

5.5 Figures

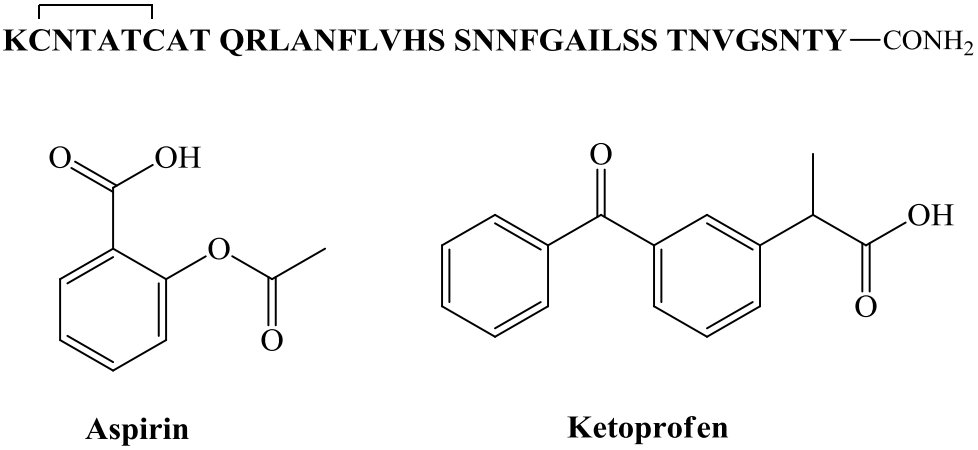

Figure 5-1: Primary sequence of human IAPP and the structure of aspirin and ketoprofen. IAPP contains a disulfide bridge between residues 2 and 7, and the C-terminus is amidated.

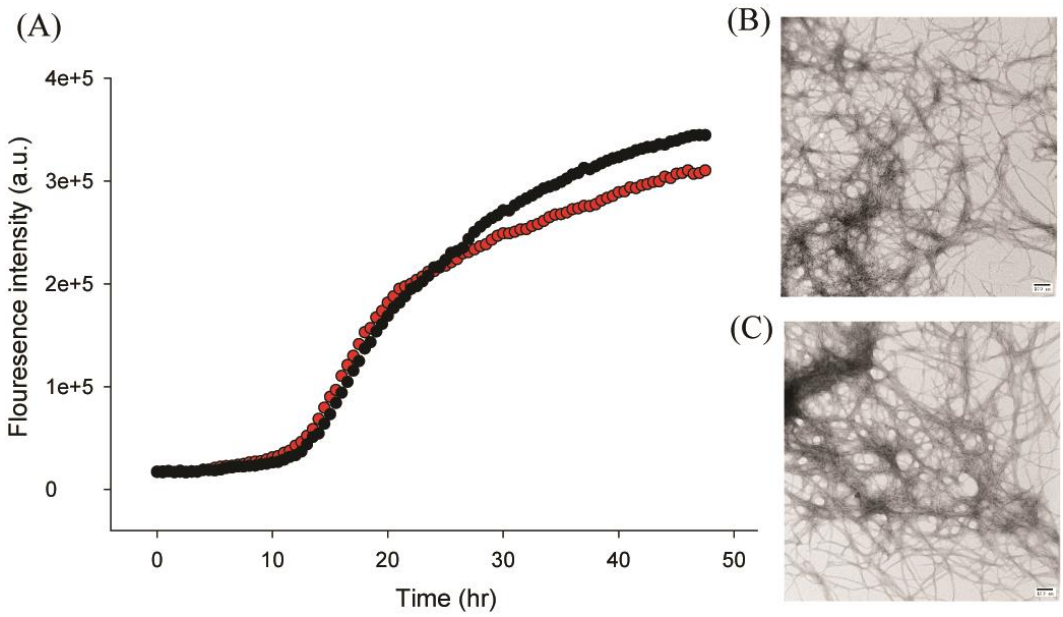

Figure 5-2: Aspirin does not inhibit amyloid formation by human IAPP. (A) Thioflavin-T fluorescence assays of the time course of amyloid formation in the absence (black) and in the presence (red) of a 20-fold excess of aspirin. (B) TEM image of the sample of IAPP without aspirin recorded at the end of the kinetic experiment. (C) TEM image of the sample of IAPP with a 20-fold excess of aspirin recorded at the end of the kinetic experiment. Scale bars represent 100 nm. Experiments were conducted at pH 7.4 and 25 ^{o}C in 20 mM Tris buffer, 0.25% DMSO (v/v) in the absence of any fluorinated alcohol co-solvent. The concentration of IAPP was 16 μM and the concentration of aspirin was 320 μM.

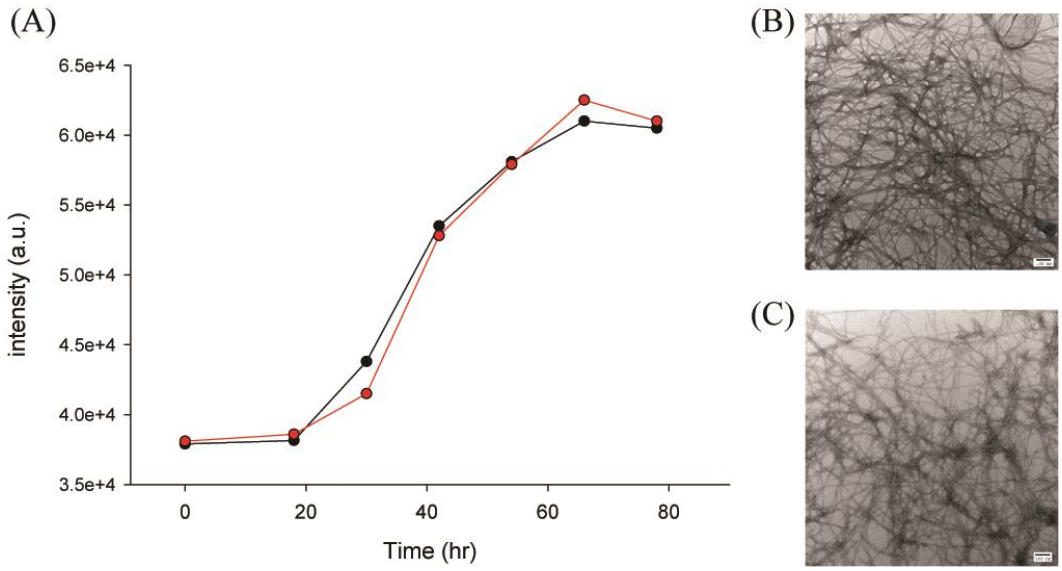

Figure 5-3: Aspirin does not inhibit amyloid formation by human IAPP. (A) RALS assays of the time course of amyloid formation in the absence (black) and in the presence (red) of a 20-fold excess of aspirin. No thioflavin-T was added to either sample (B) TEM image of the sample of IAPP without aspirin recorded at the end of the kinetic experiment. (C) TEM image of the sample of IAPP with 20-fold excess aspirin recorded at the end of the kinetic experiment. Scale bars represent 100 nm. Experiments were conducted at pH 7.4 and 25 ºC in 20 mM Tris buffer, 0.25% DMSO (v/v) in the absence of any fluorinated alcohol co-solvent. The concentration of IAPP was 16 μM and the concentration of aspirin was 320 μM.

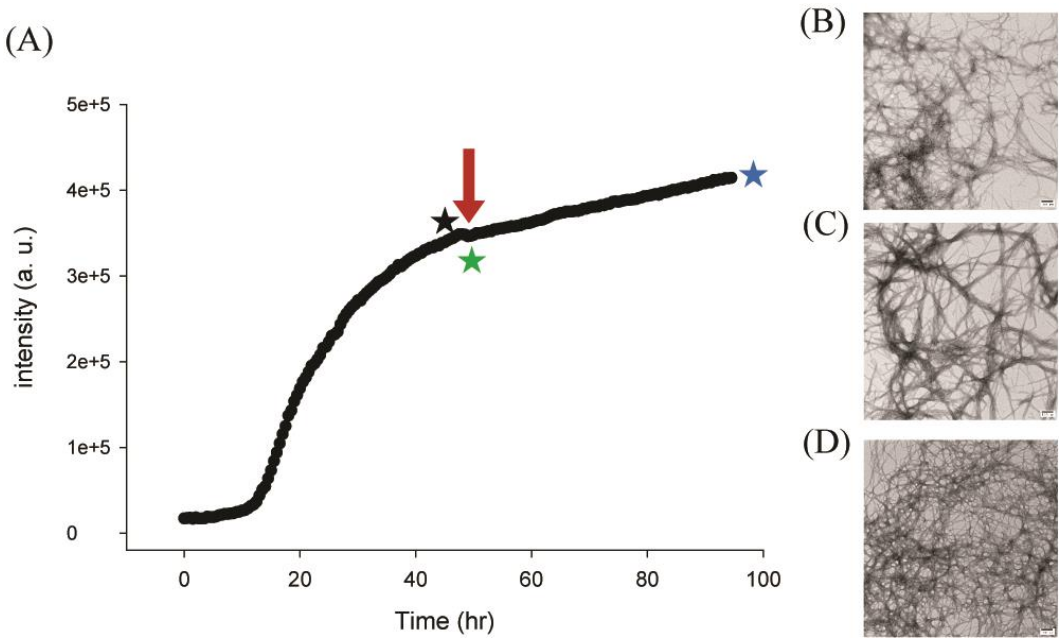

Figure 5-4: Aspirin does not disaggregate preformed human IAPP amyloid fibrils. (A) Thioflavin-T fluorescence assays of the time course of amyloid formation. A 20-fold excess of aspirin was added at the time point indicated by the red arrow. (B) TEM image of the sample just before the addition of a 20-fold excess aspirin, black star (C) TEM image of the sample just after the addition of a 20-fold excess aspirin, green star (D) TEM image of the sample 48 h after the addition of a 20-fold excess aspirin, blue star. Scale bars represent 100 nm. Experiments were conducted at pH 7.4 and 25 ^{o}C in 20 mM Tris buffer, 0.25% DMSO (v/v) in the absence of any fluorinated alcohol co-solvent. The concentration of IAPP was 16 μM and the concentration of aspirin was 320 μM.

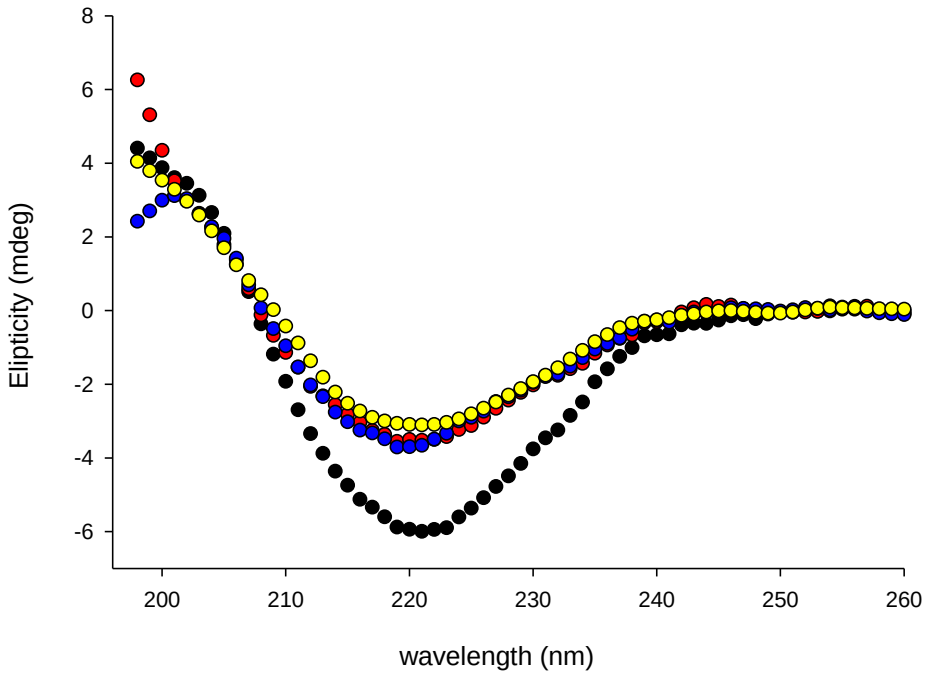

Figure 5-5: CD spectra were recorded for preformed amyloid fibrils before the addition of aspirin (Black). Red; spectrum was recorded immediately after the addition of aspirin. Blue; spectrum was recorded 1 h after the addition of aspirin. Yellow; spectrum was recorded 12 h after the addition of aspirin. The concentration of IAPP in monomeric units was 16 μM. Aspirin when added was at final concentration of 100 μM. Experiments were conducted at 25 ^{o}C, pH 7.4 Tris buffer and 1% HFIP.

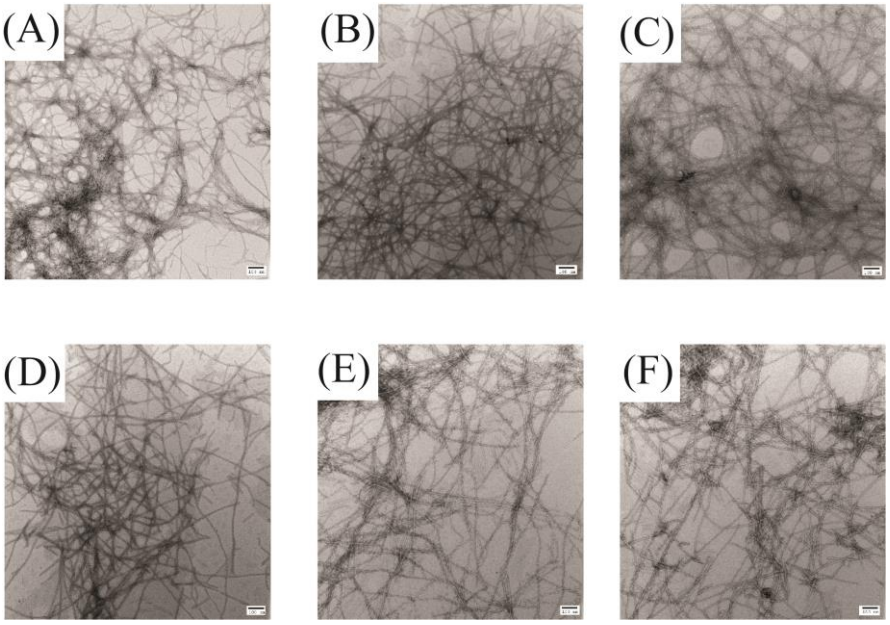

Figure 5-6: Ketoprofen does not inhibit amyloid formation by human IAPP. TEM images of samples recorded after incubating IAPP with varying amount of ketoprofen for 42 h. Scale bars represent 100 nm. (A) IAPP alone. (B) Mixture of IAPP with a 20-fold excess of ketoprofen. (C) Mixture of IAPP with a 10-fold excess of ketoprofen. (D) Mixture of IAPP with a 5-fold excess of ketoprofen. (E) Mixture of IAPP with a 2-fold excess of ketoprofen. (F) Mixture of IAPP with an equimolar amount of ketoprofen. Experiments were conducted at pH 7.4 and 25 ^{o}C in 20 mM Tris buffer, 0.25% DMSO (v/v) in the absence of any fluorinated alcohol co-solvent. The concentration of IAPP was 16 μM.

5.6 References

1. Hollander, P. A.; Levy, P.; Fineman, M.; Maggs, D. G.; Shen, L. Z.; Strobel, S. A.; Weyer, C.; Kolterman, O. G., Pramlintide as an adjunct to insulin therapy improves long-term glycemic and weight control in patients with type 2 diabetes: A 1-year randomized controlled trial. *Diabetes Care* **2003**, *26* (3), 784-790.

2. Cao, P.; Raleigh, D. P., Analysis of the inhibition and remodeling of islet amyloid polypeptide amyloid fibers by flavanols. *Biochemistry* **2012**, *51* (13), 2670-2683.

3. Meng, F. L.; Raleigh, D. P., Inhibition of glycosaminoglycan-mediated amyloid formation by islet amyloid polypeptide and proIAPP processing intermediates. *J. Mol. Biol.* **2011**, *406* (45), 491-502.

4. Porat, Y.; Mazor, Y.; Efrat, S.; Gazit, E., Inhibition of islet amyloid polypeptide fibril formation: A potential role for heteroaromatic interactions. *Biochemistry* **2004**, *43* (45), 14454-14462.

5. Meng, F. L.; Raleigh, D. P.; Abedini, A., Combination of kinetically selected inhibitors *in Trans* leads to highly effective inhibition of amyloid formation. *J. Am. Chem. Soc.* **2010**, *132* (41), 14340-14342.

6. Mishra, R.; Sellin, D.; Radovan, D.; Gohlke, A.; Winter, R., Inhibiting islet amyloid polypeptide fibril formation by the red wine compound resveratrol. *Chembiochem* **2009**, *10* (3), 445-449.

7. Kapurniotu, A.; Schmauder, A.; Tenidis, K., Structure-based design and study of non-amyloidogenic, double N-methylated IAPP amyloid core sequences as inhibitors of IAPP amyloid formation and cytotoxicity. *J. Mol. Biol.* **2002**, *315* (3), 339-350.

8. Porat, Y.; Abramowitz, A.; Gazit, E., Inhibition of amyloid fibril formation by polyphenols: structural similarity and aromatic interactions as a common inhibition mechanism. *Chem. Biol. Drug Des.* **2006**, *67* (1), 27-37.

9. Noor, H.; Cao, P.; Raleigh, D. P., Morin hydrate inhibits amyloid formation by islet amyloid polypeptide and disaggregates amyloid fibers. *Protein Sci.* **2012**, *21* (3), 373-382.

10. Thomas, T.; Nadackal, G. T.; Thomas, K., Aspirin and diabetes: Inhibition of IAPP aggregation by nonsteroidal anti-inflammatory drugs. *Exp. Clin. Endocrinol. Diabetes* **2003**, *111* (1), 8-11.

11. Ehses, J.A.; Perren, A.; Eppler, E.; Ribaux, P.; Pospisilik, J. A.; Maor-Cahn, R.; Gueripel, X.; Ellingsgaard, H.; Schneider, M. K.; Biollaz, G.; Fontana, A.; Reinecke, M.; Homo-Delarche, F.; Donath, M. Y., Increased number of islet-associated macrophages in type 2 diabetes. *Diabetes* **2007**, *56* (9), 2356-2370.

12. Donath, M. Y.; Storling, J.; Maedler, K.; Mandrup-Poulsen, T., Inflammatory mediators and islet beta-cell failure: a link between type 1 and type 2 diabetes. J. Mol. Med. **2003**, *81* (8), 455-470

13. Meier, D. T.; Morcos, M.; Samarasekera, T.; Zraika, S.; Hull, R. L.; Kahn, S. E., islet amyloid formation is essential for induction of islet inflammation in high fat fed human islet amyloid polypeptide transgenic mice. *Diabetologia* **2014**, *In Press.*

14. Masters, S. L.; Dunne, A.; Subramanian, S. L; Hull, R. L.; Tannahill, G. M.; Sharp, F. A.; Becker, C.; Franchi, L.; Yoshihara, E.; Chen, Z.; Mullooly, N.; Mielke, L. A.; Harris, J.; Coll, R. C.; Mills, K. H.; Mok, K. H; Newsholme, P.; Nuñez, G.; Yodoi, J.; Kahn, S. E.; Lavelle, E. C.; O'Neill, L. A., Activation of the NLRP3 inflammasome by islet amyloid polypeptide provides a mechanism for enhanced IL-1β in type 2 diabetes. *Nat. Immunol.* **2010**, *11* (10), 897-904.

15. Westwell-Roper, C. Y.; Ehses, J. A.; Verchere, C. B., Resident macrophages mediate islet amyloid polypeptide-induced islet IL-1β production and β-cell dysfunction. *Diabetes* **2014**, *63* (5), 1698-1711

16. Goldfine, A. B.; Silver, R.; Aldhahi, W.; Cai, D. S.; Tatro, E.; Lee, J.; Shoelson, S. E., Use of salsalate to target inflammation in the treatment of insulin resistance and type 2 diabetes. *Cts. Clin. Transl. Sci.* **2008**, *1* (1), 36-43.

17. Imai, Y.; Dobrian, A. D.; Morris, M. A.; Nadler, J. L., Islet inflammation: a unifying target for diabetes treatment? *Trends Endocrinol. Metab.* **2013**, *24* (7), 351-360.

18. Abedini, A.; Raleigh, D. P., Incorporation of pseudoproline derivatives allows the facile synthesis of human IAPP, a highly amyloidogenic and aggregation-prone polypeptide. *Org. Lett.* **2005**, *7* (4), 693-696.

19. Marek, P.; Woys, A. M.; Sutton, K.; Zanni, M. T.; Raleigh, D. P., Efficient microwave-assisted synthesis of human islet amyloid polypeptide designed to facilitate the specific incorporation of labeled amino acids. *Org. Lett.* **2010**, *12* (4), 4848-4851.

20. Abedini, A.; Singh, G.; Raleigh, D. P., Recovery and purification of highly aggregation-prone disulfide-containing peptides: Application to islet amyloid polypeptide. *Anal. Biochem.* **2006**, *351* (2), 181-186.

21. Tam, J. P.; Wu, C. R.; Liu, W.; Zhang, J. W., Disulfide bond formation in peptides by dimethyl sulfoxide- Scope and applications. *J. Am. Chem. Soc.* **1991**, *113* (17), 6657-6662.

22. Meng, F. L.; Marek, P.; Potter, K. J.; Verchere, C. B.; Raleigh, D. P., Rifampicin does not prevent amyloid fibril formation by human islet amyloid polypeptide but does inhibit fibril thioflavin-T interactions: Implications for mechanistic studies beta-cell death. *Biochemistry* **2008**, *47* (22), 6016-6024.

23. Marek, P.; Gupta, R.; Raleigh, D. P., The fluorescent amino acid *p*-cyanophenylalanine provides an intrinsic probe of amyloid formation. *Chembiochem* **2008**, *9* (9), 1372-1374.

24. Cao, P.; Tu, L. H.; Abedini, A.; Levsh, O.; Akter, R.; Patsalo, V.; Schmidt, A. M.; Raleigh, D. P., Sensitivity of amyloid formation by human islet amyloid polypeptide to mutations at residue 20. *J. Mol. Biol.* **2012**, *421*(2-3), 282-295.

25. Yanagi, K.; Ashizaki, M.; Yagi, H.; Sakurai, K.; Lee, Y. H.; Goto, Y., Hexafluoroisopropanol induces amyloid fibrils of islet amyloid polypeptide by enhancing both hydrophobic and electrostatic interactions. *J. Biol. Chem.* **2011**, *286* (27), 23959-23966.

26. Khurana, R.; Uversky, V. N.; Nielsen, L.; Fink, A. L., Is Congo red an amyloid-specific dye? *J. Biol. Chem.* **2001**, *276* (25), 22715-22721.

Chapter 6. Mutational analysis of the ability of resveratrol to inhibit amyloid formation by islet amyloid polypeptide: Critical evaluation of the importance of aromatic inhibitor and histidine inhibitor interactions

Abstract

Small molecules that block protein amyloid fibril formation or direct the process into non-toxic pathways hold promise for development as therapeutics. There are no clinically approved inhibitors of islet amyloidosis and the mode of action of existing *in vitro* inhibitors is not well understood. Resveratrol, a natural polyphenol, has been shown to inhibit amyloid formation by IAPP and by Alzheimer's disease Aβ peptide. The mechanism of action of this compound on IAPP is still known. In this study, we use a series of IAPP variants to examine the possible interactions between resveratrol and IAPP. These include His-18 mutants, truncation mutants, and mutations of each of the aromatic residues. Resveratrol exhibits different effects toward these variants. Mutation of His to Gln or Leu reduces the ability of resveratrol to inhibit amyloid formation by IAPP as does mutation of Phe-15 and Tyr-37 to Leu, as does elimination of Lys- and the N-terminal amino group. In contrast, replacement of Phe-23 with Leu has a significantly smaller effect. The data highlights Phe-15, His-18 and Tyr-37 as potential sites for IAPP resveratrol interactions and is consistent with a potential role of the N-terminus. Transmission electron microscopy demonstrates that resveratrol, unlike certain other compounds, does not effectively disaggregate IAPP fibrils, but does interfere with thioflavin-T assays.

6.1 Introduction

Polyphenols, a class of organic compounds with aromatic phenolic rings, have drawn particular attention in the inhibition of amyloid formation, including the inhibition of IAPP amyloid. For example, EGCG, the most abundant catechin in green tea, inhibits amyloid formation by Aβ, α-synuclein, IAPP and other polypeptide [1-7]. EGCG can also remodel IAPP amyloid fibrils [3, 5, 7]. This compound is believed to divert amyloidogenic peptides into off pathway aggregates that are not capable of further assembly to form amyloid. Resveratrol, a polyphenol present in red wine, has received considerable attention in the content of neurodegenerative diseases due to its anti-neuroinflammatory activity and because of its ability to inhibit amyloid formation by Aβ (Figure 1) [8-11]. By using the conformation-specific A11 and OC antibodies, resveratrol was found to be capable of selectively remolding soluble Aβ oligomers and amyloid fibrils into non-toxic insoluble disordered aggregates [11]. Proton NMR has been used to detect the direct binding of resveratrol to Aβ [12]. Work mainly done by Winter and co-workers has demonstrated that resveratrol can inhibit IAPP amyloid formation, even in the presence of anionic lipid bilayers which are known to drastically accelerate IAPP fibrillation [13, 14]. However, to date, little is known about the interaction of resveratrol with IAPP, indeed little is known about the mechanism of any anti-IAPP amyloid agent.

Recent NMR studies that made use of a non-physiological analogue of IAPP that lacks the normal amidated C-terminus have led to the proposal that His-18 and Lys-1 are involved in the binding of resveratrol [15]. The NMR spectra revealed that resonances from the side chain of His-18 exhibited the largest changes during a resveratrol titration and His-18 was proposed to be critical for resveratrol binding. Chemical shift changes for Lys-1 were also detected, suggesting

that this residue could be a second binding site for resveratrol. However, the C-terminus of IAPP has a major effect on amyloid formation and variants with a free C-terminus behave differently that the physiological form of IAPP [16]. Thus it is not clear that studies of variants with a free terminus direct translate to the natural form of IAPP. Other work has highlighted the possible role of interactions between aromatic side chains and amyloid inhibitors, but this has not been examined for the case of IAPP and resveratrol. In this study, we examine the interaction of resveratrol with a series of IAPP variants and we critically examine the ability of resveratrol to remodel preformed amyloid fibrils.

6.2 Materials and methods

6.2.1 Peptide synthesis and purification.

Peptides were synthesized on a 0.1 or 0.25 mmol scale using standard Fmoc chemistry on a CEM Liberty microwave peptide synthesizer. Fmoc-PAL-PEG-PS resin was used in order to incorporate an amidated C-terminus. Acetic anhydride was used to generate an acetylated N-terminus for the truncated 8-37 IAPP fragment. Fmoc protected pseudoproline dipeptide derivatives were incorporated at positions 9-10, 19-20, and 27-28 to facilitate the synthesis [17]. β-branched residues, Arg, and all pseudoproline dipeptide derivatives were double coupled. A maximum temperature of 50 ^{o}C was used for the coupling of His and Cys in order to reduce the possibility of racemization [18]. Peptides were cleaved from the resin by standard TFA methods. Crude peptides were partially dissolved in 20% acetic acid (v/v) and lyophilized. The dry peptide was redissolved in pure DMSO at room temperature in order to promote the formation of the disulfide bond [19]. Analytic HPLC was used to ensure the completion of oxidation. Peptides

were purified by reverse-phase HPLC using a Vydac or Proto 300 C18 preparative column (10 mm x 250 mm). A two buffer gradient system was used: buffer A consisted of 100% H_2O and 0.045% HCl (v/v) and buffer B consisted of 80% acetonitrile, 20% H_2O and 0.045% HCl. HCl was used as the counter ion because residual TFA can influence amyloid formation. HPLC method (20%B-60%B in 40 min, flow rate 10 mL/min) was applied. Peptides were collected from HPLC around 30 min after injection. Analytical HPLC was used to check the purity of peptides before use. MALDI-TOF mass spectrometry confirmed the correct molecular weight. hIAPP, expected 3903.3, observed 3902.8; H18Q-hIAPP, expected 3894.3, observed 3894.4; H18L-hIAPP, expected 3879.3, observed 3879.3; F15L-IAPP, expected 3871.3, observed 3872.0; F23L-IAPP, expected 3871.3, observed 3871.3; Y37L-IAPP, expected 3855.4, observed 3853.8; Ac 8-37 IAPP, expected 3225.5, observed 3225.1.

6.2.2 Sample preparation.

Peptides were first dissolved in 100% HFIP at a concentration of 1.6 mM and filtered to remove preformed aggregates. For kinetic studies, 8 μL aliquots were lyophilized and redissolved in 800 μL of pH 7.4, 20 mM Tris buffer with 1% DSMO. Resveratrol stock solutions were freshly prepared in pure DMSO.

6.2.3 Thioflavin-T fluorescence assays.

Lyophilized peptides were dissolved in pH 7.4, 20 mM Tris buffer solution containing thioflavin-T and resveratrol for a final peptide concentration of 16 uM. 1% DMSO was present in all solutions. Measurements were made at 25 ^{o}C using a Beckman Coulter DTX880 plate reader without stirring. An excitation wavelength of 430 nm and emission wavelength of 485 nm

was used. For amyloid fibril remolding studies, preformed fibrils were produced in advance. Thioflavin-T fluorescence was continuously monitored after the addition of resveratrol.

6.2.4 Transmission electron microscopy (TEM).

TEM was performed at the Life Science Microscopy Center at Stony Brook University. Aliquots removed from the fluorescence experiments were used for TEM analysis. 5 μL of peptide solution was placed on a carbon-coated Formvar 300 mesh copper grid for one minute and then negatively stained with saturated uranyl acetate for another minute.

6.3 Results and discussion

The primary sequence of IAPP and the IAPP variants studied here are shown in Figure 6-1. The His-18 to Gln mutant (H18Q-IAPP) and the His-18 to Leu mutant (H18L-IAPP) allow us to test the role of His-18 as potential binding site for resveratrol. A Gln substitution was chosen because Gln has roughly the same volume as His and similar hydrophobicity as a neutral His residue, while the Leu represents a more hydrophobic substitution. We used an IAPP fragment, residues 8-37 with an acetylated N-terminus (denoted Ac 8-37 IAPP), to test the importance of potential interactions with the positively charged Lys side chain and N-terminal amino group. Interactions between phenolic compounds and aromatic residues in amyloidogenic proteins have been suggested to be important for inhibitory effects [20, 21]. Thus, we prepared three aromatic to Leu point mutants including F15L-IAPP, F23L-IAPP and Y37L-IAPP to test the importance of aromatic drug interactions.

The rate of amyloid formation was monitored using thioflavin-T fluorescence binding assays. Thioflavin-T is a small dye that binds to the surface of amyloid fibrils [22]. The fluorescence quantum yield of the dye increases upon binding. Previous studies have shown that thioflavin-T can be used to monitor the kinetics of IAPP amyloid formation without altering the rate of aggregation under our conditions [23]. However, the use of this dye can sometimes be problematic for inhibition studies, since some inhibitors might inhibit thioflavin-T binding or quench the thioflavin T fluorescence and thus bias the detection of amyloid fibrils [24, 25]. Resveratrol, the inhibitor tested in our studies, has no significant absorption within the range of thioflavin-T fluorescence, but this does not mean that it will not interfere with thioflavin-T assays. One earlier study has shown that resveratrol reduces thioflavin-T fluorescence when it is added to preformed Aβ fibrils, but does not affect the thioflavin-T intensity of carboxymethylated κ-casein fibrils, suggesting that resveratrol might displace the bound thioflavin-T from Aβ fibrils [24]. However, it is not known whether resveratrol interferes with the binding of thioflavin-T to IAPP amyloid fibrils. Thus, complementary TEM studies were preformed to ensure that the results were not biased by interference between thioflavin-T and resveratrol.

6.3.1 Resveratrol prolongs the lag phase of IAPP amyloid formation

We found that resveratrol inhibits wild-type IAPP amyloid formation in a dose-dependent manner (Figure 6-2). 1:1 and 1:2 mixtures of wild-type IAPP with resveratrol exhibit a lag phase that is similar to that of wild-type IAPP in the absence of the inhibitor. However, the final thioflavin-T fluorescence intensity is greatly reduced by around 30% and 60% respectively. The lag phase is increased by a factor of 1.5 relative to the control for a 1:5 mixture of wild-type

IAPP and resveratrol, and the final fluorescence intensity of the 1:5 mixture is only 30% of that of the wild-type control. This is a very modest effect compared to EGCG, which essentially abolishes amyloid formation by IAPP at a 1:1 ratio. When the resveratrol concentration is increased to a 10-fold or a 20-fold excess, there is no detectable fluorescence intensity. The change in fluorescence intensity may be due to the formation of fewer fibrils, or interference of resveratrol with the thioflavin-T fluorescence or due to effects of resveratrol on thioflavin-T binding. TEM images recorded after 50 h of incubation show that only few short and thin fibrils are present at high ratios of resveratrol. In contrast, extensively fibrils are observed at this time point at this time point when resveratrol is absent. Large amounts of IAPP fibrils are present in the 1:10 and 1:20 samples after 126 h of incubation even though there is no increase in thioflavin-T signal. The data conclusively shows that resveratrol interferes with thioflavin-T assays of IAPP amyloid formation. However, the TEM results also confirm that resveratrol inhibits IAPP amyloid formation under the conditions examined here.

6.3.2 His-18 is important for resveratrol IAPP interaction

We next investigated the effects of resveratrol on amyloid formation by two His-18 IAPP variants, H18Q-IAPP and H18L-IAPP. The effects are noticeably less than observed with wild-type IAPP. 1:1 and 1:2 mixture of H18Q-IAPP and resveratrol have similar lag times and display the same final fluorescence intensities as observed for H18Q-IAPP alone (Figure 6-3A). The lag phase of the 1:5 H18Q-IAPP and resveratrol mixture is slightly longer relative to the H18Q-IAPP control, and the final intensity is only around 30% lower than H18Q-IAPP alone. Addition of either 10 or 20-fold excess compound also had less effect on H18Q-IAPP or H18L-IAPP than it did on wild-type IAPP. A 10-fold excess of resveratrol increased the lag phase of H18Q-IAPP by only a factor of 1.8 and dense mats of amyloid fibrils were observed in TEM images (Figure

6-3D). Although the final thioflavin-T intensity of H18Q-IAPP in the presence of a 20-fold excess of resveratrol is greatly decreased, the kinetic curve is still sigmoidal with a lag phase only 2.4-fold longer than that observed for H18Q-IAPP alone. TEM images confirmed the presence of amyloid fibrils in these samples (Figure 6-3E). These results show that mutation of His-18 significantly affects the ability of the compound to inhibit IAPP amyloid formation.

Resveratrol is even less effective at inhibiting amyloid formation by H18L-IAPP. The mutant form amyloid more rapidly that wild type. The curves quickly reach a plateau for all conditions tested (Figure 6-3B). TEM images recorded for the 1:20 H18L-IAPP and resveratrol mixture revealed large amounts of amyloid fibrils (Figure 6-3G). Figure 6-4 displays a plot of the normalized t_{50} (t_{50} in the presence of compound/ t_{50} without compound) values to facilitate comparison of the effects of resveratrol on the two variants and wild-type IAPP. One caveat with the H18L-IAPP studies is that amyloid formation is much faster for this mutant than for wild type and this might indicate a change in the mechanism. If this were the cause then the compound might still bind, but not impact the kinetics of assembly because it does not target a new rate limiting step. The mechanism of IAPP amyloid formation is not known and it is presently impossible to offer an atomic level description of consequence of the H18Lmutant, never-the-less, the H18L-IAPP is consistent with the proposed role of His-18 in resveratrol IAPP interactions.

6.3.3 The three aromatic residues in IAPP make different contributions to interactions with resveratrol

Wild-type IAPP contains three aromatic residues at position 15, 23 and 37. Aromatic interactions have been proposed to be important in amyloid formation and IAPP drug

interactions [21]. Aromatic-aromatic interactions are not required for IAPP amyloid formation although their removal does slow the process [26, 27], but it is not known whether aromatic drug interactions are important for resveratrol binding. The effects caused by single aromatic to Leu mutations on IAPP amyloid formation have been previously examined in the absence of inhibitor. All three single aromatic to Leu mutants formed amyloid fibrils and the mutations do not alter the fibril morphology [27]. We used the F15L, F23L and Y37L point mutants to test the potential role of aromatic drug interactions in the inhibition of IAPP amyloid formation by resveratrol.

Thioflavin-T fluorescence monitored kinetic curves were recorded for all three of the aromatic to Leu mutants in the absence and in the presence of different amounts of resveratrol, and are displayed in Figure 6-5. The inhibitory effects of resveratrol on F15L-IAPP amyloid formation are similar to that observed in wild-type IAPP for the lower ratios of resveratrol. The lag phase slightly increased for the 1:5 mixture of F15L-IAPP and resveratrol compared to the F15L-IAPP control. Only a few non-fibrillar aggregates were observed from wild-type IAPP with a 20-fold excess of resveratrol at 42 h and at 50 h. In contrast amyloid fibrils, albeit ones that were shorter and thinner, were found in the 1:20 mixture of F15L-IAPP and resveratrol (Figure 6-6). This indicates that the Phe-15 mutant affects IAPP resveratrol interactions and shows that Phe-15 plays a role in the interaction of resveratrol with IAPP. Resveratrol effectively inhibited F23L-IAPP amyloid formation in a dose-dependent manner. The final intensity of thioflavin-T fluorescence was drastically reduced and the lag phase of F23L-IAPP increased when a 5-fold excess of resveratrol was present. TEM images recorded for a 1:20 mixture of F23L-IAPP and resveratrol at 96 h show that no detectable fibrils were formed at that time point showing that resveratrol retards F23L-IAPP amyloid formation. This indicates that mutation of Phe-23 does not block the ability of resveratrol to inhibit amyloid formation by IAPP. By contrast, resveratrol

had no obvious inhibitory effect on Y37L-IAPP amyloid formation. Although the final fluorescence intensity of the Y37L-IAPP kinetic experiments gradually decreased upon addition of more resveratrol, the t_{50} for each condition compared to the Y37L-IAPP control were similar (Figure 6-7). TEM images show that large amounts of Y37L-IAPP fibrils were found even at high ratio of resveratrol as soon as 96 h. The data argues that Tyr-37 is important for resveratrol IAPP interactions.

6.3.4 Resveratrol does not inhibit amyloid formation by Ac 8-37- IAPP

Previous NMR studies suggested that Lys-1 was a second binding site for resveratrol [15]. We next examined the role of the N-terminal amino group and the Lys side chain in IAPP resveratrol interactions using a truncated acetylated IAPP variant, Ac 8-37-IAPP. The same approaches were used to test this fragment. Interestingly, resveratrol was not an inhibitor of amyloid formation by Ac 8-37-IAPP. Ac 8-37-IAPP quickly form amyloid fibrils even with high ratios of resveratrol present (Figure 6-8). It is hard to make conclusions based on this peptide since its lag phase is so short. The results may indicate that the N-terminal region of IAPP is important for resveratrol binding or it may be that this peptide forms amyloid fibrils aggressively, which affects resveratrol binding. Consider a simple hypothetical case; suppose there was a first fast step in the lag phase and then a slower step. Suppose resveratrol only impedes the slow step. Let us further imagine that the truncation eliminates the slow step. In this case, we would see no significant effect of resveratrol even if it still binds to IAPP. Thus the data is consistent with the proposed role of the N-terminus, but it can not definitively address that point.

Figure 6-9 summaries the TEM data collected for the various samples in the presence of a 20-fold excess of resveratrol at different time points. We collected additional TEM images of all

samples at times which corresponding to 2X t_{50} and 3X t_{50}, where t_{50} is the value of t_{50} for each individual peptide in the absence of inhibitor. These correspond to wild-type IAPP t_{50}= 16.5 h; H18Q-IAPP t_{50}= 12.5 h; H18L-IAPP t_{50}= 1.25 h; F15L-IAPP t_{50}= 20.5 h; F23L-IAPP t_{50}= 37.5 h; Y37L-IAPP t_{50}= 60.5 h; Ac 8-37-IAPP t_{50}= 4.25 h. The TEM data is included in Figure 6-10 for completeness. The data confirms that mutation of Phe-15 or Tyr-37 or His-18 has a significant effect on the ability of resveratrol to inhibit IAPP amyloid formation.

6.3.5 Resveratrol does not effectively remodel IAPP fibrils

There are conflicting reports on the ability of polyphenols to remodel amyloid fibrils. Resveratrol has been shown to remodel amyloid fibrils formed by Aβ [11]. However, the ability of resveratrol to remodel amyloid fibrils formed by IAPP has not been reported. Figure 6-11 displays the result of remodeling studies. Resveratrol was added when amyloid formation reached a plateau (black arrow), and TEM images were recorded before and directly after the addition of resveratrol (Figure 6-11B and 6-11C) as well as after 3 days and 6 days incubation. The thioflavin-T intensity initially drops after addition of resveratrol suggesting that resveratrol might interfere with thioflavin-T binding. After 3 days incubation, the thioflavin T intensity does not return to baseline. However, TEM images recorded at all time points show that numerous amyloid fibrils were present and only a small change in morphology was detected. The TEM data conclusively shows that resveratrol does not significantly remodel IAPP amyloid fibrils. In contrast, TEM studies have shown that EGCG effectively remodels IAPP fibrils [5].

6.4 Conclusions

The data presented here is consistent with previous studies that concluded that resveratrol can inhibit human IAPP amyloid formation in a dose-dependent manner. Resveratrol is a modest inhibitor of IAPP amyloid formation and is clearly less effective than EGCG. Resveratrol was less effective at inhibiting amyloid formation by some of the IAPP variants. Mutations of His-18, Phe-15, Tyr-37 and the positively charged N-terminus lead to a weaker interaction with resveratrol, or may change the aggregation pathway such that resveratrol can not target the peptide. Our data also highlights the difficulty of using fluorescence-based thioflavin-T assays in inhibition studies. Even though small molecules do not absorb at the same wavelength as thioflavin-T fluorescence, they might alter the binding of thioflavin-T on amyloid fibrils, resveratrol is a case in part. The use of electron microscopy is highly recommended to complement thioflavin-T data in inhibition studies.

Our data is consistent with previous NMR studies with a non-physiological variant of IAPP which suggested that resveratrol interacts with IAPP via binding to His-18 [15]. The work presented here also reveals the importance of Phe-15 and Tyr-37 in IAPP resveratrol interactions. The observed importance of Phe-15 and Tyr-37 consistent with the hypothesis that aromatic residues are a possible site for inhibitor protein interactions. This observation is not general since EGCG effectively inhibited variants of IAPP that lacked aromatic residues.

Seeking better inhibitors based on the structure of resveratrol would be of interest for future studies. In fact, the anti-inflammatory activity of resveratrol has received considerable attention in neurodegenerative disease and this activity seems to strongly depend on the structure features of resveratrol [28, 29]. Although it is not known what structural feature of resveratrol are important for its anti-amyloidogenic properties, other resveratrol analogues might be potentially active in inhibiting amyloid formation. Another important function that other IAPP inhibitors,

such as EGCG and Morin hydrate, have is the ability to remodel amyloid fibrils [5, 30]. Our TEM studies clearly demonstrated that resveratrol does not disaggregate fibrils, even though it induces a decrease in thioflavin-T fluorescence. These observation stress the importance of relying on more than just thioflavin-T assays in inhibitor studies. In summary, we have shown that resveratrol can retard IAPP amyloid formation, but does not completely abolish fibril formation under the conditions used here. The study highlights the role of His-18, Phe-15, and Tyr-37, but indicates that Phe-23 is not important for peptide drug interactions.

6.5 Figures

wild-type IAPP:

KCNTATCAT QRLANFLVHS SNNFGAILSS TNVGSNTY–CONH$_2$

H18Q-IAPP:

KCNTATCAT QRLANFLVQS SNNFGAILSS TNVGSNTY–CONH$_2$

H18L-IAPP:

KCNTATCAT QRLANFLVLS SNNFGAILSS TNVGSNTY–CONH$_2$

F15L-IAPP:

KCNTATCAT QRLANLLVHS SNNFGAILSS TNVGSNTY–CONH$_2$

F23L-IAPP:

KCNTATCAT QRLANFLVHS SNNLGAILSS TNVGSNTY–CONH$_2$

Y37L-IAPP:

KCNTATCAT QRLANFLVHS SNNFGAILSS TNVGSNTL–CONH$_2$

Ac 8-37-IAPP:

CH$_3$CO-AT QRLANFLVHS SNNFGAILSS TNVGSNTY–CONH$_2$

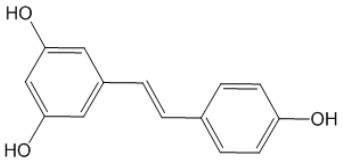

Figure 6-1: The primary sequence of IAPP and the IAPP variants studied here. The residues that differ from wild-type IAPP are highlighted in red. Except for Ac 8-37-IAPP, wild-type IAPP and IAPP variants all contain a disulfide bond between Cys-2 and Cys-7. All peptides contain an amidated C-terminus. The structure of resveratrol is shown at the bottom.

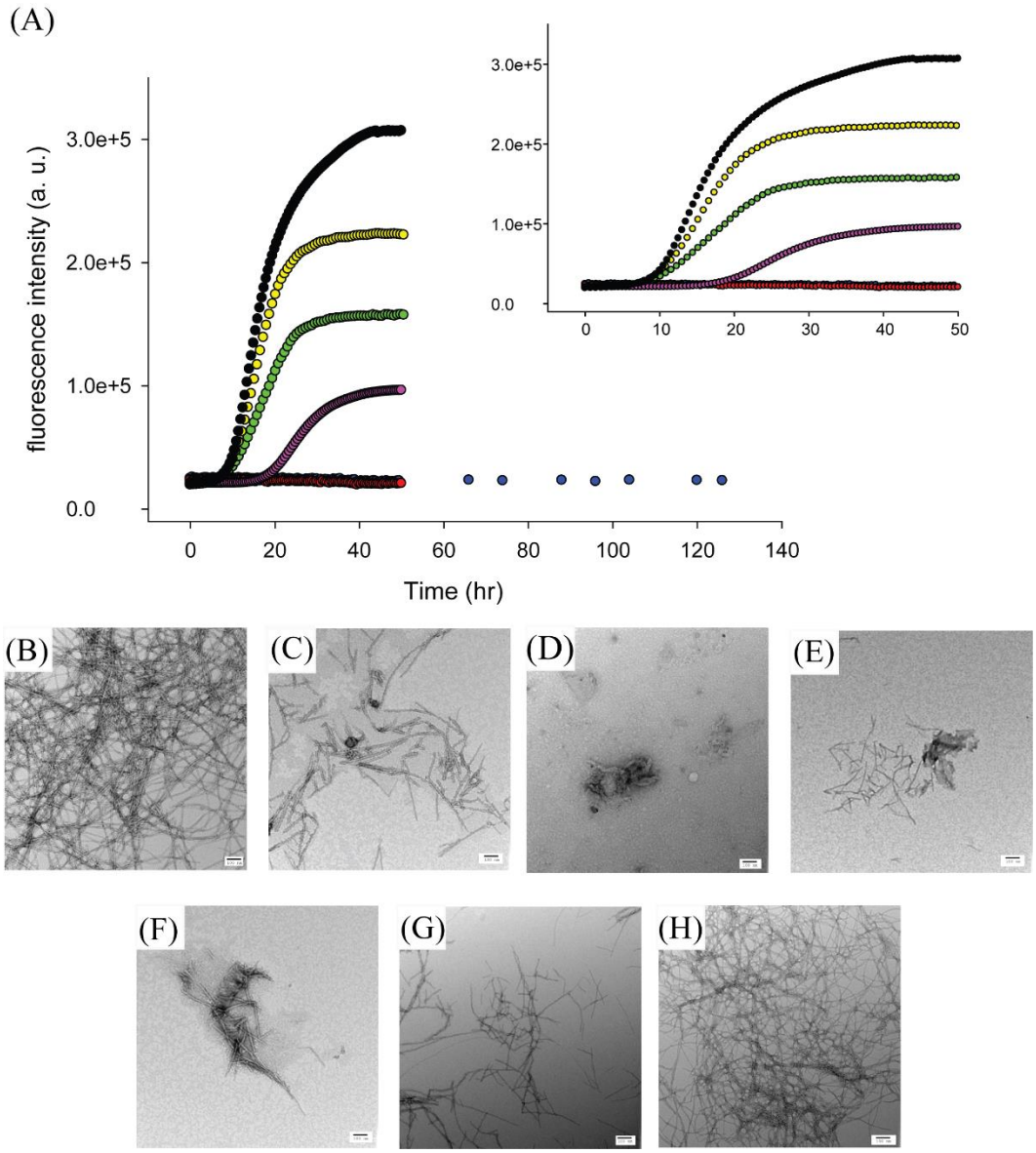

Figure 6-2: Resveratrol inhibits amyloid formation by wild-type IAPP. (A) Thioflavin-T fluorescence monitored kinetic experiments for wild-type IAPP, black; wild-type IAPP and resveratrol at a 1:1 ratio, yellow; at a 1:2 ratio, green; at a 1:5 ratio, pink; at a 1:10 ratio, red; at a 1:20 ratio, blue. The red and blue curve overlap. The insert shows an expansion of data from 0 h to 50 hr. (B) TEM image of wild-type IAPP. A sample was collected for TEM at 50 h (black

arrow). (C) TEM image of wild-type IAPP with resveratrol at a 1:10 ratio. A sample was collected for TEM at 50 h. (D) TEM image of wild-type IAPP with resveratrol at a 1:20 ratio. A sample was collected for TEM at 42 h. (E) TEM image of wild-type IAPP with resveratrol at a 1:20 ratio. A sample was collected for TEM at 50 h. (F) TEM image of wild-type IAPP with resveratrol at a 1:20 ratio. A sample was collected for TEM at 66 h. (G) TEM image of wild-type IAPP with resveratrol at a 1:20 ratio. A sample was collected for TEM at 96 h. (H) TEM image of wild-type IAPP with resveratrol at a 1:20 ratio. A sample was collected for TEM at 126 h. Samples contained 16 uM IAPP in pH 7.4, 20 mM Tris buffer with 1% DMSO. Scale bars represent 100 nm.

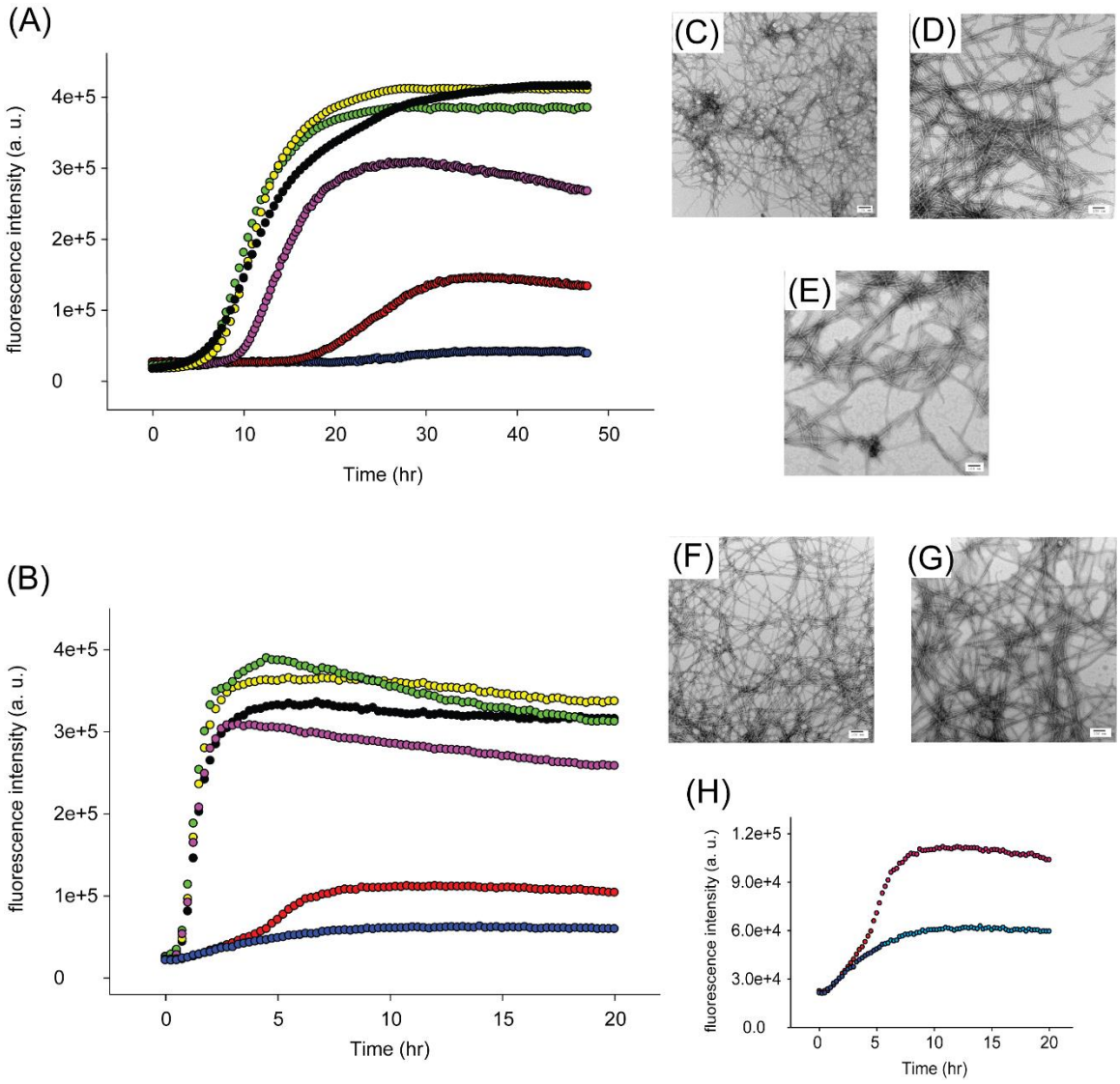

Figure 6-3: Resveratrol is not an effective inhibitor of amyloid formation by H18Q-IAPP and H18L-IAPP (A) Thioflavin-T monitored kinetic experiments for H18Q-IAPP, black; H18Q-IAPP and resveratrol at a 1:1 ratio, yellow; at a 1:2 ratio, green; at a 1:5 ratio, pink; at a 1:10 ratio, red; at a 1:20 ratio, blue. (B) Thioflavin-T monitored kinetic experiments for H18L-IAPP, black; H18L-IAPP and resveratrol at a 1:1 ratio, yellow; at a 1:2 ratio, green; at a 1:5 ratio, pink; at a 1:10 ratio, red; at a 1:20 ratio, blue. (C) TEM image for H18Q-IAPP. (D) TEM image for the

1:10 mixture of H18Q-IAPP and resveratrol. (E) TEM image for the 1:20 mixture of H18Q-IAPP and resveratrol. Samples were collected for TEM at 48 h for H18Q-IAPP with and without resveratrol. (F) TEM image for H18L-IAPP. (G) TEM image for the 1:20 mixture of H18L-IAPP and resveratrol. Samples were collected for TEM at the 22 h for H18L-IAPP with and without resveratrol. (H) An expansion of the data for H18L-IAPP with resveratrol at the 1:10 and 1:20 ratios. Samples contained 16 uM IAPP in pH 7.4, 20 mM Tris buffer with 1% DMSO. Scale bars represent 100 nm.

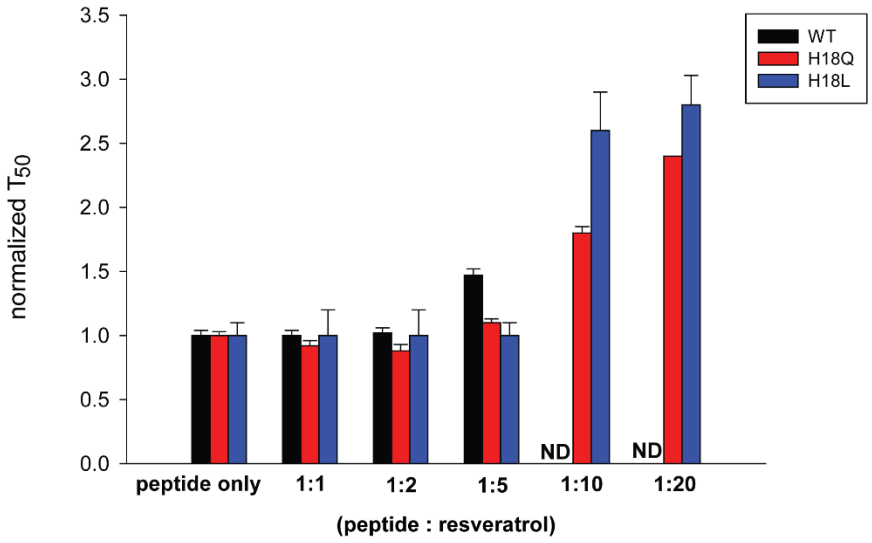

Figure 6-4: Comparison of the effect of different amounts of resveratrol on the t_{50} value for amyloid formation by wild-type IAPP (black), H18Q-IAPP (red), and H18L-IAPP (blue). ND indicates could not be determined because of lack of any fluorescence signal. The error bars represent propagation of uncertainty which is generated from 2 to 3 independent studies. The Y axis is (t_{50} with resveratrol)/ (t_{50} no resveratrol).

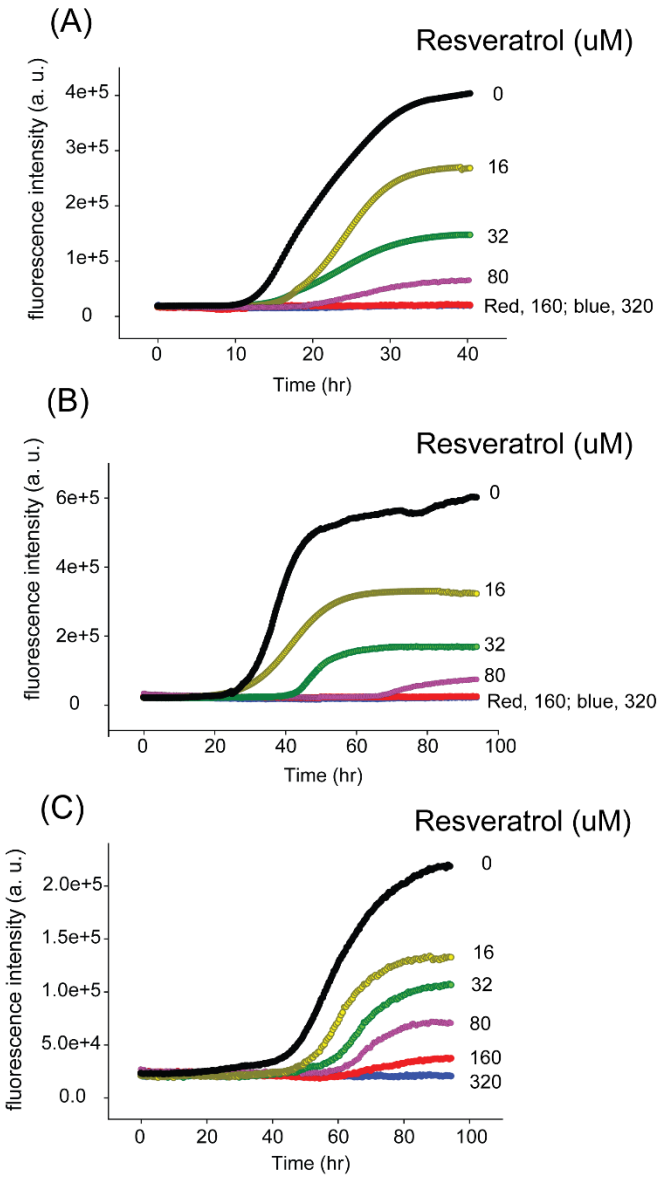

Figure 6-5: The three aromatic residues in IAPP interact differently with resveratrol. Thioflavin-T fluorescence monitored kinetic experiments for (A) F15L-IAPP, (B) F23L-IAPP and (C) Y37L-IAPP in the presence of resveratrol. Experiments were conducted at 25 ^{o}C, pH 7.4, 20 mM Tris-buffer, 16 uM mutants and 1% DMSO without stirring. In each figure, Black curve represents peptide alone; yellow, peptide with resveratrol at a 1:1 ratio; green, peptide with resveratrol at a 1:2 ratio; pink, peptide with resveratrol at a 1:5 ratio; red, peptide with resveratrol at a 1:10 ratio; blue, peptide with resveratrol at a 1:20 ratio; Red and blue curves overlap in (A) and (B).

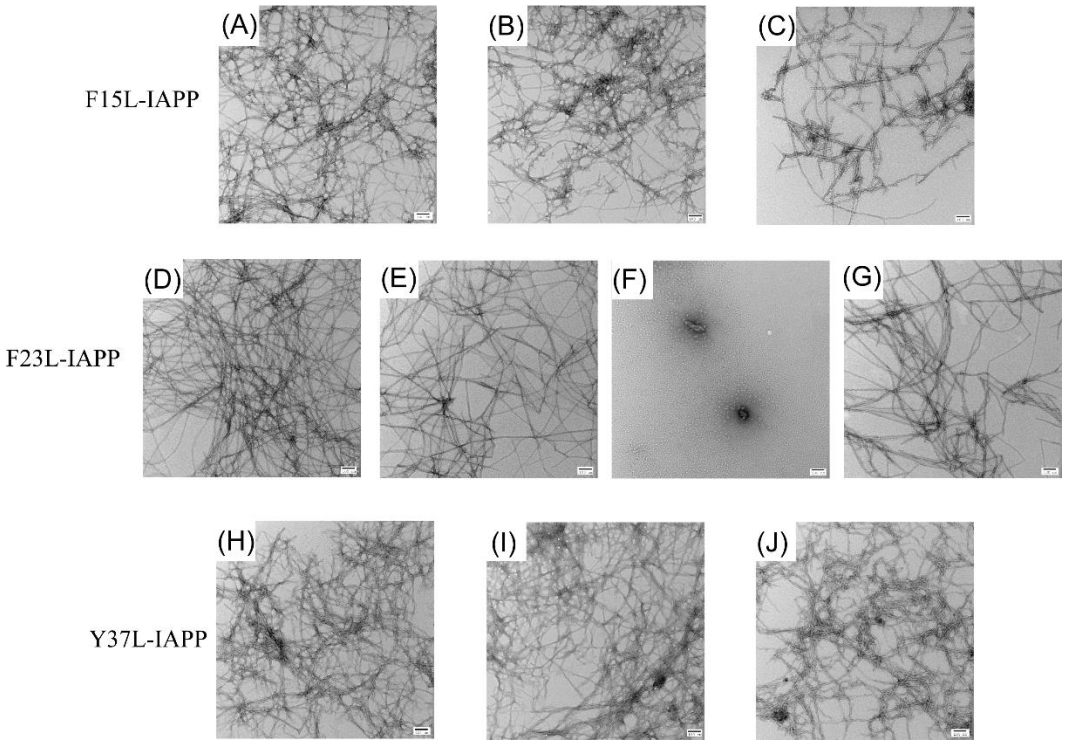

Figure 6-6: TEM images of amyloid fibrils formed by aromatic to Leu mutants and of fibrils formed in the presence of resveratrol. (A) TEM image of F15L-IAPP fibrils. (B) TEM image of F15L-IAPP fibrils with a 5-fold excess resveratrol. (C) TEM image of F15L-IAPP fibrils with a 20-fold excess resveratrol. For figure A-C, the F15L-IAPP samples were removed from thioflavin-T kinetic experiments at 42 h. (D) TEM image of F23L-IAPP fibrils. (E) TEM image of F23L-IAPP fibrils with a 5-fold excess resveratrol. (F) TEM image of F23L-IAPP fibrils with a 20-fold excess resveratrol. For figure D-F, the F23L-IAPP samples were removed from thioflavin-T kinetic experiments at 96 h. (G) TEM image of F23L-IAPP fibrils with a 20-fold excess resveratrol, but samples were removed from thioflavin-T kinetics experiments at 142 h. (H) TEM image of Y37L-IAPP fibrils. (I) TEM image of Y37L-IAPP fibrils with a 5-fold excess resveratrol (J) TEM image of Y37L-IAPP fibrils with a 20-fold excess resveratrol. For figure H-J, the Y37L-IAPP samples were removed from thioflavin-T kinetic experiments at 96 h. Scale bars represent 100 nm.

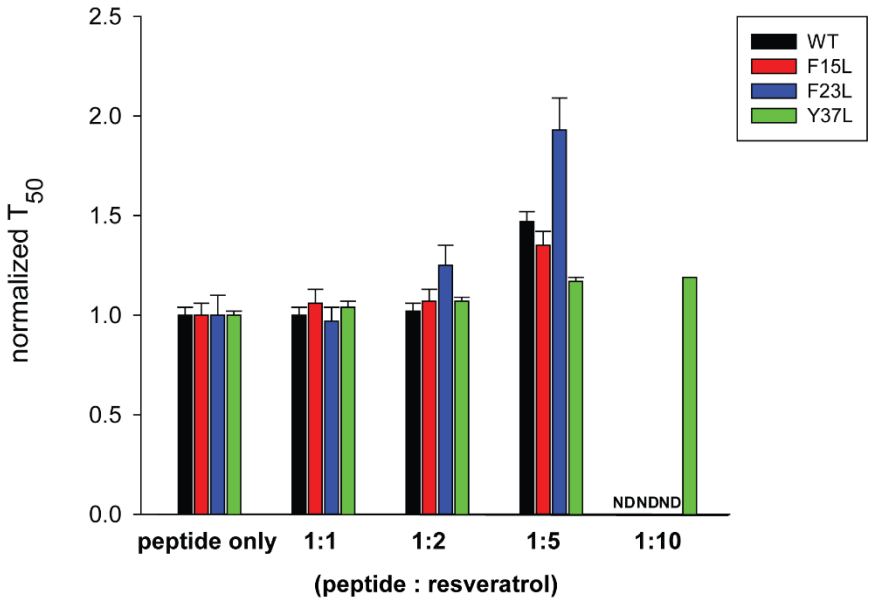

Figure 6-7: Comparison of the effect of different amounts of resveratrol on the t_{50} value for amyloid formation by wild-type IAPP (black), F15L-IAPP (red), F23L-IAPP (blue), and Y37L-IAPP (green). ND indicates could not be determined because of lack of any fluorescence signal. The error bars represent propagation of the uncertainty, generated from 2 to 3 independent studies. The Y axis is (t_{50} with resveratrol)/ (t_{50} no resveratrol)

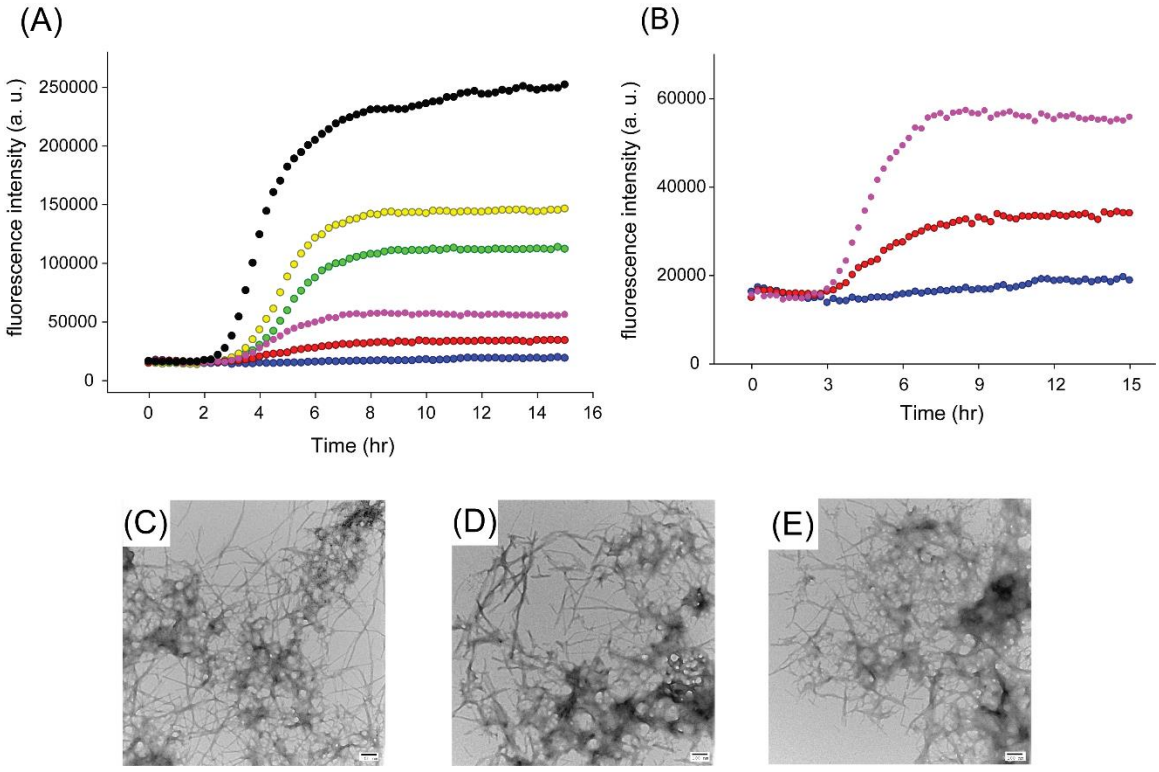

Figure 6-8: Resveratrol is not an inhibitor of amyloid formation by Ac 8-37-IAPP. (A) Thioflavin-T fluorescence monitored kinetic experiments for Ac 8-37-IAPP, black; Ac 8-37-IAPP and resveratrol at a 1:1 ratio, yellow; at a 1:2 ratio, green; at a 1:5 ratio, pink; at a 1:10 ratio, red; at a 1:20 ratio, blue. (B) An expansion of the data for Ac 8-37-IAPP with resveratrol at the 1:5, 1:10 and 1:20 ratios. (C) TEM image for Ac 8-37-IAPP. (D) TEM image for the 1:5 mixture of Ac 8-37-IAPP and resveratrol. (E) TEM image for the 1:20 mixture of Ac 8-37-IAPP and resveratrol. All Ac 8-37-IAPP samples were collected for TEM at 22 h. Samples contained 16 uM variant in pH 7.4, 20 mM Tris buffer with 1% DMSO. Scale bars represent 100 nm.

(A)

Time	peptides with 20X Resveratrol			
	Wild-type	H18Q-IAPP	H18L-IAPP	Ac-8-37-IAPP
22 h	—	—	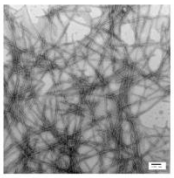	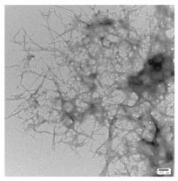
42 h	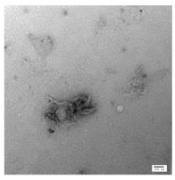	—	—	—
48 h	—	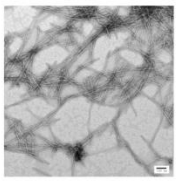	—	—
50 h	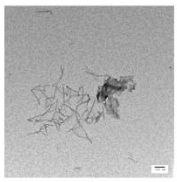	—	—	—
66 h	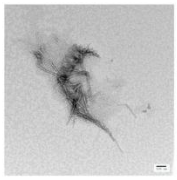	—	—	—
96 h	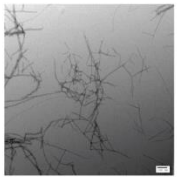	—	—	—
126 h	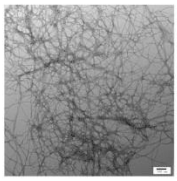	—	—	—

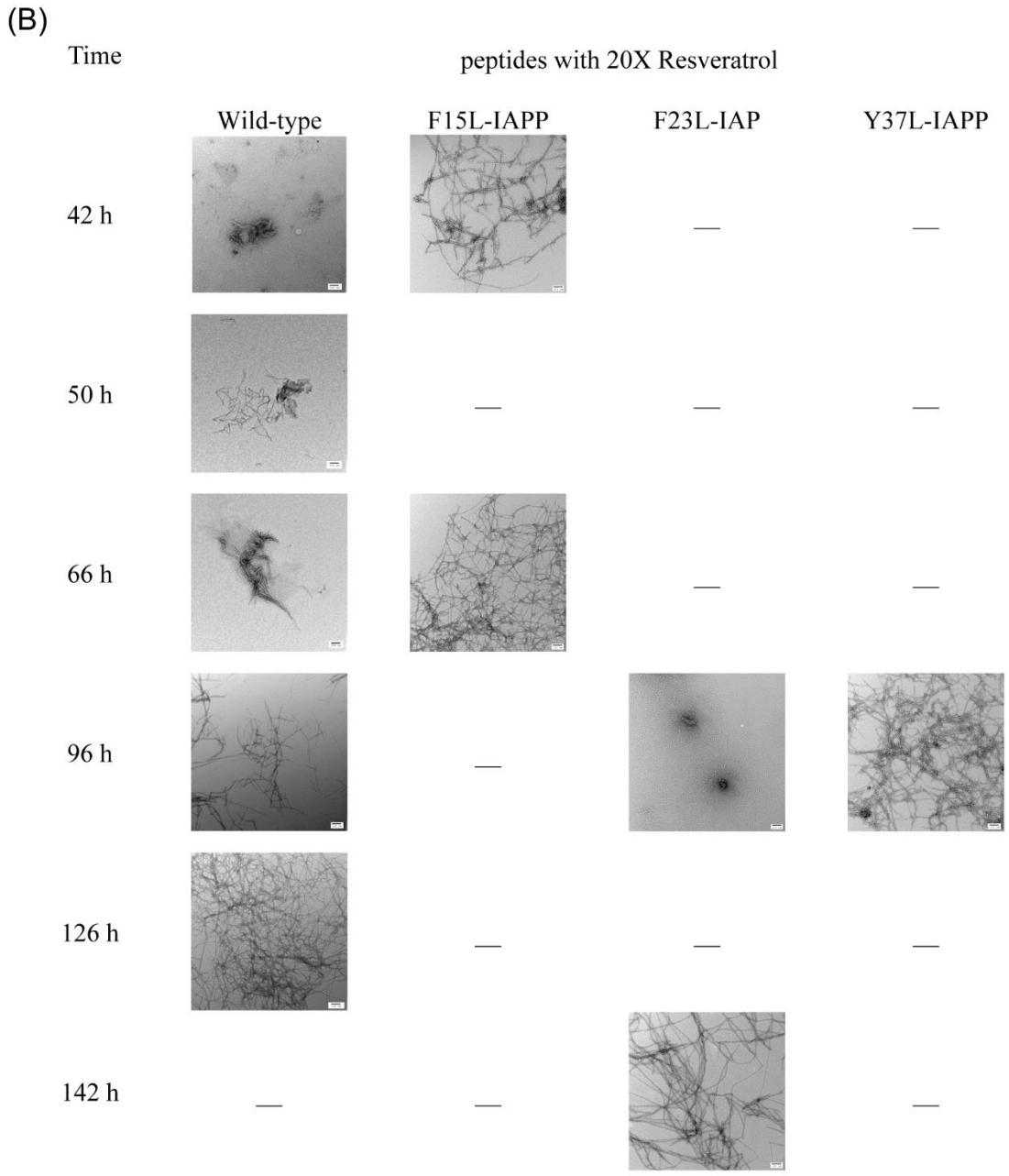

Figure 6-9: Summary of time dependent TEM dada. A — means no image recorded. All TEM samples were collected from thioflavin-T kinetic experiments. Samples contained 16 uM peptide and 320 uM resveratrol in pH 7.4, 20 mM Tris buffer with 1% DMSO. Scale bars represent 100 nm.

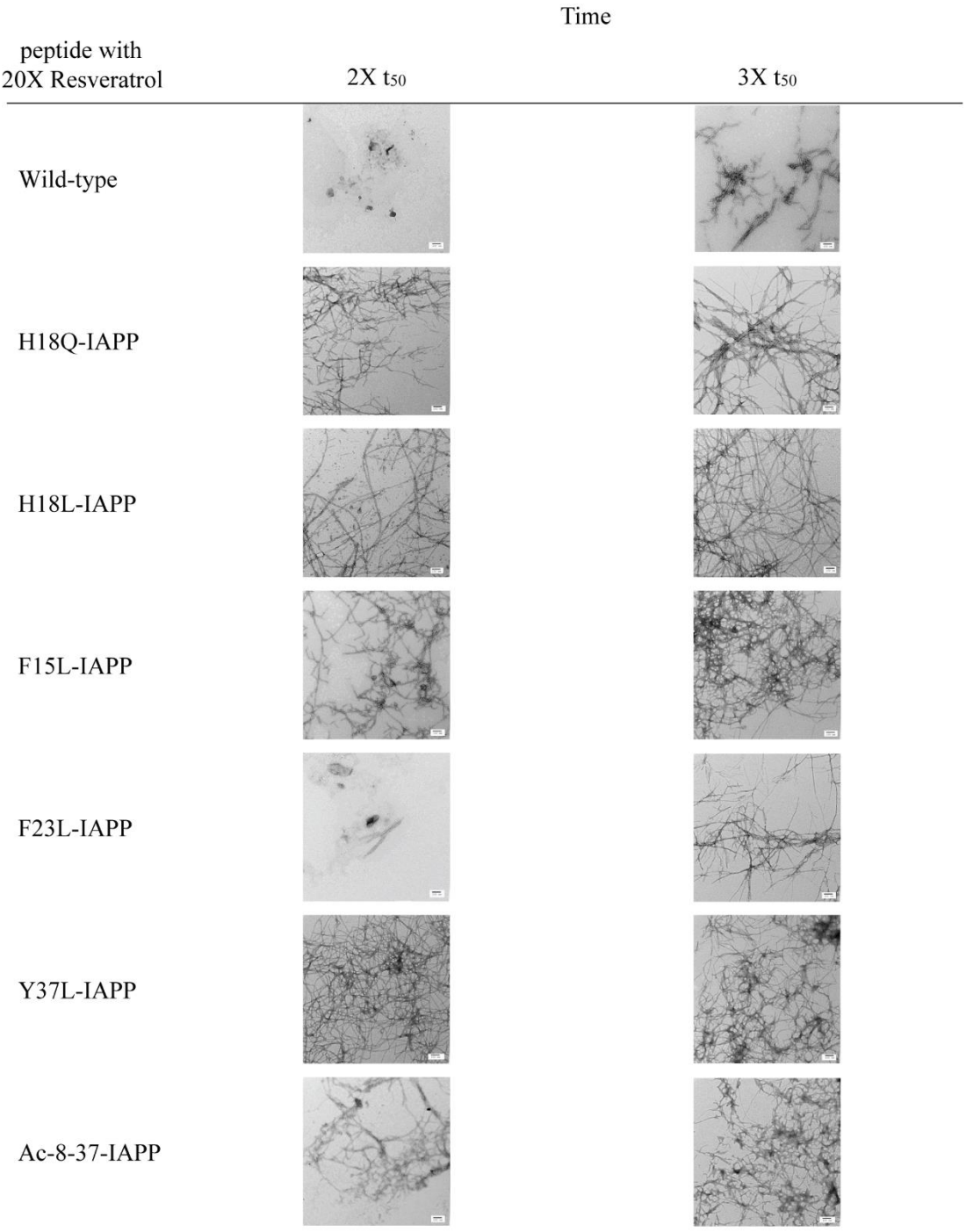

Figure 6-10: Summary of TEM data collected for each peptide in the presence of resveratrol. Images were collected at 2X and 3X the t_{50} value of the respective samples in the absence of inhibitor. Samples contained 16 uM peptide and 320 uM resveratrol in pH 7.4, 20 mM Tris buffer with 1% DMSO. Scale bars represent 100 nm.

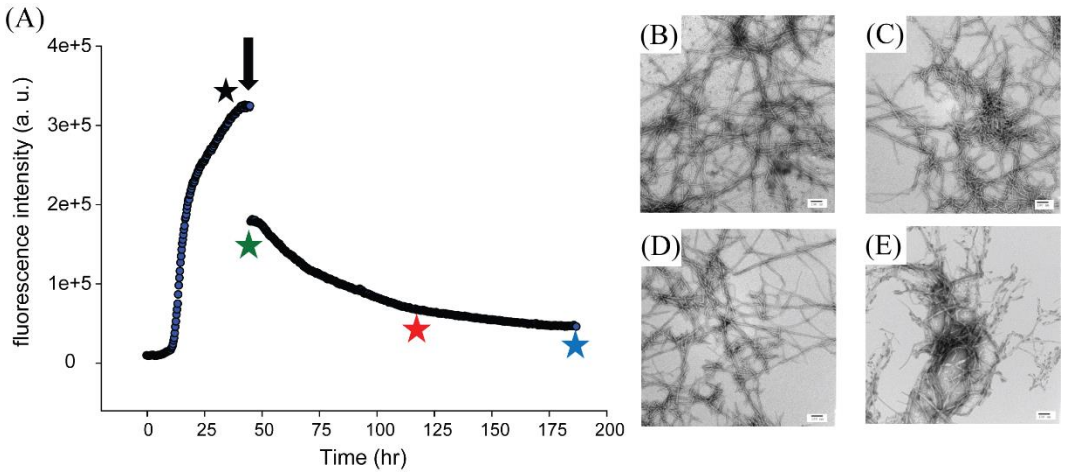

Figure 6-11: Resveratrol does not effectively remodel amyloid fibrils formed by wild-type IAPP. (A) Thioflavin-T monitored time course. Amyloid formation was allowed to proceed for 48 h and then resveratrol was added (black arrow). (B) TEM image recorded before adding resveratrol (black star). (C) TEM image recorded immediately after adding resveratrol (green star). (D) TEM image recorded after 3 days incubation (red star). (E) TEM image recorded after 6 days incubation (blue star). Experiments were conducted at 25 ^{o}C, 20 mM Tris buffer, 32 uM thioflavin-T and 16 uM IAPP. Resveratrol was added to a final concentration of 160 uM. Samples contained 1% DMSO after the addition of resveratrol.

6.6 References

1. Rezai-Zadeh, K.; Arendash, G. W.; Hou, H. Y.; Fernandez, F.; Jensen, M.; Runfeldt, M.; Shytle, R. D.; Tan, J., Green tea epigallocatechin-3-gallate (EGCG) reduces beta-amyloid mediated cognitive impairment and modulates tau pathology in Alzheimer transgenic mice. *Brain Research* **2008**, *1214*, 177-187

2. Meng, F. L.; Abedini, A.; Plesner, A.; Verchere, C. B.; Raleigh, D. P., The flavanol (-)-epigallocatechin 3-gallate inhibits amyloid formation by islet amyloid polypeptide, disaggregates amyloid fibrils, and protects cultured cells against IAPP-induced toxicity. *Biochemistry* **2010**, *49* (37), 8127-8133.

3. Bieschke, J.; Russ, J.; Friedrich, R. P.; Ehrnhoefer, D. E.; Wobst, H.; Neugebauer, K.; Wanker, E. E., EGCG remodels mature alpha-synuclein and amyloid-beta fibrils and reduces cellular toxicity. *Pro. Natl. Acad. Sci. U. S. A.* **2010**, *107* (17), 7710-7715.

4. Popovych, N.; Brender, J. R.; Soong, R.; Vivekanandan, S.; Hartman, K.; Basrur, V.; Macdonald, P. M.; Ramamoorthy, A., Site specific interaction of the polyphenol EGCG with the SEVI amyloid precursor peptide PAP 248-286. *J. Phys. Chem. B* **2012**, *116* (11), 3650-3658.

5. Cao, P.; Raleigh, D. P., Analysis of the inhibition and remodeling of islet amyloid polypeptide amyloid fibers by flavanols. *Biochemistry* **2012**, *51* (13), 2670-2683.

6. Young, L. M.; Cao, P.; Raleigh, D. P.; Ashcroft, A. E.; Radford, S. E., Ion mobility spectrometry-mass spectrometry defines the oligomeric intermediates in amylin amyloid formation and the mode of action of inhibitors. *J. Am. Chem. Soc.* **2014**, *136* (2), 660-670.

7. Palhano, F. L.; Lee, J.; Grimster, N. P.; Kelly, J. W., Toward the molecular mechanism(s) by which EGCG treatment remodels mature amyloid fibrils. *J. Am. Chem. Soc.* **2013**, *135* (20), 7503-7510.

8. Sun, A. Y.; Wang, Q.; Simonyi, A.; Sun, G. Y., Resveratrol as a therapeutic agent for neurodegenerative diseases. *Mol. Neurobiol.* **2010**, *41* (2-3), 375-383.

9. Savaskan, E.; Olivieri, G.; Meier, F.; Seifritz, E.; Wirz-Justice, A.; Muller-Spahn, F., Red wine ingredient resveratrol protects from beta-amyloid neurotoxicity. *Gerontology* **2003**, *49* (6), 380-383.

10. Marambaud, P.; Zhao, H. T.; Davies, P., Resveratrol promotes clearance of Alzheimer's disease amyloid-beta peptides. *J. Biol. Chem.* **2005**, *280* (45), 37377-37382.

11. Ladiwala, A. R. A.; Lin, J. C.; Bale, S. S.; Marcelino-Cruz, A. M.; Bhattacharya, M.; Dordick, J. S.; Tessier, P. M., Resveratrol selectively remodels soluble oligomers and fibrils of amyloid A-beta into off-pathway conformers. *J. Biol. Chem.* **2010**, *285* (31), 24228-24237.

12. Ge, J. F.; Qiao, J. P.; Qi, C. C.; Wang, C. W.; Zhou, J. N., The binding of resveratrol to monomer and fibril amyloid beta. *Neurochem. Interl.* **2012**, *61* (7), 1192-1201.

13. Evers, F.; Jeworrek, C.; Tiemeyer, S.; Weise, K.; Sellin, D.; Paulus, M.; Struth, B.; Tolan, M.; Winter, R., Elucidating the mechanism of lipid membrane-induced IAPP fibrillogenesis and its inhibition by the red wine compound resveratrol: A synchrotron X-ray reflectivity study. *J. Am. Chem. Soc.* **2009**, *131* (27), 9516-9521.

14. Radovan, D.; Opitz, N.; Winter, R., Fluorescence microscopy studies on islet amyloid polypeptide fibrillation at heterogeneous and cellular membrane interfaces and its inhibition by resveratrol. *Febs Lett.* **2009**, *583* (9), 1439-1445.

15. Wei, L.; Jiang, P.; Xu, W. X.; Li, H.; Zhang, H.; Yan, L. Y.; Chan-Park, M. B.; Liu, X. W.; Tang, K.; Mu, Y. G.; Pervushin, K., The molecular basis of distinct aggregation pathways of islet amyloid polypeptide. *J. Biol. Chem.* **2011**, *286* (8), 6291-6300.

16. Tu, L. H.; Serrano, A. L.; Zanni, M. T.; Raleigh, D. P. Mutational analysis of preamyloid intermediates: The role of His-Tyr interactions in islet amyloid formation. *Biophys. J.* **2014**, *106* (7), 1520-1527.

17. Abedini, A.; Raleigh, D. P., Incorporation of pseudoproline derivatives allows the facile synthesis of human IAPP, a highly amyloidogenic and aggregation-prone polypeptide. *Org. Lett.* **2005**, *7* (4), 693-696.

18. Marek, P.; Woys, A. M.; Sutton, K.; Zanni, M. T.; Raleigh, D. P., Efficient microwave-assisted synthesis of human islet amyloid polypeptide designed to facilitate the specific incorporation of labeled amino acids. *Org. Lett.* **2010**, *12* (21), 4848-4851.

19. Abedini, A.; Singh, G.; Raleigh, D. P., Recovery and purification of highly aggregation-prone disulfide-containing peptides: Application to islet amyloid polypeptide. *Ana. Biochem.* **2006**, *351* (2), 181-186.

20. Porat, Y.; Mazor, Y.; Efrat, S.; Gazit, E., Inhibition of islet amyloid polypeptide fibril formation: A potential role for heteroaromatic interactions. *Biochemistry* **2004**, *43* (45), 14454-14462.

21. Porat, Y.; Abramowitz, A.; Gazit, E., Inhibition of amyloid fibril formation by polyphenols: Structural similarity and aromatic interactions as a common inhibition mechanism. *Chem. Biol. Drug Des.* **2006**, *67* (1), 27-37.

22. Krebs, M. R. H.; Bromley, E. H. C.; Donald, A. M., The binding of thioflavin-T to amyloid fibrils: localisation and implications. *J. Struc. Biol.* **2005**, *149* (1), 30-37.

23. Marek, P.; Mukherjee, S.; Zanni, M. T.; Raleigh, D. P., Residue-specific, real-time characterization of lag-phase species and fibril growth during amyloid formation: A combined fluorescence and IR study of p-cyanophenylalanine analogs of islet amyloid polypeptide. *J. Mol. Biol.* **2010**, *400* (4), 878-888.

24. Hudson, S. A.; Ecroyd, H.; Kee, T. W.; Carver, J. A., The thioflavin T fluorescence assay for amyloid fibril detection can be biased by the presence of exogenous compounds. *Febs J.* **2009**, *276* (20), 5960-5972.

25. Meng, F. L.; Marek, P.; Potter, K. J.; Verchere, C. B.; Raleigh, D. P., Rifampicin does not prevent amyloid fibril formation by human islet amyloid polypeptide but does inhibit fibril thioflavin-T interactions: Implications for mechanistic studies beta-cell death. *Biochemistry* **2008**, *47* (22), 6016-6024.

26. Marek, P.; Abedini, A.; Song, B. B.; Kanungo, M.; Johnson, M. E.; Gupta, R.; Zaman, W.; Wong, S. S.; Raleigh, D. P., Aromatic interactions are not required for amyloid fibril formation by islet amyloid polypeptide but do influence the rate of fibril formation and fibril morphology. *Biochemistry* **2007**, *46* (11), 3255-3261.

27. Tu, L. H.; Raleigh, D. P., Role of aromatic interactions in amyloid formation by islet amyloid polypeptide. *Biochemistry* **2013**, *52* (2), 333-342.

28. Murias, M.; Jager, W.; Handler, N.; Erker, T.; Horvath, Z.; Szekeres, T.; Nohl, H.; Gille, L., Antioxidant prooxidant and cytotoxic activity of hydroxylated resveratrol analogues: structure-activity relationship. *Biochem. Pharm.* **2005**, *69* (6), 903-912.

29. Murias, M.; Handler, N.; Erker, T.; Pleban, K.; Ecker, G.; Saiko, P.; Szekeres, T.; Jager, W., Resveratrol analogues as selective cyclooxygenase-2 inhibitors: synthesis and structure-activity relationship. *Bioorg. Medi. Chem.* **2004**, *12* (21), 5571-5578.

30. Noor, H.; Cao, P.; Raleigh, D. P., Morin hydrate inhibits amyloid formation by islet amyloid polypeptide and disaggregates amyloid fibers. *Protein Sci.* **2012**, *21* (3), 373-382.

Complete List of References

Abedini, A.; Raleigh, D. P., The role of His-18 in amyloid formation by human islet amyloid polypeptide. *Biochemistry* **2005**, *44* (49), 16284-16291.

Abedini, A.; Raleigh, D. P., Incorporation of pseudoproline derivatives allows the facile synthesis of human IAPP, a highly amyloidogenic and aggregation-prone polypeptide. *Org. Lett.* **2005**, *7* (4), 693-696.

Abedini, A.; Raleigh, D. P., Destabilization of human IAPP amyloid fibrils by proline mutations outside of the putative amyloidogenic domain: Is there a critical amyloidogenic domain in human IAPP? *J. Mol. Biol.* **2006**, *355* (2), 274-281.

Abedini, A.; Singh, G.; Raleigh, D. P., Recovery and purification of highly aggregation-prone disulfide-containing peptides: Application to islet amyloid polypeptide. *Ana. Biochem.* **2006**, *351* (2), 181-186.

Abedini, A.; Meng, F. L.; Raleigh, D. P., A single-point mutation converts the highly amyloidogenic human islet amyloid polypeptide into a potent fibrillization inhibitor. *J. Am. Chem. Soc.* **2007**, *129* (37), 11300-11301.

Abedini, A.; Raleigh, D. P., A critical assessment of the role of helical intermediates in amyloid formation by natively unfolded proteins and polypeptides. *Protein Eng. Des. Sel.* **2009**, *22* (8), 453-459.

Abedini, A.; Raleigh, D. P., A role for helical intermediates in amyloid formation by natively unfolded polypeptides? *Phys. Biol.* **2009**, *6* (1), 15005

Abedini, A.; Schmidt, A. M., Mechanisms of islet amyloidosis toxicity in type 2 diabetes. *Febs Lett.* **2013**, *587* (8), 1119-1127.

Ahronheim, J. H., The nature of the hyaline material in the pancreatic islands in diabetes mellitus. *Am. J. Pathol.* **1943**, *19* (5), 873-882.

Armstrong, A. H.; Chen, J.; McKoy, A. F.; Hecht, M. H., Mutations that replace aromatic side chains promote aggregation of the Alzheimer's A beta peptide, *Biochemistry* **2011**, *50* (19), 4058-4067.

Ashcroft, F. M.; Rorsman, P., Diabetes mellitus and the beta cell: The last ten years. *Cell* **2012**, *148* (6), 1160-1171.

Aston-Mourney, K.; Zraika, S.; Udayasankar, J.; Subramanian, S. L.; Green, P. S.; Kahn, S. E.; Hull, R. L., Matrix metalloproteinase-9 reduces islet amyloid formation by degrading islet amyloid polypeptide. *J. Biol. Chem.* **2013**, *288* (5), 3553-3559.

Azriel, R.; Gazit, E., Analysis of the structural and functional elements of the minimal active fragment of islet amyloid polypeptide (IAPP) - An experimental support for the key role of the phenylalanine residue in amyloid formation. *J. Biol. Chem.* **2001**, *276* (36), 34156-34161.

Backstrom, J. R.; Lim, G. P.; Cullen, M. J.; Tokes, Z. A., Matrix metalloproteinase-9 (MMP-9) is synthesized in neurons of the human hippocampus and is capable of degrading the amyloid-beta peptide (1-40). *J. Neurosci.* **1996**, *16* (24), 7910-7919.

Badman, M. K.; Shennan, K. I.; Jermany, J. L.; Docherty, K.; Clark, A., Processing of pro-islet amyloid polypeptide (proIAPP) by the prohormone convertase PC2. *Febs Lett.* **1996**, 378 (3), 227-231.

Baglioni, S.; Casamenti, F.; Bucciantini, M.; Luheshi, L. M.; Taddei, N.; Chiti, F.; Dobson, C. M.; Stefani, M., Prefibrillar amyloid aggregates could be generic toxins in higher organisms. *J. Neurosci.* **2006**, *26* (31), 8160-8167.

Ban, T.; Hamada, D.; Hasegawa, K.; Naiki, H.; Goto, Y., Direct observation of amyloid fibril growth monitored by thioflavin T fluorescence. *J. Biol. Chem.* **2003**, *278* (19), 16462-16465.

Bastianetto, S.; Krantic, S.; Quirion, R., Polyphenols as potential inhibitors of amyloid aggregation and toxicity: Possible significance to Alzheimer's disease. *Med. Chem.* **2008**, *8* (5), 429-435.

Bastianetto, S.; Yao, Z. X.; Papadopoulos, V.; Quirion, R., Neuroprotective effects of green and black teas and their catechin gallate esters against beta-amyloid-induced toxicity. *Euro. J. Neurosci.* **2006**, *23* (1), 55-64.

Bellotti, V.; Chiti, F., Amyloidogenesis in its biological environment: challenging a fundamental issue in protein misfolding diseases. *Curr. Opin. Struct. Biol.* **2008**, *18* (6), 771-779.

Bennett, R. G.; Duckworth, W. C.; Hamel, F. G. Degradation of amylin by insulin-degrading enzyme. *J. Biol. Chem.* **2000**, *275* (47), 36621-36625.

Bennett, R. G.; Hamel, F. G.; Duckworth, W. C., An insulin-degrading enzyme inhibitor decreases amylin degradation, increases amylin-induced cytotoxicity, and increases amyloid formation in insulinoma cell cultures. *Diabetes* **2003**, *52* (9), 2315-2320.

Betsholtz, C.; Svensson, V.; Rorsman, F.; Engstrom, U.; Westermark, G. T.; Wilander, E.; Johnson, K.; Westermark, P., Islet amyloid polypeptide (IAPP) - cDNA cloning and identification of an amyloidogenic region associated with the species-specific occurrence of age-related diabetes-mellitus. *Expe. Cell Res.* **1989**, *183* (2), 484-493.

Bieschke, J.; Russ, J.; Friedrich, R. P.; Ehrnhoefer, D. E.; Wobst, H.; Neugebauer, K.; Wanker, E. E., EGCG remodels mature alpha-synuclein and amyloid-beta fibrils and reduces cellular toxicity. *Pro. Natl. Acad. Sci. U. S. A.* **2010**, *107* (17), 7710-7715.

Bishop, M. F.; Ferrone, F. A., Kinetics of nucleation-controlled polymerization- A perturbation treatment for use with a secondary pathway. *Biophys. J.* **1984**, *46* (5), 631-644.

Buchanan, L. E.; Dunkelberger, E. B.; Tran, H. Q.; Cheng, P. N.; Chiu, C. C.; Cao, P.; Raleigh, D. P.; de Pablo, J. J.; Nowick, J. S.; Zanni, M. T., Mechanism of IAPP amyloid fibril formation involves an intermediate with a transient beta-sheet. *Proc. Natl. Acad. Sci. U.S.A.* **2013**, *110* (48), 19285-19290.

Bulawa, C. E.; Connelly, S.; Devit, M.; Wang, L.; Weigel, C.; Fleming, J. A.; Packman, J.; Powers, E. T.; Wiseman, R. L.; Foss, T. R.; Wilson, I. A.; Kelly, J. W.; Labaudiniere, R., Tafamidis, a potent and selective transthyretin kinetic stabilizer that inhibits the amyloid cascade. *Proc. Natl. Acad. Sci. U. S. A.* **2012**, *109* (24), 9629-9634.

Butler, A. E.; Janson, J.; Bonner-Weir, S.; Ritzel, R.; Rizza, R. A.; Butler, P. C., beta-cell deficit and increased beta-cell apoptosis in humans with type 2 diabetes, *Diabetes* **2003**, *52* (1), 102-110.

Cao, D.; Zhang, Y. J.; Zhang, H. H.; Zhong, L. W.; Qian, X. H., Systematic characterization of the covalent interactions between (-)-epigallocatechin gallate and peptides under physiological conditions by mass spectrometry. *Rapid Commun. Mass Spectrom*. **2009**, *23* (8), 1147-1157.

Cao, P.; Meng, F.; Abedini, A.; Raleigh, D. P., The ability of rodent islet amyloid polypeptide to inhibit amyloid formation by human islet amyloid polypeptide has important implications for the mechanism of amyloid formation and the design of inhibitors, *Biochemistry* **2010**, *49* (5), 872-881.

Cao, P.; Raleigh, D. P., Analysis of the inhibition and remodeling of islet amyloid polypeptide amyloid fibers by flavanols. *Biochemistry* **2012**, *51* (13), 2670-2683.

Cao, P.; Tu, L. H.; Abedini, A.; Levsh, O.; Akter, R.; Patsalo, V.; Schmidt, A. M.; Raleigh, D. P., Sensitivity of amyloid formation by human islet amyloid polypeptide to mutations at residue 20. J. Mol. Biol. **2012**, *421* (2-3), 282-295.

Cao, P.; Marek, P.; Noor, H.; Patsalo, V.; Tu, L. H.; Wang, H.; Abedini, A.; Raleigh, D. P., Islet amyloid: From fundamental biophysics to mechanisms of cytotoxicity. *Febs Lett*. **2013**, *587* (8), 1106-1118.

Castano, E. M.; Prelli, F.; Wisniewski, T.; Golabek, A.; Kumar, R. A.; Soto, C.; Frangione, B., Fibrillogenesis in Alzheimers-disease of amyloid-beta peptides and apolipoprotein-E. *Biochem. J.* **1995**, *306*, 599-604.

Charge, S. B.; de Koning, E. J.; Clark, A., Effect of pH and insulin on fibrillogenesis of islet amyloid polypeptide *in vitro*. *Biochemistry* **1995**, *34* (44), 14588-14593.

Chen, M. S.; Zhao, D. S.; Yu, Y. P.; Li, W. W.; Chen, Y. X.; Zhao, Y. F.; Li, Y. M., Characterizing the assembly behaviors of human amylin: a perspective derived from C-terminal variants. *Chem. Comm*. **2013**, *49* (18), 1799-1801.

Cheng, B. A.; Liu, X. R.; Gong, H.; Huang, L. Q.; Chen, H.; Zhang, X.; Li, C. Z.; Yang, M. Y.; Ma, B. J.; Jiao, L. H.; Zheng, L.; Huan, K., Coffee components inhibit amyloid formation of human islet amyloid polypeptide *in vitro*: Possible link between coffee consumption and diabetes mellitus. *J. Agricul. Food Chem.* **2011**, *59* (24), 13147-13155.

Cheng, F.; Marzban, L., Cytotoxic effects of human islet amyloid polypeptide on primary islet alpha-cells and beta-cells: Implications for understanding the pathogenesis of type 2 diabetes. *Diabetes* **2007**, *56*, A410-A411.

Chesneau, V.; Vekrellis, K.; Rosner, M. R.; Selkoe, D. J., Purified recombinant insulin-degrading enzyme degrades amyloid beta-protein but does not promote its oligomerization. *Biochem. J.* **2000**, *351*, 509-516.

Chiti, F.; Dobson, C. M., Protein misfolding, functional amyloid, and human disease. *Annu. Rev. Biochem.* **2006**, *75*, 333-366.

Clark, A.; Lewis, C. E.; Willis, A. C.; Cooper, G. J. S.; Morris, J. F.; Reid, K. B. M.; Turner, R. C., Islet amyloid formed from diabetes-associated peptide may be pathogenic in type-2 diabetes, *Lancet* **1987**, *2* (8553), 231-234.

Clark, A.; Wells, C. A.; Buley, I. D.; Cruickshank, J. K.; Vanhegan, R. I.; Matthews, D. R.; Cooper, G. J. S.; Holman, R. R.; Turner, R. C., Islet amyloid, increased alpha-cells, reduced beta-cells and exocrine fibrosis-quantitative changes in the pancreas in type 2 diabetes. *Diabetes Res.***1988**, *9* (4), 151-159.

Coelho, T.; Maia, L. F.; da Silva, A. M.; Cruz, M. W.; Plante-Bordeneuve, V.; Lozeron, P.; Suhr, O. B.; Campistol, J. M.; Conceicao, I. M.; Schmidt, H. H. J.; Trigo, P.; Kelly, J. W.; Labaudinie, R.; Chan, J.; Packman, J.; Wilson, A.; Grogan, D. R., Tafamidis for transthyretin familial amyloid polyneuropathy a randomized, controlled trial. *Neurology* **2012**, *79* (8), 785-792.

Cooper, G. J. S.; Willis, A. C.; Clark, A.; Turner, R. C.; Sim, R. B.; Reid, K. B. M., Purification and characterization of a peptide from amyloid-rich pancreases of type-2 diabetic-patients. *Proc. Natl. Acad. Sci. U. S. A.* **1987**, *84* (23), 8628-8632.

Cooper, G. J. S.; Leighton, B.; Dimitriadis, G. D.; Parrybillings, M.; Kowalchuk, J. M.; Howland, K.; Rothbard, J. B.; Willis, A. C.; Reid, K. B. M., Amylin found in amyloid deposits in human type-2 diabetes-mellitus may be a hormone that regulates glycogen-metabolism in skeletal-muscle. *Proc. Natl. Acad. Sci. U.S.A.* **1988**, *85* (20), 7763-7766.

de Groot, N. S.; Aviles, F. X.; Vendrell, J.; Ventura, S., Mutagenesis of the central hydrophobic cluster in A beta 42 Alzheimer's peptide: Side-chain properties correlate with aggregation propensities, *Febs J.* **2006**, *273* (3), 658-668.

Demuro, A.; Mina, E.; Kayed, R.; Milton, S. C.; Parker, I.; Glabe, C. G., Calcium dysregulation and membrane disruption as a ubiquitous neurotoxic mechanism of soluble amyloid oligomers. *J. Biol. Chem.* **2005**, *280* (17), 17294-17300.

Donath, M. Y.; Shoelson, S. E., Type 2 diabetes as an inflammatory disease. *Nat. Rev. Immunol.* **2011**, *11* (2), 98-107.

Dunkelberger, E. B.; Buchanan, L. E.; Marek, P.; Cao, P.; Raleigh, D. P.; Zanni, M. T., Deamidation accelerates amyloid formation and alters amylin fiber structure. *J. Am. Chem. Soc.* **2012**, *134* (30), 12658-12667.

Dupuis, N. F.; Wu, C.; Shea, J. E.; Bowers, M. T., The amyloid formation mechanism in human IAPP: Dimers have beta-strand monomer-monomer interfaces. *J. Am. Chem. Soc.* **2011**, *133* (19), 7240-7243.

Ehses, J.A., Perren, A., Eppler, E., Ribaux, P., Pospisilik, J. A., Maor-Cahn, R., Gueripel, X., Ellingsgaard, H., Schneider, M. K., Biollaz, G., Fontana, A., Reinecke, M., Homo-Delarche, F., & Donath, M. Y. Increased number of islet-associated macrophages in type 2 diabetes. *Diabetes* **2007**, *56* (9), 2356-2370.

Esler, W. P.; Stimson, E. R.; Ghilardi, J. R.; Lu, Y. A.; Felix, A. M.; Vinters, H. V.; Mantyh, P. W.; Lee, J. P.; Maggio, J. E., Point substitution in the central hydrophobic cluster of a human beta-amyloid congener disrupts peptide folding and abolishes plaque competence. *Biochemistry* **1996**, *35* (44), 13914-13921.

Evers, F.; Jeworrek, C.; Tiemeyer, S.; Weise, K.; Sellin, D.; Paulus, M.; Struth, B.; Tolan, M.; Winter, R., Elucidating the mechanism of lipid membrane-induced IAPP fibrillogenesis and its inhibition by the red wine compound resveratrol: A synchrotron X-ray reflectivity study. *J. Am. Chem. Soc.* **2009**, *131* (27), 9516-9521.

Fandrich, M., Oligomeric intermediates in amyloid formation: Structure determination and mechanisms of toxicity. *J. Mol. Biol.* **2012**, *421* (4-5), 427-440.

Fauchere, J. L.; Charton, M.; Kier, L. B.; Verloop, A.; Pliska, V., Amino acid side chain parameters for correlation studies in biology and pharmacology. *Int. J. Pept. Protein Res.* **1988**, *32* (4), 269-278.

Feng, Y.; Wang, X. P.; Yang, S. G.; Wang, Y. J.; Zhang, X.; Du, X. T.; Sun, X. X.; Zhao, M.; Huang, L.; Liu, R. T., Resveratrol inhibits beta-amyloid oligomeric cytotoxicity but does not prevent oligomer formation. *Neurotoxicology* **2009**, *30* (6), 986-995.

Ferreira, N.; Saraiva, M. J.; Almeida, M. R., Natural polyphenols inhibit different steps of the process of transthyretin (TTR) amyloid fibril formation. *Febs Lett.* **2011**, *585* (15), 2424-2430.

Ferrone, F., Analysis of protein aggregation kinetics. *Method. Enzymol.* **1999**, *309*, 256-274.

Fox, A.; Snollaerts, T.; Casanova, C. E.; Calciano, A.; Nogaj, L. A.; Moffet, D. A., Selection for nonamyloidogenic mutants of islet amyloid polypeptide (IAPP) identifies an extended region for amyloidogenicity. *Biochemistry* **2010**, *49* (36), 7783-7789.

Gazit, E. A possible role for pi-stacking in the self-assembly of amyloid fibrils. *Febs. J.* **2002**, *16* (1), 77-83.

Gazit, E., The role of prefibrillar assemblies in the pathogenesis of amyloid diseases. *Drug Future* **2004**, *29* (6), 613-619.

Ge, J. F.; Qiao, J. P.; Qi, C. C.; Wang, C. W.; Zhou, J. N., The binding of resveratrol to monomer and fibril amyloid beta. *Neurochem. Interl.* **2012**, *61* (7), 1192-1201.

Getahun, Z.; Huang, C. Y.; Wang, T.; De Leon, B.; DeGrado, W. F.; Gai, F., Using nitrile-derivatized amino acids as infrared probes of local environment. *J. Am. Chem. Soc.* **2003**, *125* (2), 405-411.

Gilead, S.; Wolfenson, H.; Gazit, E., Molecular mapping of the recognition interface between the islet amyloid polypeptide and insulin. *Angew. Chem. Int. Ed.* **2006**, *45* (39), 6476-6480.

Glabe, C.; Kayed, R.; Sokolov, Y.; Hall, J., Common structure and mechanism of soluble amyloid oligomer pathogenesis in degenerative diseases. *Neurobiol. Aging* **2004**, *25*, S75-S76.

Goldschmidt, L.; Teng, P. K.; Riek, R.; Eisenberg, D., Identifying the amylome, proteins capable of forming amyloid-like fibrils. *Proc. Natl. Acad. Sci. U. S. A.* **2010**, *107* (8), 3487-3492.

Gordon, D. J.; Tappe, R.; Meredith, S. C., Design and characterization of a membrane permeable N-methyl amino acid-containing peptide that inhibits A beta (1-40) fibrillogenesis. *J. Pept. Res.* **2002**, *60* (1), 37-55.

Grechko, M.; Zanni, M. T., Quantification of transition dipole strengths using 1D and 2D spectroscopy for the identification of molecular structures via exciton delocalization: Application to alpha-helices. *J. Chem. Phys.* **2012**, *137* (18), 184202

Green, J.; Goldsbury, C.; Min, T.; Sunderji, S.; Frey, P.; Kistler, J.; Cooper, G.; Aebi, U., Full-length rat amylin forms fibrils following substitution of single residues from human amylin. *J. Mol. Biol*. **2003**, *326* (4), 1147-1156.

Guan, H.; Chow, K. M.; Shah, R.; Rhodes, C. J.; Hersh, L. B., Degradation of islet amyloid polypeptide by neprilysin. *Diabetologia* **2012**, *55* (11), 2989-2998.

Haass, C.; Selkoe, D. J., Soluble protein oligomers in neurodegeneration: lessons from the Alzheimer's amyloid beta-peptide. *Nat. Rev. Mol. Cell Biol*. **2007**, *8* (2), 101-112.

Haataja, L.; Gurlo, T.; Huang, C. J.; Butler, P. C., Islet amyloid in type 2 diabetes, and the toxic oligomer hypothesis. *Endocr. Rev.* **2008**, *29* (3), 303-316.

Hauber, I.; Hohenberg, H.; Holstermann, B.; Hunstein, W.; Hauber, J., The main green tea polyphenol epigallocatechin-3-gallate counteracts semen-mediated enhancement of HIV infection. *Proc. Natl. Acad. Sci. U. S. A.* **2009**, *106* (22), 9033-9038.

Heinitz, K.; Beck, M.; Schliebs, R.; Perez-Polo, J. R., Toxicity mediated by soluble oligomers of beta-amyloid (1-42) on cholinergic SN56.B5.G4 cells. *J. Neurochem*. **2006**, *98* (6), 1930-1945.

Hersh, L. B.; Rodgers, D. W., Neprilysin and amyloid beta peptide degradation. *Curr. Alzheimer Res*. **2008**, *5* (2), 225-231.

Hollander, P. A., Levy, P., Fineman, M., Maggs, D. G., Shen, L. Z., Strobel, S. A., Weyer, C. & Kolterman, O. G. Pramlintide as an adjunct to insulin therapy improves long-term glycemic and weight control in patients with type 2 diabetes: A 1-year randomized controlled trial. *Diabetes Care* **2003**, *26* (3), 784-790.

Hoppener, J. W. M.; Lips, C. J. M., Role of islet amyloid in type 2 diabetes mellitus. *Interl. J. Biochem. Cell Biol.* **2006**, *38* (5-6), 726-736.

Horovitz, A., Double-mutant cycles: A powerful tool for analyzing protein structure and function. *Fold. Des.* **1996**, *1* (6), R121-R126.

Hou, X.; Aguilar, M. I.; Small, D. H., Transthyretin and familial amyloidotic polyneuropathy - Recent progress in understanding the molecular mechanism of neurodegeneration. *Febs J.* **2007**, *274* (7), 1637-1650.

Hudson, S. A.; Ecroyd, H.; Kee, T. W.; Carver, J. A., The thioflavin T fluorescence assay for amyloid fibril detection can be biased by the presence of exogenous compounds. *Febs J.* **2009**, *276* (20), 5960-5972.

Hughes, S. R.; Goyal, S.; Sun, J. E.; GonzalezDeWhitt, P.; Fortes, M. A.; Riedel, N. G.; Sahasrabudhe, S. R., Two-hybrid system as a model to study the interaction of beta-amyloid peptide monomers. *Proc. Natl. Acad. Sci. U. S. A.* **1996**, *93* (5), 2065-2070.

Hull, R. L.; Andrikopoulos, S.; Verchere, C. B.; Vidal, J.; Wang, F.; Cnop, M.; Prigeon, R. L.; Kahn, S. E., Increased dietary fat promotes islet amyloid formation and beta-cell secretory dysfunction in a transgenic mouse model of islet amyloid. *Diabetes* **2003**, *52* (2), 372-379.

Hutton, J. C., The internal pH and membrane-potential of the insulin-secretory granule. *Biochem. J.* **1982**, *204* (1), 171-178.

Hutton, J. C. The insulin secretory granule, *Diabetologia* **1989**, *32* (5), 271-281.

Jakob-Roetne, R.; Jacobsen, H., Alzheimer's disease: From pathology to therapeutic approaches. *Angew. Chem. Int. Ed*. **2009**, *48* (17), 3030-3059.

Janson, J.; Ashley, R. H.; Harrison, D.; McIntyre, S.; Butler, P. C., The mechanism of islet amyloid polypeptide toxicity is membrane disruption by intermediate-sized toxic amyloid particles. Diabetes **1999**, *48* (3), 491-498.

Janson, J.; Soeller, W. C.; Roche, P. C.; Nelson, R. T.; Torchia, A. J.; Kreutter, D. K.; Butler, P. C., Spontaneous diabetes mellitus in transgenic mice expressing human islet amyloid polypeptide. *Proc. Natl. Acad. Sci. U.S.A.* **1996**, *93* (14), 7283-7288.

Jayasinghe, S. A.; Langen, R., Identifying structural features of fibrillar islet amyloid polypeptide using site-directed spin labeling. *J. Biol. Chem*. **2004**, *279* (46), 48420-48425.

Johnson, K. H.; Obrien, T. D.; Betsholtz, C.; Westermark, P., Islet amyloid, islet-amyloid polypeptide, and diabetes-Mellitus. *N. Engl. J. Med*. **1989**, *321* (8), 513-519.

Jurgens, C. A.; Toukatly, M. N.; Fligner, C. L.; Udayasankar, J.; Subramanian, S. L.; Zraika, S.; Aston-Mourney, K.; Carr, D. B.; Westermark, P.; Westermark, G. T.; Kahn, S. E.; Hull, R. L., beta-cell loss and beta-cell apoptosis in human type 2 diabetes are related to islet amyloid deposition. *Am. J. Pathol*. **2011**, *178* (6), 2632-2640.

Kahn, S. E.; Dalessio, D. A.; Schwartz, M. W.; Fujimoto, W. Y.; Ensinck, J. W.; Taborsky, G. J.; Porte, D., Evidence of cosecretion of islet amyloid polypeptide and Insulin by beta-cells. *Diabetes* **1990**, *39* (5), 634-638.

Kahn, S. E.; Andrikopoulos, S.; Verchere, C. B., Islet amyloid: A long-recognized but underappreciated pathological feature of type 2 diabetes. *Diabetes* **1999**, 48 (2), 241-253.

Kajava, A. V.; Aebi, U.; Steven, A. C., The parallel superpleated beta-structure as a model for amyloid fibrils of human amylin. *J. Mol. Biol.* **2005**, *348* (2), 247-252.

Kanemitsu, H.; Tomiyama, T.; Mori, H., Human neprilysin is capable of degrading amyloid beta peptide not only in the monomeric form but also the pathological oligomeric form. *Neurosci. Lett.* **2003**, *350* (2), 113-116.

Kapurniotu, A.; Schmauder, A.; Tenidis, K., Structure-based design and study of non-amyloidogenic, double N-methylated IAPP amyloid core sequences as inhibitors of IAPP amyloid formation and cytotoxicity. *J. Mol. Biol*. **2002**, *315* (3), 339-350.

Kayed, R.; Head, E.; Sarsoza, F.; Saing, T.; Cotman, C. W.; Necula, M.; Margol, L.; Wu, J.; Breydo, L.; Thompson, J. L.; Rasool, S.; Gurlo, T.; Butler, P.; Glabe, C. G., Fibril specific, conformation dependent antibodies recognize a generic epitope common to amyloid fibrils and fibrillar oligomers that is absent in prefibrillar oligomers. *Mol. Neurodegener*. **2007**, 2. 18

Kayed, R.; Head, E.; Thompson, J. L.; McIntire, T. M.; Milton, S. C.; Cotman, C. W.; Glabe, C. G., Common structure of soluble amyloid oligomers implies common mechanism of pathogenesis. *Science* **2003**, *300* (5618), 486-489.

Khemtemourian, L.; Killian, J. A.; Hoppener, J. W. M.; Engel, M. F. M., Recent insights in islet amyloid polypeptide-induced membrane disruption and its role in beta-cell death in type 2 diabetes mellitus. *Expe. Diabetes Res*. **2008**, *2008*, 421287.

Khurana, R.; Uversky, V. N.; Nielsen, L.; Fink, A. L., Is Congo red an amyloid-specific dye? *J. Biol. Chem.* **2011**, *276* (25), 22715-22721.

Kirkitadze, M. D.; Condron, M. M.; Teplow, D. B., Identification and characterization of key kinetic intermediates in amyloid beta-protein fibrillogenesis, *J. Mol. Biol*. **2001**, *312* (5), 1103

Klein, W. L.; Stine, W. B.; Teplow, D. B., Small assemblies of unmodified amyloid beta-protein are the proximate neurotoxin in Alzheimer's disease. *Neurobiol. Aging* **2004**, *25* (5), 569-580.

Kokkoni, N.; Stott, K.; Amijee, H.; Mason, J. M.; Doig, A. J., N-methylated peptide inhibitors of beta-amyloid aggregation and toxicity. Optimization of the inhibitor structure. *Biochemistry* **2006**, *45* (32), 9906-9918.

Konarkowska, B.; Aitken, J. F.; Kistler, J.; Zhang, S. P.; Cooper, G. J. S., The aggregation potential of human amylin determines its cytotoxicity towards islet beta-cells. *Febs J.* **2006**, *273* (15), 3614-3624.

Koo, B. W.; Hebda, J. A.; Miranker, A. D., Amide inequivalence in the fibrillar assembly of islet amyloid polypeptide. *Protein Eng. Des. Sel*. **2008**, *21* (3), 147-154.

Koo, E. H.; Lansbury, P. T.; Kelly, J. W., Amyloid diseases: Abnormal protein aggregation in neurodegeneration. *Pro. Natl. Acad. Sci. U. S. A.* **1999**, 96 (18), 9989-9990.

Kosowska, B.; Tokarska, M.; Januszewski, A.; Jach, H.; Bednarek-Tupikowska, G.; Zdrojewicz, Z., Amyloidosis and amyloidogenic proteins. *Med. Weter* **2001**, *57* (4), 233-237.

Krebs, M. R. H.; Morozova-Roche, L. A.; Daniel, K.; Robinson, C. V.; Dobson, C. M. Observation of sequence specificity in the seeding of protein amyloid fibrils, *Protein Sci*. **2004**, *13* (7), 1933-1938.

Krebs, M. R. H.; Bromley, E. H. C.; Donald, A. M., The binding of thioflavin-T to amyloid fibrils: localisation and implications. *J. Struc. Biol.* **2005**, *149* (1), 30-37.

Kumar, S.; Walter, J., Phosphorylation of amyloid beta (A beta) peptides - A trigger for formation of toxic aggregates in Alzheimer's disease. *Aging* **2011**, *3* (8), 803-812.

Ladiwala, A. R. A.; Lin, J. C.; Bale, S. S.; Marcelino-Cruz, A. M.; Bhattacharya, M.; Dordick, J. S.; Tessier, P. M., Resveratrol selectively remodels soluble oligomers and fibrils of amyloid A beta into off-pathway conformers. *J. Biol. Chem*. **2010**, *285* (31), 24228-24237.

Lai, Z. H.; Colon, W.; Kelly, J. W., The acid-mediated denaturation pathway of transthyretin yields a conformational intermediate that can self-assemble into amyloid. *Biochemistry* **1996**, *35* (20), 6470-6482.

Lansbury, P. T.; Lashuel, H. A., A century-old debate on protein aggregation and neurodegeneration enters the clinic. *Nature* **2006**, *443* (7113), 774-779.

Larson, J. L.; Miranker, A. D., The mechanism of insulin action on islet amyloid polypeptide fiber formation. *J. Mol. Biol*. **2004**, *335* (1), 221-231.

Lazo, N. D.; Downing, D. T., Fibril formation by amyloid-beta proteins may involve beta-helical protofibrils. *J. Pept. Res.* **1999**, *53* (6), 633-640.

Levine, H. Thioflavine-T interaction with synthetic Alzheimers-disease beta-amyloid peptides: Detection of amyloid aggregation in solution, *Protein Sci.* **1993**, *2* (3), 404-410.

Li, Y.; Xu, W. X.; Mu, Y. G.; Zhang, J. Z. H., Acidic pH retards the fibrillization of human islet amyloid polypeptide due to electrostatic repulsion of histidines. *J. Chem. Phys*. **2013**, *139* (5), 055102

Lomakin, A.; Chung, D. S.; Benedek, G. B.; Kirschner, D. A.; Teplow, D. B., On the nucleation and growth of amyloid beta-protein fibrils: Detection of nuclei and quantitation of rate constants. *Proc. Natl. Acad. Sci. U.S.A.* **1996**, *93* (3), 1125-1129.

Lorenzo, A.; Razzaboni, B.; Weir, G. C.; Yankner, B. A., Pancreatic-islet cell toxicity of amylin associated with type-2 diabetes-mellitus. *Nature* **1994**, *368* (6473), 756-760.

Luca, S.; Yau, W. M.; Leapman, R.; Tycko, R., Peptide conformation and supramolecular organization in amylin fibrils: Constraints from solid-state NMR. *Biochemistry* **2007**, *46* (47), 13505-13522.

Lutz, T.A., Control of energy homeostasis by amylin. *Cell. Mol. Life Sci.* **2012**, *69* (12), 1947–1965.

Lyu, P. C.; Sherman, J. C.; Chen, A.; Kallenbach, N. R., Alpha-helix stabilization by natural and unnatural amino-acids with alkyl side-chains. *Proc. Natl. Acad. Sci. U.S.A.* **1991**, *88* (17), 5317-5320.

Makin, O. S.; Serpell, L. C., Structural characterisation of islet amyloid polypeptide fibrils. *J. Mol. Biol.* **2004**, *335* (5), 1279-1288.

Maloy, A. L.; Longnecker, D. S.; Greenberg, E. R., The relation of islet amyloid to the clinical type diabetes. *Human Pathol*. **1981**, *12* (10), 917-922.

Marambaud, P.; Zhao, H. T.; Davies, P., Resveratrol promotes clearance of Alzheimer's disease amyloid-beta peptides. *J. Biol. Chem*. **2005**, *280* (45), 37377-37382.

Marek, P. J.; Patsalo, V.; Green, D. F.; Raleigh, D. P., Ionic strength effects on amyloid formation by amylin are a complicated interplay among Debye screening, ion selectivity, and Hofmeister effects. *Biochemistry* **2012**, *51* (43), 8478-8490.

Marek, P.; Abedini, A.; Song, B. B.; Kanungo, M.; Johnson, M. E.; Gupta, R.; Zaman, W.; Wong, S. S.; Raleigh, D. P., Aromatic interactions are not required for amyloid fibril formation by islet amyloid polypeptide but do influence the rate of fibril formation and fibril morphology. *Biochemistry* **2007**, *46* (11), 3255-3261.

Marek, P.; Gupta, R.; Raleigh, D. P., The fluorescent amino acid p-cyanophenylalanine provides an intrinsic probe of amyloid formation. *Chembiochem* **2008**, *9* (9), 1372-1374.

Marek, P.; Mukherjee, S.; Zanni, M. T.; Raleigh, D. P., Residue-specific, real-time characterization of lag-phase species and fibril growth during amyloid formation: A combined fluorescence and IR study of p-cyanophenylalanine analogs of islet amyloid polypeptide. *J. Mol. Biol*. **2010**, *400* (4), 878-888.

Marek, P.; Woys, A. M.; Sutton, K.; Zanni, M. T; Raleigh, D. P., Efficient microwave-assisted synthesis of human islet amyloid polypeptide designed to facilitate the specific incorporation of labeled amino acids. *Org. Lett*. **2010**, *12* (4), 4848-4851.

Martinez, A.; Montuenga, L. M.; Springall, D. R.; Treston, A.; Cuttitta, F.; Polak, J. M., Immunocytochemical localization of peptidylglycine alpha-amidating monooxygenase enzymes (PAM) in human endocrine pancreas. *J. Histochem. Cytochem.* **1993**, *41* (3), 375-380.

Marzban, L.; Soukhatcheva, G.; Verchere, C. B., Role of carboxypeptidase E in processing of pro-islet amyloid polypeptide in beta-cells. *Endocrinology* **2005**, *146* (4), 1808-1817.

Marzban, L.; Trigo-Gonzales, G.; Zhu, X. R.; Rhodes, C. J.; Halban, P. A.; Steiner, D. F.; Verchere, C. B., Role of beta-cell prohormone convertase (PC) 1/3 in processing of pro-islet antyloid polypeptide. *Diabetes* **2004**, *53* (1), 141-148.

Masters, S. L.; Dunne, A.; Subramanian, S. L.; Hull, R. L.; Tannahill, G. M.; Sharp, F. A.; Becker, C.; Franchi, L.; Yoshihara, E.; Chen, Z.; Mullooly, N.; Mielke, L. A.; Harris, J.; Coll, R. C.; Mills, K. H. G.; Mok, K. H.; Newsholme, P.; Nunez, G.; Yodoi, J.; Kahn, S. E.; Lavelle, E. C.; O'Neill, L. A. J., Activation of the NLRP3 inflammasome by islet amyloid polypeptide provides a mechanism for enhanced IL-1 beta in type 2 diabetes. *Nat. Immunol.* 2010, *11* (10), 897-904.

McCutchen, S. L.; Colon, W.; Kelly, J. W., Transthyretin mutation Leu-55-Pro significantly alters tetramer stability and increases amyloidogenicity. *Biochemistry* 1993, *32* (45), 12119-12127.

McGowan, D. P.; van Roon-Mom, W.; Holloway, H.; Bates, G. P.; Mangiarini, L.; Cooper, G. J. S.; Faull, R. L. M.; Snell, R. G., Amyloid-like inclusions in Huntington's disease. *Neuroscience* **2000**, *100* (4), 677-680.

McLean, C. A.; Cherny, R. A.; Fraser, F. W.; Fuller, S. J.; Smith, M. J.; Beyreuther, K.; Bush, A. I.; Masters, C. L., Soluble pool of A beta amyloid as a determinant of severity of neurodegeneration in Alzheimer's disease. *Annals Neurol.* **1999**, *46* (6), 860-866.

Meier, D. T.; Morcos, M.; Samarasekera, T.; Zraika, S.; Hull, R. L; Kahn, S. E., Islet amyloid formation is essential for induction of islet inflammation in high fat fed human islet amyloid polypeptide transgenic mice. *Diabetologia* **2014**, In Press.

Meng, F. L.; Marek, P.; Potter, K. J.; Verchere, C. B., Raleigh, D. P. Rifampicin does not prevent amyloid fibril formation by human islet amyloid polypeptide but does inhibit fibril thioflavin-T interactions: Implications for mechanistic studies of beta-cell death. *Biochemistry* **2008**, *47* (22), 6016-6024.

Meng, F. L.; Abedini, A.; Plesner, A.; Verchere, C. B.; Raleigh, D. P., The flavanol (-)-epigallocatechin 3-gallate inhibits amyloid formation by islet amyloid polypeptide, disaggregates amyloid fibrils, and protects cultured cells against IAPP-induced toxicity. *Biochemistry* **2010**, *49* (37), 8127-8133.

Meng, F. L.; Raleigh, D. P.; Abedini, A., Combination of kinetically selected inhibitors in trans leads to highly effective inhibition of amyloid formation. *J. Am. Chem. Soc.* **2010**, *132* (41), 14340-14342.

Meng, F. L.; Raleigh, D. P., Inhibition of glycosaminoglycan-mediated amyloid formation by islet amyloid polypeptide and proIAPP processing intermediates. *J. Mol. Biol.* **2011**, *406* (3), 491-502.

Meurisse, R.; Brasseur, R.; Thomas, A., Aromatic side-chain interactions in proteins: Near and far sequence His-X pairs. *Biochim. Biophys. Acta*. **2003**, *1649* (1), 85-96.

Middleton, C. T.; Woys, A. M.; Mukherjee, S. S.; Zanni, M. T., Residue-specific structural kinetics of proteins through the union of isotope labeling, mid-IR pulse shaping, and coherent 2D IR spectroscopy. *Methods*. **2010**, *52* (1), 12-22.

Minor, D. L.; Kim, P. S., Measurement of the beta-sheet-forming propensities of amino-acids. *Nature* **1994**, *367* (6464), 660-663.

Mishra, R.; Sellin, D.; Radovan, D.; Gohlke, A.; Winter, R., Inhibiting islet amyloid polypeptide fibril formation by the red wine compound resveratrol. *Chembiochem* **2009**, *10* (3), 445-449.

Mitraki, A., Protein aggregation: From inclusion bodies to amyloid and biomaterials, *Adv. Protein Chem. Str.* **2010**, *79*, 89-125.

Miyazato, M.; Nakazato, M.; Shiomi, K.; Aburaya, J.; Kangawa, K.; Matsuo, H.; Matsukura, S., Molecular-forms of islet amyloid polypeptide (IAPP amylin) in four mammals. *Diabetes Res. Clin. Pract.* **1992**, *15* (1), 31-36.

Moechars, D.; Dewachter, I.; Lorent, K.; Reverse, D.; Baekelandt, V.; Naidu, A.; Tesseur, I.; Spittaels, K.; Van Den Haute, C.; Checler, F.; Godaux, E.; Cordell, B.; Van Leuven, F., Early phenotypic changes in transgenic mice that overexpress different mutants of amyloid precursor protein in brain. *J. Biol. Chem*. **1999**, *274* (10), 6483-6492.

Moriarty, D. F.; Raleigh, D. P., Effects of sequential proline substitutions on amyloid formation by human amylin (20-29). *Biochemistry* **1999**, *38* (6), 1811-1818.

Morita, S.; Sakagashira, S.; Shimajiri, Y.; Eberhardt, N. L.; Kondo, T.; Kondo, T.; Sanke, T., Autophagy protects against human islet amyloid polypeptide-associated apoptosis. *J. Diabetes Invest.* **2011**, *2* (1), 48-55.

Mosselman, S.; Hoppener, J. W. M.; Zandberg, J.; Vanmansfeld, A. D. M.; Vankessel, A. H. M. G.; Lips, C. J. M.; Jansz, H. S., Islet amyloid polypeptide: Identification and chromosomal localization of the human-gene. *Febs Lett*. **1988**, *239* (2), 227-232.

Murias, M.; Handler, N.; Erker, T.; Pleban, K.; Ecker, G.; Saiko, P.; Szekeres, T.; Jager, W., Resveratrol analogues as selective cyclooxygenase-2 inhibitors: synthesis and structure-activity relationship. *Bioorg. Medi. Chem*. **2004**, *12* (21), 5571-5578.

Murias, M.; Jager, W.; Handler, N.; Erker, T.; Horvath, Z.; Szekeres, T.; Nohl, H.; Gille, L., Antioxidant prooxidant and cytotoxic activity of hydroxylated resveratrol analogues: structure-activity relationship. *Biochem. Pharm*. **2005**, *69* (6), 903-912.

Nakagawa, T.; Zhu, H.; Morishima, N.; Li, E.; Xu, J.; Yankner, B. A.; Yuan, J. Y., Caspase-12 mediates endoplasmic-reticulum-specific apoptosis and cytotoxicity by amyloid-beta. *Nature* **2000**, *403* (6765), 98-103.

Nanga, R. P. R.; Brender, J. R.; Xu, J. D.; Hartman, K.; Subramanian, V.; Ramamoorthy, A. Three-dimensional structure and orientation of rat islet amyloid polypeptide protein in a membrane environment by solution NMR spectroscopy. *J. Am. Chem. Soc*. **2009**, *131* (23), 8252-8261.

Narita, R.; Toshimori, H.; Nakazato, M.; Kuribayashi, T.; Toshimori, T.; Kawabata, K.; Takahashi, K.; Masukura, S., Islet amyloid polypeptide (IAPP) and pancreatic-islet amyloid deposition in diabetes and nondiabetic patients. *Diabetes Res. Clin. Pract.* **1992**, *15* (1), 3-14.

Nelson, R.; Eisenberg, D., Recent atomic models of amyloid fibril structure. *Curr. Opin. Struc. Biol.* **2006**, *16* (2), 260-265.

Nelson, R.; Sawaya, M. R.; Balbirnie, M.; Madsen, A. O.; Riekel, C.; Grothe, R.; Eisenberg, D., Structure of the cross-beta spine of amyloid-like fibrils. *Nature* **2005**, *435* (7043), 773-778.

Nishi, M.; Sanke, T.; Nagamatsu, S.; Bell, G. I.; Steiner, D. F., Islet amyloid polypeptide-a new beta-cell secretory product related islet amyloid deposits. *J. Biol. Chem.* **1990**, *265* (8), 4173-4176.

Nishi, M.; Chan, S. J.; Nagamatsu, S.; Bell, G. I.; Steiner, D. F., Conservation of the sequence of islet amyloid polypeptide in five mammals is consistent with its putative role as an islet hormone. *Proc. Natl. Acad. Sci. U.S.A.* **1989**, *86* (15), 5738-5742.

Noor, H.; Cao, P.; Raleigh, D. P., Morin hydrate inhibits amyloid formation by islet amyloid polypeptide and disaggregates amyloid fibers. *Protein Sci.* **2012**, *21* (3), 373-382.

O'Nuallain, B.; Williams, A. D.; Westermark, P.; Wetzel, R., Seeding specificity in amyloid growth induced by heterologous fibrils. *J. Biol. Chem.* **2004**, *279* (17), 17490-17499.

Padrick, S. B.; Miranker, A. D., Islet amyloid polypeptide: Identification of long-range contacts and local order on the fibrillogenesis pathway. *J. Mol. Biol.* **2001**, *308* (4), 783-794.

Padrick, S. B.; Miranker, A. D., Islet amyloid: Phase partitioning and secondary nucleation are central to the mechanism of fibrillogenesis. *Biochemistry* **2002**, *41* (14), 4694-4703.

Palhano, F. L.; Lee, J.; Grimster, N. P.; Kelly, J. W., Toward the molecular mechanism(s) by which EGCG treatment remodels mature amyloid fibrils. *J. Am. Chem. Soc.* **2013**, *135* (20), 7503-7510.

Park, K.; Jaikaran, E. T. A. S.; Clark, A.; Verchere, C. B., Increased amyloid fibril formation and beta cell toxicity of S20G mutant human islet amyloid polypeptide (IAPP). *Diabetes* **2002**, *51*, A386-A386.

Paterson, Y.; Leach, S. J., Effect of side-chain branching on theoretically predicted conformational space available to amino-acid-residues. *Macromolecules* **1978**, *11* (2), 409-415.

Paulsson, J. F.; Andersson, A.; Westermark, P.; Westermark, G. T., Intracellular amyloid-like deposits contain unprocessed pro-islet amyloid polypeptide (proIAPP) in beta cells of transgenic mice overexpressing the gene for human IAPP and transplanted human islets. *Diabetologia* **2006**, *49* (6), 1237-1246.

Petkova, A. T.; Ishii, Y.; Balbach, J. J.; Antzutkin, O. N.; Leapman, R. D.; Delaglio, F.; Tycko, R., A structural model for Alzheimer's beta-amyloid fibrils based on experimental constraints from solid state NMR. *Proc. Natl. Acad. Sci. U.S.A.* **2002**, *99* (26), 16742-16747.

Popovych, N.; Brender, J. R.; Soong, R.; Vivekanandan, S.; Hartman, K.; Basrur, V.; Macdonald, P. M.; Ramamoorthy, A., Site specific interaction of the polyphenol EGCG with the SEVI amyloid precursor peptide PAP(248-286). *J. Phys. Chem. B* **2012**, *116* (11), 3650-3658.

Porat, Y.; Abramowitz, A.; Gazit, E., Inhibition of amyloid fibril formation by polyphenols: Structural similarity and aromatic interactions as a common inhibition mechanism. *Chem. Bio. Drug Des*. **2006**, *67* (1), 27-37.

Porat, Y.; Mazor, Y.; Efrat, S.; Gazit, E., Inhibition of islet amyloid polypeptide fibril formation: A potential role for heteroaromatic interactions. *Biochemistry* **2004**, *43* (45), 14454-14462.

Potter, K. J.; Abedini, A.; Marek, P.; Klimek, A. M.; Butterworth, S.; Driscoll, M.; Baker, R.; Nilsson, M. R.; Warnock, G. L.; Oberholzer, J.; Bertera, S.; Trucco, M.; Korbutt, G. S.; Fraser, P. E. Raleigh, D. P.; Verchere, C. B., Islet amyloid deposition limits the viability of human islet grafts but not porcine islet grafts. *Proc. Natl. Acad. Sci. U.S.A.* **2010**, *107* (9), 4305-4310.

Puchtler, H.; Sweat, F., Congo red as a stain for fluorescence microscopy of amyloid. *J. Histochem. Cytochem*. **1965**, *13* (8), 693-694.

Quist, A.; Doudevski, L.; Lin, H.; Azimova, R.; Ng, D.; Frangione, B.; Kagan, B.; Ghiso, J.; Lal, R., Amyloid ion channels: A common structural link for protein-misfolding disease. *Proc. Natl. Acad. Sci. U.S.A.* **2005**, *102* (30), 10427-10432.

Radovan, D.; Opitz, N.; Winter, R., Fluorescence microscopy studies on islet amyloid polypeptide fibrillation at heterogeneous and cellular membrane interfaces and its inhibition by resveratrol. *Febs Lett*. **2009**, *583* (9), 1439-1445.

Rezai-Zadeh, K.; Arendash, G. W.; Hou, H. Y.; Fernandez, F.; Jensen, M.; Runfeldt, M.; Shytle, R. D.; Tan, J., Green tea epigallocatechin-3-gallate (EGCG) reduces beta-amyloid mediated cognitive impairment and modulates tau pathology in Alzheimer transgenic mice. *Brain Res.* **2008**, *1214*, 177-187.

Ritzel, R. A.; Meier, J. J.; Lin, C. Y.; Veldhuis, J. D.; Butler, P. C., Human islet amyloid polypeptide oligomers disrupt cell coupling, induce apoptosis, and impair insulin secretion in isolated human islets. *Diabetes* **2007**, *56* (1), 65-71.

Rivera, J. F.; Gurlo, T.; Daval, M.; Huang, C. J.; Matveyenko, A. V.; Butler, P. C.; Costes, S., Human-IAPP disrupts the autophagy/lysosomal pathway in pancreatic beta-cells: protective role of p62-positive cytoplasmic inclusions. *Cell Death Differ*. **2011**, *18* (3), 415-426.

Roberts, A. N.; Leighton, B.; Todd, J. A.; Cockburn, D.; Schofield, P. N.; Sutton, R.; Holt, S.; Boyd, Y.; Day, A. J.; Foot, E. A.; Willis, A. C.; Reid, K. B. M.; Cooper, G. J. S., Molecular and functional-characterization of amylin, a peptide associated with type-2 diabetes-mellitus. *Pro. Natl. Acad. Sci. U.S.A.* **1989**, *86* (24), 9662-9666.

Rushing P. A.; Hagan, M. M.; Seeley R. J.; Lutz, T. A.; D' Alessio, D. A.; Air, E. L.; Woods S. C., Inhibition of central amylin signaling increases food intake and body adiposity in rats. Endocrinology **2001**, *142* (11), 5035-5038

Sakagashira, S.; Hiddinga, H. J.; Tateishi, K.; Sanke, T.; Hanabusa, T.; Nanjo, K.; Eberhardt, N. L., S20G mutant amylin exhibits increased in vitro amyloidogenicity and increased intracellular cytotoxicity compared to wild-type amylin. *Am. J. Pathol*. **2000**, *157* (6), 2101-2109.

Sanke, T.; Bell, G. I.; Sample, C.; Rubenstein, A. H.; Steiner, D. F., An islet amyloid peptide is derived from an 89-amino acid precursor by proteolytic processing. *J. Biol. Chem*. **1988**, *263* (33), 17243-17246.

Saraogi, I.; Hebda, J. A.; Becerril, J.; Estroff, L. A.; Miranker, A. D.; Hamilton, A. D., Synthetic alpha-helix mimetics as agonists and antagonists of islet amyloid polypeptide aggregation. *Angew. Chem. Int. Ed*. **2010**, *49* (4), 736-739.

Savaskan, E.; Olivieri, G.; Meier, F.; Seifritz, E.; Wirz-Justice, A.; Muller-Spahn, F., Red wine ingredient resveratrol protects from beta-amyloid neurotoxicity. *Gerontology* 2003, *49* (6), 380-383.

Sawaya, M. R.; Sambashivan, S.; Nelson, R.; Ivanova, M. I.; Sievers, S. A.; Apostol, M. I.; Thompson, M. J.; Balbirnie, M.; Wiltzius, J. J. W.; McFarlane, H. T.; Madsen, A. O.; Riekel, C.; Eisenberg, D., Atomic structures of amyloid cross-beta spines reveal varied steric zippers. *Nature* **2007**, *447* (7143), 453-457.

Scherbaum, W. A., The role of amylin in the physiology of glycemic control. Exp. Clin. Endocrinol. Diabetes **1998**, *106* (2), 97-102.

Sciarretta, K. L.; Gordon, D. J.; Meredith, S. C., Peptide-based inhibitors of amyloid assembly. *Method Enzymol*. **2006**, *413*, 273-312.

Selkoe, D. J. Cell biology of protein misfolding: The examples of Alzheimer's and Parkinson's diseases, *Nat. Cell Biol*. **2004**, *6* (11), 1054-1061.

Serpell, L. C.; Sunde, M.; Benson, M. D.; Tennent, G. A.; Pepys, M. B.; Fraser, P. E., The protofilament substructure of amyloid fibrils. *J. Mol. Biol.* **2000**, *300* (5), 1033-1039.

Sharon, R.; Bar-Joseph, I.; Frosch, M. P.; Walsh, D. M.; Hamilton, J. A.; Selkoe, D. J., The formation of highly soluble oligomers of alpha-synuclein is regulated by fatty acids and enhanced in Parkinson's disease. *Neuron* **2003**, *37* (4), 583-595.

Shim, S. H.; Gupta, R.; Ling, Y. L.; Strasfeld, D. B.; Raleigh, D. P.; Zanni, M. T., Two-dimensional IR spectroscopy and isotope labeling defines the pathway of amyloid formation with residue-specific resolution, *Proc. Natl. Acad. Sci. U.S.A.* **2009**, *106* (16), 6614-6619.

Sievers, S. A.; Karanicolas, J.; Chang, H. W.; Zhao, A.; Jiang, L.; Zirafi, O.; Stevens, J. T.; Munch, J.; Baker, D.; Eisenberg, D., Structure-based design of non-natural amino-acid inhibitors of amyloid fibril formation. *Nature* **2011**, *475* (7354), 96-117.

Sipe, J. D., Amyloidosis. *Crit. Rev. Clin. Lab. Sci*. **1994**, *31* (4), 325-354.

Sipe, J. D.; Benson, M. D.; Buxbaum, J. N.; Ikeda, S.; Merlini, G.; Saraiva, M. J. M.; Westermark, P., Amyloid fibril protein nomenclature: 2012 recommendations from the nomenclature committee of the international society of amyloidosis. *Amyloid* **2012**, *19* (4), 167-170.

Stefani, M., Generic cell dysfunction in neurodegenerative disorders: Role of surfaces in early protein misfolding, aggregation, and aggregate cytotoxicity. *Neuroscientist* **2007**, *13* (5), 519-531.

Strasfeld, D. B.; Ling, Y. L.; Shim, S. H.; Zanni, M. T., Tracking fiber formation in human islet amyloid polypeptide with automated 2D-IR spectroscopy. *J. Am. Chem. Soc*. **2008**, *130* (21), 6698-6699.

Street, A. G.; Mayo, S. L., Intrinsic beta-sheet propensities result from van der Waals interactions between side chains and the local backbone, *Proc. Natl. Acad. Sci. U.S.A*. **1999**, *96* (1), 9074-9076.

Subramanian, S. L.; Hull, R. L.; Zraika, S.; Aston-Mourney, K.; Udayasankar, J.; Kahn, S. E., cJUN N-terminal kinase (JNK) activation mediates islet amyloid-induced beta cell apoptosis in cultured human islet amyloid polypeptide transgenic mouse islets. *Diabetologia* **2012**, *55* (1), 166-174.

Sun, A. Y.; Wang, Q.; Simonyi, A.; Sun, G. Y., Resveratrol as a therapeutic agent for neurodegenerative diseases. *Mol. Neurobiol*. **2010**, *41* (2-3), 375-383.

Sunde, M.; Serpell, L. C.; Bartlam, M.; Fraser, P. E.; Pepys, M. B.; Blake, C. C. F., Common core structure of amyloid fibrils by synchrotron X-ray diffraction. *J. Mol. Biol*. 1997, 273 (3), 729-739.

Suzuki, Y.; Brender, J. R.; Hartman, K.; Ramamoorthy, A.; Marsh, E. N. G., Alternative pathways of human islet amyloid polypeptide aggregation distinguished by F-19 nuclear magnetic resonance-detected kinetics of monomer consumption. *Biochemistry* **2012**, *51* (41), 8154-8162.

Swift, S. M.; Clayton, H. A.; London, N. J. M.; James, R. F. L., The potential contribution of rejection to survival of transplanted human islets. *Cell Transplant*. **1998**, *7* (6), 599-606.

Tam, J. P., Wu, C. R., Liu, W. & Zhang, J. W. Disulfide bond formation in peptides by dimethyl-sulfoxide: Scope and applications. *J. Am. Chem. Soc.* **1991**, *113* (17), 6657-6662.

Terzi, E.; Holzemann, G.; Seelig, J., Interaction of Alzheimer beta-amyloid peptide (1-40) with lipid membranes. *Biochemistry* **1997**, *36* (48), 14845-14852.

Thomas, T.; Nadackal, G. T.; Thomas, K., Aspirin and diabetes: Inhibition of amylin aggregation by nonsteroidal anti-inflammatory drugs. *Exp. Clin. Endocrinol. Diabetes* **2003**, *111* (1), 8-11.

Tjernberg, L. O.; Naslund, J.; Lindqvist, F.; Johansson, J.; Karlstrom, A. R.; Thyberg, J.; Terenius, L.; Nordstedt, C., Arrest of beta-amyloid fibril formation by a pentapeptide ligand. *J. Biol. Chem*. **1996**, *271* (15), 8545-8548.

Tracz, S. M.; Abedini, A.; Driscoll, M.; Raleigh, D. P., Role of aromatic interactions in amyloid formation by peptides derived from human amylin. *Biochemistry* **2004**, *43* (50), 15901-15908.

Tu, L. H.; Raleigh, D. P., Role of aromatic interactions in amyloid formation by islet amyloid polypeptide. *Biochemistry* **2013**, *52* (2), 333-342.

Tu, L.H.; Serrano, A. L.; Zanni, M. T. Raleigh, D. P., Mutational analysis of preamyloid intermediates: The role of His-Tyr interactions in islet amyloid formation. *Biophys. J*. **2014**, *106* (7), 1520-1527.

Tucker, M. J.; Oyola, R.; Gai, F., A novel fluorescent probe for protein binding and folding studies: p-cyano-phenylalanine. *Biopolymers* **2006**, *83* (6), 571-576.

Vaiana, S. M.; Ghirlando, R.; Yau, W. M.; Eaton, W. A.; Hofrichter, J., Sedimentation studies on human amylin fail to detect low-molecular-weight oligomers. *Biophys. J.* **2008**, *94* (7), L45-L47.

Valincius, G.; Heinrich, F.; Budvytyte, R.; Vanderah, D. J.; McGillivray, D. J.; Sokolov, Y.; Hall, J. E.; Losche, M., Soluble amyloid beta-oligomers affect dielectric membrane properties by bilayer insertion and domain formation: Implications for cell toxicity. *Biophys. J.* **2008**, *95* (10), 4845-4861.

Van der Wel, P. C. A.; Lewandowski, J. R.; Griffin, R. G., Solid-state NMR study of amyloid nanocrystals and fibrils formed by the peptide GNNQQNY from yeast prion protein Sup35p. *J. Am. Chem. Soc.* **2007**, *129* (16), 5117-5130.

Verchere, C. B.; DAlessio, D. A.; Palmiter, R. D.; Weir, G. C.; BonnerWeir, S.; Baskin, D. G.; Kahn, S. E., Islet amyloid formation associated with hyperglycemia in transgenic mice with pancreatic beta cell expression of human islet amyloid polypeptide. *Proc. Natl. Acad. Sci. U.S.A.* **1996**, *93* (8), 3492-3496.

Wang, J.; Dickson, D. W.; Trojanowski, J. Q.; Lee, V. M. Y., The levels of soluble versus insoluble brain A beta distinguish Alzheimer's disease from normal and pathologic aging. *Expe. Neurol.* **1999**, *158* (2), 328-337.

Wang, J.; Xu, J.; Finnerty, J.; Furuta, M.; Steiner, D. F.; Verchere, C. B., The prohormone convertase enzyme 2 (PC2) is essential for processing pro-islet amyloid polypeptide at the NH2-terminal cleavage site. *Diabetes* **2001**, *50* (3), 534-539.

Wei, L.; Jiang, P.; Xu, W. X.; Li, H.; Zhang, H.; Yan, L. Y.; Chan-Park, M. B.; Liu, X. W.; Tang, K.; Mu, Y. G.; Pervushin, K., The molecular basis of distinct aggregation pathways of islet amyloid polypeptide. *J. Biol. Chem.* **2011**, *286* (8), 6291-6300.

Weise, K.; Radovan, D.; Gohlke, A.; Opitz, N.; Winter, R., Interaction of hIAPP with model raft membranes and pancreatic beta-cells: Cytotoxicity of hIAPP oligomers. *Chembiochem* **2010**, *11* (9), 1280-1290.

Westerma. P., Quantitative studies of amyloid in islets of Langerhans. *Ups. J. Med. Sci*. **1972**, *77* (2), 91-94.

Westermark, G. T.; Falkmer, S.; Steiner, D. F.; Chan, S. J.; Engstrom, U.; Westermark, P., Islet amyloid polypeptide is expressed in the pancreatic islet parenchyma of the teleostean fish, Myoxocephalus (cottus) scorpius. *Comp. Biochem. Physiol. B Biochem. Mol. Biol.* **2002**, *133* (1), 119-125.

Westermark, G. T.; Westermark, P.; Nordin, A.; Tornelius, E.; Andersson, A., Formation of amyloid in human pancreatic islets transplanted to the liver and spleen of nude mice, *Upsala J. Med. Sci.* **2003**, *108* (3), 193-203.

Westermark, G. T.; Westermark, P.; Berne, C.; Korsgren, O.; Nordic Network Clin Islet, T., Widespread amyloid deposition in transplanted human pancreatic islets, *N. Engl. J. Med.* **2008**, *359* (9), 977-979.

Westermark, P.; Wernstedt, C.; Wilander, E.; Hayden, D. W.; Obrien, T. D.; Johnson, K. H., Amyloid fibrils in human insulinoma and islets of Langerhans of the diabetic cat are derived from a neuropeptide-like protein also present in normal islet cells, *Proc. Natl. Acad. Sci. U.S.A.* **1987**, *84* (11), 3881-3885.

Westermark, P.; Engstrom, U.; Johnson, K. H.; Westermark, G. T.; Betsholtz, C., Islet amyloid polypeptide: pinpointing amino acid residues linked to amyloid fibril formation. *Proc. Natl. Acad. Sci. U.S.A.* **1990**, *87* (13), 5036-5040.

Westermark, P.; Andersson, A.; Westermark, G. T., Islet amyloid polypeptide, Islet amyloid, and diabetes mellitus, *Physiol. Rev.* **2011**, *91* (3), 795-826.

Weyer, C.; Maggs, D. G.; Young, A. A.; Kolterman, O. G., Amylin replacement with pramlintide as an adjunct to insulin therapy in type 1 and type 2 diabetes mellitus: A physiological approach toward improved metabolic control. *Curr. Pharma. Des.* **2001**, *7* (14), 1353-1373.

Williamson, J. A.; Miranker, A. D., Direct detection of transient alpha-helical states in islet amyloid polypeptide. *Protein Sci.* **2007**, *16* (1), 110-117.

Williamson, J. A.; Loria, J. P.; Miranker, A. D., Helix stabilization precedes aqueous and bilayer-catalyzed fiber formation in islet amyloid polypeptide. *J. Mol. Biol.* **2009**, *393* (2), 383-396.

Wiltzius, J. J. W.; Sievers, S. A.; Sawaya, M. R.; Cascio, D.; Popov, D.; Riekel, C.; Eisenberg, D., Atomic structure of the cross-beta spine of islet amyloid polypeptide (amylin). *Protein Sci.* **2008**, *17* (9), 1467-1474.

Wiltzius, J. J. W.; Sievers, S. A.; Sawaya, M. R.; Eisenberg, D., Atomic structures of IAPP (amylin) fusions suggest a mechanism for fibrillation and the role of insulin in the process, *Protein Sci.* **2009**, *18* (7), 1521-1530.

Winner, B.; Jappelli, R.; Maji, S. K.; Desplats, P. A.; Boyer, L.; Aigner, S.; Hetzer, C.; Loher, T.; Vilar, M.; Campionic, S.; Tzitzilonis, C.; Soragni, A.; Jessberger, S.; Mira, H.; Consiglio, A.; Pham, E.; Masliah, E.; Gage, F. H.; Riek, R., In vivo demonstration that alpha-synuclein oligomers are toxic. *Proc. Natl. Acad. Sci. U.S.A.* **2011**, *108* (10), 4194-4199.

Wood, S. J.; Wetzel, R.; Martin, J. D.; Hurle, M. R., Prolines and amyloidogenicity in fragments of the Alzheimer's peptide beta/A4. *Biochemistry* **1995**, *34* (3), 724-730.

Xue, W. F.; Homans, S. W.; Radford, S. E., Systematic analysis of nucleation-dependent polymerization reveals new insights into the mechanism of amyloid self-assembly. *Proc. Natl. Acad. Sci. U.S.A.* **2008**, *105* (26), 8926-8931.

Yagui, K.; Yamaguchi, T.; Kanatsuka, A.; Shimada, F.; Huang, C. I.; Tokuyama, Y.; Ohsawa, H.; Yamamura, K. I.; Miyazaki, J. I.; Mikata, A.; Yoshida, S.; Makino, H., Formation of islet amyloid fibrils in beta-secretory granules of transgenic mice expressing human islet amyloid polypeptide amylin. *Euro. J. Endocrol.* **1995**, *132* (4), 487-496.

Yan, P.; Hu, X. Y.; Song, H. W.; Yin, K. J.; Bateman, R. J.; Cirrito, J. R.; Xiao, Q. L.; Hsu, F. F.; Turk, J. W.; Xu, J.; Hsu, C. Y.; Holtzman, D. M.; Lee, J. M., Matrix metalloproteinase-9 degrades amyloid-beta fibrils in vitro and compact plaques in situ. *J. Biol. Chem.* **2006**, *281* (34), 24566-24574.

Yanagi, K.; Ashizaki, M.; Yagi, H.; Sakurai, K.; Lee, Y. H.; Goto, Y., Hexafluoroisopropanol induces amyloid fibrils of islet amyloid polypeptide by enhancing both hydrophobic and electrostatic interactions. *J. Biol. Chem.* **2011**, *286* (27), 23959-23966.

Young, D. A.; Deems, R. O.; Deacon, R. W.; McIntosh, R. H.; Foley, J. E., Effects of amylin on glucose-metabolism and glycogenolysis in vivo and in vitro. *Am. J. Physiol.* **1990**, *259* (3), E457-E461.

Young, L. M.; Cao, P.; Raleigh, D. P.; Ashcroft, A. E.; Radford, S. E., Ion mobility spectrometry-mass spectrometry defines the oligomeric intermediates in amylin amyloid formation and the mode of action of inhibitors. *J. Am. Chem. Soc.* **2014**, *136* (2), 660-670.

Zhang, S. P.; Liu, J. X.; Dragunow, M.; Cooper, G. J. S., Fibrillogenic amylin evokes islet beta-cell apoptosis through linked activation of a caspase cascade and JNK1. *J. Biol. Chem.* **2003**, *278* (52), 52810-52819.

Zhang, X.; Cheng, B. A.; Gong, H.; Li, C. Z.; Chen, H.; Zheng, L.; Huang, K., Porcine islet amyloid polypeptide fragments are refractory to amyloid formation. *Febs Lett.* **2011**, *585* (1), 71-77.

Zierath, J. R.; Galuska, D.; Engstrom, A.; Johnson, K. H.; Betsholtz, C.; Westermark, P.; Wallberghenriksson, H., Human islet amyloid polypeptide at pharmacological levels inhibits insulin and phorbol ester-stimulated glucose-transport in vitro incubated human muscle strips. *Diabetologia* **1992**, *35* (1), 26-31.

Zraika, S.; Hull, R. L.; Udayasankar, J.; Clark, A.; Utzschneider, K. M.; Tong, J.; Gerchman, F.; Kahn, S. E., Identification of the amyloid-degrading enzyme neprilysin in mouse islets and potential role in islet amyloidogenesis. *Diabetes* **2007**, *56* (2), 304-310.

Zraika, S.; Hull, R. L.; Udayasankar, J.; Aston-Mourney, K.; Subramanian, S. L.; Kisilevsky, R.; Szarek, W. A.; Kahn, S. E., Oxidative stress is induced by islet amyloid formation and time-dependently mediates amyloid-induced beta cell apoptosis. *Diabetologia* **2009**, *52* (4), 626-635.

Zraika, S.; Hull, R. L.; Verchere, C. B.; Clark, A.; Potter, K. J.; Fraser, P. E.; Raleigh, D. P.; Kahn, S. E., Toxic oligomers and islet beta cell death: guilty by association or convicted by circumstantial evidence? *Diabetologia* **2010**, *53* (6), 1046-1056.

Zraika, S.; Aston-Mourney, K.; Marek, P.; Hull, R. L.; Green, P. S.; Udayasankar, J.; Subramanian, S. L.; Raleigh, D. P.; Kahn, S. E., Neprilysin impedes islet amyloid formation by inhibition of fibril formation rather than peptide degradation. *J. Biol. Chem.* **2010**, *285* (24), 18177-18183.